



HAL
open science

Study of the dynamics of physiological and metabolic responses of *Yarrowia lipolytica* to environmental physico-chemical perturbations

Asma Timoumi

► **To cite this version:**

Asma Timoumi. Study of the dynamics of physiological and metabolic responses of *Yarrowia lipolytica* to environmental physico-chemical perturbations. Microbiology and Parasitology. INSA de Toulouse, 2017. English. NNT: 2017ISAT0009 . tel-01628212

HAL Id: tel-01628212

<https://theses.hal.science/tel-01628212>

Submitted on 3 Nov 2017

HAL is a multi-disciplinary open access archive for the deposit and dissemination of scientific research documents, whether they are published or not. The documents may come from teaching and research institutions in France or abroad, or from public or private research centers.

L'archive ouverte pluridisciplinaire **HAL**, est destinée au dépôt et à la diffusion de documents scientifiques de niveau recherche, publiés ou non, émanant des établissements d'enseignement et de recherche français ou étrangers, des laboratoires publics ou privés.



Université
de Toulouse

THÈSE

En vue de l'obtention du

DOCTORAT DE L'UNIVERSITÉ DE TOULOUSE

Délivré par :

Institut National des Sciences Appliquées de Toulouse (INSA de Toulouse)

Cotutelle internationale avec :

Présentée et soutenue par :

Asma TIMOUMI

Le jeudi 29 juin 2017

Titre :

Study of the dynamics of physiological and metabolic responses of *Yarrowia lipolytica* to environmental physico-chemical perturbations

ED SEVAB : Ingénieries microbienne et enzymatique

Unité de recherche :

Laboratoire d'Ingénierie des Systèmes Biologiques et des Procédés (LISBP)

Directeur(s) de Thèse :

Luc FILLAUDEAU (DR INRA, LISBP, Toulouse)

Carole MOLINA-JOUE (PR INSA, LISBP, Toulouse)

Nathalie GORRET (CR INRA, LISBP, Toulouse)

Rapporteurs :

Hela KALLEL (DR, Institut Pasteur, Tunis)

Jack LEGRAND (PR, GEPEA, Nantes)

Autre(s) membre(s) du jury :

Cécile NEUVEGLISE (DR INRA, MICALIS, Jouy-en-Josas)

Nom: Timoumi

Prénom: Asma

Titre: Etude des dynamiques de réponses physiologiques et métaboliques de *Yarrowia lipolytica* à des perturbations environnementales physico-chimiques

Année: 2017

Nombre de pages: 238

Spécialité: Ingénieries microbienne et enzymatique

Lieu: INSA Toulouse

Résumé

En raison d'un mélange non-idéal, des hétérogénéités au sein des bioréacteurs se produisent régulièrement soit à l'échelle pilote, soit lors de l'extrapolation à l'échelle industrielle. En conséquence, les microorganismes circulant au sein de ces bioréacteurs sont continuellement exposés à des gradients locaux de paramètres tels que le pH, la température, la concentration en substrat et en oxygène dissous, le cisaillement, etc. Ces fluctuations spatiales et temporelles peuvent affecter la physiologie des cellules (croissance, métabolisme, morphologie) en fonction de leur nature, intensité, durée et/ou fréquence. L'objectif de ce travail est l'étude qualitative et quantitative de l'impact des fluctuations de pH et d'oxygène dissous sur le comportement dynamique (morphologique et métabolique) de *Yarrowia lipolytica*, une levure avec un potentiel biotechnologique prometteur. Pour répondre à cet objectif, des cultures en bioréacteur en conditions d'environnement contrôlé ont été mises en œuvre afin d'établir un lien de causalité entre la perturbation et la réponse observée. L'implémentation de deux modes de cultures différents (discontinu et continu) a permis de caractériser le comportement dynamique des populations cellulaires dans des états physiologiques différents. En mode continu (en régime permanent), toutes les cellules sont dans le même état physiologique et se multiplient à la même vitesse spécifique de croissance, alors que des sous-populations de levures dans des états physiologiques distincts peuvent cohabiter dans les cultures en mode discontinu. Un effort important a été consacré au développement et validation des méthodes (à partir de particules modèles et de cellules) pour une quantification rigoureuse des évolutions morphologiques de *Y. lipolytica*. Le comportement macroscopique de la levure a été caractérisé par l'évaluation des dynamiques de croissance, la viabilité, les vitesses de consommation du glucose et d'oxygène, ainsi que les vitesses de production d'acide organique et de dioxyde de carbone. Trois techniques, à savoir la cytométrie en flux (CYT), la morphogranulométrie (MG) et la diffraction dynamique de la lumière laser (DLS) ont été employé pour la quantification et la caractérisation de la transition mycélienne. Les résultats ont démontré l'adéquation du modèle cylindre pour quantifier la population filamentée, ainsi que l'importance de la longueur (complémentaire du diamètre équivalent) pour qualifier l'intensité du dimorphisme. Aucun effet significatif des fluctuations de pH et d'oxygène dissous sur le comportement macroscopique (vitesses spécifiques, rendements, viabilité) de la levure n'a été observé. En revanche, une transition mycélienne a été induite en réponse aux deux facteurs de stress (pH and pO_2) seulement en conditions d'excès de glucose durant les cultures discontinues et continues (après limitation d'oxygène), suggérant ainsi un rôle de la concentration résiduelle de glucose sur la régulation de dimorphisme chez *Y. lipolytica*. Le contrôle et la régulation de la concentration en glucose dans le milieu pourrait ainsi contribuer à une meilleure maîtrise des changements morphologiques de *Y. lipolytica* en réponse à des stimuli de l'environnement.

Mots clés: *Yarrowia lipolytica*, Batch, Chemostat, Réponse dynamique, Métabolisme, Morphologie, Sous-populations, Cytométrie, Perturbation, Stress pH, Disponibilité d'oxygène

Last-name: Timoumi

First-name: Asma

Title: Study of the dynamics of physiological and metabolic responses of *Yarrowia lipolytica* to environmental physico-chemical perturbations

Year: 2017

Number of pages: 238

Specialty: Microbial and Enzymatic Engineering

Place: INSA Toulouse

Abstract

Due to limited mixing capacities, heterogeneities regularly occur when scaling-up bioreactors for large-scale production. Microbial cultures are continuously exposed to local gradients in fundamental process parameters such as substrate, pH, temperature and dissolved oxygen DO concentration. These micro-environmental fluctuations may have detrimental effects on cellular growth, metabolism and morphology, depending on the nature, intensity, duration and/or frequency of the fluctuations encountered. The aim of this study was to investigate the impact of pH and DO fluctuations on the dynamic behavior of *Yarrowia lipolytica*, a microorganism with a promising biotechnological potential, at both morphological and metabolic levels. For this purpose, batch and continuous cultivations modes were preferentially adopted, as it enabled respectively, the study of the stress response of yeast populations growing at their maximum specific rate, and at various controlled specific growth rates in physiological steady-states. In addition, an important effort was devoted to the development and validation of morphological methods (using model particles and yeast cells) in order to acquire qualitative and quantitative characterization of the response dynamics at the population scale. The macroscopic behavior of *Y. lipolytica* was assessed through examining the patterns of growth, viability, glucose uptake, oxygen consumption, organic acid and carbon dioxide production rates. Changes in the yeast morphology were characterized at the cell population level by means of flow cytometry, morphogranulometry and diffraction light scattering techniques. The results demonstrated the accuracy of the cylinder model for elongated-shaped cells, and emphasized the importance of examining the length parameter to assess the dimorphism magnitude. Additionally, no significant effect of pH and DO fluctuations on the macroscopic behavior (specific rates, yields, viability) of the yeast was observed. Nevertheless, mycelial growth was induced upon exposure to both stressors, only in glucose-excess environments, suggesting therefore an impact of glucose levels on the regulation of dimorphic transition in *Y. lipolytica*. Controlling residual glucose concentrations in *Y. lipolytica* fermentations may thus contribute to a better monitoring of the morphological changes in response to environmental stimuli.

Keywords: *Yarrowia lipolytica*, Batch, Chemostat, Dynamic response, Metabolism, Morphology, Subpopulations, Cytometry, Perturbation, pH stress, Oxygen availability

ACKNOWLEDGMENTS

A PhD thesis is not possible without the contribution of several people. For this reason, I dedicate here my most sincere thanks to all those people.

I would like to express my thanks to the rapporteurs, Professors Hela KALLEL and Jack LEGRAND, for accepting to examine my PhD thesis. A special thanks to Cécile NEUVÉGLISE, DR INRA, for agreeing to act as an external examiner for this doctoral thesis. I am deeply grateful to all members of the jury for their participation in my PhD defense, and their valuable discussions, suggestions and comments.

I would like to express my sincere gratefulness to my supervisor Luc FILLAUDEAU, DR INRA, for his academic supervision, excellent scientific knowledge and advices. I also like to extent my thanks to my co-supervisor Carole MOLINA-JOUVE, PR INSA, for investing time and providing interesting and valuable feedbacks despite an exceedingly busy schedule. My deep gratitude goes to my co-supervisor Nathalie GORRET, CR INRA, for her excellent supervision, scientific guidance, continuous support and patience. Her selfless help and encouragement were great motivation for my research and writing of this thesis. Without their dedication and commitment to my research, I would have not been able to carry out the research and finish the thesis in the present form.

I acknowledge the assistance of Yohan ALLOUCHE, the Head of Acoustic Testing department of Airbus, who offered me valuable suggestions for this study. Thank you, most sincerely, for our fruitful cooperation during the preparation of the thesis.

I would like to acknowledge Airbus industry for the funding granted through the project ProBio3 “Biocatalytic production of lipidic bioproducts from renewable resources and industrial by-products: BioJet Fuel Application” for my research works.

I would like to thank all the members of the “Fermentation Advances and Microbial Engineering” team for the great work environment. And also to my friends and colleagues with whom I shared my daily life during my time in the Lab or outside: “Arnaud, Aurore, Carlos, Catherine, Elise, Florence, Jillian, Julie, Lucile, Marine, Nicolas, Rana, Tuan, Xiaomin, Yannik, Yassim”. To the entire “FAME” team, I thank you all for the amusing moments.

A very special thanks to Fradj for his unconditional support during all these years and for all his love. I dedicate this thesis to you.

And of course, to finalize, my most profound recognition goes to my parents Houcine and Om-saad. I thank you all for all the love, the constant encouragement, trust and for being always with me supporting my professional and personal projects. I know you are very proud! A special thanks to my sisters Sihem and Zina. I dedicate this thesis to you.

To those I forgot to thank directly, a big thank to you all!

Asma TIMOUMI

PUBLICATIONS AND COMMUNICATIONS

International journals

Timoumi A, Cléret M, Bideaux C, E. Guillouet S, Allouche Y, Molina-Jouve C, Fillaudeau L, Gorret N (2017): Dynamic behavior of *Yarrowia lipolytica* in response to pH perturbations: dependence of the stress response on the culture mode. *Appl Microbiol Biotechnol* 101:351-366 doi:10.1007/s00253-016-7856-2

Timoumi A, Bideaux C, E. Guillouet S, Allouche Y, Molina-Jouve C, Fillaudeau L, Gorret N: Investigation of the effect of oxygen availability on the metabolism and morphology of *Yarrowia lipolytica*: more insights into the impact of glucose levels on dimorphism. *Appl Microbiol Biotechnol* 101:351-366 doi:10.1007/s00253-016-7856-2

Timoumi A, Nguyen T.C, Molina-Jouve C, Gorret N, Fillaudeau L: Comparison of optical methodologies for morphology and size distribution characterization of model particles and complex-shaped biological matrices (*under preparation*).

International conferences

➤ Oral presentation

Timoumi A, Cléret M, Allouche Y, Molina-Jouve C, Fillaudeau L, Gorret N. (2015): Study of the dynamics of metabolic and physiological responses of *Yarrowia lipolytica* to pH perturbations under well-controlled conditions in batch and continuous modes of culture. *Microbial Stress Congress: From Molecules to Systems, Sitges, Spain*.

Timoumi A, Cléret M, Allouche Y, Molina-Jouve C, Fillaudeau L, Gorret N. (2016): Dynamic behavior of *Yarrowia lipolytica* to well-controlled pH and oxygen perturbations: dependence of the stress response on the culture mode. *17th European Congress on Biotechnology (ECB), Krakow, Poland*.

Timoumi A, Cléret M, Allouche Y, Molina-Jouve C, Fillaudeau L, Gorret N. (2016): Dynamics of metabolic and physiological responses of *Yarrowia lipolytica* to well-controlled pH and oxygen perturbations in batch and continuous operating modes. *6th Conference on Physiology of Yeasts and Filamentous Fungi (PYFF6), Lisbon, Portugal*.

Timoumi A, Nguyen T.C, Le T, Anne-archard D, Bideaux C, Cameleyre X, Lombard E, Molina-Jouve C, To K.A, Gorret N, Fillaudeau L. (2016): Optical methods and their limitation to characterize the morphology and granulometry of complex shape biological materials. *Journées Internationales de Biotechnologie, Sousse, Tunisie*.

➤ Poster presentation

Timoumi A, Allouche Y, Plateau J, Molina-Jouve C, Fillaudeau L, Gorret N. (2015): Comparison of optical methods to characterize morphology and size distribution of model particles and mycelial transition of *Yarrowia lipolytica*. *ECCE10-ECAB3-EPIC5 Congress, Nice, France*.

Timoumi A, Allouche Y, Plateau J, Molina-Jouve C, Fillaudeau L, Gorret N. (2015): Comparison of optical methods to characterize morphology and size distribution of model particles and mycelial transition of *Yarrowia lipolytica*. *Journées Internationales de Biotechnologie, Djerba, Tunisie*.

TABLE OF CONTENTS

INTRODUCTION AND CONTEXT OF THE STUDY	1
PART I: LITERATURE REVIEW	7
I.1 Bioreactor heterogeneities and bioperformances	9
I.1.1 Origin of heterogeneities inside bioreactor	10
I.1.2 Nature of heterogeneities in industrial bioreactors	10
I.1.3 Impact on bioprocess performances	17
I.2 Physiological responses of <i>Yarrowia lipolytica</i> to stress conditions	18
I.2.1 General description of <i>Yarrowia lipolytica</i>	18
I.2.2 Morphological changes in <i>Yarrowia lipolytica</i> : dimorphism phenomena	19
I.2.3 Metabolic responses of <i>Yarrowia lipolytica</i> to adverse environmental conditions	35
I.2.4 Mechanisms regulating stress responses in <i>Yarrowia lipolytica</i>	37
I.3 Conclusions and objectives of the study	38
PART II: MATERIALS AND METHODS	41
II.1 Strain and culture media.....	42
II.1.1 Strain	42
II.1.2 Culture media	42
II.2 Culture conditions	44
II.2.1 Strain preservation.....	44
II.2.2 Inoculum preparation	44
II.2.3 Bioreactor fermentation.....	45
II.3 Model particles	48
II.3.1 Calibration particles: from 1 to 15 μm -diameter.....	48
II.3.2 Calibration particles: 40 and 80 μm -diameter.....	48
II.4 Analytical methods.....	49
II.4.1 Biomass characterization.....	49
II.4.2 Determination of glucose and organic acids concentrations	62
II.4.3 Gas analysis.....	67
II.5 Methodology for data treatment.....	67

II.5.1	Rates expression for gas-phase reactions	67
II.5.2	Rate expressions for liquid-phase reactions	73
II.5.3	Determination of overall yields	74
II.5.4	Carbon and redox balances	74
II.5.5	Smoothing and reconciliation of the experimental data	75
PART III: RESULTS AND DISCUSSION.....		76
Chapter III-1: Development and validation of methodologies for the quantification and characterization of morphological changes in <i>Yarrowia lipolytica</i>		
		78
III.1.1	Introduction	80
III.1.2	Experimental strategy.....	81
III.1.3	Results and discussion.....	82
III.1.4	Conclusion.....	95
III.1.5	Results synthesis	97
Chapter III-2: Characterization of the mycelial transition of <i>Yarrowia lipolytica</i> by morphogranulometric measurements		
		99
III.2.1	Introduction	101
III.2.2	Experimental strategy.....	102
III.2.3	Results and discussion.....	102
III.2.4	Conclusions	114
III.2.5	Results synthesis	115
Chapter III-3: Dynamic behavior of <i>Yarrowia lipolytica</i> in response to pH perturbations: dependence of the stress response on the culture mode		
		117
III.3.1	Introduction	119
III.3.2	Publication: Dynamic behavior of <i>Yarrowia lipolytica</i> in response to pH perturbations: dependence of the stress response on the culture mode.....	120
III.3.3	Results synthesis	150
Chapter III-4: Investigation of the effect of oxygen availability on the metabolism and morphology of <i>Yarrowia lipolytica</i> : more insights into the impact of glucose levels on dimorphism.....		
		152
III.4.1	Introduction	154

III.4.2	Publication: Investigation of the effect of oxygen availability on the metabolism and morphology of <i>Yarrowia lipolytica</i> : more insights into the impact of glucose levels on dimorphism	155
III.4.3	Results synthesis	182
GENERAL DISCUSSION, CONCLUSIONS AND PERSPECTIVES		184
REFERENCES		195

LIST OF FIGURES

Figure 0-1: The PhD research focus and experimental strategy	5
Figure I-1: Schematic illustration of the irreducible couplings between physico-chemical phenomena (control of cellular environment) and biotic responses of microorganisms. Figure adapted from Asenjo and Merchuk (1994).....	10
Figure I-2: Predicted gas holdup (A) and local dissolved oxygen concentration (B) in a 3 m ³ triple-impeller stirred bioreactor (vessel diameter :1.3 m; liquid height: 2.3 m; impeller speed: 180 rpm; vvm: 1; pressure: 2.5 atm; circulation time: 10 s) (Zahradnik et al. 2001)	12
Figure I-3: Comparison of DO readings from the top and bottom probes in a 20-L (A) and 5000-L bioreactor: Equivalent specific power inputs (100 W m ⁻³ , air sparging rates (0.0013 vvm) and liquid aspect ratio were used for both 20- and 5000-L bioreactors (Xing et al. 2009)	13
Figure I-4: pH variations after base addition (Na ₂ CO ₃) either at the liquid surface (A) or in the impeller region (B) of a 8 m ³ stirred bioreactor (vessel diameter D: 2m; liquid height: 1.3D; impeller diameter: 0.225D; impeller speed: 60 rpm; vvm: 0.005) (Langheinrich and Nienow 1999)	14
Figure I-5: pH gradients simulated in the scale down-system during engineered <i>E. coli</i> cultures at residence times of 60 (A), 120 (B), 180 (C), and 240 s (D). The dark lines correspond to the pH values in the stirred tank reactor simulating the well-mixed region near the impeller (STR1). The gray lines correspond to the pH values in the stirred tank reactor simulating the region of alkali addition (STR2) (Cortes et al. 2016)	15
Figure I-6: CFD simulation of instantaneous glucose concentration in a 22 m ³ bioreactor fed with a 500 g L ⁻¹ solution at a rate of 180 L h ⁻¹ (Enfors et al. 2001)	16
Figure I-7: CFD simulation of glucose concentration fluctuations: (A) at one point close to the feed point; and (B) at two points (pos 1 and pos 2) close to the vessel wall in a 22 m ³ bioreactor (Enfors et al. 2001)	17
Figure I-8: Morphology of <i>Yarrowia lipolytica</i> W29 cells cultivated with shaking at 28 °C in Yeast Nitrogen Base (YNB) medium containing 1 % glucose, 0.5 % (NH ₄) ₂ SO ₄ and 50 mM phosphate or citrate buffer. A and C: pH 3 medium with phosphate or citrate buffer. B and D: pH 7 medium with phosphate or citrate buffer (Ruiz-Herrera and Sentandreu 2002)	21
Figure I-9: Kinetic of hyphae formation during thermal stress application: a control system; b after 1 h of the thermal shift; c after 2 h of the thermal shift (Kawasse et al. 2003)	24

Figure I-10: Elongation factor distribution for: a control system; b thermal stress conditions (Kawasse et al. 2003)	24
Figure I-11: Total hyphal length determined for: a control system; b oxidative stress conditions (Kawasse et al. 2003)	25
Figure I-12: Growth kinetics of <i>Y. lipolytica</i> cultivated in flasks containing olive oil as sole carbon source and changes in dissolved oxygen concentration (DOC). Light micrographs showing the morphology of the yeast as growth proceeded. (a) Single cells; (b) pseudomycelia and single cells; (c) true mycelia and yeast cells (images were taken at magnifications of 1000x) (Bellou et al. 2014)	26
Figure I-13: Growth, DOC and morphology of <i>Y. lipolytica</i> during the transition from low to high oxygen concentration at steady state (dilution rate, 0.032 h ⁻¹). (a) True mycelia and a few pseudomycelia were predominant; (b) pseudomycelia and a few single cells; (c) single cells and a few pseudomycelia (images were taken at magnifications of 400x) (Bellou et al. 2014)	27
Figure I-14: Scanning electron micrographs of <i>Yarrowia lipolytica</i> cells: a) control; b) in the presence of 9 % NaCl (Andreishcheva et al. 1999)	28
Figure I-15: Cell size distribution for <i>Yarrowia lipolytica</i> W29 cells at: atmospheric pressure (black bar), 4 bar (white bar) and 8 bar (grey bar) (Lopes et al. 2008)	29
Figure I-16: Morphology of <i>Yarrowia lipolytica</i> grown as yeast in YNBGlc medium (a and c), or as mycelium in YNBGlcNAc medium, after a heat shock (b and d), after 12h (a, b) or 24 h (c, d) incubation (Guevaraolvera et al. 1993)	31
Figure I-17: Dependence of cellular morphology on organic sources of nitrogen. <i>Yarrowia lipolytica</i> cells were incubated for 18-20 h at 28 °C in minimal YNB medium with the addition of 0- 5 % mg mL ⁻¹ of peptone, or 0-5 mg mL ⁻¹ of each amino acid (Szabo and Stofanikova 2002)	33
Figure II-1: Experimental setup of the continuous bioreactor (Sunya 2012)	47
Figure II-2: Schematic representation of a typical flow cytometer setup (Diaz et al. 2010)....	51
Figure II-3: BD Accuri C6 [®] optical configuration	52
Figure II-4: Main steps of a measurement/analysis procedure by the Malvern Morphology [®] G3 instrument	59
Figure II-5: Operating principle of the diffraction light scattering device – Example of result presentation (Nguyen 2014)	61
Figure II-6: Schematic representation of the system considered for gas balances calculations	

.....	68
Figure III-1: Calibration curves of the particle diameter (A) and length (B) over a size range from 1 to 15 μm	84
Figure III-2: Comparison between the theoretical and experimental data (diameter, length) quantified by flow cytometry	85
Figure III-3: Calibration of the morphogranulometer apparatus with the model particles over a size range from 1 to 80 μm	86
Figure III-4: Calibration of the dynamic light scattering device with the model particles over a size range from 1 to 80 μm	87
Figure III-5: Distribution and cumulative distribution functions, in number (E, $F_n(d)$) (A) and in volume (E, $F_v(d)$) (B), measured by the different methods for the particles of 15 μm -diameter. Average values of the mean, 10 th , 50 th (median), and 90 th percentile of the particle diameter, quantified in number (C) and in volume (D) by the three methods for the 15 μm -beads	88
Figure III-6: Morphogranulometric images for the A-(1/15 μm); and B-(4/6 μm) mixed bead subpopulations. Analyses were performed at a magnification of x20 under bright field mode	91
Figure III-7: Number distribution, $E_n(d_{SE}$ or $d_{CE})$ and cumulative number distribution, $F_n(d_{SE}$ or $d_{CE})$ functions for the 1-15 μm (A, B), and 4- 6 μm mixed beads (C, D)	92
Figure III-8: Evolution of the ratio between the volumes of particle determined according to the sphere, elliptic or cylinder models	94
Figure III-9: Comparison between sphere and cylinder models and their impact on cumulative volume distribution functions with two morphologically-distinct yeast populations: (A) ovoid-shaped cells with $AR=0.52$ and (B) filamentous cells with $AR=0.11$ (Raw data: number distribution of d_{CE} , length and width from Morphology G3S)	95
Figure III-10: Microscopic observations of the initial cell populations at pH 4.5; 5.6 and 7. Images were taken under a light microscope, without oil fixation and at magnifications of 40 \times . The image size (width x height) is 54 μm x 44 μm	103
Figure III-11: Graphical illustration of the log-normality of the size distribution for the initial cell populations: comparing number distribution function of the equivalent circle diameter (d_{CE}) between the three pH conditions	104
Figure III-12: Morphology of <i>Y. lipolytica</i> at the end of the culture under pH 4.5; 5.6 and 7. Observations were performed with a light microscope, without oil fixation and at magnifications of 40 \times . Image size (width x height): 54 μm x 44 μm	105

Figure III-13: Evolutions of the cumulative number distribution functions of the equivalent circle diameter, $F_n(d_{CE})$ during the cultures at pH 4.5, 5.6 and 7	106
Figure III-14: Evolution of the cumulative distribution function in volume of the equivalent circle diameter, $F_v(d_{CE})$ during the time course of fermentation at the different pH considering the sphere and cylinder models	109
Figure III-15: Cumulative number distribution of the fiber length, $E_n(l_f)$ during the cultures at different pH	111
Figure III-16: Cumulative volume distribution of the fiber length, $E_v(l_f)$ during the cultures at different pH	113
Figure III-17: Evolution of the mean values for the fiber length, in volume, for the three pH conditions. Average values are expressed with their associated standard deviation	114
Figure III-18: Dynamic evolutions of biomass (A) and glucose (B) concentrations, biomass production (C), glucose uptake (D), oxygen consumption and carbon dioxide production (E) specific rates, and respiratory quotient (F) during batch cultures at different pH values: Black, red, blue and green lines correspond respectively to the cultures at pH 4.5; 5.6; 7 and with a pulse perturbation at pH 7. In Figures (A-B), the symbols indicate measured values; the lines correspond to smoothed data. Dash lines in Figure (E) represent the specific oxygen uptake rates. The arrow in Figure (A) indicates the moment of pH pulse application	135
Figure III-19: A. Images taken during growth of <i>Yarrowia lipolytica</i> W29 under batch culture mode at various pH conditions (i, pH 4.5; ii, pH 5.6; iii, pH 7 and iv, pH pulse from 5.6 to 7) for biomass concentration of 0.3; 1 and 5 gCDW L ⁻¹ . The morphology was observed under a light microscope, without oil fixation and at magnifications of 40 x. Image size is 54 μm in width and 44 μm in height. B. Quantification of the mycelial transition of <i>Yarrowia lipolytica</i> W29 by morphogranulometric measurements. Evolutions of the filamentous subpopulation, in number and in volume, were followed during the time course of fermentation	138
Figure III-20: Multiparameter dot plots of <i>Y. lipolytica</i> W29 representing cFDA (FL1) versus PI fluorescence (FL3) and cFDA (FL1) versus Sytox (FL4) fluorescence for the cFDA/PI and cFDA/Sytox double-stained cells respectively. Samples were taken at the end of each batch culture (A, pH 4.5; B, pH 5.6; C, pH 7 and D, pH pulse from 5.6 to 7). Two main subpopulations of untreated (culture sample/ red color) and dead (control sample/ blue color) cells can be readily differentiated through overlapping their respective plots. The quadrants of the dot plots were set on the double-stained dead cells that appeared in the lower left quadrant. Q1 and Q2 quadrants represent viable subpopulation in the cFDA/Sytox and cFDA/PI double-stained culture samples respectively. Q3 quadrant represents dead subpopulation. Q4 quadrant (represents injured damaged) cells. The indicated percentages in the four quadrants correspond to the untreated sample (culture sample / red color)	140
Figure III-21: Morphology of <i>Y. lipolytica</i> W29 during the steady state (SS, pH 5.6), pulses (P, pH 7) and Heaviside (HS, pH 7) stress phases of the continuous culture at a dilution rate of	

0.10 h⁻¹. Images were taken through a light microscope, with oil fixation, under phase contrast mode, and at magnifications of 40 x. Image size is 54 μm in width and 44 μm in height143

Figure III-22: A. Box plots comparing the evolution of cell length distribution during the batch culture at pH 5.6, the phase I (steady state at pH 5.6) and the phase II (pluses at pH 7) of the continuous experiments performed at dilution rates of 0.03, 0.07, 0.10 and 0.20 h⁻¹. B. Box plots comparing the dynamics of cell length distribution between the batch culture at pH 7 and the phase III (Heaviside at pH 7) of the chemostat experiments carried out at dilution rates from 0.03 to 0.20 h⁻¹. The boundary of the box closest to zero indicates the 25th percentile, a black line within the box marks the median, a red line within the box marks the mean and the boundary of the box farthest from zero indicates the 75th percentile. Whiskers above and below the box indicate the 90th and 10th percentiles. The black dot indicates the 95th and 5th percentiles145

Figure III-23: Dynamic evolutions of biomass concentration, oxygen uptake and carbon dioxide production rates of *Y. lipolytica* W29 in response to controlled fluctuations in dissolved oxygen (DO) levels under batch cultivation mode. (A, B) Measured values from the continuous anoxic perturbations of 1 h. (C, D) Measured values from the discontinuous (switch between air and nitrogen gas every 20 min) anoxic perturbations of 1 h. In Figures (A, C), open symbols represent changes in DO levels, and filled symbols correspond to biomass concentrations. In Figures (B, D), red and blue lines correspond to oxygen consumption and carbon dioxide production rates, respectively. The vertical dashed lines (grey) delimit the stress phases166

Figure III-24: A. Light micrographs showing morphological changes of *Yarrowia lipolytica* W29 in response to fluctuations in dissolved oxygen (DO) concentration during the batch cultures. The morphology was compared before and after exposure to (i) three and (ii) nine successive anoxic perturbations of 60 and 20 min, respectively. As growth processed, observations were performed using a light microscope, without oil fixation, and at magnifications of 40 x. Image size is 54 μm in width and 44 μm in height. B. Dynamic evolution of the filamentous subpopulation, in number and in volume, during the DO oscillating batch cultures of *Y. lipolytica*. Data were quantified by morphogranulometric measurements based on the cylinder model (for calculation details, see the Electronic supplementary material (Timoumi et al. 2017))167

Figure III-25: Flow cytometry multiparameter dot plots representing cFDA (FL1) versus PI fluorescence (FL3) and cFDA (FL1) versus Sytox (FL4) fluorescence of the cFDA/PI and cFDA/Sytox double-stained *Y. lipolytica* cells, respectively. Data is presented for biomass samples taken at the end of each batch run (A, three DO perturbations of 60 min; B, nine DO perturbations of 20 min). Untreated (culture sample/ red color) and dead (control sample/ blue color) cells can be clearly discriminated by overlapping their respective plots. The quadrants were set so that the double-stained dead cells appeared in the lower left quadrant. Percentages of cells indicated in each quadrant correspond to the culture sample (red color). Q1 and Q2 quadrants represent viable subpopulations in the cFDA/Sytox and cFDA/PI double-stained cells, respectively. Q3 quadrant represents the dead subpopulation. Q4 quadrant represents

injured (damaged) cells168

Figure III-26: A. Effect of dissolved oxygen (DO) fluctuations on *Y. lipolytica* morphology in glucose-limited chemostat cultures at a dilution rate of 0.10 h^{-1} . Microscopic observations comparing (i) unstressed (steady state phase), and stressed cells exposed to consecutive DO fluctuations of (ii) 60, (iii) 20 and (iv) 5 min. Images were taken at magnifications of 40 x under oil immersion using phase contrast mode. The image size (width x height) is $54 \mu\text{m} \times 44 \mu\text{m}$. B. Box plots comparing the time-evolution of length distribution measurements for cells under steady state and oxygen perturbed environments (data quantified by flow cytometry). The boundary of the box closest to zero indicates the 25th percentile, a black line within the box marks the median, a red line within the box marks the mean and the boundary of the box farthest from zero indicates the 75th percentile. Whiskers above and below the box indicate the 90th and 10th percentiles. The black dot indicates the 95th and 5th percentiles.....173

Figure III-27: A. Light micrographs illustrating the morphological changes of *Y. lipolytica* following the transition from low ($p\text{O}_2 \approx 2 \%$) to limited DO conditions ($p\text{O}_2 = 0 \%$, 75 % of cell needs). The morphology was examined under phase contrast mode using an oil immersion objective at a magnification of 40 x. Image dimension (width x height): $54 \mu\text{m} \times 44 \mu\text{m}$. B. Dynamics of cell length distribution of *Y. lipolytica* subpopulations in the continuous cultures at high (steady state phase), low ($p\text{O}_2 2 \%$) and limited ($p\text{O}_2 0 \%$) oxygen supply. Cell length measurements were performed by flow cytometry C. Evolution of the filamentous subpopulation (in volume) and the residual glucose concentration during the oxygen-limited phase of the chemostat culture174

LIST OF TABLES

Table I-1: Effectors inducing dimorphism in <i>Yarrowia lipolytica</i>	20
Table I-2: Effect of pH on the dimorphic transition of <i>Yarrowia lipolytica</i> strain W29, cultivated in liquid Yeast Nitrogen Base (YNB) medium containing 1 % glucose, 0.5 % (NH ₄) ₂ SO ₄ and 50 mM phosphate or citrate buffer. Cultures were incubated with shaking at 28 °C for 10-20 h (Ruiz-Herrera and Sentandreu 2002)	21
Table I-3: Effect of pH on mycelium formation by <i>Yarrowia lipolytica</i> W29 (Gonzalez-Lopez et al. 2006)	22
Table I-4: Effect of pH and calf serum on mycelium formation by <i>Yarrowia lipolytica</i> SY21 (Gonzalez-Lopez et al. 2006)	22
Table I-5: Effects of carbon source and pH on the morphology of <i>Yarrowia lipolytica</i> NCIM 3589 (Zinjarde et al. 2008)	23
Table I-6: Relative increase of cells in hyphae form (H) obtained in the central composite design CCRD 2 ² for hyphae formation by the dimorphic yeast <i>Y. lipolytica</i> (Nunes et al. 2013)	29
Table I-7: Effect of nitrogen source on mycelial growth: cells of <i>Yarrowia lipolytica</i> W29 were incubated at 28 °C in YNB medium containing 1 % glucose and 50 mM phosphate buffer (pH 7) plus 0.5 % of the indicated nitrogen sources (– No growth) (Ruiz-Herrera and Sentandreu 2002)	32
Table I-8: Potential methods for the characterization of morphology and size distribution	35
Table II-1: Composition of the YPD and PCA rich media.....	43
Table II-2: Composition of the minimum medium	44
Table II-3: Characteristics of the six polystyrene microsphere samples	48
Table II-4: Characteristics of the fluorescent probes used for the determination of yeast cell viability.....	53
Table II-5: Definitions of number, dimension, surface and volume based distributions (Nguyen 2014)	55
Table II-6: Criteria to evaluate the normality of a distribution	57
Table II-7: Standard operating procedure for morphogranulometry measurements.....	60

Table II-8: Retention times of the compounds quantified by HPLC.....	63
Table II-9: KOH gradient program for organic acid quantification by ionic chromatography (linear profile between the points).....	64
Table II-10: Retention times of the organic acids quantified by HPIC.....	65
Table II-11: Potential waveform for the detection of glucose	66
Table III-1: Technical specifications of the particle size characterization techniques	81
Table III-2: Experimental protocol for the qualitative validation of the methods (the cross mark indicates the technique used)	82
Table III-3: Experimental protocol for the quantitative validation of the methods based on subpopulation mixtures (the cross mark indicates the method employed)	82
Table III-4: Error calculation associated with the use of the power-law calibration to convert FSCA and width signals into diameter and length of particles	84
Table III-5: Comparison of the particle diameter determined by flow cytometry (based on power-law calibration), morphogranulometry (direct measurement) and diffraction light scattering (using sphere model approximation) measurements on the basis of number (D[1,0]) and volume (D[4,3]) size distribution: average equivalent diameters are expressed with their associated standard deviation	90
Table III-6: Comparison of subpopulation proportions between flow cytometry and morphogranulometry	93
Table III-7: Projected surface and volume formula for the sphere, ellipse and cylinder forms	93
Table III-8: Morphological characteristics of the initial populations: Mean values of the equivalent circle diameter (d_{CE}), aspect ratio (AR), fiber length (L_f) and fiber width (W_f) are expressed with their associated standard deviations	103
Table III-9: Determination of mean, standard deviation and normality criteria for the initial cell populations	104
Table III-10: Qualitative and quantitative investigation of the mycelial behavior of <i>Y. lipolytica</i> considering number-based distribution of the equivalent diameter (d_{CE})	107
Table III-11: Qualitative and quantitative assessment of the filamentous behavior of <i>Y. lipolytica</i> based on the sphere and cylinder models: comparison between cultures at pH 4.5; 5.6 and 7	109
Table III-12: Qualitative and quantitative characterization of the mycelial growth in <i>Y.</i>	

<i>lipolytica</i> based on number distribution of the cell length	112
Table III-13: Qualitative and quantitative analysis of mycelial growth intensity based on volume distribution of the cell length	114
Table III-14: Comparison of kinetic parameters of the continuous cultures: Average values of specific rates, yields, respiratory quotients, carbon and redox recoveries were expressed with their associated standard deviations	142
Table III-15: Effect of different conditions of oxygen availability on the kinetic growth parameters of <i>Y. lipolytica</i> in glucose-limited chemostat cultures: values of specific rates, yields, respiratory quotients, carbon and redox recoveries were expressed as mean± <i>standard deviation</i>	171
Table III-16: Average percentage of viable cells during the chemostat experiments	175

LIST OF ABBREVIATIONS

μ	Specific biomass growth rate
AR	Aspect ratio
CYT	Flow cytometry
d	Diameter
D[1,0]	Mean number diameter
D[4,3]	Mean volume diameter
d _{CE}	Equivalent circular diameter
DLS	Dynamic light scattering
DO	Dissolved oxygen
d _{SE}	Equivalent spherical diameter
d _{St}	Stokes diameter
En	Number distribution function
Ev	Volume distribution function
FBRM	Focused beam reflectance measurement
F _n	Cumulative number distribution function
FSC	Forward Scattered Light
F _v	Cumulative volume distribution function
L	Length
l _c	Chord length
MAD	Mean absolute deviation
MG	Morphogranulometry
P	Product
P	Pressure
P-exo	Exocellular products
P-intra	Intracellular products
Pop.	Population
Pr	Prandtl number
qCO ₂	Specific carbon dioxide production rate
qO ₂	Specific oxygen consumption rate
qS	Specific substrate consumption rate
rCO ₂	Carbon dioxide production rate
rO ₂	Oxygen consumption rate
RQ	Respiratory quotient
rS	Substrate consumption rate
rX	Biomass production rate
S	Substrate
STDV	Standard Deviation
t _c	Circulation time
t _m	Mixing time
TSL	Turbiscan™ LAB Stability Analyzer
U	Velocity
W	Width
X	Biomass

Introduction and context of the study

INTRODUCTION AND CONTEXT OF THE STUDY

The current worldwide consumption of jet fuel by the aviation industry is about 200 million tons per year, representing approximately 5 % of world oil demand [1]. Fuel consumption is increasing by 1 to 2 % every year and would even reach 3 % at the 2050 horizon [2]. Moreover, aviation is responsible for 2-3 % of all human-induced carbon dioxide (CO₂) emissions, compared to 13.5 % from transport sector [3, 4]. In order to secure a future energy supply, aeronautic industry has identified the production of sustainable fuels as a promising solution for reducing the environmental impact of its activity as well as its energy costs [4]

In this context, numerous researches in the field of bio jet fuels were implemented in order to provide at least 2 million tonnes of biofuels per annum for European aviation by 2020 [5]. Among the fossil fuels alternatives identified, lipid-based biofuels represent an attractive substitute. Lipids can be extracted from oleaginous plants, preferentially from non-food crops such as camelina and jatropha. A series of test flight have been flown successfully using blends of camelina or jatropha biofuel with conventional kerosene. Oleaginous microorganisms such as bacteria, fungi, yeast or microalgae are also able to accumulate oils up to 86 % of its dry weight under some specific cultivation conditions (Babau et al. 2013; Meng et al. 2009; Metting 1996; Ratledge 1982; Xu et al. 2006). Yeasts have been identified as promising producers of lipids, mostly triacylglycerols (Ratledge 1982). *Yarrowia lipolytica* is recognized as a non-conventional yeast whose intracellular lipid accumulation level can reach 50 % of cell dry weight (Papanikolaou et al. 2003). Specifically, accumulated lipids contain high proportion of linoleic acid (C18:2) (Ratledge and Wynn 2002).

Within the different phases of a new bioprocess development, the scale-up from laboratory to larger scale is still a critical issue due to the occurrence of local gradients in fundamental process parameters, such as temperature, pH, dissolved oxygen, substrate and metabolite concentration (Collignon et al. 2010; Enfors et al. 2001; Hewitt and Nienow 2007; Lara et al. 2006; Takors 2012). These micro-environmental fluctuations may represent various stress conditions affecting microorganism metabolism and physiology (Amanullah et al. 2001; Bylund et al. 1998; Carlquist et al. 2012; Delvigne et al. 2009; Enfors et al. 2001; Lara et al. 2006; Lejeune et al. 2013; Olmos et al. 2013). Nature, intensity, duration and/or frequency of the stress encountered would be responsible for different cellular behaviors leading thereby to the generation of phenotypic variabilities at the population level (Han et al. 2013; Jazini et al. 2014; Sunya et al. 2012). This is expected to cause performance variabilities in terms of yield,

titer and/or productivity in industrial bioreactors comparing to small-scale bioreactors (Delvigne and Goffin 2014; Enfors et al. 2001; Lara et al. 2006). Therefore, identification and quantification of the impacts of these fluctuations on microbial dynamics is necessary to achieve optimal performances at the industrial level.

Research studies presented in this manuscript focus on the characterization and quantification of the microbial dynamics in response to controlled perturbations in bioreactor using *Y. lipolytica*, a microorganism with a promising biotechnological potential, as a model system. Acquisition of new insights on the physiology of *Y. lipolytica* is necessary for an efficient control and monitoring of fermentation processes at the industrial scale, where environmental fluctuations are frequently encountered. The Lipid production process involves three main phases: (I) growth phase, (II) transition phase, and (III) nutrient (usually nitrogen) limitation phase. During the growth phase (I), biomass was produced under controlled glucose feeding strategy (fed-batch mode) without any other nutrient limitation. The transition phase (II) was initiated when a nutrient limitation occurs in the presence of excess carbon. During this phase, the nitrogen concentration decreased until the stabilization of the carbon/nitrogen (C/N) ratio. The lipid accumulation phase (III) began when the C/N ratio reached a critical level (Cescut 2009; Ochoa-Estopier 2012). In this work, stress responses were particularly examined during the biomass production phase and not during the lipid production phase. The aim was to ensure a better monitoring of the biomass propagation phase (growth kinetics, metabolism and morphology) in order to promote consequent enhancement of the yeast productivity.

The experimental strategy consists firstly in developing a literature review of previous researches focusing on heterogeneities in bioreactors and their impact on *Y. lipolytica* metabolism and morphology. The objective was to identify the nature, origin and amplitude of these fluctuations, the potential inducers of stress responses in the yeast, as well as the experimental tools and methodologies used for analyzing the resulting responses. Considering their inevitable appearance in large scale bioreactors and notably their significant impact on the morphology of *Y. lipolytica*, controlled fluctuations in pH and dissolved oxygen concentration were examined in the present work. Then, appropriate methodologies were developed and optimized in order to provide pertinent characterization of the dynamics of the microbial responses at the population scale. Bioreactor fermentations were then performed under pH and oxygen perturbed environments using specific cultivation modes (batch and continuous). The implementation of two modes of cultures aimed to investigate the response of cell populations with different physiological states: in continuous bioreactors, all the cells

are in the same physiological state and grow at the same specific rate, while in batch cultures cell subpopulations with different physiological states growing at various specific rates may cohabit at the same time. Finally, a discussion of the results in the context of previous findings was carried out. A synthetic scheme presenting the positioning of this PhD work regarding the lipid production bioprocess, as well as the experimental strategy adopted in this thesis is depicted in Figure 0-1.

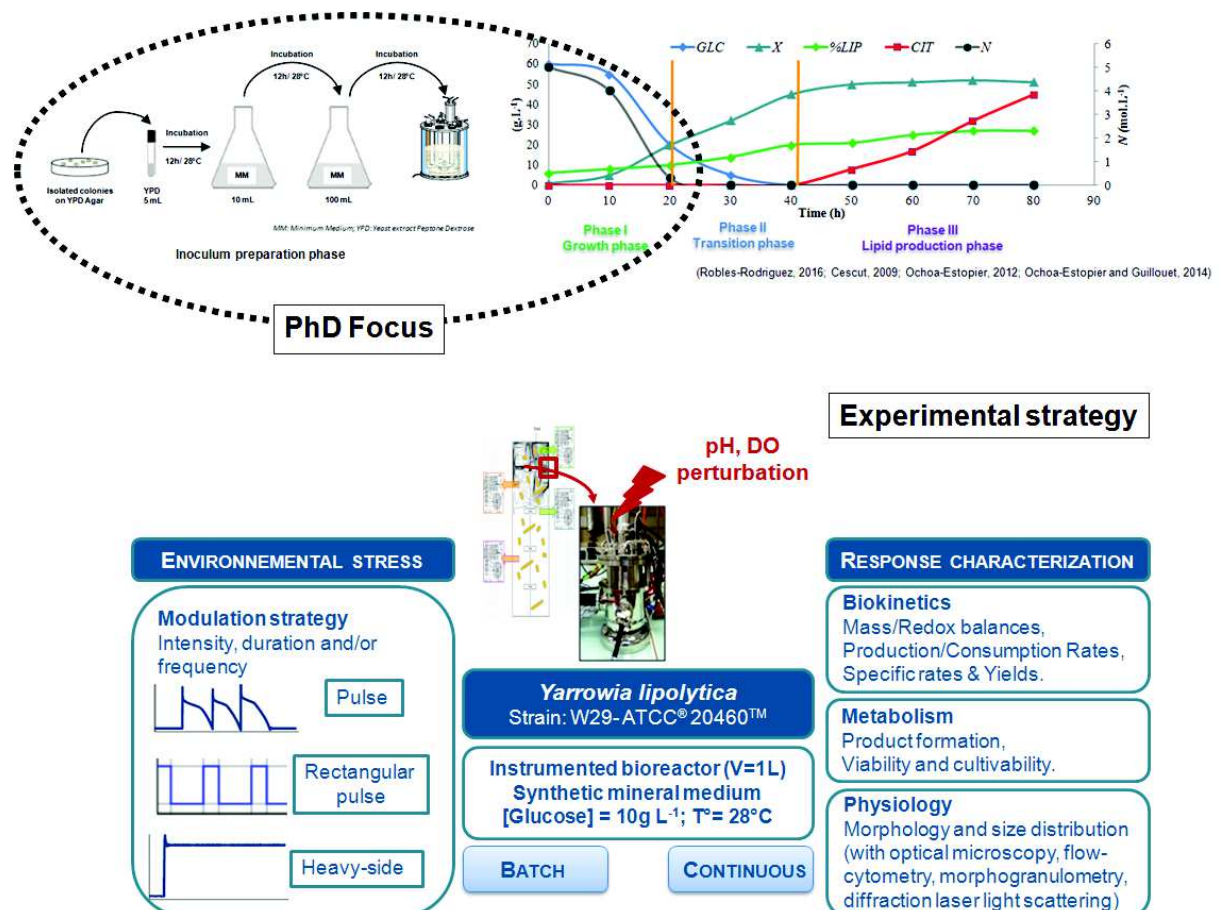


Figure 0-1: The PhD research focus and experimental strategy

The thesis is structured in four parts as follows:

First part of the manuscript concerns literature review, where a general overview of previous studies related to large-scale bioreactor heterogeneities is presented. The physiology of the microorganism of interest “*Y. lipolytica*”, as well as the current state of knowledge regarding its behavior in response to environmental fluctuations is described.

In the second section, a detailed description of material and methods used in the experiments is given

The third part presents and discusses the research findings. The “Results and discussion” section is organized in four chapters:

Chapter 1 is devoted to the development and validation of methodologies for the quantification of morphological changes in *Y. lipolytica*. The approach is based on the characterization of model particles, with known geometric properties, by means of different optical methods (flow cytometry, morphogranulometry, diffraction light scattering). Once validated, these methods are used to characterize morphology and size distribution of biological matrices (*Y. lipolytica* cells) with different shape and forms (spherical/ovoid and filamentous forms) at the cell population level.

Chapter 2 is dedicated to the analysis of morphology and size distribution during the yeast-to-mycelium transition of *Y. lipolytica* by means of morphogranulometric measurements. Considering different morphometric criteria (equivalent diameter, length, width, aspect ratio) and their associated number and volume distributions, dynamics of changes in the yeast morphology were analyzed. Two different geometric models (sphere and cylinder) were compared regarding their accuracy to quantify the filamentous subpopulation.

Chapter 3 presents a study on the impacts of pH perturbations of different types (pulse, Heaviside) on the dynamics of growth, physiology and metabolism of *Y. lipolytica* cultivated in batch and continuous bioreactors. The implementation of two different modes of cultures aims to investigate the response of cell populations with different physiological states: cells growing at their maximum specific rate, and at various controlled specific growth rates in physiological steady-states. This chapter is presented in the form of a research article currently published in “Applied Microbiology and Biotechnology”.

Chapter 4 focuses on the influence of dissolved oxygen fluctuations of different frequencies and durations on the metabolism and morphology of *Y. lipolytica*. Microbial behaviors under low and limited-oxygen conditions were similarly characterized in batch and glucose-limited chemostat bioreactors. The results achieved were discussed and compared with the data from the pH stress study (chapter 3). The findings presented in this chapter were submitted to “Applied Microbiology and Biotechnology” for publication.

Finally, **the last part provides a general discussion** on the previous findings and draws **overall conclusions** as well **perspectives for future work**.

Part I: Literature review

PART I: LITERATURE REVIEW

In industrial bioreactors, microbial cultures are continuously exposed to local gradients in fundamental process parameters. These heterogeneities may have detrimental effects on cellular growth, metabolism and morphology, depending on the microorganism and on the nature, intensity, duration and/or frequency of the fluctuations encountered. In this chapter, the focus was given to:

- ⇒ review the origins of gradients in large scale bioreactors, their different natures as well as their concomitant effects on bioprocess performances.
- ⇒ present the actual scientific knowledge on the physiology of *Yarrowia lipolytica* and its dynamic responses to environmental stress conditions.
- ⇒ describe the regulatory mechanisms underlying adaptation to stress and particularly dimorphic transition in *Y. lipolytica*.

I.1 Bioreactor heterogeneities and bioperformances

During cell cultures in bioreactors, interactions between physico-chemical parameters (microorganism environment) and biological systems (bio-reactivity) affect bioprocess performances. These phenomena were previously described and explained in several handbooks (Asenjo and Merchuk 1994; Kent 2012; Soetaert and Vandamme 2010). The scientific and technological continuum relies on three major contributions: bioreactor design, transfer control and microorganism metabolism. Consequently, bioperformances result from the control and the understanding of both physical and biological responses at global and local scales (Figure I-1).

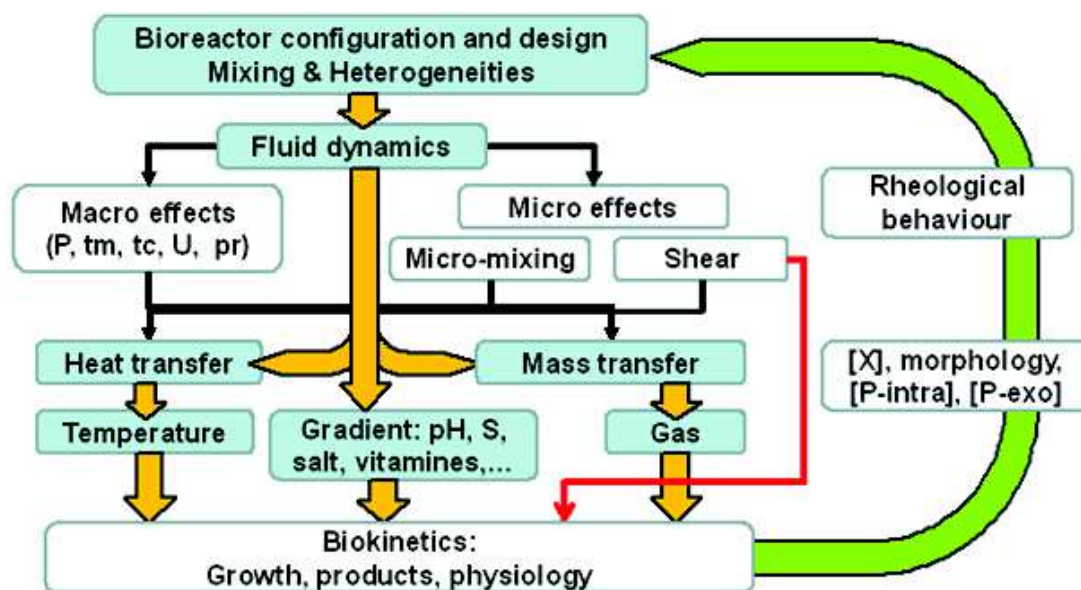


Figure I-1: Schematic illustration of the irreducible couplings between physico-chemical phenomena (control of cellular environment) and biotic responses of microorganisms. Figure adapted from Asenjo and Merchuk (1994)

I.1.1 Origin of heterogeneities inside bioreactor

Bench-scale bioreactors with cultivation volumes typically ranging from 0.2 to 20 L are generally considered as perfectly mixed. Such bioreactors are usually equipped with adequate mixing systems that ensure a good homogeneity of the fermentation broth and therefore high mass and heat transfer capabilities. When scaling up a bioprocess to an industrial production scale, the increase in size of bioreactors is often associated with a poor mixing efficiency, which leads to mass and heat transfer limitations and consequently causing inhomogeneities within large volume cultures (Carlquist et al. 2012; Delvigne and Goffin 2014; Enfors et al. 2001; Hewitt et al. 2007; Lara et al. 2006; Muller et al. 2010; Palomares and Ramirez 2000).

I.1.2 Nature of heterogeneities in industrial bioreactors

Heterogeneities in industrial bioreactors, as absolute values or generated gradients, have been identified and documented in several handbooks (Asenjo and Merchuk 1994; Kent 2012; Soetaert and Vandamme 2010) and scientific papers (Amanullah et al. 2001; Baert et al. 2016; Bylund et al. 1998; Carlquist et al. 2012; Enfors et al. 2001; Fernandes et al. 2012; Kuschel et al. 2017; Langheinrich and Nienow 1999; Lara et al. 2006; Larsson et al. 1996; Manfredini et al. 1983; Nagy et al. 1995; O'Beirne and Hamer 2000; Phue and Shiloach 2005; Schweder et al. 1999; Tsao et al. 1992; Varma and Palsson 1994; Wick et al. 2001; Xu et al. 1999). It affects fundamental culture parameters such as shear rate, dissolved oxygen concentrations, substrate concentrations, pH, temperature and osmotic pressure.

I.1.2.1 Shear rate

Cells are transiently exposed to different shear forces as they circulate throughout the various zones of a bioreactor. Duration and intensity of such forces depend on the impeller type, agitation, aeration rate, and reactor configuration. Several deleterious effects of shear have been observed in cultured cells. Animal and fungal cells are especially the most sensitive to mechanical stress (Chisti 2001; Cruz et al. 1998; Manfredini et al. 1983; Palomares et al. 2006). Plant cells and microbial cultures may also be influenced by the effects of shear (Sahoo et al. 2006; Taticek et al. 1991; Toma et al. 1991).

Shear rates of 1482 s^{-1} have been observed to cause loss in viability in *B. subtilis* cell cultures (Sahoo et al. 2006). It may trigger several physiological responses, which lower biomass and product yield or affect product quality (Lu et al. 1995; McDowell and Papoutsakis 1998;

Senger and Karim 2003). Besides, shearing flow can induce transcription factors (Ranjan et al. 1996) and can influence DNA synthesis rate and the proliferative state of cells (Lakhotia et al. 1992). Nevertheless, in some cases, positive effects of shear have been observed within certain limits. In fact, it has been proved that shear may improve the Microcin B17 (antibiotic) production by *Escherichia coli* ZK650 strain (Gao et al. 2001). Such positive effects may be due to enhancement of heat and mass transfer rates (Asenjo and Merchuk 1994).

I.1.2.2 Dissolved oxygen concentration

The oxygen transfer rate is a critical parameter in bioreactors. Cells passing through the oxygen-limited zones sense and respond to oxygen depletion, leading to the activation of microaerobic or anaerobic metabolism and therefore to the accumulation of by-products.

Experiments carried out by Larsson et al. (1996) demonstrated that oxygen gradients vary with stirrer speed, the time of cultivation and the organism type and process. Oosterhuis and Kossen (1984) identified oxygen gradients ranging from 22 % (with respect to air saturation) in well-mixed zones to 0 % in stagnant regions of a 19 m³ bioreactor. In 1994, Reuss and co-workers (1994) employed computational fluid dynamics (CFD) techniques to simulate oxygen distribution within a 100 L bioreactor. They predicted a 64-fold difference between maximum and minimum oxygen concentrations within the reactor. Similarly, Zahradnik and colleagues (2001) developed a model based on the Networks-of-Zones approach for the description of gas-liquid flow in a 3 m³ triple-impeller stirred bioreactor. The Networks-of-Zones approach is based on a spatial subdivision of the reactor into finite volumes. These computations are more tractable than full computational fluid dynamics (CFD) and provide a realistic picture of the internal behavior of a reactor. Results showed spatial non-uniformities in the gas holdup varying from 2 to 80 % (with a mean value of 17 ± 0.9 %) (Figure I-2A) and local dissolved oxygen concentrations ranging from 3 to 49 % (with a mean value of 35 ± 0.24 %) (Figure I-2B). Under considered operating conditions, this simulation shows the importance of dissolved oxygen variations in different zones of a 3 m³ bioreactor.

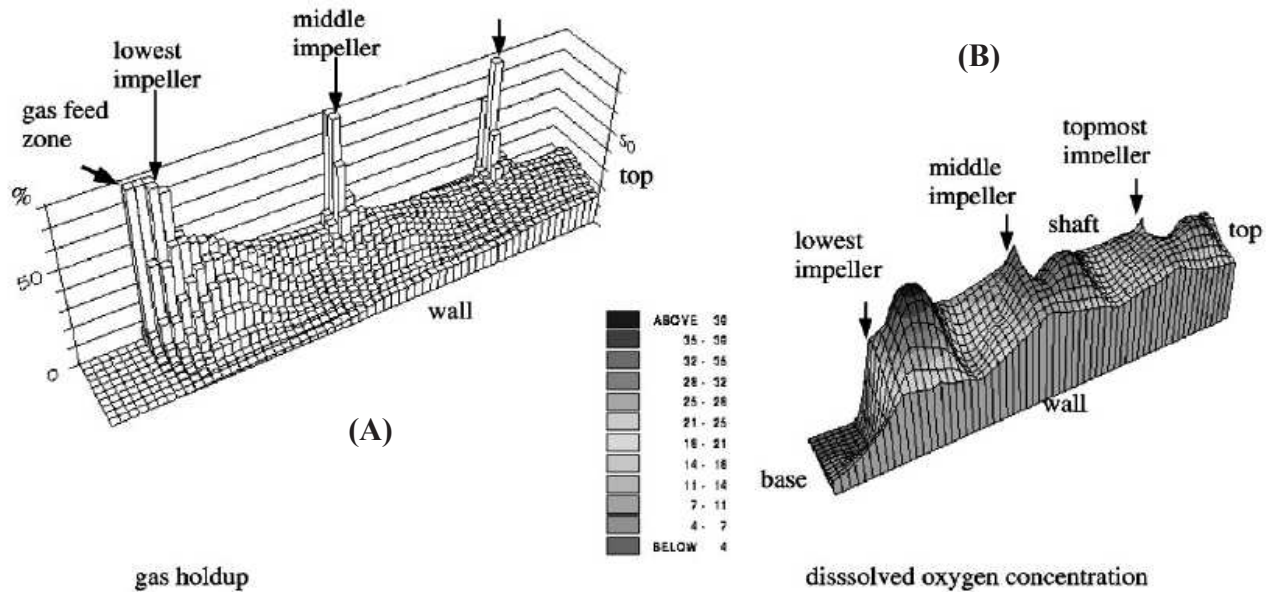


Figure I-2: Predicted gas holdup (A) and local dissolved oxygen concentration (B) in a 3 m³ triple-impeller stirred bioreactor (vessel diameter :1.3 m; liquid height: 2.3 m; impeller speed: 180 rpm; vvm: 1; pressure: 2.5 atm; circulation time: 10 s) (Zahradnik et al. 2001)

Further experiments based on the simulations of gas-liquid flow, using CFD techniques coupled with population balance equations have been run in a 20 L multi-impeller bioreactor (equipped with six-bladed Rushton impellers located at the center of the vessel) (Zhang et al. 2009). Population balance is a well-established method used to analyze the size distribution of the dispersed phase and accounting for breakage and coalescence effects. An inhomogeneous distribution of gas bubble size, gas holdup and turbulent energy dissipation has been predicted throughout the whole bioreactor. These perturbations are thought to be very important in determining the health and viability of microorganisms.

Moreover, experiments using a dual probe technique demonstrated the existence of dissolved oxygen (DO) gradients in a 5000-L bioreactor (Xing et al. 2009). Two DO probes, one placed at the bottom of the bioreactor and the other was located just below the liquid phase on the opposite side, were utilized to measure differences in the DO readings between the top and bottom of 20- and 5000-L bioreactors. Each bioreactor was equipped with three impellers, and a sparger containing holes of 15 μm (20-L bioreactor) and 1.8 mm (5000-L bioreactor) diameters. As shown in Figure I-3A, the top and bottom DO profiles were approximately identical in the 20-L vessel. Nevertheless, DO readings were different between both probe locations in the 5000-L bioreactor (Figure I-3B). Besides, the bottom DO probe responds more rapidly than the top probe that did not respond for over 6 min. These gradients were thought to be attributed to the lower mixing efficiency at the large scale.

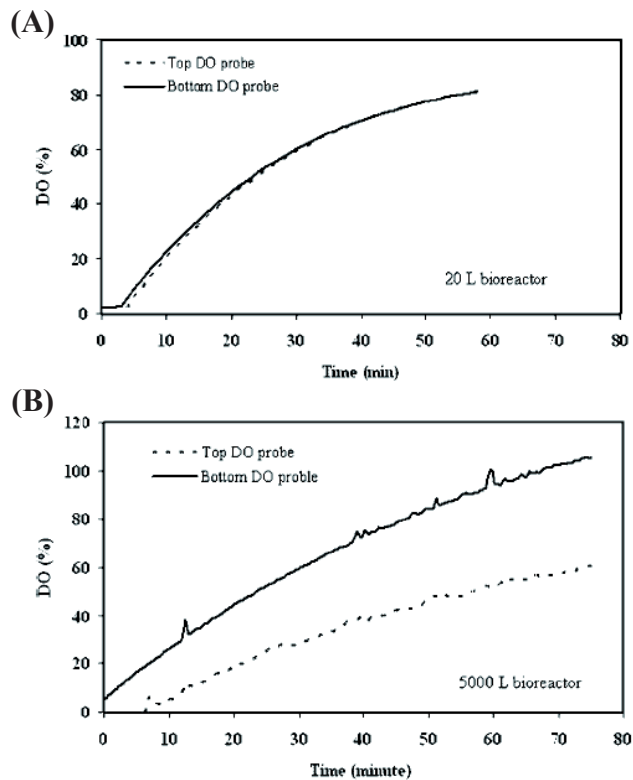


Figure I-3: Comparison of DO readings from the top and bottom probes in a 20-L (A) and 5000-L bioreactor: Equivalent specific power inputs (100 W m^{-3} , air sparging rates (0.0013 vvm) and liquid aspect ratio were used for both 20- and 5000-L bioreactors (Xing et al. 2009)

I.1.2.3 pH

pH is an important parameter that must be carefully measured and controlled during bioprocessing. Spatial pH fluctuations can occur in large-scale reactors near the base or acid addition points as a consequence of a deficient mixing. In addition, accumulation of by-products (e.g. organic acids) can generate low pH zones when cells are exposed to high substrate concentrations (overflow metabolism) or oxygen-limited conditions (micro/anaerobic metabolism). pH fluctuations may affect product quality, culture viability and biological functions (Amanullah et al. 2001; Onyeaka et al. 2003).

Structured models for predicting pH profiles in a 100 L bioreactor have been designed by Reuss et al. (1994). They predicted pH variations from 4.0 in the bulk liquid to 9.0 in the alkali addition zones. Langheinrich and Nienow (1999) found pH gradients of up to 1 unit between the base-feeding zone (liquid surface) and the bulk liquid in an industrial scale 8 m^3 stirred bioreactor fitted with a Rushton turbine. Two pH probes were used to detect pH variations: one situated at the liquid surface (position 1) and the second in the impeller plane (position 3). They also demonstrated that changing the point of alkali addition from the liquid

surface (Figure I-4A) to the well-mixed impeller regions (Figure I-4B) can reduce pH heterogeneities inside bioreactor.

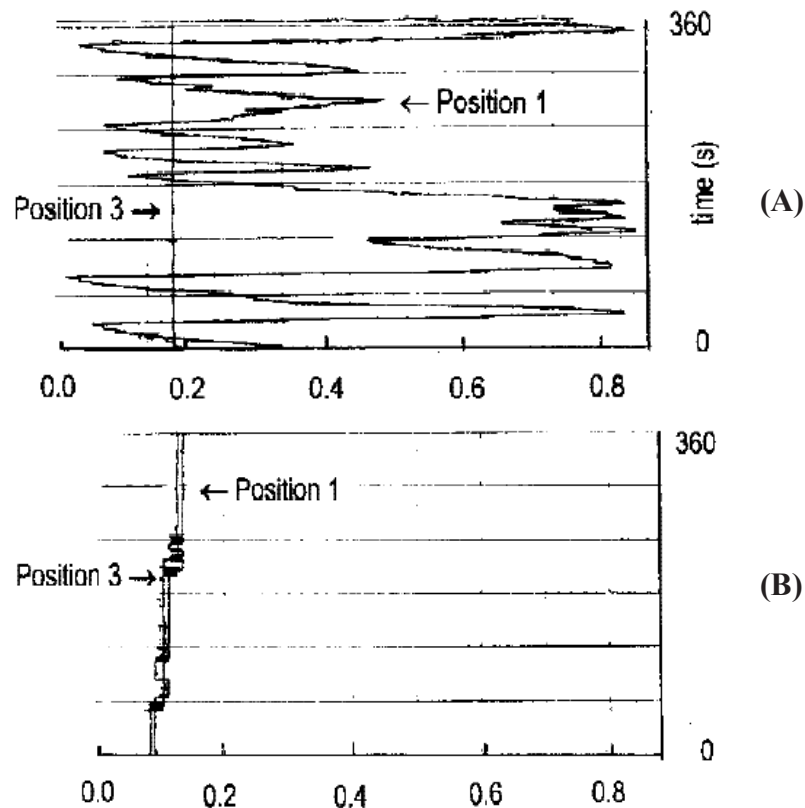


Figure I-4: pH variations after base addition (Na_2CO_3) either at the liquid surface (A) or in the impeller region (B) of a 8 m^3 stirred bioreactor (vessel diameter D : 2m; liquid height: $1.3D$; impeller diameter: $0.225D$; impeller speed: 60 rpm; vvm: 0.005) (Langheinrich and Nienow 1999)

A Similar approach based on dual pH probes measurements was used to investigate the occurrence of pH gradients in a 5000-L bioreactor (Xing et al. 2009). The two pH sensors were placed at distinct position in the vessel: at the bottom of the bioreactor and at the liquid surface (on the opposite side). The obtained results showed differences in the pH probes responses when adding the tracer at the liquid surface. Indeed, the top probe response was characterized by a rapid peak (pH overshoot) followed by a steady state decline until the final pH value, whereas the bottom sensor response showed a steady state increase up to a the same final pH. The pH overshoot in the 5000-L bioreactor was approximately 1.67 units. It was reduced when decreasing the bioreactor volume up to 0.08 and 0.81 units for 5- and 20-L reactors, respectively.

A recent study (Cortes et al. 2016) provided a simulation of the pH gradients during batch cultures of an engineered *Escherichia coli* strain via a two-compartment scale-down system.

The system was composed of two interconnected stirred tank reactors (STR): one representing the conditions of the bulk of the fluid (well-mixed region) (STR1), and the second corresponding to alkali addition zone for pH regulation (STR2). A continuous circulation of cells between the two vessels was ensured by means of an external peristaltic pump. pH values were monitored at various residence times (t_R) of 60, 120, 180 and 240 s. The residence times were simulated by setting a recirculation flow between the vessels. Figure I-5 represents the simulation of pH gradients at each residence time during the time course of fermentation. The pH gradient was present through almost the entire duration of the culture. Values of pH gradients up to 2 units were attained in the alkali addition region at a $t_R = 240$ s. The largest pH gradient observed at a $t_R = 60$ s was around 0.2 units.

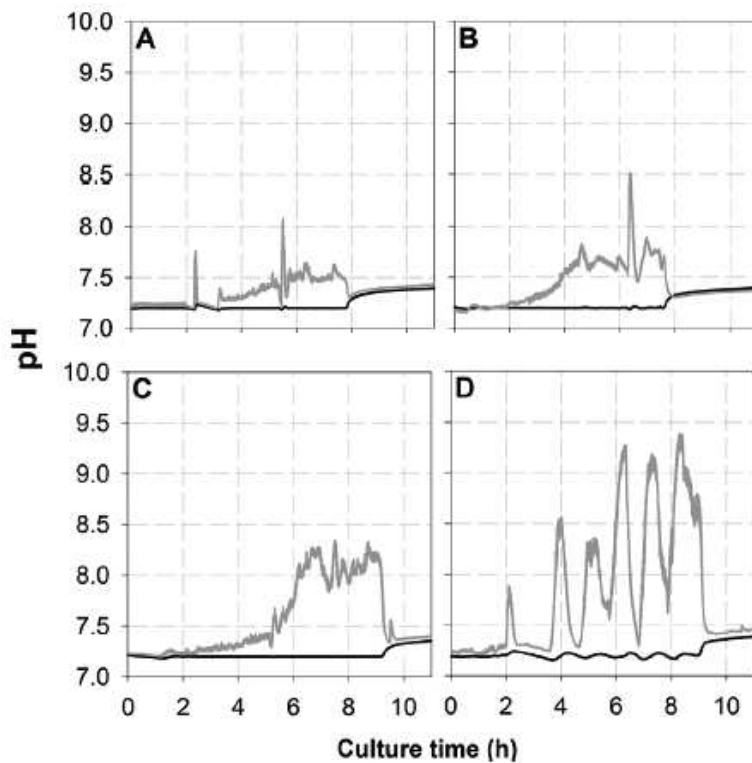


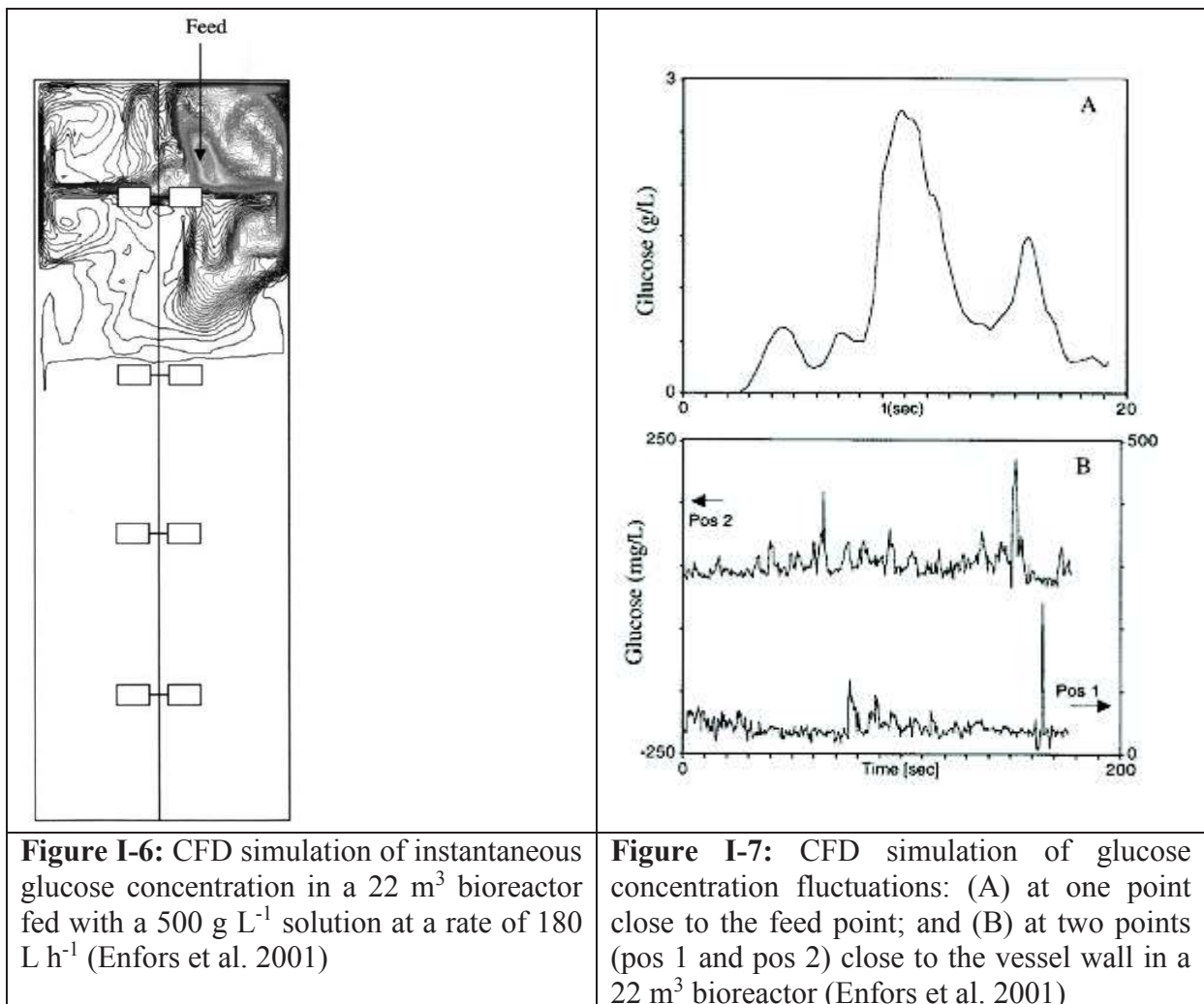
Figure I-5: pH gradients simulated in the scale down-system during engineered *E. coli* cultures at residence times of 60 (A), 120 (B), 180 (C), and 240 s (D). The dark lines correspond to the pH values in the stirred tank reactor simulating the well-mixed region near the impeller (STR1). The gray lines correspond to the pH values in the stirred tank reactor simulating the region of alkali addition (STR2) (Cortes et al. 2016)

I.1.2.4 Substrate concentration

Many industrial bioprocesses usually use fed-batch mode where high concentration of feed substrate is added at one point on the top of bioreactor leading to spatial substrate gradients within the culture broth.

Bylund and co-workers (1998) have predicted an inhomogeneous distribution of glucose concentrations in a 12 m³ fed-batch bioreactor, equipped with three Rushton turbines. The feed solution was highly concentrated (552 g L⁻¹) in order to avoid dilution of bioreactor. The results demonstrated a gradual decrease of glucose concentrations away from the feed point, and concentrations of up to 400-fold the mean value were found at the level closest to the addition zone: concentrations changed from 5 mg L⁻¹ most distant from the feed point up to almost 2000 mg L⁻¹ close to the substrate addition level.

Similarly, Enfors et al. (2001) have predicted by CFD calculations the existence of glucose gradients when a 500 g L⁻¹ glucose solution was added at the top of a 22 m³ fed-batch bioreactor, fitted with four Rushton turbines (Figure I-6). Substrate concentrations varying from around 0 to 3 g L⁻¹ have been expected in the vicinity of the feed point (Figure I-7A). Whereas, glucose fluctuations (almost from 0 to 20 mg L⁻¹ (Pos 2) and from 50 up to 250 mg L⁻¹ (Pos 1)) have been observed in two points of the bulk liquid (distant from the feed point) (Figure I-7B).



I.1.2.5 Temperature

Temperature gradients are not typically expected in large scale bioreactors (Manfredini et al. 1983). This parameter is routinely well controlled and maintained constant during cell culture. However, under some conditions (e.g. inefficient cooling systems, exothermic reactions) cells could be exposed to temperature fluctuations which may represent an environmental stress affecting their viability and activity. Specifically, Tsao et al. (1992) have observed that heat shock (from 37 to 42 °C during 1 h) induces different stress responses in mammalian CHO cell cultures, such as reduction of heterologous protein production, decrease of RNA translation rates, and in extreme cases, cell death. Furthermore, Gorenflo et al. (2007) have predicted the existence of temperature gradients in a 10 L culture of CHO cells. They observed a decrease in growth rate when cells were repeatedly exposed to 1 min excursions from 37 to 27 °C.

I.1.3 Impact on bioprocess performances

Local environmental gradients are typically encountered in many industrial scale fermentation processes. Cultivated microorganisms are then forced to experience sudden environmental changes as they circulate from one zone to the other. These perturbations may pose different types of stress (e.g. oxidative, temperature, pH) on the cells and affect their metabolism and physiology (Amanullah et al. 2001; Bylund et al. 1998; Carlquist et al. 2012; Delvigne et al. 2009; Enfors et al. 2001; Kuschel et al. 2017; Takors 2012). Nature, intensity, duration and/or frequency of these stress conditions would be responsible for different metabolic and physiological cell behaviors within the culture broth. The resulted various types of cell responses are expected to cause performance variability in terms of yield, titer and/or productivity in industrial bioreactors comparing to small-scale bioreactors (Enfors et al. 2001; Lara et al. 2006; Muller et al. 2010). Identification and quantification of the impacts of these heterogeneities on microbial dynamics is therefore necessary to achieve optimal performances at the industrial level.

The microorganism of interest in this research “*Yarrowia lipolytica*” is an ascomycete yeast with biotechnological potential to produce notably specific lipids for bio-jet fuels synthesis (Cescut 2009; Portelli 2011). Under partially controlled conditions (in presence of stress), the fungus is characterized by its ability:

- ✓ to mediate metabolic shifts (e.g. production of organic acids) (Beopoulos et al. 2009), which may affect the conversion yields of substrate into biomass ($Y_{X/S}$) and/or lipids ($Y_{Lip/S}$) causing thereby a decrease in the bioprocess performances.
- ✓ to undergo a dimorphic transition from yeast to the mycelium forms in response to environmental stressors (Barth and Gaillardin 1997; Bellou et al. 2014; Braga et al. 2016; Kim et al. 2000; Palande et al. 2014; Ruiz-Herrera and Sentandreu 2002). The presence of mycelial cells affects significantly the rheological behavior of the broths (Kraiem et al. 2013) and the transfer phenomena in bioreactors (Kar et al. 2011; O'Shea and Walsh 2000) leading consequently to the deterioration of the cell productivity (Fickers et al. 2009; Galvagno et al. 2011).

To ensure a successful scale-up of *Y. lipolytica*-based processes from laboratory to production scale, it is of utmost importance to characterize the dynamics of its responses to perturbations in the growth environment, at both metabolic and morphological levels.

I.2 Physiological responses of *Yarrowia lipolytica* to stress conditions

I.2.1 General description of *Yarrowia lipolytica*

Yarrowia lipolytica (formerly known as *Candida*, *Endomycopsis* or *Saccharomycopsis lipolytica*) is a strictly aerobic yeast, belonging to the family of Hemiascomycetes (Barth and Gaillardin 1996; Barth and Gaillardin 1997). This yeast is usually isolated from dairy products such as cheese, yogurt, and sausages (Barth and Gaillardin 1996), from oily environments such as polluted soils, raw poultry or dairy products (Deak 2001; Lanciotti et al. 2005; Sinigaglia et al. 1994; Yalcin and Ucar 2009), as well as from marine and hypersaline media (Beopoulos et al. 2009).

Y. lipolytica is unable to grow above 32 °C. It is considered non-pathogenic and several processes based on this microorganism were classified as Generally Recognized As Safe (GRAS) by the Food and Drug Administration (FDA, USA) (Barth and Gaillardin 1996; Barth and Gaillardin 1997; Fickers et al. 2005).

Y. lipolytica is an industrially important microorganism capable to metabolize a wide variety of carbon substrates (e.g. glucose, alcohols, acetate and hydrophobic substrates) (Fickers et al. 2005; Finogenova et al. 2002; Papanikolaou et al. 2006), to degrade efficiently several low-value or toxic compounds (e.g. raw glycerol, olive mill wastewater) (Levinson et al. 2007;

Makri et al. 2010; Rymowicz et al. 2006; Sarris et al. 2011), and to produce a broad spectrum of valuable metabolites (e.g. organic acids, lipids, enzymes and proteins) (Bellou et al. 2016; Bussamara et al. 2010; Lopes et al. 2009a; Madzak et al. 2004; Papanikolaou and Aggelis 2009; Papanikolaou et al. 2007; Parfene et al. 2013; Ron and Rosenberg 2002; Sauer et al. 2008). These potentialities have increased interest in the exploitation of *Y. lipolytica* in numerous biotechnological and environmental applications (Coelho et al. 2010; Goncalves et al. 2014; Ledesma-Amaro and Nicaud 2016; Liu et al. 2015; Zinjarde 2014).

In its natural biotope, *Y. lipolytica* has the capacity to grow in the yeast-like or mycelial forms, depending on the environmental conditions and the genetic background of the strain. This property is of practical importance especially when biotechnological applications are designed. Indeed, dimorphism is generally characterized by a presence of many intermediate morphological forms, displaying a broad distribution of cell sizes and shapes. This wide morphology spectrum affects significantly the fermentation performances, since it induces rheological changes and consequently leads to heat and mass transfer alterations in the bioreactor at local and global levels. Hence, monitoring changes in the cell morphology became an important key to enhance and optimize productivity (O'Shea and Walsh 2000).

I.2.2 Morphological changes in *Yarrowia lipolytica*: dimorphism phenomena

The growing scientific interest on *Y. lipolytica* is illustrated by an increasing number of publications (around 85 scientific articles annually) devoted to this yeast. Number of papers focusing on dimorphism, as a specific response of *Y. lipolytica* to adverse environmental conditions (210 publications in total) is quite limited compared to similar studies with other yeasts or fungi (almost 41905 publications). Dimorphic behavior of *Y. lipolytica* represents a topic of interest that requires further research and investigation.

I.2.2.1 Effectors involved in dimorphism

The environmental conditions that induce the yeast-to-mycelium transition in *Yarrowia lipolytica* are extremely variable. They can be classified into three main groups (Table I-1): physico-chemical (pH, temperature and dissolved oxygen concentration), mechanical (pressure and mixing) and nutritional (carbon source, nitrogen source and metal ions).

Most of the studies focused on the physico-chemical (almost 67 % of studies) and nutritional (around 83 % of studies) effectors. However, the mechanical perturbations have rarely been investigated (about 11 % of the studies). In the majority of studies, several effectors were

examined simultaneously and the observed cellular responses were multifactorial in most of the cases.

Table I-1: Effectors inducing dimorphism in *Yarrowia lipolytica*

Effectors		Nature
Physico-chemical		pH Temperature Dissolved oxygen Osmotic pressure
Mechanical		Pressure Mixing (shear rate/stress)
Nutritional	Carbon source	N-acetylglucosamine (GlcNAc) Serum (BSA, calf serum...) Fatty acids and glycerides: olive oil, triolein, oleic acid Glycerides: coconut oil, palm kernel oil
	Nitrogen source	Proteins: bovine mil casein (BSA), soybean fraction, meat extract Ammonium salts ((NH ₄) ₂ SO ₄ ; (NH ₄) ₂ HPO ₄) Organic sources of nitrogen (amino acids, peptone)
	Metal ions	Mg ²⁺ ions Fe ³⁺ ions

I.2.2.1.1 Physico-chemical effectors

I.2.2.1.1.1 pH

pH was identified as the most important factor involved in the dimorphic transition. Most studies have focused on the effect of varying pH levels, typically from pH 3.0 to 7.0, on the yeast morphology. The pH effect was usually dependent on the nature of buffer used (phosphate or citrate buffer), as well as on the presence of another nutritional stimulus (e.g. N-acetylglucosamine (GlcNAc) or serum) (Gonzalez-Lopez et al. 2006; Ruiz-Herrera and Sentandreu 2002; Zinjarde et al. 2008). Results demonstrated that mycelium formation was maximal at pH near neutrality and decreased as pH lowers to become almost null at pH 3. The intensity of filament formation was variable depending on the operating conditions and the strains used.

In the experiments carried by Ruiz-Herrera and Sentandreu (2002), the effect of pH (from 3.0 to 7.0) on the dimorphic transition of *Y. lipolytica* W29 was examined using different buffers. Results (Table I-2, Figure I-8) showed a maximal mycelium formation at neutral pH (87 and 98 % with phosphate and citrate buffer respectively) in contrast to pH 3. Nevertheless, the impact of pH on the dimorphic switch was not only coupled with the chemical composition of the buffer but also with the temperature. Indeed, cells were subjected to thermal shock (at 37-

38 °C for 15 min) immediately preceding their inoculation into a dimorphism inducing medium. This pre-treatment has been shown to make cells more sensitive to stimuli and increases mycelium formation (Guevaraolvera et al. 1993).

Table I-2: Effect of pH on the dimorphic transition of *Yarrowia lipolytica* strain W29, cultivated in liquid Yeast Nitrogen Base (YNB) medium containing 1 % glucose, 0.5 % (NH₄)₂SO₄ and 50 mM phosphate or citrate buffer. Cultures were incubated with shaking at 28 °C for 10-20 h (Ruiz-Herrera and Sentandreu 2002)

Initial pH	Buffer	Final pH	Growth Dry weight (mg ml ⁻¹)	Morphology (%)	
				Yeasts	Mycelium
3.0	Phosphate	2.69	1.08	95	5 ^a
3.0	Citrate	2.87	0.50	80	20 ^a
4.0	Citrate	3.87	1.50	66	34 ^a
5.0	Citrate	5.18	1.30	20	80
6.0	Phosphate	5.63	1.45	32	68
6.0	Citrate	5.80	0.80	10	90
7.0	Phosphate	6.92	1.85	13	87
7.0	Citrate	6.05	0.80	2	98

^a Very short cells

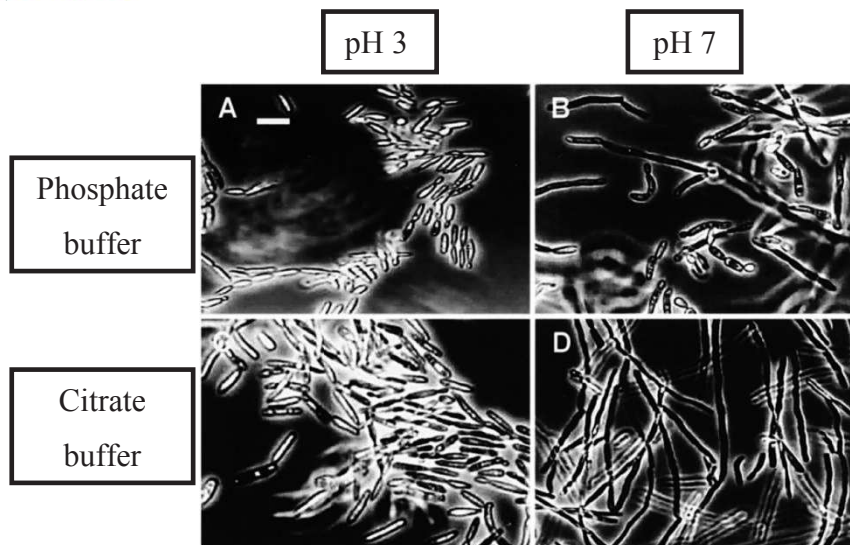


Figure I-8: Morphology of *Yarrowia lipolytica* W29 cells cultivated with shaking at 28 °C in Yeast Nitrogen Base (YNB) medium containing 1 % glucose, 0.5 % (NH₄)₂SO₄ and 50 mM phosphate or citrate buffer. A and C: pH 3 medium with phosphate or citrate buffer. B and D: pH 7 medium with phosphate or citrate buffer (Ruiz-Herrera and Sentandreu 2002)

Other studies carried out by Gonzalez-Lopez et al. (2006) confirmed, using the wild-type strain W29, that the dimorphic transition of the fungus was controlled by the pH of the medium. At pH 3, mycelial growth did not exceed 2 % compared to 50 % or more at pH 7 (Table I-3). The effect of carbon source (GlcNAc) was not significant when citrate buffer was employed to control the pH of the medium (Table I-3).

Table I-3: Effect of pH on mycelium formation by *Yarrowia lipolytica* W29 (Gonzalez-Lopez et al. 2006)

Initial pH	Carbon source	Final pH	OD ₆₀₀	Mycelium (%)
3	Glucose	2.9	5.6	0
7	Glucose	5.9	7.8	50
3	GlcNAC	3.6	6.2	2
7	GlcNAC	6.2	7.3	52

The effect of pH in the presence of serum (a nutritional inducer of dimorphism) was also determined using the strain SY21 (Gonzalez-Lopez et al. 2006). These studies employed a phosphate buffer that was not shown to induce mycelial growth (Ruiz-Herrera and Sentandreu 2002). Results demonstrated that the positive effect of serum was dependent on pH. No mycelial growth occurred at pH 3, whereas at pH 7, 98 % mycelium was formed in media containing 5 % serum (Table I-4).

Overall, the data presented in this study (Gonzalez-Lopez et al. 2006) highlighted that pH is an important effector of dimorphism in *Y. lipolytica*, at least for the strains W29 and SY21 examined.

Table I-4: Effect of pH and calf serum on mycelium formation by *Yarrowia lipolytica* SY21 (Gonzalez-Lopez et al. 2006)

Initial pH	Serum (%)	Final pH	OD ₆₀₀	Mycelium (%)
3.0	0	3.1	1.5	0
3.0	2.5	2.9	2.4	0
3.0	5.0	3.7	3.6	0
7.0	0	5.1	2.6	0
7.0	2.5	4.3	4.7	90
7.0	5.0	5.1	4.4	98

Zinjarde and co-workers (2008) investigated the effect of pH on the yeast morphology for cells grown on different carbon sources (Table I-5). The optimal mycelium formation (95 %) was observed at pH 7.0 when cells were cultivated on coconut oil or palm kernel oil. Meanwhile, under the conditions of an uncontrolled pH (pH drop from 4.0 to 7.0/ unbuffered medium), mycelial growth was not detected.

Table I-5: Effects of carbon source and pH on the morphology of *Yarrowia lipolytica* NCIM 3589 (Zinjarde et al. 2008)

Carbon source	pH	Percentage of mycelia
Glucose, N-acetylglucosamine, n-dodecane	4.0 to 7.0	ND
Peanut oil, olive oil, sesame oil	4.0 to 7.0	40
Coconut oil, palm kernel oil	5.0	60
Coconut oil, palm kernel oil	6.0	90
Coconut oil, palm kernel oil	7.0	95

I.2.2.1.1.2 Temperature

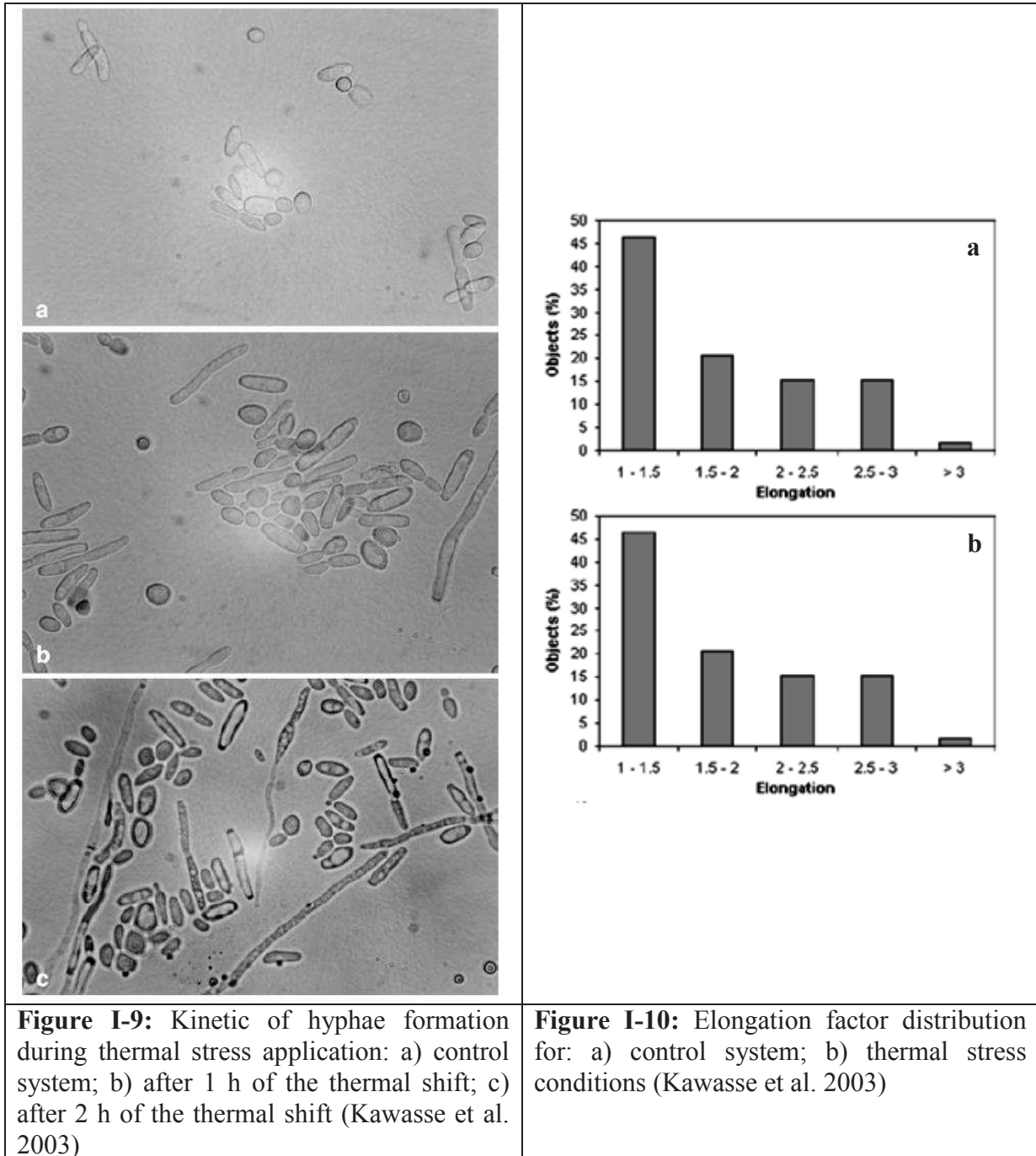
Thermal shock has been identified to induce morphological changes in *Y. lipolytica*. Indeed, experiments carried out by Guevaraolvera et al. (1993) demonstrated that if the cultures were starved at 4 °C for at least 15 min (cold shock) prior to the morphogenetic switch (using GlcNAc as inducer), 90 % of the cells (strain SA-1) germinated and gave rise to long and branched hypha. In addition, further experiments (Ruiz-Herrera and Sentandreu 2002) showed that a heat shock applied at 37- 38 °C for 15 min (hot shock) preceding the inoculation of *Y. lipolytica* makes cells more sensitive to environmental stimuli and increase mycelium formation.

Research studies carried out by Kawasse et al. (2003) analyzed the effect of temperature separately from other stimuli. Thermal stress experiments were performed by applying a temperature shift from 29 to 37 °C during 1 or 2 h during the exponential growth phase. The authors reported a significant increase in the capacity of *Y. lipolytica* to form elongated hyphae (Figure I-9). Quantitative measurements based on image analysis approach (Figure I-10) showed a net increase of around 25 % in the elongation factor defined as the ratio between hyphal length and hyphal width. Hyphal length and hyphal width were determined as the maximum Feret diameter (F_{max}) and minimum Feret diameter (F_{min}) respectively. The Feret diameter is given by the distance between two parallel tangents in any given direction (Kim et al. 2000):

$$\text{Elongation} = \frac{F_{max}}{F_{min}} = \frac{\text{Hyphal length}}{\text{Hyphal width}}$$

Additionally, the morphology of the cells observed in Figure I-9 illustrated the presence of intermediate morphological forms in conjunction with hyphae and unicellular ones during the dimorphic transition. Similar morphological behavior was previously reported for other

dimorphic yeasts, such as the case of *Kluyveromyces marxianus* (O'Shea and Walsh 2000; O'Shea and Walsh 1996).



I.2.2.1.1.3 Dissolved oxygen (DO) concentrations

The amount of oxygen available to the cells may directly impact the morphology of *Y. lipolytica*. The influence of DO concentration on the yeast morphology was generally examined under semi-anoxic environments since the microorganism has a strict aerobic metabolism and unable to grow under strict anaerobic conditions. In most of the previous studies, cultures were performed in sealed bottles (with limited and gradually decreasing

dissolved oxygen levels by varying headspace volume) (Zinjarde et al. 1998) , test tubes (under layer of mineral oil) (Ruiz-Herrera and Sentandreu 2002) or flasks (by addition of 20 mM H₂O₂) (Kawasse et al. 2003; Kim et al. 2000). Generally, oxidative stress has been shown to induce the formation of extremely long hypha.

In the studies of Zinjarde et al. (1998), decreasing the culture head space up to less than 5 % induced an increase in the proportion of mycelia until 60 % in media containing GlcNAc as carbon source. Ruiz-Herrera and Sentandreu (2002) demonstrated that the semi-anoxic conditions provided in liquid or solid media promoted the formation of extremely long hyphae in *Y. lipolytica*.

Further researches carried out by Kim et al. (2000) assayed the effect of the oxidative stress combined with another nutritional stimuli (GlcNAc or serum), on the morphology of the fungus. Results showed that the oxidative stress (by addition of 20 mM H₂O₂) inhibited the dimorphic transition induced by N-acetylglucosamine, but did not suppress the mycelial growth triggered by serum.

Changes in *Y. lipolytica* morphology upon exposure to oxidative stress were examined by digital image analysis processing tools (Kawasse et al. 2003). H₂O₂ addition (concentrations from 0 to 20 mM) at the exponential growth phase led to more than 25 % increase of the elongation factor (F_{\max}/F_{\min}). Additionally, oxidative stress conditions applied induced a significant increase in the characteristic hyphal length (defined as the maximum Feret diameter, F_{\max}) (Figure I-11).

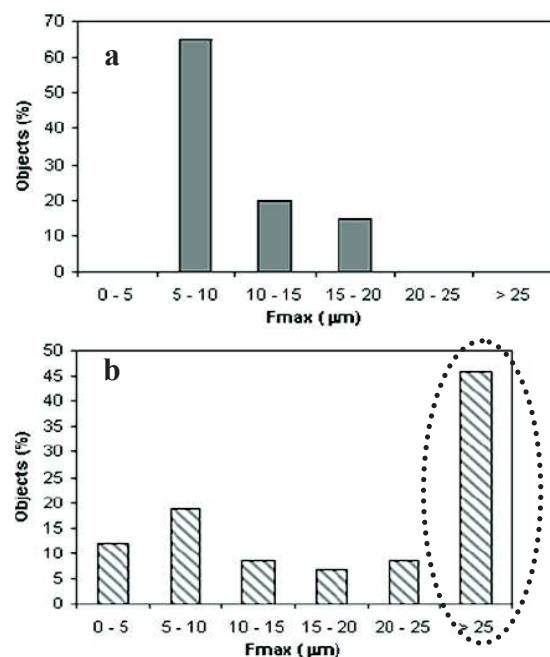


Figure I-11: Total hyphal length determined for: a control system; b oxidative stress conditions (Kawasse et al. 2003)

More recently, experiments carried out by Bellou and co-workers (2014), showed that the DO concentration is the most important inducer of dimorphism in *Y. lipolytica*, compared to the carbon and the nitrogen sources. Indeed, under batch cultivation mode, and at low or zero dissolved oxygen concentrations, filamentous cells predominated ovoid ones (Figure I-12). In addition, when DO levels gradually increased from 0.1 to 1.5 mg L⁻¹, a progressive transition from the mycelium to the yeast form was observed in continuous cultures of *Y. lipolytica* (Figure I-13).

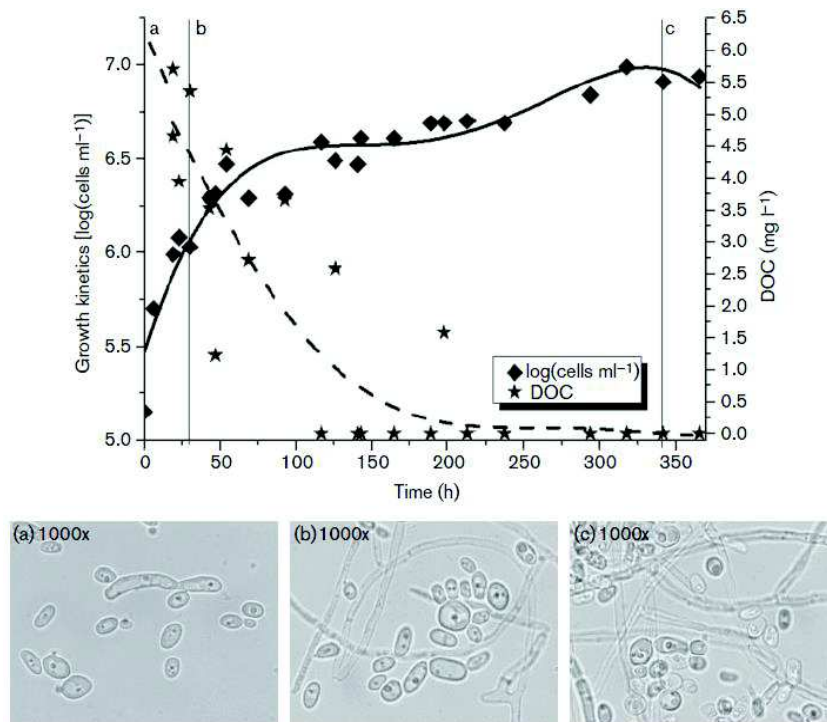


Figure I-12: Growth kinetics of *Y. lipolytica* cultivated in flasks containing olive oil as sole carbon source and changes in dissolved oxygen concentration (DOC). Light micrographs showing the morphology of the yeast as growth proceeded. (a) Single cells; (b) pseudomycelia and single cells; (c) true mycelia and yeast cells (images were taken at magnifications of 1000x) (Bellou et al. 2014)

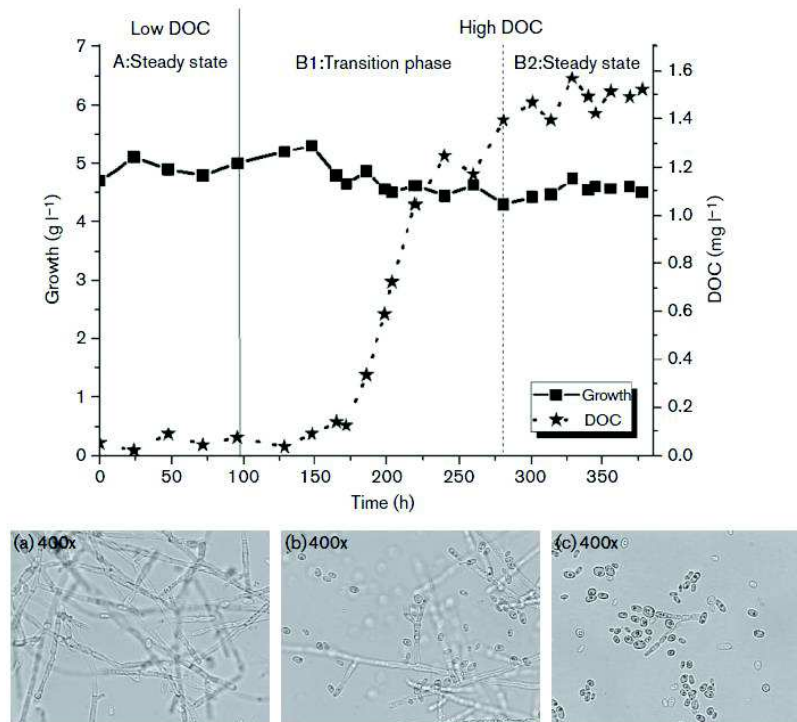


Figure I-13: Growth, DOC and morphology of *Y. lipolytica* during the transition from low to high oxygen concentration at steady state (dilution rate, 0.032 h^{-1}). (a) True mycelia and a few pseudomycelia were predominant; (b) pseudomycelia and a few single cells; (c) single cells and a few pseudomycelia (images were taken at magnifications of 400x) (Bellou et al. 2014)

I.2.2.1.1.4 Osmotic stress (salinity)

There are few studies on the effect of osmotic stress on the morphology of *Y. lipolytica* (Andreishcheva et al. 1999; Kim et al. 2000). The studies carried by Andreishcheva and colleagues (1999) demonstrated that when cells are incubated in the presence of 9 % NaCl, a rapid change in their size and shape was observed. Surprisingly, cells became progressively more ovoid and decreased in size (Figure I-14). This decline in cell size enabled cells to rapidly increase their intracellular concentrations of solutes and therefore to counterbalance the elevated external osmotic pressure in their environment. Other experiments performed by Kim et al. (2000) studied the effect of osmotic stress but coupled with a nutritional inducer (carbon source: GlcNAc or serum). Experimental data demonstrated that applying an osmotic stress (by addition of 0.2 M NaCl) inhibited mycelium formation induced by GlcNAc, and had no significant effect on the hypha formation triggered by serum.

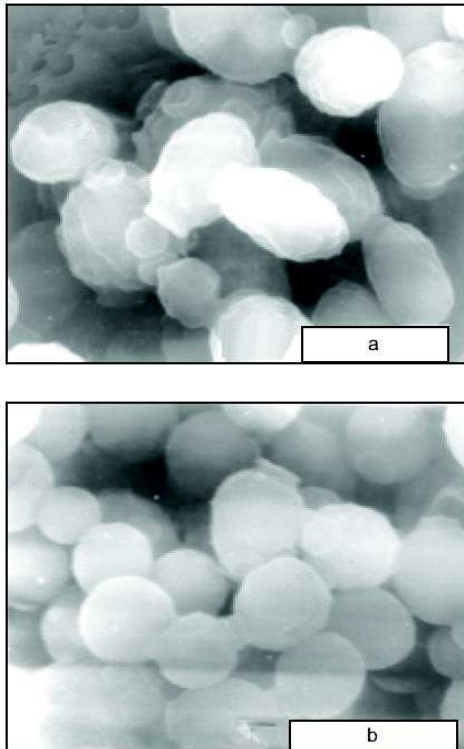


Figure I-14: Scanning electron micrographs of *Yarrowia lipolytica* cells: a) control; b) in the presence of 9 % NaCl. 5000× magnification (Andreishcheva et al. 1999)

I.2.2.1.2 Mechanical effectors

Only a few studies have examined the impact of mechanical stressors, such as mixing or pressure on the morphological behavior of *Y. lipolytica*.

I.2.2.1.2.1 Mixing

A recent research study (Nunes et al. 2013) showed that agitation rate during culture of *Y. lipolytica* impacted the intensity of hyphal growth. The effect of modulating mixing levels (from 60 to 160 rpm) on the microorganism morphology was assessed in the presence of serum (a potential inducer of mycelial growth) using a central composite rotatable design CCRD 2². Hyphae formation was inhibited at the high agitation rate even in the presence of 6 % of serum known as strong inducer of dimorphism (Table I-6). The relative increase of the cells with the hyphal morphotype was around 0.86 % at the higher mixing level (160 rpm) compared to 5.81 % at 60 rpm. High agitation rate seemed to alleviate the formation of filamented cells.

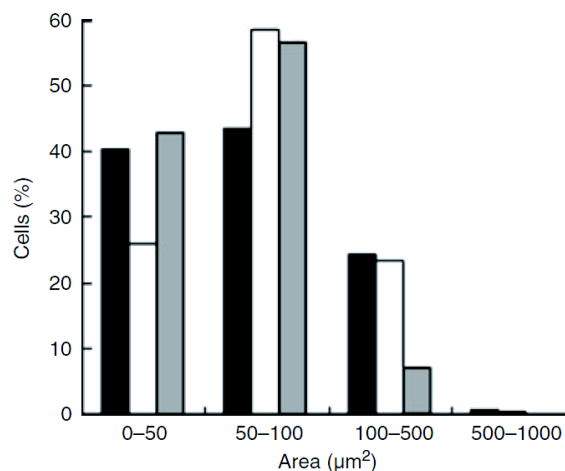
Table I-6: Relative increase of cells in hyphae form (H) obtained in the central composite design CCRD 2² for hyphae formation by the dimorphic yeast *Y. lipolytica* (Nunes et al. 2013)

Assay	Agitation		Bovine calf serum		<i>H</i> ^a
	Code	Value (rpm)	Code	Value (%)	
1	-1	74.5	-1	1.74	5.13
2	+1	145.5	-1	1.74	0.03
3	-1	74.5	+1	10.26	4.13
4	+1	145.5	+1	10.26	1.17
5	0	110.0	0	6.00	0.70
6	0	110.0	0	6.00	0.65
7	-1.41	60.0	0	6.00	5.81
8	+1.41	160.0	0	6.00	0.86
9	0	110.0	-1.41	0	0.89
10	0	110.0	+1.41	12.00	1.40

^a Relative increase of cells in hyphae form (*H*), $H = \frac{H_{15h} - H_{0h}}{H_{0h}}$

I.2.2.1.2.2 Pressure

Batch cultures of *Y. lipolytica* were conducted in a pressurized bioreactor at 4 and 8 bar of air pressure and the cell morphology was compared with cultures at atmospheric pressure (Lopes 2013; Lopes et al. 2008). Cells displayed a typical oval form in all the assays with elongation factors below 2.0 for the majority of cells (more than 85 % of cells). Figure I-15 compares the size distribution of yeast cells exposed to hyperbaric pressures and those grown at atmospheric pressure. A decrease in the percentage of cells with a projected area higher than 100 μm² was obtained at 8 bar (7 %) compared to 25 % of cells with similar size at 4 bar at and at atmospheric pressure. Air pressure rise did not inflict oxidative stress to the cells since their morphology was slightly altered.

**Figure I-15:** Cell size distribution for *Yarrowia lipolytica* W29 cells at: atmospheric pressure (black bar), 4 bar (white bar) and 8 bar (grey bar) (Lopes et al. 2008)

I.2.2.1.3 Nutritional effectors

Studies on various *Y. lipolytica* strains showed that nutritional factors may influence significantly the cell morphology. The nutritional factors identified include the carbon and nitrogen sources, and metal ions.

I.2.2.1.3.1 Carbon source

Carbon sources namely N-acetylglucosamine (GlcNAc), serum and hydrophobic substrates (such as fatty acids and oils) were among the major parameters affecting *Y. lipolytica* dimorphism.

The impact of GlcNAc on the dimorphic transition of the yeast was widely studied in literature. It was reported that mycelial growth was induced in the presence of GlcNAc at concentrations of 0.5 to 1 %. Significant amounts of mycelia (higher than 90 %) were obtained after short incubation periods (5- 16 h).

In minimal medium containing N-acetylglucosamine as sole carbon source instead of glucose, mycelium formation was maximal within 12 to 15 h of incubation (Rodriguez and Dominguez 1984). Percentages of filamentous cells were between 60 to 90 % depending on the strain.

Experiments conducted by Guevaraolvera and co-workers (1993) revealed the development of almost 90 % of long and unbranched hyphae (strain SA-1) in GlcNAc inducing medium after exposure to thermal shock at (4 °C) (Figure I-16).

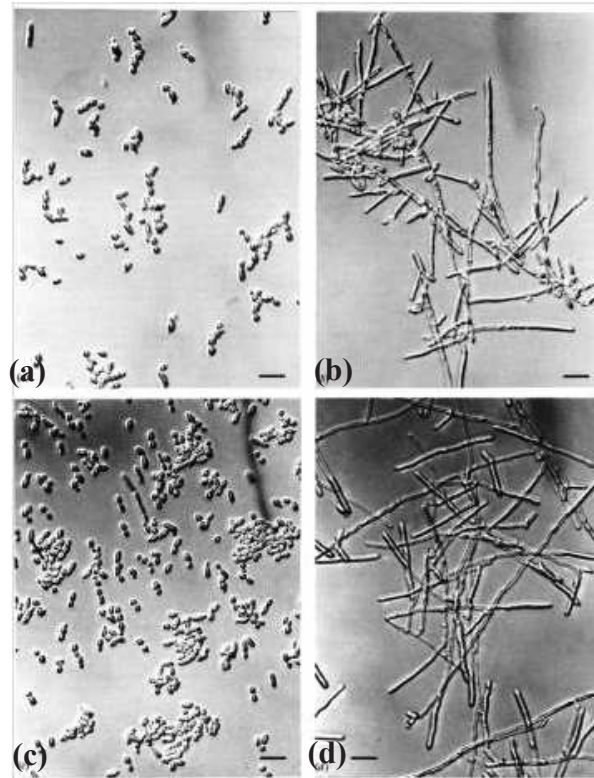


Figure I-16: Morphology of *Yarrowia lipolytica* grown as yeast in YNBGlc medium (a and c), or as mycelium in YNBGlcNAc medium, after a heat shock (b and d), after 12h (a, b) or 24 h (c, d) incubation (Guevaraolvera et al. 1993)

Other studies carried out by Novotny and co-workers (1994) demonstrated that in media containing GlcNAc as the sole carbon source at pH 6.0, the proportion of filaments in biomass (for *Y. lipolytica* 29-26-8 strain) reached about 78 and 89 % in the presence of phosphate and citrate buffer respectively. However, Ruiz-Herrera and Sentandreu (2002) have proven that morphological alterations induced by GlcNAc occurred exclusively in citrate medium at neutral pH. Only 8 % of the cells (W29 strain) developed mycelia in phosphate medium. This discrepancy may be dependent on the strain, the buffer and the operating conditions (W29 cells were exposed to thermal shock before induction of dimorphism).

On another hand, Dominguez et al. (2000) and Perez-Campo and Dominguez (2001) demonstrated that adding serum in the growing media allowed an induction of germ tube formation in more than 90 % of cells after 4 to 6 h of incubation. Similar observation was also obtained with GlcNAc as carbon source. On solid media, serum has been shown to induce invasive growth (Perez-Campo and Dominguez 2001) as it was previously described for *S. cerevisiae* by Roberts and Fink (Roberts and Fink 1994). In addition, studies carried out by Kim and colleagues (2000) demonstrated that serum is the most powerful inducer of

dimorphism in *Y. lipolytica* SMS397 strain. Indeed, it triggered hyphal growth more rapidly (4 h) than N-acetylglucosamine (10 h).

Y. lipolytica strains are mostly isolated from environments containing hydrophobic substrates such as fatty acids and glycerides. This fungus was found to undergo a dimorphic transition from the yeast form to the mycelial form in these media. Experiments developed by Ota et al. (1984) demonstrated that olive oil and its derivatives including triolein, oleic acid, linoleic acid and oleyl alcohol caused development of mycelial cells in presence of the casein. Mycelial cell ratios higher than 55 % were reported in *S. lipolytica* CBS 6303 strain. Morphological transition of *Y. lipolytica* in response to hydrophobic substrates was further examined by Zinjarde et al. (2008). The results showed the formation of mycelium in about 95 % of cells growing on media with coconut oil or palm kernel oil (rich in lauric (45- 48 %) and myristic acids (18 %)) at neutral pH.

I.2.2.1.3.2 Nitrogen source

Nitrogen sources have also been found to affect *Y. lipolytica* morphology. The influence of different nitrogen source on the mycelial growth was examined by Ruiz-Herrera and Sentandreu (2002). Their results, depicted in Table I-7, illustrated that ammonium salts ((NH₄)₂SO₄; (NH₄)₂HPO₄) are the most effective inducers of dimorphism (62 and 90 % of mycelial cells) whereas glutamate and glutamine inhibited dimorphism (0 % of mycelia). By contrast, the use of lysine or proline as nitrogen source induced the yeast-to-mycelium transition for *Y. lipolytica* SA-1 strain (Perez-Campo and Dominguez 2001). Furthermore, the simultaneous addition of casein and olive oil appeared to be required for dimorphism induction. Without casein, olive oil did not trigger filamentation (Ota et al. 1984) .

Table I-7: Effect of nitrogen source on mycelial growth: cells of *Yarrowia lipolytica* W29 were incubated at 28 °C in YNB medium containing 1 % glucose and 50 mM phosphate buffer (pH 7) plus 0.5 % of the indicated nitrogen sources (– No growth) (Ruiz-Herrera and Sentandreu 2002)

Nitrogen source	Final pH	Growth Dry weight (mg ml ⁻¹)	Morphology (%)	
			Yeasts	Mycelium
(NH ₄) ₂ SO ₄	6.07	1.15	38	62
(NH ₄) ₂ HPO ₄	6.45	1.90	10	90
NH ₄ CH ₃ COO	7.12	1.90	93	7
KNO ₃	7.09	–	–	–
Glutamate	7.31	0.75	100	0
Glutamine	6.55	2.55	100	0

Organic sources of nitrogen, amino acids and peptone were also identified as strong inducers of dimorphism in *Y. lipolytica* (Szabo and Stofanikova 2002). Amino acids such as lysine, leucine, sodium glutamate, glycine and histidine, as well as peptone have positive effects on the filamentous growth (Figure I-17).

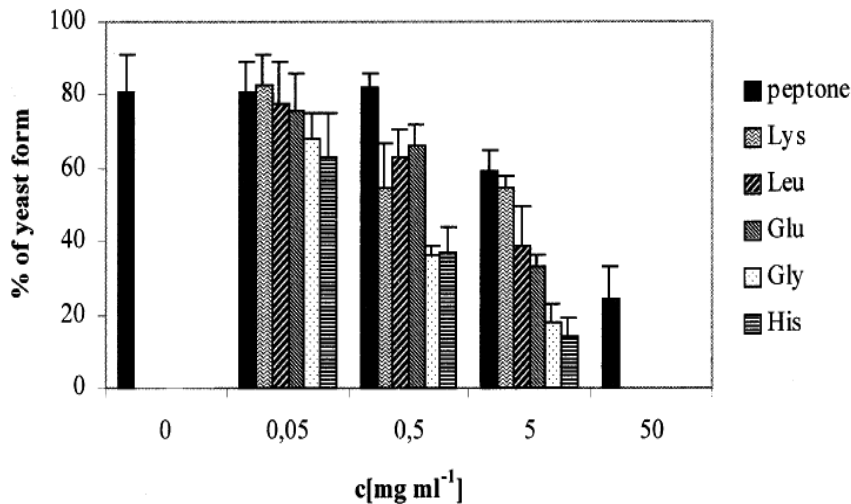


Figure I-17: Dependence of cellular morphology on organic sources of nitrogen. *Yarrowia lipolytica* cells were incubated for 18-20 h at 28 °C in minimal YNB medium with the addition of 0- 5 % mg mL⁻¹ of peptone, or 0-5 mg mL⁻¹ of each amino acid (Szabo and Stofanikova 2002)

I.2.2.1.3.3 Metal ions

The effect of deficiency in metal ions, such as magnesium (Mg²⁺), ferric (Fe³⁺) and calcium (Ca²⁺) ions on the dimorphic transition of *Y. lipolytica* was examined in the work of Ota et al. (1984). Concentrations higher than 2×10⁻⁵ M of Mg²⁺ ions appeared to be required to induce dimorphism. It was also reported that a minimal Fe³⁺ concentrations of 10⁻⁷ M is necessary for filamentation. However, addition or absence of Ca²⁺ ions had no significant effects on the filamentous growth.

Further research (Zinjarde et al. 1998) confirmed the role of magnesium in the morphogenetic switch. Supplementation with magnesium chloride (MgCl₂) increased the proportion of mycelial cells in a NCIM 3589 *Y. lipolytica* strain isolated from sea water. A maximal proportion of mycelial cells (70 %) were obtained with another marine isolate (NCYC 789) when cells were grown in media containing magnesium ions and GlcNAc as carbon sources.

I.2.2.2 Culture conditions for studying dimorphism in *Yarrowia lipolytica*

In previous research, most of the studies on *Y. lipolytica* dimorphism were performed under a batch culture mode (typically in flasks, tubes or bottles) in small reacting volumes (between 1

and 100 mL), and during short incubation periods (from few hours up to a maximum of 96 h). Furthermore, these culture systems were usually uncontrolled and thereby subjected to wide fluctuations in main culture parameters, such as pH or dissolved oxygen concentration. The cell response to an environmental perturbation in an uncontrolled environment will be certainly dependent on other stimuli related to the culture conditions (multifactorial stress responses). Bellou et al. (2014) conducted the only study to date examining the effect of DO availability on the morphology of *Y. lipolytica* under controlled conditions in bioreactor, thereby establishing a direct correlation between the perturbation and the morphological response.

I.2.2.3 Dimorphism quantification and characterization methods

Up to now, characterization of the mycelial transition of *Y. lipolytica* at the population level through analysis of cell size distribution profiles has never been considered. Such approach may provide a realistic description of the morphological heterogeneity of the culture and allows the subcategorization of yeast population into the yeast-like (ovoid or spherical single cells) and filamentous (elongated cells and pseudomycelia) forms.

In previous reports, optical microscopy was the most widely used technique. It allowed the observation of cells and was often associated with direct counting methods using a haemocytometer or a counting chamber (Guevaraolvera et al. 1993; Ota et al. 1984; Zinjarde et al. 2008; Zinjarde et al. 1998). An automatic image processing methodology was sometimes applied to extract individual properties of cells, such as area, hyphal length, hyphal width and elongation factor (Kawasse et al. 2003; Lopes et al. 2008; Nunes et al. 2013).

Cell morphology was also monitored by means of electronic microscopic techniques, mainly the transmission electron microscopy (TEM) and the scanning electron microscopy (SEM) (Dominguez et al. 2000; Herrero et al. 1999; Rodriguez and Dominguez 1984). These techniques were most commonly used to analyze the surface details and the germ tube emission during the yeast-to-mycelium transition.

Furthermore, a coulter counter approach was applied to determine the size distribution and the mean volume of cells (Rodriguez and Dominguez 1984). Segregation between yeast and filamentous cells was based on the difference in volume. The volume of the yeast form (almost spherical shape) was considered to be higher than that of the mycelial one (almost cylindrical shape). Ota and co-workers (1984) described a different method to determine the

mycelial cell ratio. The method consists on the separation between the two cell forms on the basis of differences in cellular specific gravity (Density gradient centrifugation).

Most of the studies quantify the dimorphism phenomena by determining the percentage of filamentous cells within the population. Data on the population distribution according to the size are quite lacking in previous research. Besides, discriminatory parameters used to distinguish between filamentous and ovoid cells were rarely mentioned in literature. Only few morphological criteria were reported:

- ✓ Elongation factor (> 2.0) (Lopes et al. 2008; Nunes et al. 2013);
- ✓ Length-(daughter cells) germ tube $>$ diameter-(mother cells) (Guevaraolvera et al. 1993);
- ✓ Cellular gravity (filamentous cells) $<$ (ovoid cells) (Novotny et al. 1994; Ota et al. 1984).

Furthermore, statistical analyses of observed cells were not well-detailed. The number of analyzed images and/or the number of counted cells were also rarely indicated in previous studies (Gonzalez-Lopez et al. 2006; Guevaraolvera et al. 1993; Lopes et al. 2008; Ruiz-Herrera and Sentandreu 2002). Most of the analyzed samples were not statistically representative of the cell population.

In addition to numerous experimental methods and modeling techniques for the description of cell population heterogeneity regarding physiology and cell activity (Fernandes et al. 2012), several methods could be used to investigate (qualitatively and quantitatively) the morphological behavior of *Y. lipolytica* in response to environmental stress conditions (Table I-8).

Table I-8: Potential methods for the characterization of morphology and size distribution

Method	Dimension	Measured parameters	Statistical representatively
Optical microscopy	2D	d_{CE} , L, W, AR	∅
Morphogranulometry (MG)	3D	d_{CE} , L, W, AR, perimeter, area, circularity	⊕
Dynamic light scattering (DLS)	3D	d_{SE}	⊕
Flow cytometry (CYT)	3D	d_{SE} , L	⊕

AR: aspect ratio=width/length; d_{CE} : equivalent circular diameter; d_{SE} : equivalent spherical diameter; L: length; W: width

I.2.3 Metabolic responses of *Yarrowia lipolytica* to adverse environmental conditions

The growth of *Y. lipolytica* and the secretion of metabolites (organic acids, lipids and lipase among others) are influenced by changes in the physico-chemical properties of their growth

environment (Coelho et al. 2010). Metabolic behaviors of *Y. lipolytica* in response to external perturbations have not been widely documented in the published literature.

I.2.3.1 Effect of pH

pH is a variable that affects directly several metabolic pathways in *Y. lipolytica*. Initial pH values in the range of 5.2 to 7.0 allowed an enhanced production of citric acid by different *Y. lipolytica* strains. pH levels outside this range caused a considerable decrease in citric acid concentrations (Yalcin et al. 2010). On the other hand, varying pH of the culture (from 4 to 7) during the lipogenic phase resulted in a small increment in the lipid content of *Y. lipolytica* cells (Enshaeieh et al. 2013). In the literature, pH values in the range between 5.0 and 7.0 were the mostly employed during cultivation of *Y. lipolytica* for lipid synthesis (Fontanille et al. 2012; Najjar et al. 2011; Papanikolaou et al. 2001; Papanikolaou et al. 2002; Sarris et al. 2011). Additionally, production and properties of lipases secreted by *Y. lipolytica* are influenced by changes in medium pH. A slight decrease in the specific rate of lipase production has been noted when promoting pH gradients in batch bioreactors (Kar et al. 2008). An optimum lipase production was detected for pH values ranging between 4.4 and 4.8 for different yeast strains (Corzo and Revah 1999; Kebabci and Cihangir 2012). Lipases from *Y. lipolytica* were found to be active between pH 6.0 and 10.0 with an optimum activity observed at pH 6.0, 7.0 or 9.0 depending on the strain used (Brígida et al. 2007; Fickers et al. 2011).

I.2.3.2 Effect of dissolved oxygen concentration

Oxygen is a key substrate in aerobic bioprocesses. An increased oxygen supply has been shown to enhance cellular growth of *Y. lipolytica*. Indeed, the specific growth rate and the biomass production were enhanced 3.4 and 5-fold, respectively by an increase in air pressure up to 6 bar compared to the atmospheric conditions (Lopes et al. 2009). Besides, the maximum specific growth rate of the yeast was greatly inhibited when reducing oxygen saturation levels from 90-95 to 28-30 %. DO levels were monitored through modulating agitation and aeration rates. At 28-30 % O₂ saturation, the yeast growth was inhibited, and the specific growth rate ($\mu_{\max}=0.12 \text{ h}^{-1}$) was almost 2-fold lower than during the culture at 90-95 % saturation ($\mu_{\max}=0.23 \text{ h}^{-1}$) (Finogenova et al. 1991).

Lipase synthesis, γ -decalactone secretion and organic acid production by *Y. lipolytica* were also affected by oxygen availability in the culture medium (Kar et al. 2008; Lopes et al.

2008). In fact, oxygen transfer rate (OTR) improvement by increasing air pressure in bioreactor resulted in a significant enhancement of lipase production by the yeast: the enzyme activity was increased from 96.6 U l⁻¹ at 1 bar to 533.5 U l⁻¹ at 8 bar (Lopes et al. 2008). In addition, higher γ -decalactone concentration was reached at high OTR (by increasing aeration from 1.7 to 5.4 L min⁻¹ and agitation from 400 to 650 rpm) compared with that obtained using low aeration (Braga and Belo 2015). Furthermore, citric acid synthesis appeared to be dependent on dissolved oxygen concentration. Specific citric acid productivity was increased by approximately 55 % as the concentration of dissolved oxygen was enhanced from 20 to 80 %. At a biomass concentration of 5% w/v, citric acid productivity evolved from 11 to 20 mg citric acid. g_{cell}⁻¹ h⁻¹ over the range of DO concentrations examined (Rane and Sims 1994). Similarly, an improvement of the initial oxygen volumetric mass transfer coefficient (K_LA) from 7 up to 55 h⁻¹ has been shown to enhance citric acid final concentration by 7.8 times (Ferreira et al. 2016a).

On another hand, some studies have indicated that conditions of low (≤ 5 % of saturation) and/or limited (0 % of saturation) DO tensions were often required for an efficient production of certain valuable metabolites, such as mannitol, arabitol, citric acid, succinic acid by *Y. lipolytica* (Kamzolova et al. 2003, Workman et al. 2013, Jost et al. 2015).

I.2.4 Mechanisms regulating stress responses in *Yarrowia lipolytica*

An important progress has been made recently in the elucidation of molecular mechanisms underlying adaptation to extracellular stress factors, and in particular the dimorphic transition of *Y. lipolytica*.

The tolerance of *Y. lipolytica* to different agents of oxidative stress was examined in some previous researches (Biryukova et al. 2006; Lopes et al. 2009b; Lopes et al. 2013). In the work carried out by Biryukova et al. (2006), the yeast cells showed a high resistance against oxidants, including hydrogen peroxide (H₂O₂), menadione, and juglone. This behavior was associated with an increase in the activity of cellular catalase, superoxide dismutase, glucose-6-phosphate dehydrogenase, and glutathione reductase, the main enzymes involved in cell defense against oxidative stress. Defense mechanisms of *Y. lipolytica* against oxidative stress were also found to be effective under increased oxygen availability (Lopes et al. 2009b; Lopes et al. 2013). Indeed, a pressure rise from 1 to 6 bar (6-fold increase in DO concentration) caused the induction of the antioxidant enzyme superoxide dismutase. The

activity of the enzyme at 6 bar was 53.4-fold higher than that obtained under atmospheric pressure.

Regarding resistance to pH stress, previous reports showed that adaptation to alkaline pH is under the control of the Pal/Rim signaling pathway regulating the expression of many pH-dependent genes (Gonzalez-Lopez et al. 2002; Lambert et al. 1997). Furthermore, proteomic analysis enabled the identification of major proteins involved in the pH adaptive ability of *Y. lipolytica* (Epova et al. 2012; Guseva et al. 2010). Adaptation to pH changes was found to be related to the activation of antioxidant systems preventing the development of oxidative stress in cells: an enhanced production of reactive oxygen species (ROS) was shown during the growth at pH 4.5 and 9.0, contrarily to the culture at pH 5.5 (ROS generation was almost 1.5-fold lower). Superoxide dismutase (SOD) activity was significantly increased under both acid and alkaline conditions (by 2.5 and 4 times at pH 4.5 and pH 9.0 respectively) (Sekova et al. 2015).

Specifically, regulation of the dimorphic transition in *Y. lipolytica* is based on the operation of the mitogen-activated protein kinase (MAPK) and protein kinase A (PKA) signaling pathways. These pathways operate in opposition during the yeast-to-mycelium transition: MAPK pathway is necessary for mycelial growth whereas PKA pathway is required for growth in the yeast-like form (Cervantes-Chavez et al. 2009; Cervantes-Chavez and Ruiz-Herrera 2006; Cervantes-Chavez and Ruiz-Herrera 2007). Several genes involved in dimorphism have been isolated and characterized, Rho family among others. These genes are not only implicated in dimorphism but also in a variety of other cellular activities (such as cell wall organization and biogenesis and membrane trafficking) (Cervantes-Chavez et al. 2009; Hurtado et al. 2000; Martinez-Vazquez et al. 2013; Topiltin Morales-Vargas et al. 2012). Proteins implicated in the yeast-to-mycelium transition have been also identified in order to understand the regulatory mechanisms involved in dimorphism (Morin et al. 2007).

I.3 Conclusions and objectives of the study

Bioprocess design for an industrial production occurs after optimization at laboratory scale, a critical transition step for successful technology transfer and commercialization of product of interest (Fu et al. 2014). Physiological and metabolic behaviors of microorganisms face environmental heterogeneities should be taken into consideration to achieve high performances (productivities, qualities and/or yields of products of interest).

The first part of the literature review described major environmental gradients frequently encountered in large-scale bioreactors, based on major handbooks and scientific papers. Fundamental culture parameters, such as shear stress, pH, temperature or concentration of nutrients may be prone to heterogeneities. As cells travel through various gradients in bioreactor, they are exposed to changing environments. This may act as stress effector and affects microbial dynamics (physiology, metabolism). Nonetheless, the complex interplay between environmental changes and cellular responses is yet not fully understood, and the integration of this new knowledge into the strategies for design, operation and control of bioprocesses is far from being an established reality (Fernandes et al. 2012).

The second part of this chapter focused on the establishment of the main working database on *Y. lipolytica*, and its morphological and metabolic responses to environmental perturbations. The current knowledge about the mycelial transition of *Y. lipolytica* in response to different environmental fluctuations was described. Studies correlating a single perturbation to yeast morphology are quite lacking. In fact, most of studies were conducted under uncontrolled culture conditions which give rise to multi-effector responses. Well-controlled culture conditions and perturbations using fully instrumented bioreactors may be proposed in order to establish a direct causal link between the stress and the cell response. Furthermore, comparing the morphological evolutions between the different studies seems to be quite complex. Analytical methods and discriminatory criteria used to distinguish between filamentous and ovoid cells are non-standardized, sometimes subjective and dependent on the culture conditions. Additionally, in none of the studies, the effect of a modulated stress under controlled culture conditions in bioreactors has been investigated. Controlled perturbations in the form of pulse, Heaviside and/or rectangular perturbations might be examined to highlight the effect of the intensity, duration and/or frequency of cell exposure to stress conditions on the microbial response.

Considering their implications on lipid-production performances, identification and characterization of the dynamic responses of *Y. lipolytica* to heterogeneities inside bioreactors appears therefore essential to optimize the process. For this purpose, the following main scientific questions were addressed:

- ⇒ What are the methods to be developed for the characterization of the morphological response at the cell population level? What is the methodology implemented to quantify subpopulations with distinct morphotypes within the culture?

- ⇒ What are the dynamics of metabolic and morphological behavior of *Y. lipolytica* in response to pH stress? What are the effects of the cell growth rate and culture mode on the microbial response?
- ⇒ What are the impacts of fluctuations in dissolved oxygen (DO) levels on the metabolism and morphology of *Y. lipolytica*? How this yeast behaves in perturbed, low ($pO_2 \approx 2\%$) and limited DO ($pO_2 \approx 0\%$) environments?

Part II: Materials and methods

PART II: MATERIALS AND METHODS

This chapter describes the experimental methods and materials used to accomplish the objectives of the thesis. It includes a presentation of the strain and culture media employed, culture conditions adopted, as well as the characteristics of the model particles used for the validation of the size characterization techniques. In addition, the analytical methods used to characterize the dynamics of growth; metabolism and morphology of *Y. lipolytica* were described in detail. Finally, the methodology employed for the treatment of the kinetic data (rates, yields, carbon and redox balances...), as well as smoothing and reconciliation of the experimental results are duly presented.

II.1 Strain and culture media

II.1.1 Strain

The strain used in this study was the wild-type *Y. lipolytica* W29 (ATCC® 20460™) strain originated from the American Type Culture Collection (ATCC, Manassas, VA). Most commonly, the optimal growth conditions of *Y. lipolytica* W29 strain on minimum medium were: temperature: 28 °C and pH: 5.6 (Cescut 2009; Faure 2002; Ochoa Estopier 2012).

II.1.2 Culture media

Two types of growth media were used for *Y. lipolytica* cell culture: rich (YPD and PCA) and minimum medium. All reagents used for medium preparation were of the highest grade commercially available.

II.1.2.1 Rich media

II.1.2.1.1 YPD (Yeast extract Peptone Dextrose) medium

The Yeast extract Peptone Dextrose (YPD) rich medium was used for colony isolation (in solid form by the addition of agar) and for cell revivification (in liquid form). The composition of YPD medium is presented in Table II-1. The medium was prepared with deionized water and sterilized by autoclaving at 121 °C for 20 min.

II.1.2.1.2 PCA (Plate Count Agar) medium

The composition of the PCA (Plate Count Agar) medium is presented in Table II-1. Pre-sterilized PCA plates were supplied by BioMerieux (France). This medium was used in solid form (in the presence of Agar) for cell enumeration by the surface inoculation method.

Table II-1: Composition of the YPD and PCA rich media

Compound	Concentration (g L ⁻¹)		
	YPD liquid	YPD Agar	PCA
Yeast extract	10.0	10.0	2.5
Peptone	10.0	10.0	-
Casein peptone (tryptone)	-	-	5.0
Glucose	10.0	10.0	1.0
Agar	-	20.0	15.0

II.1.2.2 Minimum medium

The defined minimum medium (MM) used for all bioreactor fermentations, as well as for the two last steps of inoculum preparation was the following (Table II-2). It is a synthetic medium with an optimized composition adapted to *Y. lipolytica* cell needs. Stock solutions (1000-fold concentrated) of each oligo-element were prepared separately and sterilized by autoclaving at 121 °C for 20 min. In order to avoid iron oxidation, the iron (II) sulfate (FeSO₄) solution was sterilized by filtering through a 0.22 µm syringe-fitted filter. Vitamins were made as a 500-fold concentrated stock solution, filter sterilized (0.22 µm membrane filter) and kept refrigerated at 4 °C. Glucose was also prepared as a stock solution (600 g L⁻¹) and autoclaved separately. In a first step, the macro-elements were mixed in deionized water according to the composition presented in Table II-2. After mixing the components, the pH was adjusted to 5.6 by addition of 2M potassium hydroxide solution and the mixture was sterilized for 20 min at 121 °C. After cooling, oligo-elements, vitamin and glucose solutions were added aseptically, from their respective stock solutions, to the medium mixture at the target concentration (Table II-2).

Table II-2: Composition of the minimum medium

	Compound	Concentration (g L ⁻¹)
Macro-elements	(NH ₄) ₂ SO ₄	2.5
	KH ₂ PO ₄	6.0
	MgSO ₄	2.0
Oligo-elements	EDTA-Na ₂ . 2H ₂ O	0.03750
	ZnSO ₄ . 7H ₂ O	0.02810
	MnCl ₂ . 4H ₂ O	0.00250
	CoCl ₂ . 6H ₂ O	0.00075
	CuSO ₄ . 5H ₂ O	0.00075
	Na ₂ MoO ₄ . 2H ₂ O	0.00005
	CaCl ₂ . 2H ₂ O	0.01250
	FeSO ₄ . 7H ₂ O	0.00875
	H ₃ BO ₃	0.00250
Vitamins	D-Biotin	0.00025
	DL-Pantothenic acid	0.00100
	Nicotinic acid	0.00100
	Myo-inositol	0.00625
	Thiamine. HCl	0.00100
	Pyridoxine	0.00100
	Para-aminobenzoic acid	0.00020
Carbon source	Glucose	10

II.2 Culture conditions

II.2.1 Strain preservation

At the beginning of the thesis work, *Y. lipolytica* cell frozen stock was prepared as follows: From a YPD agar plate of *Y. lipolytica* W29 strain, a single colony was picked and transferred into a 10-mL sterile tube containing 5 mL of YPD medium. After incubation for 16 h at 28 °C and 110 rpm, 3 mL of the culture was used to inoculate 27 mL of the same medium in a 100-mL baffled-shake flask. The flask was then incubated for 16 h at 28 °C and 110 rpm. The culture (21 mL) was mixed with 9 mL of pure sterile glycerol solution to reach a final concentration of 30 % (v/v). Finally, the prepared stock culture was aliquoted into sterile cryotubes (1 mL each) and stored at -80 °C. Sterilization of glycerol and YPD medium was carried out by autoclaving at 121 °C for 20 min. All the experiments presented in the manuscript were performed with cells from the same lot of glycerol stock.

II.2.2 Inoculum preparation

For each culture, one glycerol stock kept à -80 °C was streaked on YPD agar plate and incubated at 30 °C for 48 h. Well-isolated single colony from YPD agar plate (incubation at 30 °C for 48 h) was used for inoculum preparation. The isolated colony was transferred into a

sterile tube containing 5 mL of YPD rich medium. Subsequently, a second sub-culturing at 10 % (v/v) was carried out on minimum medium supplemented with 10 g L⁻¹ glucose. Cells arising from the second subculture were used to inoculate at 10% (v/v) an Erlenmeyer flask containing 100 mL of the same minimum medium. The 100 mL inoculum was then used to inoculate the bioreactor at an initial biomass concentration of 0.3 gCDW L⁻¹. The three successive pre-cultures were incubated at 28 °C for 12 h exactly at 130 rpm to obtain well-standardized inoculums. One drop of polypropylene glycol (antifoam PPG) was added to the third subculture in order to avoid foam formation. As a precautionary measure against contamination, all pre-cultures were performed in duplicate.

II.2.3 Bioreactor fermentation

II.2.3.1 Experimental setup

Bioreactor batch and continuous cultures were made in a 1.6 L stainless-steel stirred tank bioreactor (BIOSTAT® Bplus, Sartorius, Germany) (1 L working volume), fitted with two six-bladed Rushton impellers and four equally spaced baffles (1 cm width). The system is equipped with precise control systems of pH (*EasyFerm Plus K8 160, Hamilton, Suisse*), temperature, dissolved oxygen (*OxyFerm FDA 160, Hamilton, Suisse*), agitation speed and air flow rate. MFCS/win 2.1 software was used for data acquisition of the online measurements during fermentation. Each culture was operated and automatically controlled with the BIOSTAT® Bplus control tower.

II.2.3.2 Process control and regulation

Temperature was regulated at 28 °C by fluid circulation in the jacket surrounding the reactor. pH was maintained at the set point by automatic addition of 2M potassium hydroxide solution. Temperature and pH control systems consist of probe and electrode linked to PID controller modules.

In order to ensure highly aerobic conditions throughout the batch cultures, a partial oxygen pressure (pO₂) higher than 40 % of saturation was maintained by manually increasing agitation and aeration rates from 100 to 800 rpm and 0.1 to 0.35 vvm respectively. During continuous runs, pO₂ value was stabilized at around 65 % of saturation by maintaining agitation and aeration rates at constant levels.

In order to avoid mass transfer limitation due to foam formation, the antifoam (polypropylene glycol) was periodically added by means of a peristaltic pump (controlled pulse-based addition) in the continuous bioreactors. A nearly constant concentration of 1 mL L^{-1} was maintained all along the cultures. For the batch cultivations, antifoam was added at the same concentration (1 mL L^{-1}) prior to reactor sterilization.

II.2.3.3 Batch cultures

The minimum medium (composed only of the macro-elements) containing 1 mL of antifoam (PPG) was sterilized directly in the bioreactor by autoclaving for 20 min at $121 \text{ }^\circ\text{C}$. After cooling, pre-sterilized stock solutions of oligo-elements (1000-fold concentrated), vitamins (500-fold concentrated) and glucose (600 g L^{-1}) were injected into the bioreactor, via a septum using sterile syringes, according to their concentrations presented in Table II-2. To ensure sterility, the incoming gas passed through PTFE membrane filters of $0.2 \text{ }\mu\text{m}$ pore size (Midisart®, Sartorius). The pH probe was calibrated before sterilization using standard buffer solutions. Calibration of the dissolved oxygen probe was carried out after sterilization. The culture vessel was inoculated with 100 mL of exponentially growing pre-culture, by means of a stainless steel cannula introduced in the bulk culture medium.

II.2.3.4 Continuous cultures

Glucose-limited chemostat cultures were established by feeding the bioreactor with fresh medium (MM supplemented with 10 g L^{-1} glucose) through a calibrated peristaltic pump at a defined constant flow rate. The working volume was kept constant at 1 L by removing the overflow broth by means of a stainless steel cannula placed at the upper level of the culture. The outflow cannula was connected to a peristaltic pump operating at a slightly higher rate than the inflow pump. Figure II-1 presents the experimental setup of the continuous bioreactor. Steady state conditions were reached after at least five residence times. The steady state phase was assessed through constant measurements of biomass and residual glucose concentrations, as well as stable compositions of the exhaust gases.

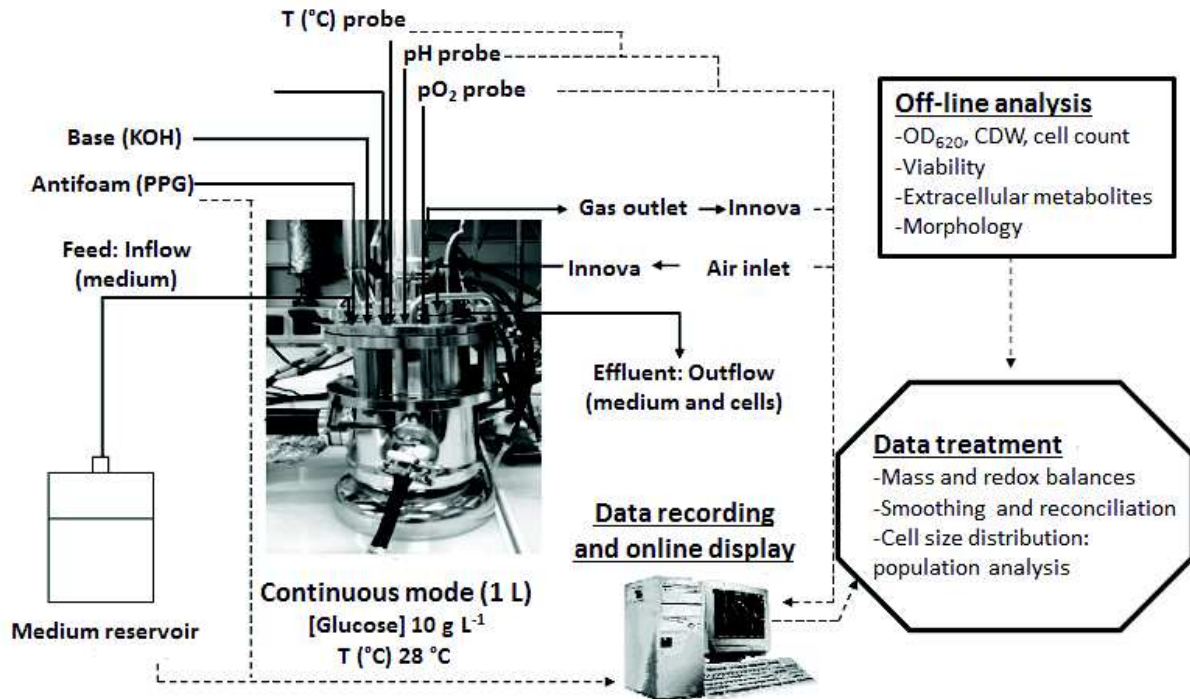


Figure II-1: Experimental setup of the continuous bioreactor (Sunya 2012)

II.2.3.5 Sampling procedure description

For each mode of culture (batch or continuous), a different sampling procedure was adopted:

- *Batch mode*: for the pH stress experiments, broth samples were harvested at approximately 1-h intervals all along the fermentation. Higher sampling frequency was applied (every 30 min) during the cultures with fluctuations in dissolved oxygen (DO) concentrations. Samples of 10 to 40 mL, representing 1-4 % of the total volume, were taken aseptically from the bioreactor, and characterized by the following measurements: optical density (DO), cell dry weight (DCW), cell counting, viability assessment, extracellular metabolite (glucose and organic acids) quantification and morphological characterization (with microscopy, morphogranulometry, diffraction light scattering and flow cytometry).
- *Continuous mode*: the steady state phase was characterized by taking-up three samples per day (approximately every 8h hour) during a period corresponding to at least five residence times. Depending on the type and nature of perturbation applied, samples were collected at time intervals of 2 to 4-h in order to study the impact of stress on the macroscopic and microscopic behavior of the yeast. To this end, 15-20 mL samples

(i.e. 1.5-2 % of the total volume of the culture) were taken and characterized using the same measurements as for the batch runs.

II.3 Model particles

Two sets of model particles with different size ranges were used as a reference for the validation of the morphological methods:

II.3.1 Calibration particles: from 1 to 15 μm -diameter

Polystyrene microspheres with diameters ranging from 1 to 15 μm (Flow Cytometry Size Calibration Kit (F-13838), Molecular probes, Invitrogen, USA) were used. The microspheres were supplied as aqueous solutions in water containing Tween[®] 20 (0.05%) and sodium azide (2 mM). All the particles have the same refractive index (1.591 at 590 nm) so that the differences in the forward scattered light (FSC) intensity reflect directly their relative size. The particles were packaged in convenient 1 mL flip flop dropper bottles at different concentrations. Their actual diameters are precisely determined by transmission electron microscopy. Nominal (approximate) and actual diameters, as well as the density of each set of particles are presented in Table II-3.

Table II-3: Characteristics of the six polystyrene microsphere samples

Provider information Nominal diameter, d_{SE} (μm)	Actual diameter (μm)	Density (beads mL^{-1})
1	1.1	$\sim 6 \times 10^7$
2	2.0	$\sim 3 \times 10^7$
4	4.2	$\sim 3 \times 10^7$
6	5.9	$\sim 2 \times 10^7$
10	9.9	$\sim 2 \times 10^7$
15	15.4	$\sim 2 \times 10^7$

d_{SE} : equivalent spherical diameter

II.3.2 Calibration particles: 40 and 80 μm -diameter

Polystyrene microbeads Dynoseeds[®] TS-40 and TS-80, of average diameter 40 and 80 μm respectively, as reported by the manufacturer (Microbeads AS, Skedsmokorset, Norway) were used. The particles exhibited a spherical shape and very smooth surface. These beads have a polydispersity lower than 10 % and a density of 1050 Kg m^{-3} (at 20 °C) (Boyer et al. 2011; Khidas et al. 2015; Pakpour 2013). They were mixed with water in the presence of a surfactant (Triton X-100, 0.2 %) in order to create a suspension. Characterization of these beads was carried out at a concentration of 1 % (w/v).

II.4 Analytical methods

II.4.1 Biomass characterization

II.4.1.1 Biomass concentration

II.4.1.1.1 Optical density

Yeast growth was monitored by spectrophotometric measurements at 620 nm in a spectrophotometer (Biochrom Libra S4, UK) with a 2 mm path length absorption cell (Hellma). Culture samples were diluted so that the absorbance reading is within the linear working range of the spectrophotometer (between 0.1 and 0.7 unit absorbance).

II.4.1.1.2 Cell dry weight

Dry cellular weight (DCW), expressed in g L^{-1} , was determined by gravimetry. A defined volume of culture broth was filtered by using vacuum pump through a 0.45 μm pore-size pre-dried and weighed polyamide membrane (Sartorius Biolab Product). The membrane was then washed twice with deionized water in order to remove traces of salts, and dried in an oven (HERAEUS, France) at 60 °C under partial vacuum (200 mmHg) for at least 48 h. The dry biomass concentration (g L^{-1}) was calculated by dividing the difference in the weight of the filter over the sample volume. For each sample, the quantified biomass was superior to 10 mg in order to be in the precision range of the scales. 1 unit in $\text{OD}_{620\text{nm}}$ corresponded to 0.92 g CDW L^{-1} during the batch mode and 1.07 g CDW L^{-1} during the steady-state continuous cultures.

II.4.1.1.3 Elemental analysis: C.H.O.N determination

The elemental composition of the biomass was determined by C.H.O.N elemental analysis on freeze-dried samples of *Y. lipolytica* W29 cells collected during the fermentation under continuous mode (steady-state phase). Analyses were performed at the laboratory of microanalysis at the “Institut de Chimie des Substances Naturelles” (ICSN) (<http://www.icsn.cnrs-gif.fr>) of the CNRS.

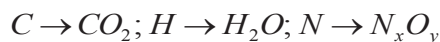
II.4.1.1.3.1 Sample preparation

During fermentation, 20 mL broth samples were centrifuged (5810R, Eppendorf, Hamburg, Germany) in sterile falcon tubes at 400 rpm for 10 min at 4 °C. The pellet was washed 5 times in physiological saline (0.9 % NaCl) at 4 °C, and stored at -80 °C.

Prior to C.H.O.N. analysis, the pellet was lyophilized for 24 h and stored in falcon tubes containing silica gel. At least, a quantity of 10 mg cell dry matter was required to accurately determine the elemental composition of the biomass.

II.4.1.1.3.2 Measurement principle

- The elements Carbon (C), Hydrogen (H) and Nitrogen (N) were detected by combustion of the analysis sample at 1050 °C in an oxygen (O₂)/ helium (He) gas flow. Under these conditions, carbon, hydrogen and nitrogen interact with O₂ as follows:



In the presence of copper (Cu) at 450 °C, the gaseous nitrogen oxide (N_xO_y) undergoes reduction to N₂. The products of combustion (CO₂, H₂O and N₂) were then quantified by gas chromatography (catharometric detection).

- The element Oxygen (O): was quantified by pyrolysis of the sample, over carbon, at 1120 °C in a nitrogen flow: $O + C \rightarrow CO$. Carbon monoxide (CO) was then fractionated on a chromatographic column and measured by a specific infrared detector.

II.4.1.1.3.3 Elemental composition of the biomass

The elemental analysis of *Y. lipolytica* biomass composition was performed on different broth samples taken at different times during the steady state phase of the continuous fermentation. The elementary formula of *Y. lipolytica* W29 strain was: CH_{1.675}O_{0.523}N_{0.153} with a molecular weight of 25.59 g Cmol⁻¹ considering 5.7 % of ashes.

II.4.1.1.4 Cell Cultivability

The number of viable and cultivable cells was determined using a simple plate count technique on Plate Count Agar (PCA) medium. One milliliter of broth was serially diluted with 9 mL sterile NaCl 0.85 % (w/v) physiological solution (BioMerieux®, France), and a precise volume (50 µL) of the resulting cell suspension was plated out, in triplicate, onto PCA medium by means of a Whitley Automatic Spiral Plater-WASP (Don Whitley Scientific Limited, UK). The plates were then incubated for 48 h at 28 °C and the colonies were manually counted. The counting results were expressed as number of colony forming units per milliliter of sample volume (CFU mL⁻¹). 1 g of cell dry matter per liter corresponded to 4

$\times 10^7$ CFU mL⁻¹ in batch cultures, and 3×10^8 CFU mL⁻¹ under steady state regime in continuous bioreactors.

II.4.1.2 Cell viability

During the time course of fermentation, yeast viability was monitored by flow cytometric measurements of fluorescence emission after staining cells with fluorescent dyes.

II.4.1.2.1 Operating principle of the flow cytometer

Flow cytometry is a laser-based technology allowing the characterization of cell populations at the single cell level through analysis of light scattering and fluorescence signals. The principle of flow cytometry is based on a single-file cell stream through a laser focused beam. Scattered light and fluorescence emissions generated by each cell particle are collected by detectors and sent to a computer for analysis by suitable software. Acquired data are displayed as a number distribution of the population with respect to the different cell parameters. A typical flow cytometer is composed of different main units: the light source, the flow cell, the hydraulic fluidic system, several optical filters, a group of detectors and a data processing unit (Chapman 2000; Givan 2001; Robinson 2004; Shapiro 2003) (Figure II-2).

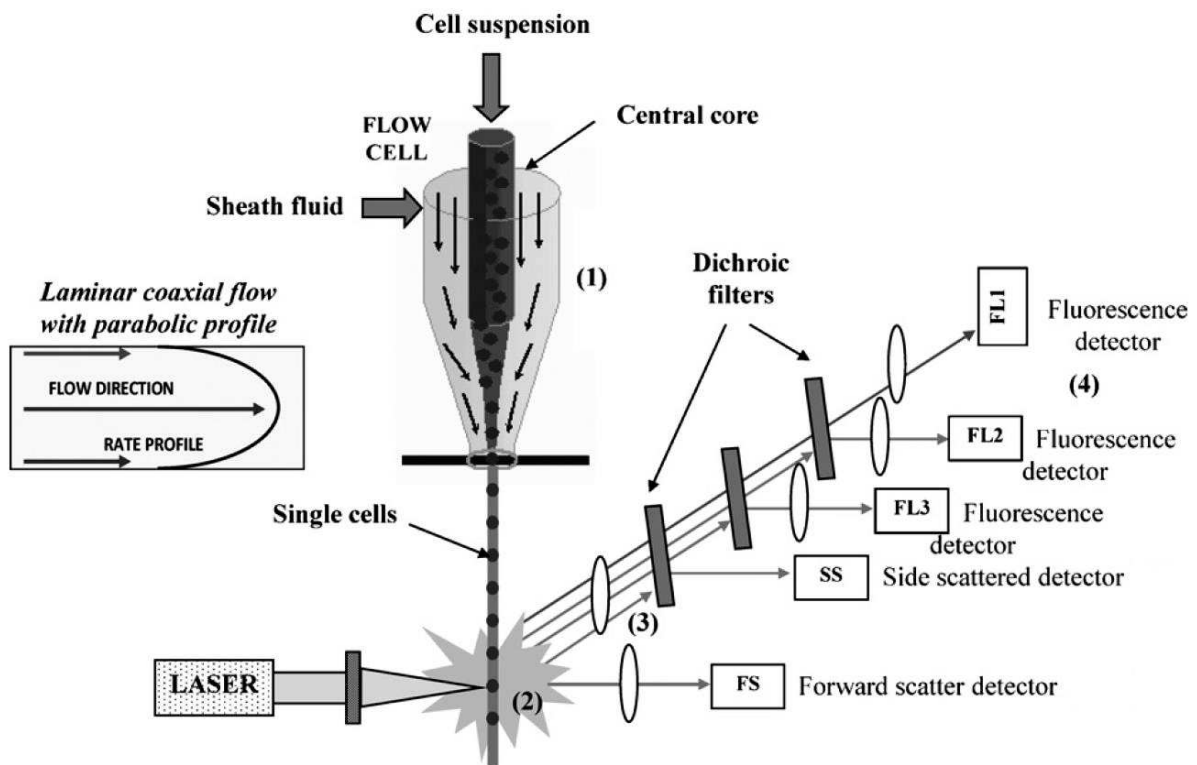


Figure II-2: Schematic representation of a typical flow cytometer setup (Diaz et al. 2010).

The system used in the current study was the BD Accuri C6[®] flow cytometer (BD Biosciences). The apparatus is configured with blue (488 nm) and red (640 nm) excitation lasers. Light scatter is collected at two angles: forward (FSC, 0 degrees, ± 13) and side (SSC, 90 degrees, ± 13) scatter. FSC and SSC signals are correlated to the cell size and internal complexity, respectively. Fluorescence intensity was collected in FL1 (533/30nm), FL2 (585/40), FL3 (>670 nm) and FL4 (675/25) bandpass/long pass optical filter/photomultiplier detector systems. The optical bench of the BD Accuri C6[®] flow cytometer is shown in Figure II-3.

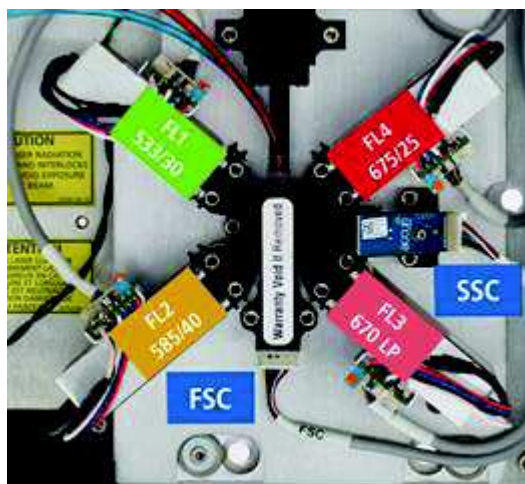


Figure II-3: BD Accuri C6[®] optical configuration

II.4.1.2.2 Experimental protocol for cell viability assessment

The use of fluorochromes may provide additional information about the physiological status of cells. Single and double staining assays were performed to monitor yeast viability throughout the fermentation. Three different fluorescent probes were used: carboxyfluorescein diacetate (cFDA), propidium iodide (PI) and Sytox[®] red (Molecular probes, Invitrogen, USA). cFDA was used to evaluate cell esterase activity, whereas PI and Sytox were employed to assess membrane integrity. Two staining combinations (cFDA/PI and cFDA/Sytox) were employed for the discrimination between dead and viable subpopulations in the culture. The green fluorescence emitted by the cFDA-stained cells was detected through the FL1 channel, and the red fluorescence of the PI and Sytox signal was collected in the FL3 and FL4 channels respectively. Spectral properties of the fluorescent dyes used, as well as their target substrates and applications are summarized in Table II-4.

Table II-4: Characteristics of the fluorescent probes used for the determination of yeast cell viability

Dye	Excitation wavelength (λ_{\max}) (nm)	Emission wavelength (λ_{\max}) (nm)	Emission detector	Cell substrate	Applications
carboxyfluorescein diacetate (cFDA)	492	517	FL1	Esterase activity	Metabolic activity
propidium iodide (PI)	490	635	FL3	DNA,RNA	Membrane permeability
Sytox® red	640	658	FL4	DNA,RNA	Membrane permeability

A stock solution of cFDA (3 g L^{-1}) was prepared by dissolving 5 mg of cFDA in 500 μL of anhydrous DMSO and 1 mL of pluronic (F-127, Molecular probes, Invitrogen, USA), and stored at room temperature, in the dark, in a desiccator cabinet. cFDA solution was thereafter used at a concentration of 3 mg L^{-1} of cell suspension. PI and Sytox® red stains were supplied by the manufacturer at 20 mM and 5 μM solutions in dimethyl sulfoxide solvent (DMSO) respectively, and were used as the working solutions at a concentration of $1 \mu\text{L mL}^{-1}$ of cell culture. Before staining, yeast cells were collected by centrifugation (13400 rpm, 3 min), and washed twice in the McIlvaine buffer (pH 4.5) (McIlvaine 1921) in order to remove residual medium components. The pellet of washed cells was resuspended in the same buffer, and diluted until a concentration of approximately $10^6 \text{ cells mL}^{-1}$. The cells were then labeled and incubated in the dark for 20 min at 37 °C. Heat-treated cells (70 °C for 20 min) served as 100 % dead control samples. Measurements with flow cytometry were performed with a fixed sample volume (20 μL), and at slow flow rate ($14 \mu\text{L min}^{-1}$) of the sheath fluid (MilliQ water). For all viability assays, the instrument trigger was set on the FSC signal (threshold value of 30000). Data were collected with BD Accuri CFlow® software and analyzed with FlowJo software (Tree Star).

II.4.1.3 Cell morphology and size distribution

In a first stage, basic concepts related to the definition and characterization of size distribution functions are introduced. In a second stage, different techniques dedicated to morphological analysis were described. These methods generate statistically representative data at the population level.

II.4.1.3.1 Theoretical aspects related to distribution functions

II.4.1.3.1.1 Definition of distribution functions

- Definition of distribution functions and associated moments

Because of the non-uniform particle size, changes in the population size are presented as a size distribution. Distribution profiles can be defined by distribution functions $E(x)$ or cumulative distribution $F(x)$. Distributions can be discrete or described by a continuous function as given by:

	Distribution function $E(x)$	Cumulative distribution function $F(x)$
Continuous	$E(x).dx = \frac{dn}{n}$	$F(x) = \int_0^{\infty} E(x).dx = 1$
Discrete	$p_i = \frac{dn}{n}$	$F_i = \sum_{i=0}^{\infty} p_i = 1$

Eq. 1

Where p_i is the probability corresponding to the size class i , and n is the number of particles

Each distribution function, $E(x)$ is characterized by a set of moments and centered moments of order j (Danckwerts 1953; Ham and Platzer 2004; Villermaux 1993).

$$\Gamma^i = \int_0^{\infty} x^i .E(x).dx \quad \text{and} \quad \Gamma^{i'} = \int_0^{\infty} (x - \bar{x})^i .E(x).dx \quad \text{Eq. 2}$$

The distribution function $E(x)$ is characterized by a mean value (\bar{x}), which represents the moment of order 1 (Γ^1). The variance (σ^2) and reduced variance $\beta^2 = \sigma^2/\bar{x}^2$ corresponds to the centered moment of order 2 ($\Gamma^{2'}$), which characterize the dispersion of the distribution curve. The centered moment of order 3 ($\Gamma^{3'}$) estimates the skewness, which represents the deviation from a symmetrical distribution ($S = 0$). A left-skew distribution exists for $S < 0$ and a right skew for $S > 0$. The centered moment of order 4 ($\Gamma^{4'}$) evaluates the spread of the distribution curve (Kurtosis) (Nguyen 2014).

- From morphological complexity to equivalent diameters

Different morphological descriptors were defined to characterize the particle size. They can be directly related to visual or microscopic measurements (length, width, aspect ratio...) or they are based on the concept of equivalent diameter. The equivalent circular diameters (d_{CE}) and the equivalent spherical diameters (d_{SE}) were examined in this study. d_{CE} represents the

diameter of the circle having the same projected area as the particle, and d_{SE} defines the diameter of the sphere with the same volume as the particle being examined.

Particle size characterization techniques provide measurements of size distribution based on the number, length, surface or volume of the particles. According to the classes of particles, different types of distribution were defined (Table II-5).

Table II-5: Definitions of number, dimension, surface and volume based distributions (Nguyen 2014)

Distribution	Signification	Formula
Distribution in number	Percentage in number associated with each class	$p_{n_i} = \frac{n_i}{\sum n_i}$
Distribution in dimension	Percentage in dimension associated with each class	$p_{d_i} = \frac{n_i \cdot d_i}{\sum n_i \cdot d_i}$
Distribution in surface	Percentage in surface associated with each class	$p_{s_i} = \frac{n_i \cdot d_i^2}{\sum n_i \cdot d_i^2}$
Distribution in volume	Percentage in volume associated with each class	$p_{v_i} = \frac{n_i \cdot d_i^3}{\sum n_i \cdot d_i^3}$

Considering the complexity of particle shape and morphology, it is convenient to consider a mean diameter (and its associated standard deviation describing the width of the distribution around the mean value) for a given particle population (Nguyen 2014). For instance, the average diameter can be defined by:

$$d_{p,q} = \left[\frac{\sum n_i \cdot d_i^p}{\sum n_i \cdot d_i^q} \right]^{1/p-q} \quad \text{Eq. 3}$$

With n_i : the number of particles of diameter d_i , and p, q are the integers ($p = q + 1$ with $q = 0, 1, 2, 3$ for number-, length-, surface- and volume-weighted, respectively) (Allen 1968; Brittain 2001; Tourbin 2006). Based on these notations: $d_{1,0}$ is the number-average diameter, $d_{2,0}$ is the quadratic mean diameter, $d_{3,0}$ is the cube average diameter, $d_{4,3}$ is the mass or volume mean diameter, and $d_{3,2}$ is the area-average diameter or Sauter diameter .

II.4.1.3.1.2 Statistical analysis and comparison of distribution functions

II.4.1.3.1.2.1 Normality of distribution functions

Several parametric statistical tests are based on the assumption of normally distributed data. In current study, graphical (visual) and numerical (statistical tests) inspection were used for

assessing normality of size distribution within a cell population (Dart and Chatellier 2002; Rakotomalala 2011):

- Graphical method: boxplot

Boxplot represents a convenient tool for graphically depicting an empirical distribution data by means of their quartiles. The first (25th percentile) and third (75th percentile) quartiles represents respectively the bottom and the top of the box. The horizontal line inside the box corresponds to the median (second quartile, 50th percentile). The interquartile range (IQR, range between the 25th to 75th percentiles) represents the length of the box. The whiskers (lines extending vertically from the box) represent the minimum and maximum values when they are within $1.5 \times \text{IQR}$ from either end of the box. Scores greater than $1.5 \times \text{IQR}$ are out of the boxplot and are considered as outliers, and those greater than $3 \times \text{IQR}$ are extreme outliers (Ghasemi and Zahediasl 2012). When the boxplot is symmetric and showing the median line at approximately the center of the box with symmetric whiskers slightly longer than the subsections of the center box, the data might be *expected to be normally distributed* (Elliott and Woodward 2006).

- Moments tests

The “moment” method is based on the fact that a normal distribution can be characterized by moments and centered moments. Based on these parameters, different criteria (Table II-6) were analyzed in order to estimate a possible fit between the empirical distribution and the Gaussian law. As shown in Table II-6, theoretical values could be expected for each criterion and deviation from normality could therefore be considered as acceptable, tolerate (deviation) or rejected. First criterion, C1 is based on the trends towards convergence (mode, mean and median are theoretically equal). The mean/median ratio should be then close to 1. Second criterion, C2 named «Geary test» is based on another feature of the Gaussian law, the ratio between the mean absolute deviation (MAD) and the standard deviation. This criterion is asymptotically equal to $(\sqrt{2/\pi} \approx 0.7979)$. Third criterion, C3 (Skewness) represents the asymmetry of the distribution that can be described with centered moment of order 3 (Γ^3/σ^3) . This coefficient is null, negative or positive when the distribution is symmetric, skewed to the left or to the right respectively. If the Skewness coefficient is higher than 1, distribution deviates from the normality. This deviation is more noticeable when values are greater than 2. Fourth criterion, C4 describes the flattening of a distribution named «Kurtosis» and can be

defined by the centered moment of order 4 (Γ^4/σ^4). If the Kurtosis coefficient is higher than 4, the distribution is deviated from the Gaussian law. This deviation is more important were values are higher than 7.

Table II-6: Criteria to evaluate the normality of a distribution

Criteria	Range	
Mean/Median	$C1 = \frac{\bar{x}}{F(x=0.5)} \rightarrow 1$	If $0.95 < C1$ or $C1 > 1.05$: deviation If $0.90 < C1$ or $C1 > 1.10$: rejected
MAD/STDV	$C2 = \frac{MAD}{\sigma} \rightarrow \sqrt{\frac{2}{\pi}}$	If $0.95 \times 0.798 < C2$ or $C2 > 1.05 \times 0.798$: deviation If $0.90 \times 0.798 < C2$ or $C2 > 1.10 \times 0.798$: rejected
Skewness	$C3 = \frac{\Gamma^3}{\sigma^3} \rightarrow 0$	If $C3 > 1$: deviation If $C3 > 2$: rejected
Kurtosis	$C3 = \frac{\Gamma^4}{\sigma^4}$	If $C4 > 4$: deviation If $C4 > 7$: rejected

$x(F=0.5)$: median; MAD: mean absolute deviation; STDV: standard deviation

II.4.1.3.1.2.2 Similarity of distribution functions

In order to assess the agreement or similarity between size distribution functions of independent cell populations, two statistical tests; Student test and overlapping coefficient determination; were carried out.: overlapping coefficient (all distributions) and Student test (Gaussian distribution) formula and applications are presented below.

- Overlapping coefficient

The overlapping coefficient (OVL coefficient) is a measure of the agreement or similarity between two probability distributions. It refers to the intersected area between both probability distribution functions. The OVL coefficient is defined as:

$$\delta(f_1(x), f_2(x)) = \int_{-\infty}^{+\infty} \text{Min}(f_1(x), f_2(x)).dx \quad \text{Eq. 4}$$

Where $f_1(x)$ and $f_2(x)$ are two distribution functions

The OVL coefficient ranges between zero and unity. It is 0 when the two distributions are completely distinct and is 1 when the two distributions are totally identical. Similarity criteria can be classified and distributions can be therefore considered as identical ($0.9 < \text{OVL}$), conform ($0.7 < \text{OVL} < 0.9$) or different ($\text{OVL} < 0.7$).

- Student's t-test

Student's t-test is used to compare the degree of similarity between populations described by a normal distribution. For two independent samples of sizes n_1 and n_2 , the test is conducted with considering the function:

$$T = \frac{\bar{x}_1 - \bar{x}_2}{\sqrt{\frac{S}{n_1} - \frac{S}{n_2}}} \quad \text{with} \quad S^2 = \frac{\sum(x - \bar{x}_1)^2 + \sum(x - \bar{x}_2)^2}{n_1 + n_2 - 2} \quad \text{Eq. 5}$$

Where \bar{x}_1 and \bar{x}_2 are the sample means, and S^2 the common variance.

Under the null hypothesis H_0 “population means are equal”, T follows a Student law to ($n_1 + n_2 - 2$) degree of freedom. T value is compared to the appropriate critical value (T_{critical}) in the student table. If the absolute value of T is greater than the critical value, the null hypothesis is rejected and the samples are considered as significantly different.

II.4.1.3.2 Optical microscopy

Microscopic observations were performed using an Olympus BH-2 microscope (Olympus optical Co., Ltd, Tokyo, Japan), which includes several magnifications (x10, x20; x40 and x100) enabling observations in direct light and contrast phase (under oil). This microscope is equipped with a color digital camera (Nikon’s Digital System DS-Ri1, Surrey, UK). Digital images were produced with a size of 1280x1024 pixels (dimensions: 2200x1760 μm^2 without magnification). The resolution of the instrument allowed observing details in the size of 0.2 μm .

Sample preparation represents a critical step to obtain accurate and precise measurements with the microscope and the morpho-granulometer. Broth samples taken during batch and chemostat runs were diluted (from 1:1 to 1:10) up to concentrations ranging between 0.3 and 0.5 gCDW L^{-1} , and homogenized using a vortex. A Droplet of about 5 μL of the cell suspension was deposited between cover glass and slide. The slides were previously cleaned with ethanol. In microscopy, three to five images were taken by sample. For morpho-granulometry measurements, the cover glass was sealed with a nail in order to avoid sample drying during conservation at 4 °C prior to analysis.

II.4.1.3.3 Morphogranulometry (MG)

II.4.1.3.3.1 Operating principle

Changes in cell morphology were characterized using a morpho-granulometer (Mastersizer G3S, Malvern Instruments Ltd. SN: MAL1033756, software Morphologi v7.21). The instrument is composed of a system of lens (magnification: from x1 to x50, particle dimension: from 0.5 to 3000 μm), an optical device (Nikon CFI60 Bright/ Dark field) and a camera (IEEE1394a, Fire Wire™, 2592x1544 pixels). The morphogranulometer is a particle size analyzer providing the ability to measure morphological characteristics of individual cells, and to report cell size distribution within a culture sample. The main steps of a measurement/analysis procedure by the morphogranulometer apparatus are presented in Figure II-4. The measuring principle is based on the capture of composite image on defined sample area, the on-line image processing, and the identification and analysis of geometric properties of individual cells (such as diameter, aspect ratio, circularity). Multiple morphometric criteria were calculated for each cell particle and associated distributions (in number and in volume) were generated for each parameter.

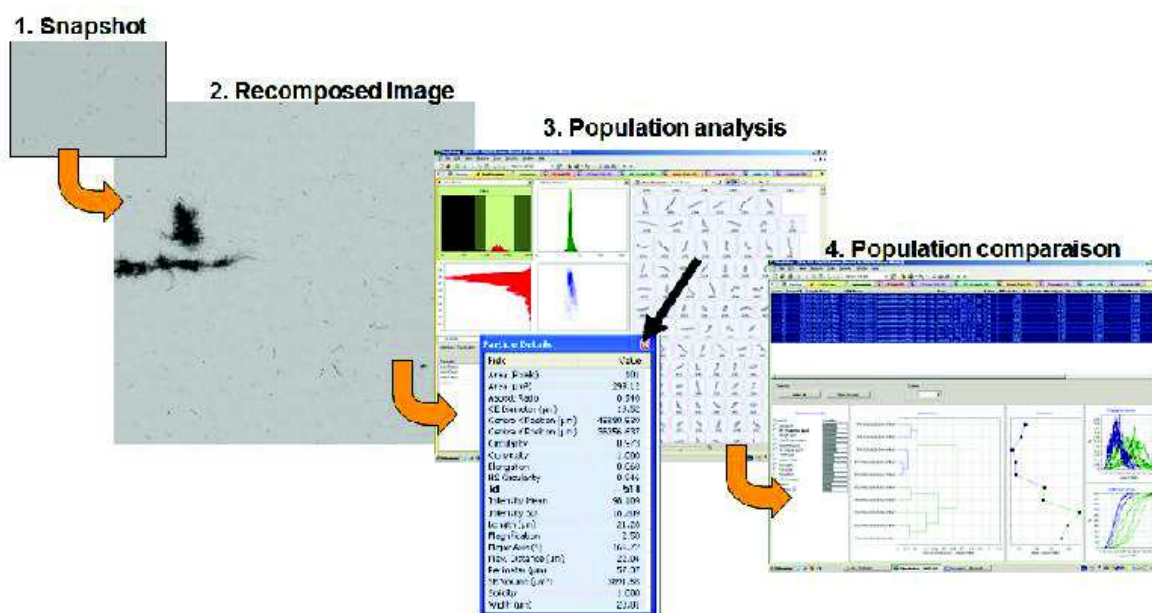


Figure II-4: Main steps of a measurement/analysis procedure by the Malvern Morphology® G3 instrument

II.4.1.3.3.2 Experimental protocol

Sample preparation procedure was similar to microscopy. A surface of (2x2 mm²) was selected by the operator and analyzed under the standardized operating conditions, presented

in Table II-7. Recorded images were then filtered and analyzed to determine cell size distribution at the population level.

Table II-7: Standard operating procedure for morphogranulometry measurements

Sample carrier	Plate glass Compensate for plate tilt
Illumination	Episcopic light source (dark field) Light intensity: 100%; Exposure time: 300 ms
Optic selection	Magnification: x20 Manual focus, no z stacking
Threshold	Threshold for particle detection: [50-100]
Scan area	Square area: 2x2 mm ² Enable refine position before measurement
Analysis setting	Soft analysis ID: 3.00 Trash size: 10 pixels Calculate fiber parameters No fill holes
Filters	None

II.4.1.3.4 Diffraction light scattering (DLS)

II.4.1.3.4.1 Operating principle

The size distribution of cells within the culture was characterized through a diffraction light scattering device (Mastersizer 2000 Hydro, Malvern Instruments Ltd. SN: 34205-69, range from 0.02 to 2000 μm). The working principle is based on the time-resolved measurement of the scattered light intensity generated by the passage of a dispersed cell sample through a laser beam, as illustrated in Figure II-5. The light scattering angle is directly related to the size of the particles. Large particles scatter light at small angles, whereas small particles scatter light at wider angles. The scattering data is then analyzed to determine the size of the cell responsible for creating the scattering pattern, by the application of the Mie theory. Mie theory predicts scattering intensity as a function of the angle at which light is scattered at the point of interaction with a spherical particle (Webb 2000). The cell size is then reported as a volume equivalent sphere diameter.

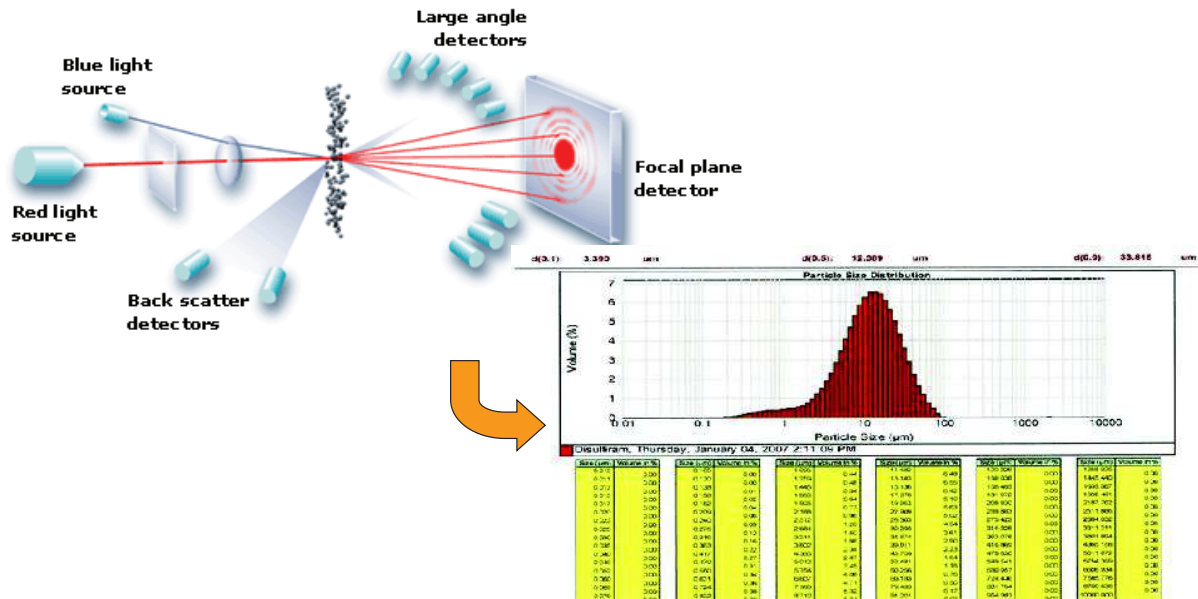


Figure II-5: Operating principle of the diffraction light scattering device – Example of result presentation (Nguyen 2014)

II.4.1.3.4.2 Experimental protocol

The passage of a homogeneous stream of cells through the laser beam is required for reproducible measurements. A defined volume of the cell suspension (1 mL) was added into a water circulation loop (volume: 50 mL; refractive index of the dispersant agent: 1.33). Constant circulation of the transporting fluid, as well as gentle agitation (with magnetic stirring bar) of the suspension was maintained during analysis, in order to avoid cell decantation. Measurements were conducted at room temperature (20°C) with obscuration rates (red $\lambda=632.8$ nm and blue $\lambda=470.0$ nm lights) ranging between 10 and 40 %. This analysis is based on the sphere-shaped model and employs by default the refractive index of organic compounds (1.569 at 20 °C).

II.4.1.3.5 Flow cytometry

Single-cell light scattering measurements were carried out with the BD Accuri C6[®] flow cytometer (BD Biosciences). The principle of the measurement, as well as the equipment specifications are described above (Paragraph II.4.1.2.1). Cell size and internal granularity were correlated with the forward scattered (FSC, 0 degrees, ± 13) and side scattered (SSC, 90 degrees, ± 13) light respectively. Cell size was estimated from the FSC signal using a calibration curve established by a set of polystyrene microspheres with diameters ranging between 1 and 15 μm (Flow Cytometry Size Calibration Kit (F-13838), Molecular probes, Invitrogen, USA). The width of the FSC signal representing the time of flight of the cell

though the laser beam was analyzed to determine the length distribution of cell subpopulations. Before analysis, broth samples were diluted (from 1:10 to 1:500) to reach a concentration of 10^6 cells mL⁻¹ and homogenized using a vortex. In order to discard background noise, due to the presence of salt particles and cell debris in the broth culture, a threshold of 30000 was applied on the forward scatter channel (FSCH). All measurements were performed at a pre-set flow rate of 14 μ L min⁻¹ using MilliQ grade water as sheath fluid, and with a defined sample volume of 20 μ L.

Flow cytometric data were recorded and processed using the BD Accuri CFlow[®] software. The FlowJo software (Tree Star) was used for the analysis of the collected data.

II.4.2 Determination of glucose and organic acids concentrations

II.4.2.1 High-performance liquid chromatography (HPLC)

During the cultures under batch mode, glucose and organic acids (acetate, pyruvate, succinate and citrate) concentrations were quantified by high performance liquid chromatography (HPLC). 1 mL broth samples were centrifuged (MiniSpin, Eppendorf, USA) in Eppendorf tubes at 13400 rpm for 3 min, and the supernatants were stored at -20°C. Prior to HPLC analysis, supernatants were thawed at room temperature, filtered on Minisart filters with 0.45 μ m pore diameter polyamide membranes (SARTORIUS, Germany), and diluted (when required) with Milli-Q grade water (18.2 m Ω -cm resistance).

II.4.2.1.1 Equipment description and operating conditions

HPLC analyses were performed using a Dionex UltiMate 3000 HPLC system (California, USA). The instrument is equipped with:

- an autosampler (CTC Analysis, PAL System, HTC PAL).
- a pump (Ultimate 3000 Pump).
- a pre-column (Micro-Guard IG Cation H, BIO-RAD).
- a column Aminex HPX-87H⁺ (Bio-RAd, US).
- an UV detector (Ultimate 3000 Photodiode Array Detector).
- a refractometer (Shodex RI-101).
- a software system for data acquisition and processing (Chromeleon, Chromatography Management System version 6.80).

Separation of metabolites on the Aminex HPX-87H⁺ column was performed using a 5 mM H₂SO₄ eluent under isocratic conditions. The flow rate of the mobile phase was 0.5 mL min⁻¹, the column temperature was set at 50 °C and the processed samples were kept in the HPLC autosampler at 5 °C. The injected sample volume was 20 µL and the running time of the chromatographic method was 30 min. Organic acid detection was performed using dual UV and refractive index (RI) detectors. Glucose was quantified employing the refractive index (RI) detector.

II.4.2.1.2 Experimental protocol

A standard stock solution was prepared with Milli-Q grade water (18.2 mΩ-cm resistance) in a gauged flask. The standards used for metabolite detection and quantification were glucose acetate, pyruvate, succinate and citrate. The stock solution was composed of 20 g L⁻¹ of glucose and 5 g L⁻¹ of each organic acid. From this stock solution, 1:5, 2:5, 3:5 and 4:5 (v/v) dilutions were made in order to establish a 6-point calibration curve. The retention time, the concentration range and the appropriate detector for each compound are shown in Table II-8.

Table II-8: Retention times of the compounds quantified by HPLC

Compound	Retention time (min)	Concentration range (g L ⁻¹)	Detector	
			RI	UV
Citrate	10.0	0 - 5	x	x
Glucose	11.2	0 - 20	x	-
Pyruvate	11.8	0 - 5	x	x
Succinate	14.5	0 - 5	x	x
Acetate	18.6	0 - 5	x	x

In order to check the stability of the system and the quality of measurements, calibration standards were injected at the start and end of the sample sequence. In addition, one standard solution was analyzed after every 10 samples of the sequence.

II.4.2.2 High-performance ionic chromatography (HPIC)

II.4.2.2.1 Conductometric detection

High-performance ionic chromatography with conductometric detection was used to quantify organics acids present at low concentrations in the continuous cultures. Before HPIC analysis, culture supernatants, appropriately stored à -20 °C, were thawed at room temperature, diluted at 1:10 (v/v) with Milli-Q grade water (18.2 mΩ-cm resistance), and filtered with 0.45 µm

pore diameter polyamide membranes (SARTORIUS, Germany). The dilution is required to reduce the ionic content of the broth sample (salts of the culture medium).

II.4.2.2.1.1 Equipment description and operating conditions

An ICS-3000 system (Dionex, USA) equipped with a CD conductivity detector was used. The system is configured with:

- an autosampler (AS autosampler, Dionex).
- a pump (SP, Dionex).
- a pre-column (AG11, Dionex).
- a column (IonPac AS11-HC, Dionex).
- an eluent generator cartridge (EGC II KOH, Dionex).
- anion suppressors (ASRS® 300 and CR-ATC, Dionex).
- a conductometric detector (CD 40, Dionex).
- a software system for data acquisition and processing (Chromeleon, Chromatography Management System version 6.80).

The mobile phase (KOH) was produced online using a KOH EGC II eluent generator and further purified by a continuously regenerated anion trap column (CR-ATC). An optimized eluent gradient was used to carry out separations on the IonPac AS11 column. The KOH gradient elution program used is presented in Table II-9. The flow rate of the mobile phase was kept at 1.5 mL min⁻¹ and the sample injection volume was 40 µL. The column temperature and autosampler temperature were maintained at 30 and 5 °C, respectively. After suppression (ASRS® 300), the effluent was conductometrically monitored: the HPIC system was coupled with a conductometric detector (CD 40) providing an output signal proportional to the concentration of the individual components of the mixture.

Table II-9: KOH gradient program for organic acid quantification by ionic chromatography (linear profile between the points)

Time (min)	KOH concentration (mM)
0	1
13	1
25	15
35	30
45	60
50	60
55	1
65	1

II.4.2.2.1.2 Experimental protocol

The organic acids searched for detection and quantification were acetate, pyruvate, succinate, malate, fumarate and citrate. A standard stock solution containing 10 mg L⁻¹ of each organic acid was prepared in the minimum medium used for fermentation. To generate the calibration standards, dilutions at 1:5, 2:5, 3:5 and 4:5 (v/v) of the stock solution were carried out with the same minimum medium. Table II-10 presents the retention times of the identified compounds.

Table II-10: Retention times of the organic acids quantified by HPIC

Compound	Retention time (min)
Acetate	7.3
Pyruvate	11.7
Succinate/ Malate	26.1
Fumarate	29.9
Citrate	37.6

II.4.2.2.2 Amperometric detection

During the chemostat experiments, residual glucose concentrations in the culture medium were determined by ion chromatography using pulsed amperometric detection. Measurements were performed on the supernatants of centrifuged culture samples (3 min, 13400 rpm), previously filtered and diluted (if necessary).

II.4.2.2.2.1 Equipment description and operating conditions

The ion chromatograph used was an ICS-3000 system (Dionex, USA) composed of:

- an autosampler (AS autosampler, Dionex).
- a pump (SP, Dionex).
- a pre-column (CarboPacTM PA1 guard, 4 mm x 5 mm, Dionex).
- a column (CarboPacTM PA1, 4 mm x 250 mm, Dionex).
- a gold working electrode and pH-Ag/AgCl reference electrode (Dionex).
- an amperometric detector (ED 40, Dionex).
- a software system for data acquisition and processing (Chromatography Management System version 6.80).

Glucose was separated on an anion-exchange column (CarboPac PA1) using 15 mM NaOH (isocratic elution) as a mobile phase, at a flow rate of 1.0 mL min⁻¹ for 15 min at 30 °C. At

high pH, glucose (weak acid, $pK_a=12.28$ in water at 25 °C) is partially ionized, and can thus be separated by anionic exchange mechanisms. After each run, the column is regenerated with 200 Mm NaOH in order to remove compounds that may potentially contaminate the column (e.g. carbonates, peptides and amino acids). After each regeneration, the column must be equilibrated with the working concentration of the eluent (15 mM NaOH) during 10 min before the next sample injection.

The detection of glucose is performed using pulsed amperometric detection: the analyte is adsorbed onto the surface of a gold working electrode with a potential of 0.1 V, and later detected by an oxidation desorption process. Following the detection, an oxidative cleaning of the electrode surface was carried out by applying another potential. The potential wavelength of the pulsed amperometric detection used is shown in Table II-11. In this study, the potential applied for the integration was 0.10 V, and the integration time was set between 0.2 - 0.4 s.

Table II-11: Potential wavelength for the detection of glucose

Time (s)	Potential (V)	Integration	Operating steps
0.00	0.10		
0.20	0.10	Begin	Glucose oxidation
0.40	0.10	End	
0.41	-2.00		
0.42	-2.00		Electrode cleaning
0.43	0.60		
0.44	-0.10		
0.50	-0.10		

II.4.2.2.2.2 Experimental protocol

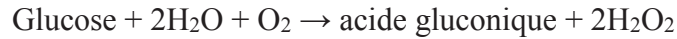
The eluent was prepared by the dilution of a concentrated NaOH stock solution of analytical grade 46/ 51 % (w/w) (Fisher Scientific, UK) in Milli-Q grade water (18.2 mΩ-cm resistance). Glucose standard solutions were prepared from the stock solution prepared with ultrapure water. Glucose calibration standards with concentrations of 4, 8, 12, 16 and 20 mg L⁻¹ of glucose were prepared by diluting the stock solution at 500 mg L⁻¹ of glucose in the fermentation medium (MM). Under these conditions, glucose was eluted at a retention time of 3.0 min.

II.4.2.3 Biochemical analysis: YSI (Glucose)

During the time course of fermentation, residual glucose concentrations were analyzed using a YSI Model 2700 analyzer (Yellow Springs Instruments, Yellow Springs, Ohio, USA).

II.4.2.3.1 Operating principle

The measurement is based on the detection of hydrogen peroxide (H₂O₂) released during the conversion of glucose into gluconic acid by means of an immobilized glucose oxidase:



The hydrogen peroxide is then oxidized at a platinum electrode to yield 2H⁺+O₂+2e (electrons). The electron flow generated will give rise to an electrical current proportional to the glucose concentration in the sample.

II.4.2.3.2 Experimental protocol

Assays were performed on culture supernatants. The yeast suspension is briefly centrifuged (13400 rpm for 3 min) to pellet the cells. For reliable measurements, supernatants should be diluted into the linear range of the instrument (0 – 2.5 g L⁻¹). The analyzer is calibrated using a single point calibration standard (2.50 g L⁻¹ glucose) (YSI 2776 Standard, Yellow Springs, Ohio, USA). The apparatus provides a direct reading of the glucose concentration, expressed in g L⁻¹. The accuracy of the measurement is approx. ± 2 %.

II.4.3 Gas analysis

During batch and continuous bioreactor cultures, the inlet and outlet gas composition were measured using a fermentation gas monitor system (LumaSense Technologies Europe). The instrument is composed of a multipoint sampler 1309 (INNOVA 1309) combined with a gas analyzer (INNOVA 1313). It allows accurate and simultaneous measurements of oxygen (O₂) and carbon dioxide (CO₂) fractions by magneto-acoustic and photo-acoustic spectroscopic methods. Gas analysis data were recorded every min along fermentation with the BZ 6003 software. To ensure accuracy of measurements, the gas analyzer was calibrated before each experiment. The calibration procedure consists of two steps: (i) checking the zero for oxygen (O₂) with the nitrogen gas and (ii) calibrating carbon dioxide (CO₂) using a standard gas mixture (5 % CO₂ and 10 % O₂).

II.5 Methodology for data treatment

II.5.1 Rates expression for gas-phase reactions

Oxygen consumption (r_{O_2}) and carbon dioxide production (r_{CO_2}) rates were calculated from the mass balances in the gas and liquid phases taking into account the inlet and outlet gas

compositions, and the evolutions of temperature, pH, salinity, and liquid volume in the bioreactor. The gas balance is determined in the reactor system illustrated in the Figure II-6.

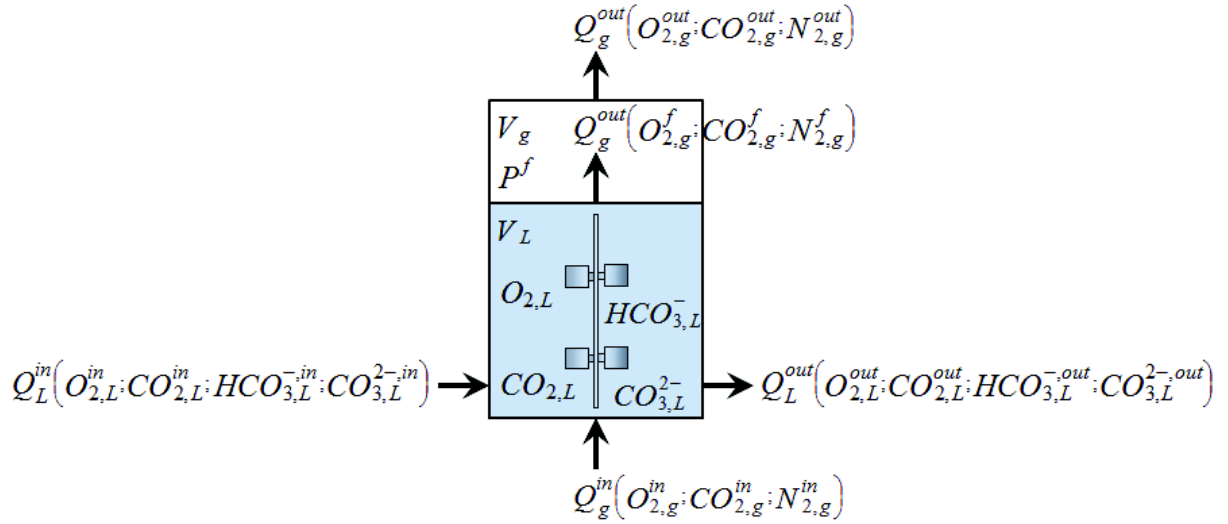


Figure II-6: Schematic representation of the system considered for gas balances calculations

During the course of bioreactor fermentation, the gas analyzer (INNOVA 1313) did not allow quantification of nitrogen (N_2) and argon (Ar) fractions in the inlet air and outlet gas streams. The molar fractions of N_2 and Ar can be deduced from measurements of O_2 and CO_2 molar fractions, by assuming a constant ratio between the volume fractions of N_2 and Ar (Eq. 6):

$$N_2 = \frac{(1 - O_{2,g}^{out} - CO_{2,g}^{out})}{\left(1 + \frac{Ar^{dry\ air}}{N_2^{dry\ air}}\right)} \quad \text{with} \quad \frac{Ar^{air\ sec}}{N_2^{air\ sec}} = 1.19 \times 10^{-2} \quad \text{Eq. 6}$$

$$Ar = 1 - O_2^{out} - CO_2^{out} - N_2$$

II.5.1.1 Overall balance on compound B

The mass conservation equation of a gas compound B in the bioreactor is written as:

$$\text{Accumulation} = [\text{Inlet} - \text{Outlet}] + \text{Reaction}$$

$$\frac{d(B_L \cdot V_L)}{dt} + \frac{d(B_g \cdot V_g)}{dt} = (Q^{in} \cdot B^{in} - Q^{out} \cdot B^{out}) + r_B \cdot V_L \quad \text{Eq. 7}$$

Where:

- V_L and V_g represent the volumes of the liquid and gas phase, respectively (NL),
- Q^{in} and Q^{out} represent the inlet and outlet gas flow rates, respectively (mol h^{-1}),

- B^{in} and B^{out} represent the fraction of compound B in the inlet and outlet gas stream,
- r_B represents the production/consumption rate of the compound B (r_B is positive for production and negative for consumption) (mol h^{-1}).

The global transfer flow term (Φ_B) regroups the accumulation term in the liquid phase and production or consumption term:

$$\frac{d(B_g \cdot V_g)}{dt} = (Q_g^{in} \cdot B^{in} - Q_g^{out} \cdot B^{out}) + \Phi_B \quad \text{Eq. 8}$$

$$\text{with } \Phi_B = -\frac{d(B_L \cdot V_L)}{dt} + r_B \cdot V_L \quad \text{Eq. 9}$$

II.5.1.2 Nitrogen balance

Nitrogen is an inert gas which is neither produced nor consumed by the microorganism. It undergoes only transport processes in the liquid phase without any conversion. Given that the nitrogen gas is slightly soluble in the liquid phase, the term $\frac{dN_{2,g}}{dt}$ can be neglected. The global transfer flow term can be neglected as well. The nitrogen balance allows then the estimation of the outlet gas flow rate Q_g^{out} , from the measurements of the inlet gas flow rate Q_g^{in} and nitrogen fractions in the inlet N_2^{in} and outlet N_2^{out} gas streams.

$$Q_g^{out} = \frac{\frac{d(V_g \times N_2^{in})}{dt} + Q_g^{in} \times N_2^{in}}{N_2^{out}} \quad \text{Eq. 10}$$

With the outlet gas flow, the oxygen and carbon dioxide transfer flows (in mol h^{-1}) can be expressed by:

$$\Phi_{CO_2} = \frac{d(V_g \times CO_2^{out})}{dt} - Q_g^{in} \times CO_2^{in} + Q_g^{out} \times CO_2^{out} \quad \text{Eq. 11}$$

$$\Phi_{O_2} = \frac{d(V_g \times O_2^{out})}{dt} - Q_g^{in} \times O_2^{in} + Q_g^{out} \times O_2^{out} \quad \text{Eq. 12}$$

Finally, the conversion rate of the compound B is given by:

$$r_B = \frac{\Phi_B + \frac{d(V_L \cdot B_L)}{dt}}{V_L} \quad \text{Eq. 13}$$

with $\Phi_B > 0$ if production and $\Phi_B < 0$ if consumption.

II.5.1.3 Oxygen balance and determination of the oxygen uptake rate

II.5.1.3.1 Dissolved oxygen solubility

The solubility of oxygen (C_S) can be calculated using Benson and Krause algorithm (Benson and Krause 1984):

$$C_S = \exp\left(-135.29996 + \frac{1.572288 \times 10^5}{T_L} - \frac{6.637149 \times 10^7}{T_L^2} + \frac{1.243678 \times 10^{10}}{T_L^3} - \frac{8.621061 \times 10^{11}}{T_L^4} - \left(0.020573 - \frac{12.142}{T_L} + \frac{2.3631 \times 10^3}{T_L^2}\right) \times S\right)$$

Eq. 14

Where:

- S: salinity ($\text{g}_{\text{salts}} \text{Kg}_{\text{culture medium}}^{-1}$)
- T: Temperature (Kelvin)

The equation 14 is applicable for temperature values comprised between 0 and 70 °C.

The Henry's constant can be determined by the following equation:

$$H_0 = \frac{C_S \times 10^6}{0.2094}$$

where the value "0.2094" correspond to the mole fraction of oxygen molecules in the dry air.

II.5.1.3.2 Oxygen consumption rate

For the continuous operating mode, it is necessary to take into account the dissolved oxygen levels via the medium feed and the culture withdrawal, in the balance equation for the liquid phase:

$$\frac{d(O_{2,L} \times V_L)}{dt} = r_{O_{2,L}} \cdot V_L + \Phi_{O_{2,L}} \times V_L \quad \text{Eq. 15}$$

$$\text{with } \Phi_{O_{2,L}} \times V_L = \varphi_{O_2} \times V_L + (Q_L^{in} \times O_{2,L}^{in} - Q_L^{out} \times O_{2,L}^{out}) \quad \text{Eq. 16}$$

$$\text{and } \varphi_{O_2} \times V_L = k_L a \cdot \text{Grad}_{O_2} = (Q_g^{in} \times O_{2,g}^{in} - Q_g^{out} \times O_{2,g}^f) \quad \text{Eq. 17}$$

According to the mass balance for the gas phase, the molar fraction of the oxygen at the outlet of the liquid phase ($O_{2,g}^f$) is expressed by the following equation:

$$O_{2,g}^f = \frac{1}{Q_g^{out}} \times \frac{d(O_{2,g}^{out} \times V_g)}{dt} + O_{2,g}^{out} \quad \text{Eq. 18}$$

Finally, the oxygen consumption rate (r_{O_2}) can be expressed, from the equations 15, 16, 17 and 18, by the formula:

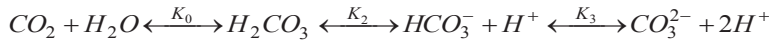
$$r_{O_2} = \frac{(Q_g^{out} \times O_{2,g}^{out} - Q_g^{in} \times O_{2,g}^{in} + Q_L^{out} \times O_{2,L}^{out} - Q_L^{in} \times O_{2,L}^{in}) + \frac{d(O_{2,L} \times V_L)}{dt} + \frac{d(O_{2,g}^{out} \times V_g)}{dt}}{V_L} \quad \text{Eq. 19}$$

where $O_{2,L} = pO_2 \times H_0 \times O_2^{in} \times P_{abs}$ and $P_{abs} = \frac{P_{atm} + P^f}{P_{atm}}$ Eq. 20

II.5.1.4 Carbon dioxide balance and determination of the carbon dioxide production rate

II.5.1.4.1 Equilibrium constants

In the liquid phase, the carbon dioxide is found in different forms with variable proportions depending on the pH and salinity of the liquid phase: carbon dioxide (CO₂), carbonic acid (H₂CO₃), hydrogencarbonate ion (HCO₃⁻) and the carbonate ion (CO₃²⁻). The equilibrium between the various forms can be expressed by:



K₀, K₁ and K₂ are the equilibrium constants of the corresponding reactions. These constants can be computed using (Weiss 1974) and (Lueker et al. 2000) algorithms, taking into account the pH, salinity (S) and temperature (T) measurements for the liquid phase.

$$K_0 = \exp\left(\frac{9345.17}{T} - 60.2409 + 23.3585 \times \ln\left(\frac{T}{100}\right) + (0.023517 - 2.3656 \times 10^{-4} \times T + 4.7036 \times 10^{-7} \times T^2) \times S\right) \quad \text{Eq. 21}$$

$$K_1 = 10^{\left(\frac{-363386}{T} + 61.2172 - 9.6777 \times \ln(T) + 1.011555 \times S - 0.0001152 \times S^2\right)} \quad \text{Eq. 22}$$

$$K_2 = 10^{\left(\frac{47178}{T} - 25.929 + 3.16967 \times \ln(T) + 0.0178 \times S - 0.000112 \times S^2\right)} \quad \text{Eq. 23}$$

Assuming that the equilibrium between these forms is established instantaneously, the ratio of each form relative to the total CO₂ can be determined by the following expressions:

$$\frac{CO_2}{CO_{2,total}} = \frac{H^2}{H^2 + K_1 H + K_1 K_2} \quad \text{Eq. 24}$$

$$\frac{HCO_3^-}{CO_{2,total}} = \frac{K_1 H}{H^2 + K_1 H + K_1 K_2} \quad \text{Eq. 25}$$

$$\frac{CO_3^{2-}}{CO_{2,total}} = \frac{K_1 K_2}{H^2 + K_1 H + K_1 K_2} \quad \text{Eq. 26}$$

with $CO_{2,total} = CO_2 + HCO_3^- + CO_3^{2-}$ and $H = 10^{-pH}$ Eq. 27

II.5.1.4.2 Carbon dioxide production rate

The concentrations of carbon dioxide dissolved in the liquid phase, supplied by the medium feeding and removed by withdrawing are considered in the determination of the carbon dioxide production rate (r_{CO_2}). The mass balance on the carbon dioxide can be described by the equation:

$$\frac{d(CO_{2,L}^{total} \times V_L)}{dt} = r_{CO_2} \times V_L + \varphi_{CO_2} \times V_L + (Q_L^{in} \times CO_{2,L}^{total,in} - Q_L^{out} \times CO_{2,L}^{total}) \quad \text{Eq. 28}$$

with $\varphi_{CO_2} \times V_L = k_L a \times Grad_{CO_2} = (Q_g^{in} \times CO_{2,g}^{in} - Q_g^{out} \times CO_{2,g}^f)$ Eq. 29

According to the mass balance for the gas phase, the molar fraction of the carbon dioxide at the outlet of the liquid phase ($CO_{2,g}^f$) is expressed by the following equation:

$$CO_{2,g}^f = \frac{1}{Q_g^{out}} \times \frac{d(CO_{2,g}^{out} \times V_g)}{dt} + CO_{2,g}^{out} \quad \text{Eq. 30}$$

From the equation 28, the gas-liquid transfer flux and the gas-liquid transfer gradient can be calculated according to the following equations:

$$\varphi_{CO_2} \times V_L = (Q_g^{in} \times CO_{2,g}^{in} - Q_g^{out} \times CO_{2,g}^f) \quad \text{Eq. 31}$$

$$Grad_{CO_2} = \frac{\varphi_{CO_2} \times V_L}{k_L a_{CO_2}} \quad \text{Eq. 32}$$

If k_{LaCO_2} and k_{LaO} values are equal, the concentration of dissolved carbon dioxide is determined by the equation:

$$CO_{2,L} = \frac{pCO_2^{*,in} * K_0 - \exp\left(\frac{(pCO_2^{*,in} - pCO_2^{*,f}) \times K_0}{Grad_{CO_2}}\right) \times pCO_2^{*,f} \times K_0}{1 - \exp\left(\frac{(pCO_2^{*,in} - pCO_2^{*,f}) \times K_0}{Grad_{CO_2}}\right)} \quad \text{Eq. 33}$$

$$\text{with } pCO_2^{*,in} = CO_{2,g}^{in} \times P_{abs}, \quad pCO_2^{*,f} = CO_{2,g}^{out} \times P_{abs} \quad \text{and} \quad P_{abs} = \frac{P_{atm} + P^f}{P_{atm}} \quad \text{Eq. 34}$$

Considering the equilibrium between the different forms, the total concentration of the dissolved CO₂ is calculated according to the equation:

$$CO_{2,L}^{total} = \frac{CO_{2,L} \times (H^2 + K_1 \times H + K_1 \times K_2)}{H^2} \quad \text{Eq. 35}$$

Finally, the carbon dioxide production rate (r_{CO_2}) can be determined, from the equations 27 and 28, according to the following formula:

$$r_{CO_2} \cdot V_L = \frac{d(CO_{2,L}^{total} \times V_L)}{dt} - \varphi_{CO_2} \times V_L - Q_L^{in} \times CO_{2,L}^{total,in} + Q_L^{out} \times CO_{2,L}^{total} \quad \text{Eq. 36}$$

The respiratory quotient (RQ) is the ratio: $QR = \frac{r_{CO_2}}{r_{O_2}} = \frac{q_{CO_2}}{q_{O_2}}$

II.5.2 Rate expressions for liquid-phase reactions

Glucose consumption (r_s) and biomass production (r_x) rates were determined based on their experimental measurements and their respective mass balance equations. The inlet and outlet volumetric flow rates were considered in calculating these rates during the continuous cultures. The mass balance of a compound F on the liquid phase can be expressed by the following equation:

$$\frac{d(F \times V_L)}{dt} = r_F \times V_L + Q_F^{in} \times F^{in} - Q_F^{out} \times F_{residual}^{out} - Q_{sampling} \times F_{residual} \quad \text{Eq. 37}$$

where:

- Q_F^{in} , Q_F^{out} and $Q_{sampling}$ represent the inlet, outlet and sampling flow rates of compound F, respectively (L h⁻¹),
- F^{in} and $F_{residual}$ represent the concentrations of compound F in the feed medium and in the bioreactor, respectively (g L⁻¹),

- V_L represents the volume of the liquid phase in the bioreactor (L),
- r_F represents the global reaction rate of compound F ($\text{g L}^{-1} \text{h}^{-1}$).

Under steady state conditions (continuous mode), the concentration of compound F and the volume of the bioreactor are constants $\left(\frac{dF}{dt} = 0\right)$ and $\left(\frac{dV_L}{dt} = 0\right)$, and the sampling flow rate is null. The inlet and outlet liquid flow rates are equal ($Q_F^{in} = Q_F^{out}$). The reaction rate of compound F can be therefore determined according to the equation:

$$r_F = \frac{Q_F^{out} \times F_{residual}^{out} - Q_F^{in} \times F^{in}}{V_L} = D(F_{residual}^{out} - F^{in}) \quad \text{Eq. 38}$$

with: D the dilution rate (h^{-1}), expressed as: $D = \frac{Q_F^{out}}{V_L} = \frac{Q_F^{in}}{V_L}$

II.5.3 Determination of overall yields

The yields on the carbon source (glucose) are determined according to the following equations:

$$R_{X/S} = \frac{r_X}{r_{glucose}} \quad \text{Cmol Cmol}^{-1}$$

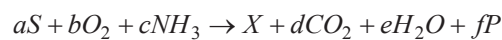
$$R_{O_2/S} = \frac{r_{O_2}}{r_{glucose}} \quad \text{Cmol Cmol}^{-1}$$

$$R_{CO_2/S} = \frac{r_{CO_2}}{r_{glucose}} \quad \text{Cmol Cmol}^{-1}$$

II.5.4 Carbon and redox balances

In order to validate the experimental data, carbon and redox balances were calculated for each fermentation.

Generally, a biological reaction follows the equation:



Where S, X and P are the substrate, biomass and product respectively.

Only the carbon-containing compounds are accounted in calculating the carbon balance, according to the following expression:

$$\sum \Phi_i = 0 \text{ where } \Phi_i \text{ is the flux in Cmol of a compound } i$$

The carbon balance is therefore defined by the equation: $-\Phi_S + \Phi_X + \Phi_{CO_2} + \Phi_P = 0$

The redox balance is computed with all compounds comprising at least one of the elements C, H, N or N, according to the following formula.

$$\sum \gamma_i \Phi_i = 0 \text{ where } \gamma_i \text{ the degree of reduction of the compound } i$$

The redox sheet equation is then expressed as follows: $-\gamma_S \cdot \Phi_S - \gamma_{O_2} \cdot \Phi_{O_2} + \gamma_X \cdot \Phi_X + \gamma_P \cdot \Phi_P = 0$

The degrees of reduction of the different elements are: $\gamma_C = 4$; $\gamma_H = 1$; $\gamma_O = -2$; $\gamma_N = -3$.

II.5.5 Smoothing and reconciliation of the experimental data

The smoothing procedure aims to deal with the experimental uncertainties and to calculate interpolated, derivatives and integrals values of the process variables, which would give access to the rates, specific rates and yields of the biological reactions.

The smoothing of the fermentation data were performed using LIREC software (internally developed software). The calculation is based on a polynomial regression in a moving window that allows the interpolation of data recorded and the approximation of results to smoothed curves.

The smoothed data was then reconciled according to the method of (Vanderheijden et al. 1994) by means of the same software (LIREC). Reconciliation is a statistical technique that evaluates the consistency of data and attempts to reduce errors in measured variables by checking balances. The verification of elemental balances allows to detect eventual anomalies in mass and redox balances, and to estimate the reaction rates enabling to close these balances. Integration of a reconciled rate data provides thereby the reconciled values of a variable.

Part III: Results and discussion

PART III: RESULTS AND DISCUSSION

Chapter III-1: Development and validation of methodologies for the quantification and characterization of morphological changes in *Yarrowia lipolytica*

Chapter III-1: Development and validation of methodologies for the quantification and characterization of morphological changes in *Yarrowia lipolytica*

III.1.1 Introduction

Biomass morphology is increasingly targeted as a key process parameter during process development because of the indisputable links between morphology, transport phenomena and related productivity (Krull et al. 2010; Papagianni 2004; Wucherpfennig et al. 2010). A prerequisite for reliable morphology analysis and control during bioprocesses is the development of accurate techniques to characterize the shape, size and distribution of cells in the population. A broad portfolio of methods is currently available to characterize the size and shape of particles, including mainly the optical microscopy, morphogranulometry (microscopy associated with automatic image acquisition and particle analysis), dynamic light scattering, flow cytometry, tomography, scanning electron microscopy, settling velocity and focused beam reflectance measurements. Table III-1 provides a brief description of the basic technical specifications of these instruments. Among the exciting techniques, three methods (in addition to optical microscopy) were selected for this study: dynamic light scattering (DLS), morphogranulometry (MG) and flow cytometry (CYT). These methods enable measurements of the size distribution profiles (either in number, E_n ; or in volume, E_v) at the entire population level (statistically representative), and are also adapted to our case study (yeast cells suspensions). All three instruments provide a measure of the particle diameter. Length, width and aspect ratio dimensions were particularly determined with the MG device. Although settling velocity and focused beam reflectance techniques provide statistically representative measurements of the cell size, their application were not retained. Indeed, data derived from settling velocity analysis are difficult to interpret and to compare with other techniques. Besides, focused beam reflectance measurement (FBRM) is an *in-situ* technique that requires insertion of a probe into the culture broth during fermentation. Such method may thus cause sterility problems inside the bioreactor.

Size characterization is simple for regular-shaped model particles, and a single method can be sufficient to analyze their morphological properties. However, for irregular or complex shaped materials, such as the case of filamentous microorganisms, a combination of methods

is typically required to provide more accurate quantification of size and shape parameters (Staniforth and Hart 1987).

Yarrowia lipolytica, the microorganism of interest in this study, possesses the ability to undergo a yeast-to-mycelium transition in response to environmental conditions. This yeast is capable to develop into two distinct morphotypes: yeast (ovoid/spherical single cells) and filamentous (elongated cells and mycelia) forms (Bellou et al. 2014; Braga et al. 2016; Ruiz-Herrera and Sentandreu 2002). In this chapter, the focus was given to develop and to validate methods in order to assess the dynamic of changes in the yeast morphology. Validation of CYT, MG and DLS techniques was carried out using model particles with known geometric properties (sphere). Measurements with particles of known size, shape and composition permit a direct comparison of the different techniques.

Table III-1: Technical specifications of the particle size characterization techniques

Method	Dimension	Measured parameter	Statistical representativity	Size distribution
Optical microscopy	2D	d_{CE} , L, W, AR	∅	En
Morphogranulometry (MG)	2D	d_{CE} , L, W, AR, perimeter, area, circularity	⊕	En
Dynamic light scattering (DLS)	3D	d_{SE}	⊕	Ev
Flow cytometry (CYT)	3D	d_{SE} , L	⊕	En
Tomography	3D	d_{SE} , L, W, thickness, specific surface	∅	Ev
Scanning electron microscopy	3D	d_{SE} , L, W, thickness	∅	En
Settling velocity (TSL)	3D	d_{St}	⊕	Ev
Focused beam reflectance measurement (FBRM)	2D	l_c	⊕	En

AR: aspect ratio; d_{CE} : equivalent circular diameter; d_{SE} : equivalent spherical diameter; d_{St} : stokes diameter; En: number distribution function; Ev: volume distribution function; L: length; l_c : chord length (the straight-line distance from one edge of a particle or particle structure to another edge); W: width

III.1.2 Experimental strategy

This part presents the experimental strategy implemented in this study. Characteristics of the models particles, main specifications of the instruments used, as well as basic principles of particle size analysis and size distribution calculations are described in the “Materials and Methods” section of the thesis.

A set of polystyrene particles with average diameters ranging from 1 to 80 μm were used as model matrices in order to evaluate the accuracy, precision and dispersion of the measurement

methods. To this end, single and intermixed particle suspensions were qualitatively (Table III-2) and quantitatively (Table III-3) analyzed by each of the techniques. The qualitative investigation was based on single particle analysis (monomodal sample), and aimed to compare methods in terms of means values and size distribution. The quantitative approach relies on the analysis of particle mixtures (bimodal samples) in order to examine the ability of the methods to quantify subpopulations with close and different (distant) sizes.

Table III-2: Experimental protocol for the qualitative validation of the methods (the cross mark indicates the technique used)

	Provider information particle diameter, d (μm)	Methods		
		CYT	MG	DLS
Single suspension Qualitative analysis	1.1	×	×	–
	2.0	×	×	–
	4.2	×	×	–
	5.9	×	×	–
	9.9	×	×	×
	15.4	×	×	×
	40.0	–	×	×
	80.0	–	×	×

CYT: flow cytometry; DLS: dynamic scattering; MG: morphogranulometry

Table III-3: Experimental protocol for the quantitative validation of the methods based on subpopulation mixtures (the cross mark indicates the method employed)

		Volume fraction (%)		Methods	
		Pop.1 (1μm)	Pop.2 (15μm)	CYT	MG
Intermixed suspension Quantitative analysis	Mix 1-15 μm	75	25	×	×
		50	50	×	×
		25	75	×	×
	Mix 4-6 μm	Pop.1 (4 μm)	Pop.2 (6 μm)	CYT	MG
		75	25	×	×
		50	50	×	×
	25	75	×	–	

III.1.3 Results and discussion

III.1.3.1 Raw data generated by each method: calibration step

In this part, the size of the model particles was determined by the three methods and compared with the supplier specifications. Uncertainties in size measurements and deviation from the expected data were accordingly evaluated.

III.1.3.1.1 Flow cytometry (CYT)

Raw data generated by flow cytometry are displayed as a number distribution of the forward scattered light (FSC), which is proportional to the particle size. Analysis of these data involved a preliminary step where a set of gates are defined to identify the population of interest. A generalized calibration curve, following a power-law, was used to correlate the FSC measurements to the equivalent spherical diameter (d_{SE}) of the microsphere (Figure III-1A). This generalized curve was established from independent passages (five times) of the calibration beads on the flow cytometer. Using this generalized plot, the diameter of the microspheres was then re-calculated, and compared with diameter measurements provided by the other methods. The diameter of the microsphere can be also correlated with the width of the FSC signal, as shown in Figure III-1B. The width represents the time of flight of the particle through the laser beam which is proportional to its length. For both signals, FSCA and width, the calibration curve was described by a power-law. Nevertheless, the exponent of the power law was approximately three-fold higher with the width parameter. This implies that the application of the power-law regression for the calibration of the width signal may generate greater uncertainty on the length estimation, compared to the FSCA signal. Errors in particle size determination associated with the use of the power-law equation ($y(x) = ax^n$) for the calibration of the signals were examined. In this equation, y represents the particle diameter given by the manufacturer, and x corresponds to the FSCA or width signal. The coefficient n is called the power law exponent, and a is a constant

Table III-4 provides values of mean and standard deviation for the coefficients a and n . An estimate of the resulting error (uncertainty) related to the power-law calibration was then determined for the FSC and width measurements. Results showed that the overall error committed in measuring the particle diameter by means of the FSC calibration did not exceed 10 % for all particle sizes. Nonetheless, with the width calibration, the error evolved from 27 to 32 % (depending on the particle diameter).

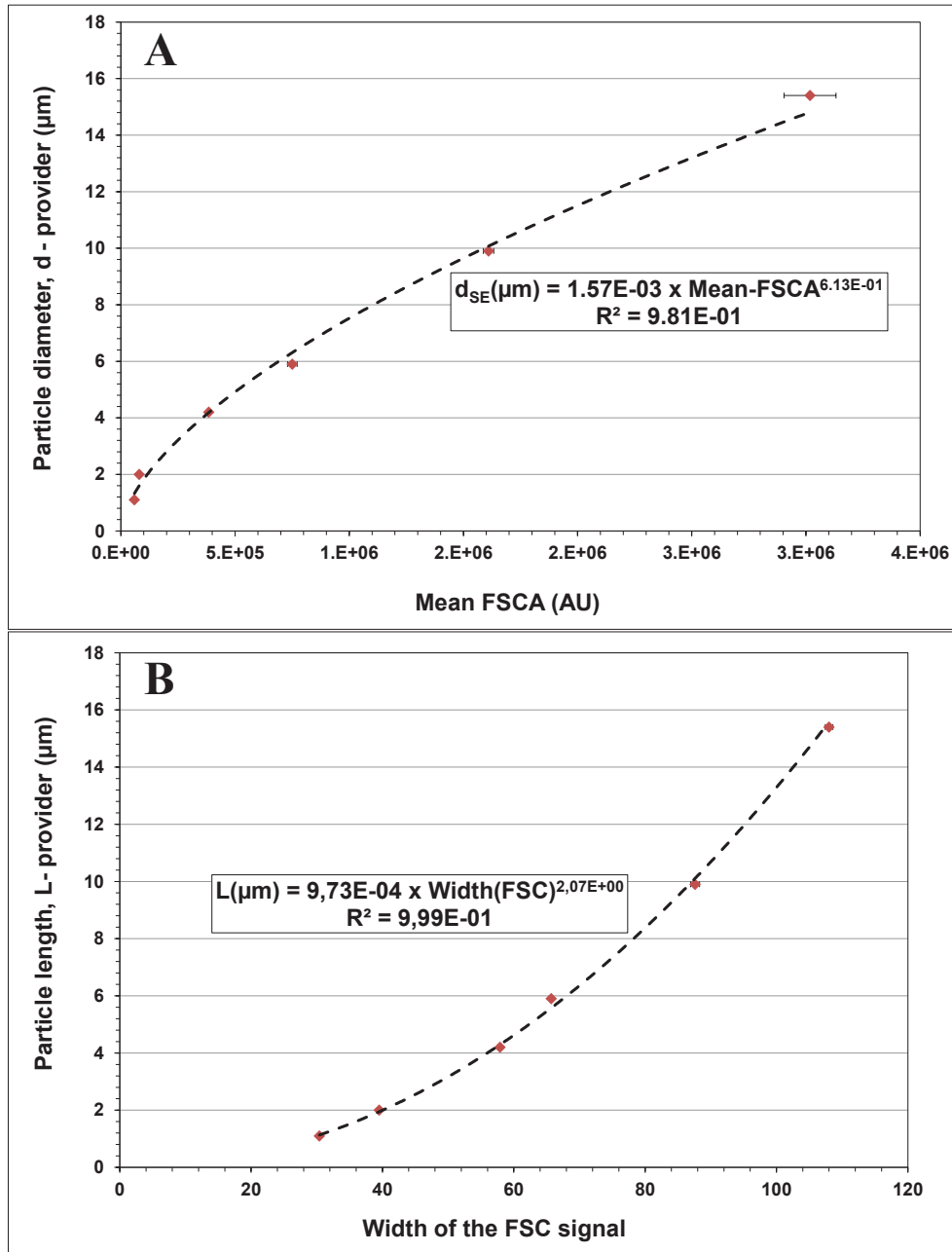


Figure III-1: Calibration curves of the particle diameter (A) and length (B) over a size range from 1 to 15 μm

Table III-4: Error calculation associated with the use of the power-law calibration to convert FSCA and width signals into diameter and length of particles

Parameter	a	n	Error (%)
FSCA	0.00157 ± 0.00110	0.613 ± 0.050	± 10
Width	$9.73 \cdot 10^{-4} \pm 1.44 \cdot 10^{-4}$	2.07 ± 0.04	From ± 27 to 32

A comparison was subsequently conducted between the recalculated dimensions (diameter, length) and the manufacturer information. As shown in Figure III-2, a good fit of the mean value with the theoretical diameter was proved for both parameters. In addition, standard

deviation around the mean value was quite negligible for the small particles (1 and 2 μm - diameter). However, for the particles with diameter higher than 6 μm , deviation from the mean value was more noticeable. This variance might be attributed to the error caused by the calibration curve approximation: almost $\pm 10\%$ and $\pm 30\%$ on the diameter and length measurements, respectively.

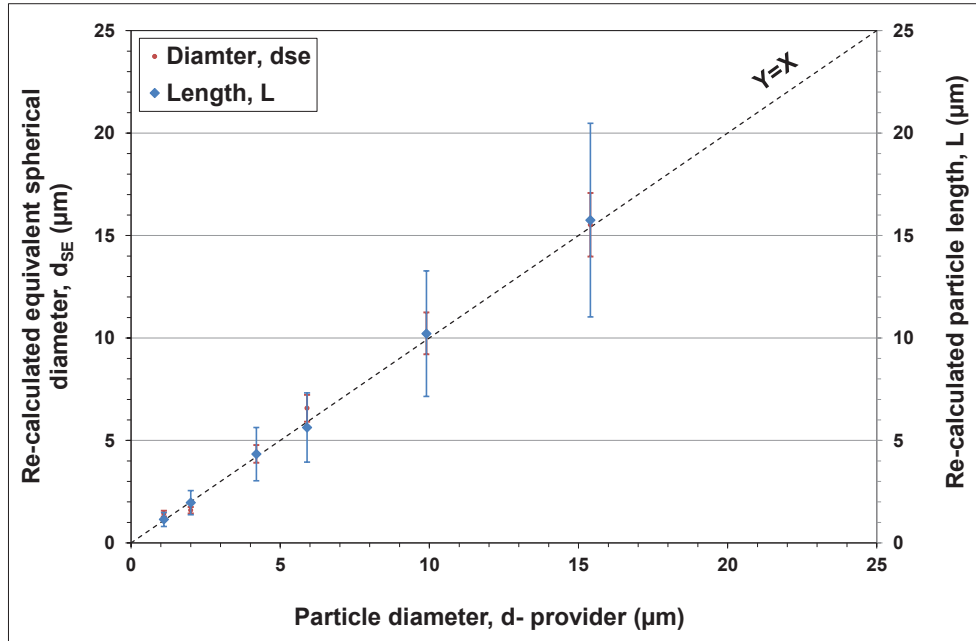


Figure III-2: Comparison between the theoretical and experimental data (diameter, length) quantified by flow cytometry

III.1.3.1.2 Morphogranulometry (MG)

Morphogranulometric analyses provide measurements of the equivalent circular diameter (d_{CE}) of each individual particle, and generate number and volume distribution of the particle equivalent diameter in the sample. Following MG measurements, acquired data were filtered according to the circularity criteria (values between 0.7 and 1) in order to remove particle agglomerates in the sample. A special attention was paid to perform analysis under bright field mode. Dark field measurement (based on reflected light) is not recommended since it induces the formation of luminous halos around the particles, which may overestimate their actual size. Data derived from MG measurements (Figure III-3) correlated well with the provider information and this is over a wide range of diameter: from 1 to 80 μm . Indeed, the deviation from linearity of the calibration curve did not exceed 3%. In addition, precision on the size measurements with the morphogranulometer was approximately $\pm 2\%$. The cumulative error remains therefore lower than 5% for all particle sizes. Such agreement between the theoretical and measured diameter was expected since an internal calibration of

the magnification and focus through four gratings of different pitches was carried out before each analysis. These calibration gratings allowed covering a size range from 0.2 to 200 μm with the instrument. As depicted in Figure III-3, the standard deviation was more noticeable with the larger beads (40 and 80 μm). These results were in agreement with the particles specifications. In fact, measurements were performed with two different sets of beads with distinct specifications. The particles with diameter ranging from 1 to 15 μm (Molecular probes, Invitrogen) are highly monodisperse. Whereas, the *Dynoseeds* particles (Microbeads AS) are characterized by a weak polydispersity (standard deviation around 5 %) (Garland et al. 2013; Pakpour 2013).

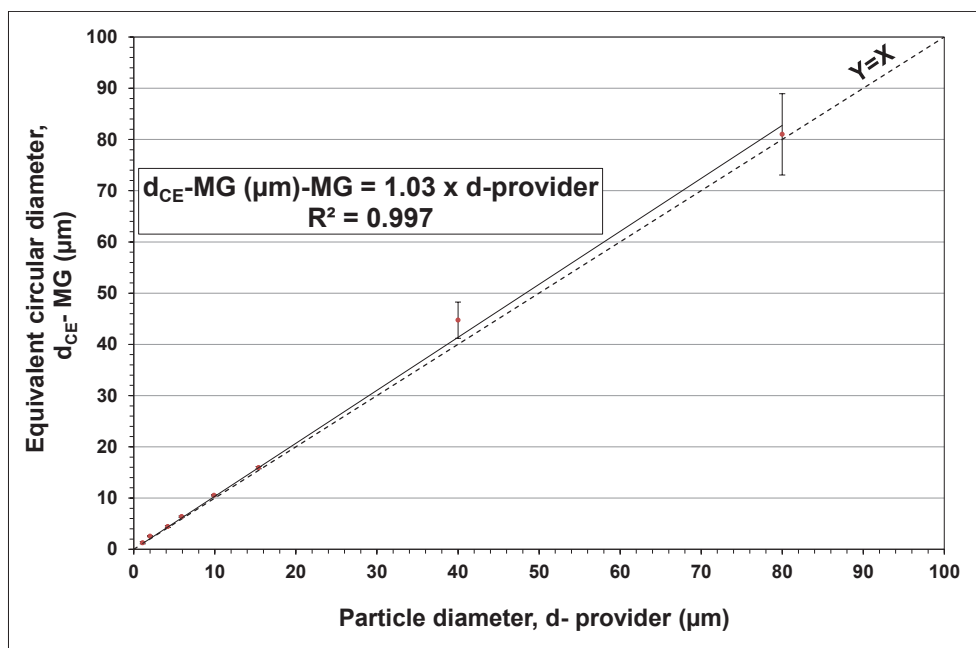


Figure III-3: Calibration of the morphogranulometer apparatus with the model particles over a size range from 1 to 80 μm

III.1.3.1.3 Dynamic light scattering (DLS)

The diffraction light scattering apparatus converts the detected scattered light into a volume size distribution of the equivalent spherical diameter (d_{SE}). Compared to MG and CYT measurements, deviation from the theoretical diameter was more noticeable (Figure III-4). These disparities would be certainly related to the assumption used (sphere model approximation) in the data processing algorithm of the DLS device. The linearity between the measured and theoretical diameter was verified but with a slope smaller than 1. That means that the diameter given by DLS measurements was underestimated compared to the provider information. The deviation from the linearity was approximately 14 %. Precision on the size determination with DLS was around 1 %, resulting thereby in a cumulative error of 15 %.

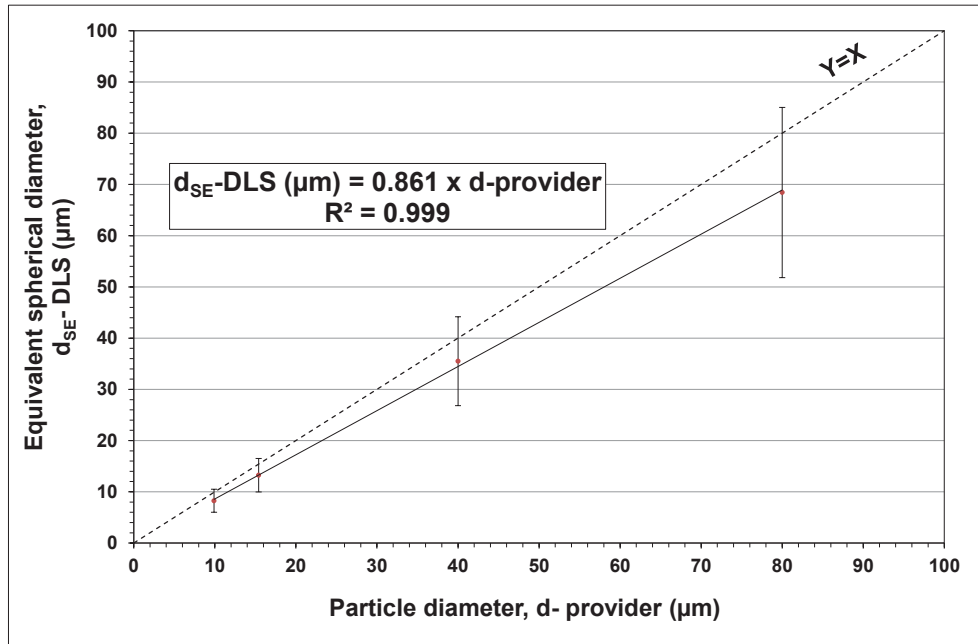


Figure III-4: Calibration of the dynamic light scattering device with the model particles over a size range from 1 to 80 μm

III.1.3.2 Comparison between the different techniques

Number and volume size distribution profiles provided by the three methods were compared for the 15 μm microsphere suspensions, as depicted in Figure III-5 (A, B). Flow cytometry and morphogranulometry results exhibited centered narrow peak representing the population. Nevertheless, broader size distributions were derived from the DLS measurements. This coarser distribution implied a limited capability of the DLS method to precisely resolve narrow sized populations in a mixed suspension. This results from the fact that DLS measures the scattering intensity which is proportional to the sixth power of the particle diameter. Hence, in the case of polydisperse suspension, the scattered light from the larger particles will overlay that from the smaller particles (Fissan et al. 2014). In addition, methods were also compared in terms of mean values. Figures III-5(C) and III-5(D) display the average values of the mean, 10th, 50th (median), and 90th percentile of the diameter for the three techniques. Results showed that dispersion in the particle diameter has tendency to increase gradually with morphogranulometry, cytometry and dynamic light scattering, respectively. This was expected since measurements rely on several mathematical models (sphere model) for flow cytometry and DLS, whereas no approximations were used in morphogranulometric (2D image analysis) analyses.

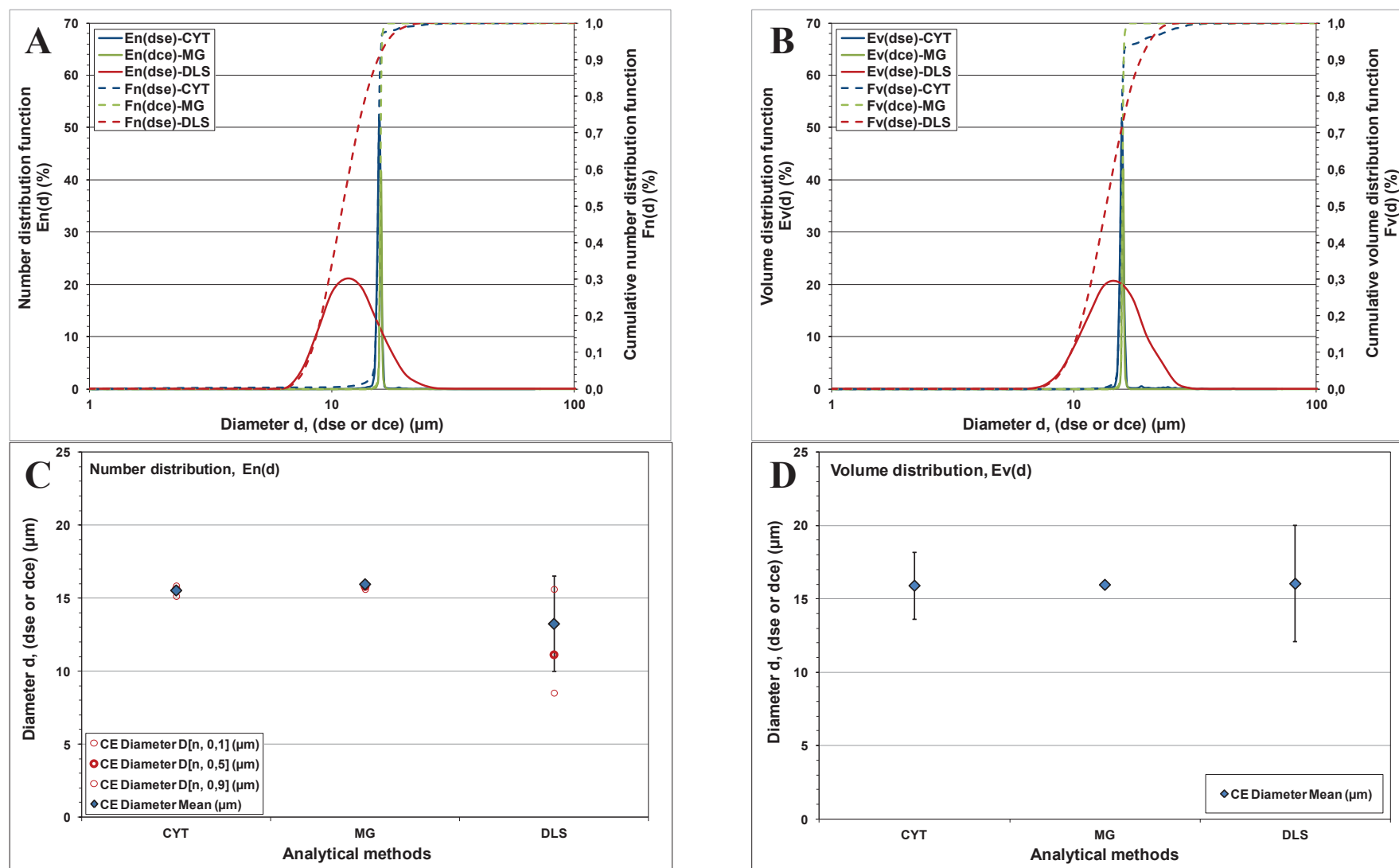


Figure III-5: Distribution and cumulative distribution functions, in number (E, $F_n(d)$) (A) and in volume (E, $F_v(d)$) (B), measured by the different methods for the particles of $15\mu\text{m}$ -diameter. Average values of the mean, 10th, 50th (median), and 90th percentile of the particle diameter, quantified in number (C) and in volume (D) by the three methods for the $15\mu\text{m}$ -beads

Mean diameters were also compared for all particle sizes (Table III-5). Acquired data revealed good agreements between methods. All three instruments provided approximately similar estimates of the average particle size. Specifically for flow cytometry and morphogranulometry techniques, a slight deviation was detected for the small particles (mean diameter of 1 and 2 μm). For both methods, results were quite similar for the larger beads (diameter higher than 4 μm), and were relatively close to the theoretical diameters. Diffraction light scattering measurements provided less accurate estimation of the size for the particles with 10, 15, 40 and 80 μm -diameter. Besides, the spread of the size distribution was more noticeable compared to flow cytometry and morphogranulometry methods. In the literature, studies comparing the size of model particles using a combination of these three methods are quite lacking. The technique of dynamic light scattering has been widely employed for sizing particles in liquid phase (Berne and Pecora 2000). Generally, DLS measurements lead to reasonably accurate results for monodisperse particle suspensions (Fissan et al. 2014). The broader standard deviation range covered by the DLS instrument for the larger particles (diameter higher than 10 μm) was in agreement with previous data reported in the literature. Indeed, (Kaye et al. 1997) reported that broader distribution for three different types of iron powders was observed with the laser diffraction than image analysis technique. The authors pointed out that artifacts resulting from the processing algorithm used in the DLS device was the cause of this difference (Yu and Erickson 2008). Flow cytometry is routinely used for the characterization of nanoparticles in cells (Nakamura and Ishimura 2010). No studies have been reported on the analysis of particle size over a range of diameters from 1 to 15 μm by flow cytometry. The polystyrene beads examined in this work were commonly used to calibrate particle size (FSC signal) on flow cytometers (Molecular probes, Invitrogen). On another hand, the low accuracy in size measurements of the small particles (1- and 2- μm diameter) compared with the manufacturer's data might be probably attributed to the errors associated with the power-law calibration of the FSC signal (as discussed in §.III.1.3.1.1). Morphogranulometry data (Table III-5) revealed considerable consistency with the measurements provided by the flow cytometer and diffraction light scattering devices. Image analysis of model particles using the Morphologi[®] G3 particle characterization system (morphogranulometer) has been previously reported for polystyrene beads of average diameter 40 and 140 μm (*Dynoseeds*[®], Microbeads AS) (Garland et al. 2013). Their results revealed that both distributions exhibited a well-defined peak close to the mean diameter: 37 μm for the TS-40 and 130 μm for the TS-140. Nevertheless, the authors showed that size

distributions for both particle sizes (40 and 140 μm) were far from monodisperse, as small fractions of particles with larger diameter were detected in the samples.

Table III-5: Comparison of the particle diameter determined by flow cytometry (based on power-law calibration), morphogranulometry (direct measurement) and diffraction light scattering (using sphere model approximation) measurements on the basis of number (D[1,0]) and volume (D[4,3]) size distribution: average equivalent diameters are expressed with their associated standard deviation

Provider information	MG		DLS		CYT	
d (μm)	D[1,0]	D[4,3]	D[1,0]	D[4,3]	D[1,0]	D[4,3]
1.1	1.28 \pm 0.20	1.34 \pm 0.11	–	–	1.44 \pm 0.14	1.45 \pm 0.15
2.0	2.57 \pm 0.12	2.59 \pm 0.09	–	–	1.60 \pm 0.16	1.60 \pm 0.16
4.2	4.44 \pm 0.20	4.47 \pm 0.25	–	–	4.35 \pm 0.43	4.35 \pm 0.44
5.9	6.38 \pm 0.13	6.38 \pm 0.13	–	–	6.64 \pm 0.66	6.64 \pm 0.66
9.9	10.5 \pm 0.1	10.5 \pm 0.1	8.3 \pm 2.2	10.4 \pm 2.8	10.3 \pm 1.0	10.3 \pm 1.0
15.4	16.0 \pm 0.2	16.0 \pm 0.2	13.2 \pm 3.3	16.0 \pm 4.0	15.7 \pm 1.6	15.7 \pm 1.6
40.0	44.7 \pm 3.5	45.5 \pm 3.5	35.5 \pm 8.7	42.9 \pm 10.6	–	–
80.0	81.0 \pm 7.9	83.3 \pm 8.2	68.4 \pm 16.6	82.5 \pm 20.3	–	–

III.1.3.3 Ability to discriminate spherical populations with close and different size

In order to evaluate the ability of the instruments to discriminate close (4- 6 μm) and different (1- 15 μm) size mixed subpopulations, volumetric mixtures of particles were prepared and characterized by CYT and MG methods (Table III-3). Particle mixtures were prepared by adding a number of drops from each standard. As precise drop dispensation was not provided in a homogenous way between the different assays, number proportions based on particle counting by flow cytometry were adopted. Beforehand, the accuracy of counting by flow cytometry was checked by means of a calibrated microspheres suspension (CountBright™ Absolute Counting Beads (C36950), Molecular probes, Invitrogen, USA): a value of $0.53 \cdot 10^5 \pm 0.01 \cdot 10^5$ events/ 50 μL was obtained for a calibrated solution containing $0.51 \cdot 10^5$ events/ 50 μL . Number proportions quantified by flow cytometry were thereafter compared with those determined by morphogranulometry. Images for the 1/15 and 4/6- μm beads are presented in Figure III-6 (data derived from morphogranulometry).

Figure III-7 compares the profiles of size distribution $En(d)$ and cumulative size distribution $Fn(d)$ between the two techniques for both particles mixtures (1/15- μm and 4/6- μm). Quantification data of each bead subpopulation are summarized in Table III-6. The results demonstrated the ability of flow cytometry and morphogranulometry instruments to discriminate and quantify subpopulations with close and distant size. Nevertheless, a sliding

effect towards smaller diameters was particularly observed with the morphogranulometer. This observation may be explained by a low focus on the finer particles when adjusting the microscope focus on the larger beads in the sample. This phenomenon was detected for the particle mixtures with distant diameters (1/15- μm), and was expected to be negligible for the particle suspensions of close sizes (4/6- μm). In both cases, number of particles in each subpopulation remains however correct, as particles with different size can be readily distinguished.

No similar approach was previously developed to assess the reliability of subpopulation quantification according to their size by the morphogranulometry analyzer. Troussellier et al (1999) showed that several bacterial cell groups having different apparent size can be discriminated by flow cytometry. This discriminatory power was also demonstrated by (Xiong et al. 2012) who analyzed a mixture of absolute counting standard particles (7.6 μm) and calibration beads (0.5; 0.9 and 3 μm) by flow cytometry. Indeed, their findings showed that distinct subpopulations can be readily identified for each particle size. In addition, in our study, comparing quantification data of the different size beads subpopulation (Table III-6) revealed slight differences between both methods. These disparities would be related to differences in the operational principle of each technique. Besides, different types of raw data were provided by each of the methods: the flow cytometer give number distributions of the equivalent spherical diameter (d_{SE}) using a single cell analysis approach. Whereas, the morphogranulometer provide size distribution based on equivalent circular diameter (d_{CE}) since the analysis relies on 2D image processing of particles. Comparing size distribution based on two different equivalent diameters (“ d_{CE} ”: circle model, and “ d_{SE} ”: spherical model) should be viewed cautiously.

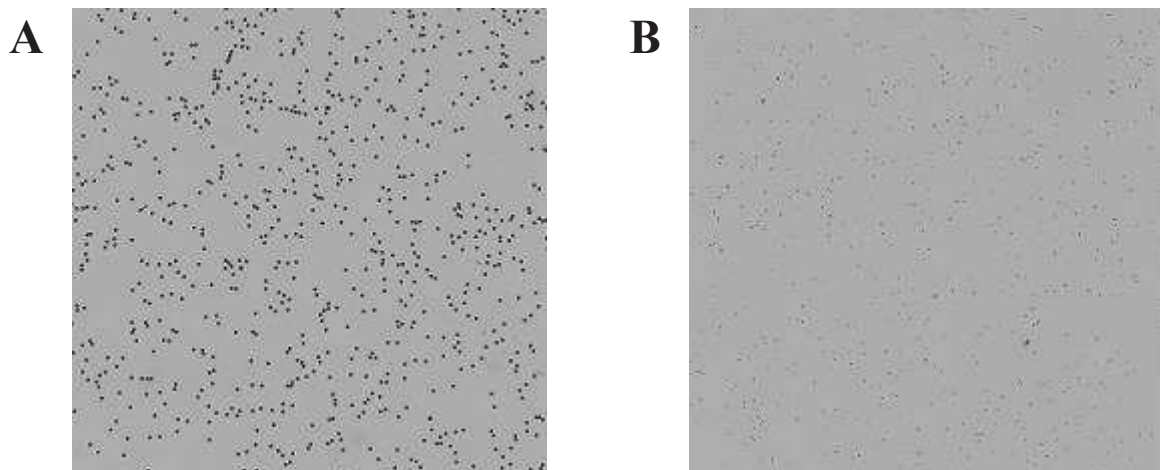


Figure III-6: Morphogranulometric images for the A-(1/15 μm); and B-(4/6 μm) mixed bead subpopulations. Analyses were performed at a magnification of x20 under bright filed mode

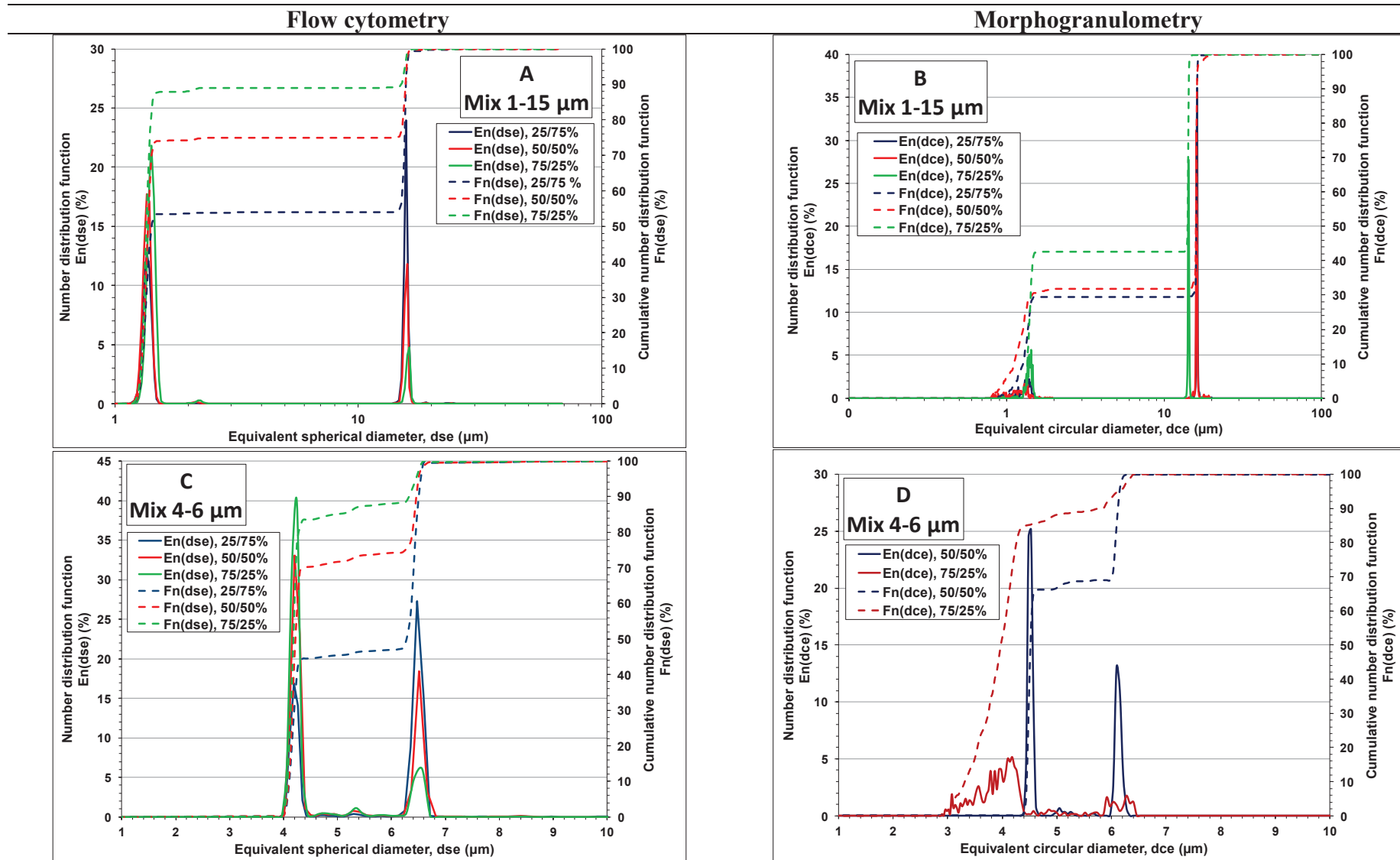


Figure III-7: Number distribution, $En(d_{SE}$ or d_{CE}) and cumulative number distribution, $Fn(d_{SE}$ or d_{CE}) functions for the 1-15 μm (A, B), and 4-6 μm mixed beads (C, D)

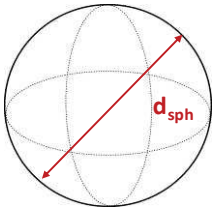
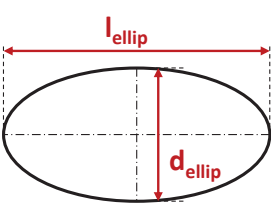
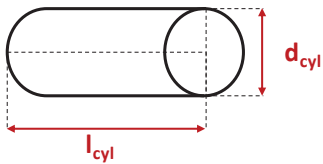
Table III-6: Comparison of subpopulation proportions between flow cytometry and morphogranulometry

Flow cytometry		Morphogranulometry	
Number proportion (%)		Number proportion (%)	
Mix 1-15 μm			
Pop. 1 (1- μm)	Pop. 2 (15- μm)	Pop. 1 (1- μm)	Pop. 2 (15- μm)
75	25	71	29
89	11	81	19
54	46	43	57
Mix 4-6 μm			
Pop. 1 (4- μm)	Pop. 2 (6- μm)	Pop. 1 (4- μm)	Pop. 2 (6- μm)
73	27	66	34
87	13	79	21
46	54	–	–

III.1.3.4 Sphere, elliptic and cylinder models: theoretical approach and impact on volume distribution

In order to properly describe the morphological evolutions in complex-shaped structures, elliptic and cylinder geometric models were analyzed and compared with the usual sphere model. The modeling approach relies on accurately calculating the projected surface and volume of each particle in the sample. 2D image analysis by morphogranulometry provides access to the different dimensional criteria of a particle, namely the diameter, the length and the width. The projected surface and volume for the sphere, ellipse and cylinder forms can therefore be expressed as follows (Table III-7):

Table III-7: Projected surface and volume formula for the sphere, ellipse and cylinder forms

	Sphere	Ellipse	Cylinder
Geometry			
Projected area	$S = \frac{1}{4}\pi (d_{sph})^2$	$S = \frac{1}{4}\pi d_{ellip} l_{ellip}$	$S = d_{cyl} l_{cyl}$
Volume	$V = \frac{1}{6}\pi (d_{sph})^3$	$V = \frac{1}{6}\pi (d_{ellip})^2 l_{ellip}$	$V = \frac{1}{4}\pi (d_{cyl})^2 l_{cyl}$

Assuming that particle volume calculated on the basis of the sphere approximation (V_{sph}) is equal to that determined according to the elliptic (V_{ellip}) or cylinder (V_{cyl}) models, volume size distribution can be calculated for each geometric form. Differences between sphere, elliptic or cylinder models can therefore be evaluated through the ratio between their corresponding volumes as a function of the aspect ratio AR, as follows:

$$\frac{V_{sph}}{V_{cyl}} = \frac{16}{3\pi^{3/2}} AR^{-1/2} \approx 0.958AR^{-1/2}; \quad \frac{V_{sph}}{V_{ellip}} = AR^{-1/2}$$

where AR is the aspect ratio, defined as the ratio between width (d) and length (L) of cells. The aspect ratio is a measure of particle elongation and has values in the range 0-1 (0: infinite line, 1: sphere).

A graphical illustration of the deviation between sphere/cylinder and sphere/elliptic models is presented in Figure III-8. Differences between elliptic and cylinder approximations is negligible ($\leq 5\%$). For elongated population (mycelial transition), elliptic and cylinder geometry appeared the most suitable for modeling the elongation phenomena and to estimate an accurate particle volume. The sphere model is totally inappropriate for low AR. In fact, if the AR are equal to 1; 0.5; 0.1 and 0.01, the volume ratio (V_{cyl}/V_{sph}) are 1.044; 0.738; 0.33 and 0.104, respectively. The error committed on the particle volume is significant: superior to 35% for AR equal to 0.5 and may reach 900% for AR of 0.01.

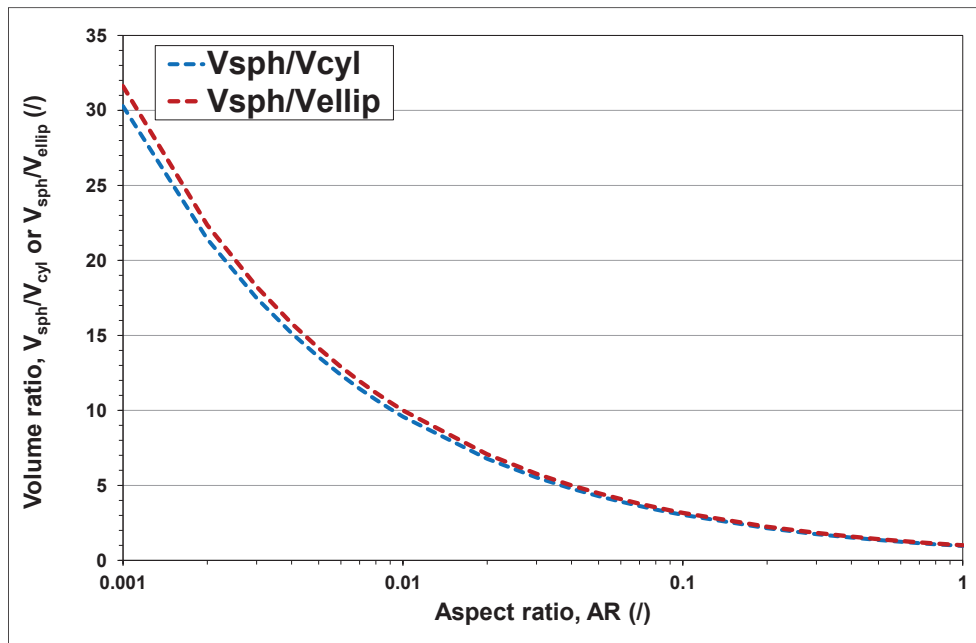


Figure III-8: Evolution of the ratio between the volumes of particle determined according to the sphere, elliptic or cylinder models

Accordingly, the choice of the geometric model is of major importance to accurately characterize morphology and size distribution. Figure III-9 presents an illustration of the deviation between the sphere and cylinder models for microbial populations with distinct morphologies. Volume distribution based on the sphere or cylinder models provided approximately similar results with the ovoid-shaped cells ($AR \approx 0.52$). Nevertheless, deviation

between both models was more noticeable with the elongated particles ($AR \approx 0.11$) and has tendency to increase with the raise of the aspect ratio.

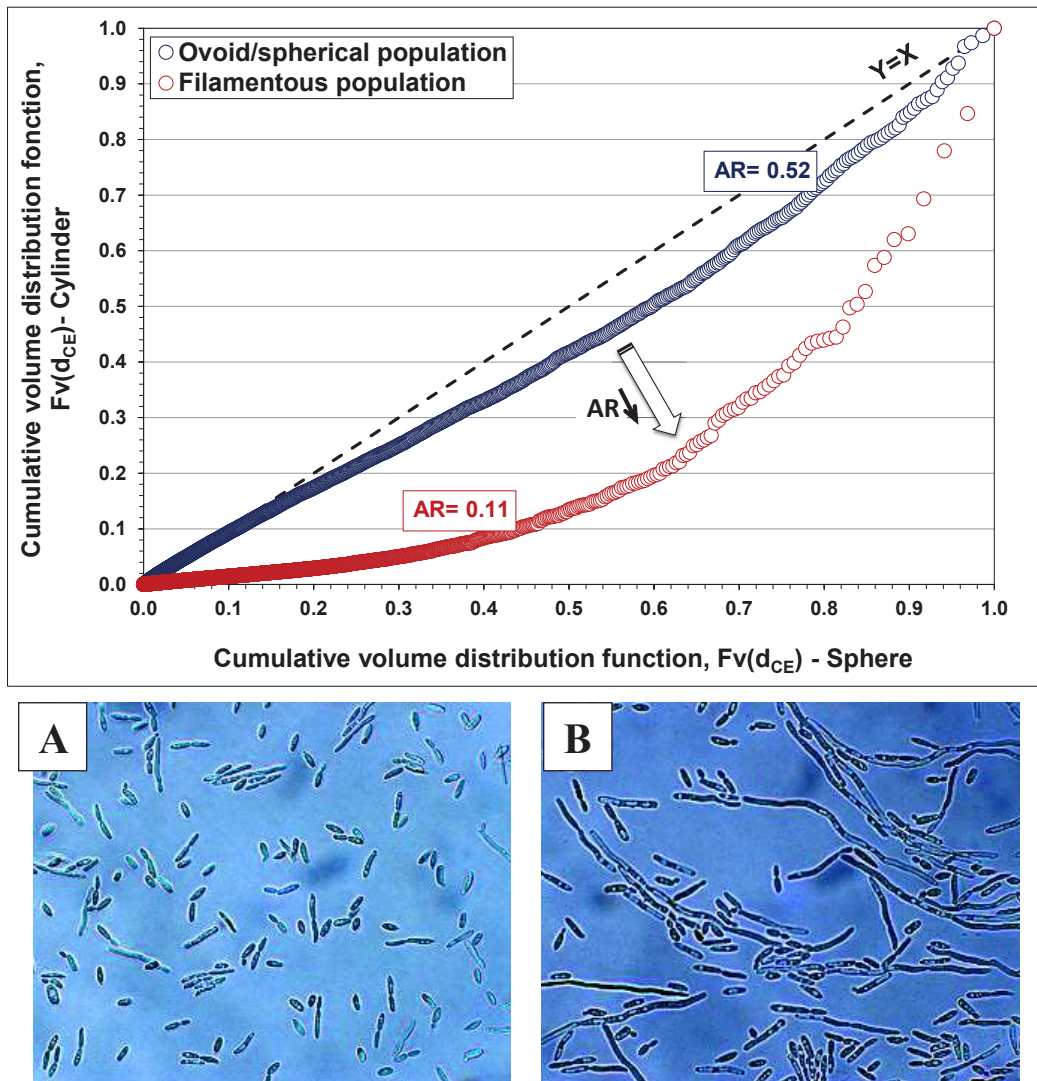


Figure III-9: Comparison between sphere and cylinder models and their impact on cumulative volume distribution functions with two morphologically-distinct yeast populations: (A) ovoid-shaped cells with $AR=0.52$ and (B) filamentous cells with $AR=0.11$ (Raw data: number distribution of d_{CE} , length and width from Morphology G3S)

III.1.4 Conclusion

In summary, characterizing suspensions comprised of a single monodisperse microsphere population by the three instruments provided similar measures of average particle size, and that agreed well with the actual bead size reported by the manufacturer. However, the techniques used in this study employ distinct principles for detecting and sizing particles and have different resolution capabilities, thus some disparities in size distribution patterns and derived particle dimensions were observed. Overall, these results are encouraging and suggest

that a combination of all the three techniques may provide a good approach for characterizing morphological changes in *Y. lipolytica*, the microorganism of interest in this study, at the population cell level. Nevertheless, it is important to stress that these methods may probably lead to different trends with the yeast cells since their morphology is much more complex than that of the regular-shaped model particles: under stress conditions, the microorganism has tendency to develop a heterogeneous morphology comprised primarily of mycelial cells. Besides, examining shape parameters more rich than a single diameter, such as the length, width and aspect ratio might be approached for an accurate description of the elongation phenomena.

III.1.5 Results synthesis

The capabilities of three particle sizing techniques; flow cytometry, morphogranulometry and diffraction light scattering; for the characterization of morphology and size distribution of *Y. lipolytica* populations were investigated using a set of microsphere standards across a diameter range from 1 to 80 μm . The presented results allow the following conclusions to be drawn:

- ⇒ Differences in the nature of the data generated by each technique should be considered in order to interpret and compare the results: the CYT technique provide an estimation of the diameter and length of the particles using a power-law calibration of the FSC and width signals according to an equivalent sphere model (by means spherical calibration beads of diameter in the range of 1 to 15 μm). Whereas, MG measurements, which are based on microscopic observations with image analysis, provided a direct measurement of the particle dimensions (without an approximation model). For the DLS apparatus, the equivalent diameter of the particles was calculated according to a sphere model.
- ⇒ Flow cytometry and morphogranulometry instruments provided generally mean diameter values similar to each other and that agreed well with the reported size of the standard. However, dynamic light scattering measurements underestimated the actual particle size by almost 14 %.
- ⇒ The magnitude of standard deviation extensively varies between techniques: for flow cytometry, standard deviation evolved from 10 to approximately 32 % on the diameter and length measures, respectively. This was due to the errors associated with the power-law calibration of the FSC and width signal derived from the device. Standard deviation was less pronounced with the data derived from morphogranulometry ($\approx 5\%$) for the particles of 1 to 15 μm -diameter. Nevertheless, deviation was more noticeable with the larger beads, which was in concordance with the manufacturer specifications (weak polydispersity of the larger particle suspensions). The DLS analysis induced a measurement error of 15 % on the particle diameter.
- ⇒ Regarding number and volume distributions, flow cytometry and morphogranulometry accurately identify individual narrow peaks in each particle suspension. Such small scale

features are not capable of being resolved with the DLS device. In fact, data are represented by a single broader peak with almost 7 times the width of the peaks determined by both other methods. Besides, the conversion of number distribution into volume distribution should be carefully scrutinized.

- ⇒ Both flow cytometry and morphogranulometry results showed accuracy and very high capability for resolving narrow (4-6 μm) and distant (1-15 μm) peaks in the distribution. However, some disparities in the quantitative proportions of the distinct sized subpopulations were observed. This might be probably attributed to variability in operational principle and nature of raw data generated by each of the technique.
- ⇒ The importance of choice of the geometric model that describes properly the shape of particle was demonstrated through comparing sphere, elliptic and cylinder modeling approaches: with ovoid/spherical populations, differences between models are negligible. However, as the aspect ratio of particles increased, deviation between sphere and cylinder models increased accordingly. The cylinder model provides more accurate description of the elongated shaped materials.

PART III: RESULTS AND DISCUSSION

Chapter III-2: Characterization of the mycelial transition of *Yarrowia lipolytica* by morphogranulometric measurements

Chapter III-2: Characterization of the mycelial transition of *Yarrowia lipolytica* by morphogranulometric measurements

III.2.1 Introduction

Yarrowia lipolytica, a yeast strain with a huge biotechnological potential, is subjected to mycelial transition induced by pH changes in the growth environment. This fungus is capable to grow as a mixture of yeast-like (ovoid/spherical forms) and mycelial (elongated forms) cells (Coelho et al. 2010). This behavior is of practical importance and should be carefully considered, especially when industrial applications are designed. In fact, the presence of filaments within the culture would greatly impact the rheological behavior of the fermentation broth, the heat, mass and momentum transfers, and consequently results in bioprocess performances deterioration (Fickers et al. 2009; Galvagno et al. 2011).

In the present chapter, the focus was placed on the characterization of morphology and size distribution during mycelial transition of *Y. lipolytica* through morphogranulometric analyses. Among the three techniques previously evaluated (*Chapter III.1*), morphogranulometry method was preferentially selected as it provides different dimensional parameters for each cell particle (diameter, length, width...), and permit thereby the application of cylinder model for the quantification of elongated subpopulations. First part of this study was dedicated to the standardization of inoculum morphology prior to inoculation into bioreactor. The objective was to ensure homogenous starting cultures between the independent pH levels, in order to provide more accurate understanding and interpretation of the morphological evolutions. Second part was devoted to the assessment of cell size distribution profiles, in number and in volume, during the time course of fermentation at the various pH (4.5; 5.6 and 7). Cylinder and sphere models were compared according to their accuracy in quantifying the mycelial subpopulation. In addition, the magnitude (intensity) of the filamentous behavior was examined through fiber length and aspect ratio measurements. Volume distribution based on this criterion was accordingly evaluated and compared between the different pH conditions. Finally, the last part summarizes the overall conclusions of this study.

Up to date, such a methodology has never been applied for characterizing mycelial growth in *Y. lipolytica*. The results presented in this chapter, in combination with the data on the validation of size characterization techniques (*Chapter III.1*), are structured in the form of a method article that will be submitted to a scientific journal for publication.

III.2.1 Experimental strategy

In this part, the ability of the morphogranulometric technique to quantify the dimorphic behavior of *Y. lipolytica* cells was examined. Dynamic evolutions in cell size distributions during the yeast growth was characterized and compared between different growth conditions. Three independent cultures of *Y. lipolytica* were carried out on minimum medium (MM) containing 10 g L⁻¹ glucose under dimorphism inducing conditions (pH stress). The pH was selected as an inducer of filamentous growth: acidic (pH 4.5) and neutral pH (pH 7) conditions were tested, and morphological evolutions were compared with a reference culture under a non-filament inducing condition (pH 5.6, optimal condition). The purpose of evaluating two distinct stressful pH levels (pH 4.5 and 7) was to assess the capability of the method to quantify the filamentous behavior at different level of intensity. The strain used in this study was the wild-type *Y. lipolytica* W29 (ATCC® 20460™). Medium composition, culture conditions (bioreactor fermentations), sampling strategy, as well as the analytical tools employed for biomass characterization are described in details in the “Materials and Methods” part of the thesis.

III.2.3 Results and discussion

III.2.3.1 Standardization of initial cell population morphology

In order to compare the morphological evolutions between the different culture conditions (pH 4.5; 5.6 and 7), similarities in the morphology and size distribution profiles of the initial cell populations need to be checked. For each culture, inoculum cultures were prepared under the same optimized conditions (medium composition, incubation conditions). Figure III-10 represents microscopic observations of the initial cultures for each pH condition. In the three independent cultures, *Y. lipolytica* exhibited a homogenous morphology comprised predominately of ovoid-shaped cells. Average cell diameters ranged between 8.08±2.12; 7.94±2.13 and 7.34±1.86 μm under pH 4.5; 5.6 and 7 respectively. Additional morphological characteristics (fiber length, fiber width and aspect ratio) of the initial populations are presented in Table III-8.

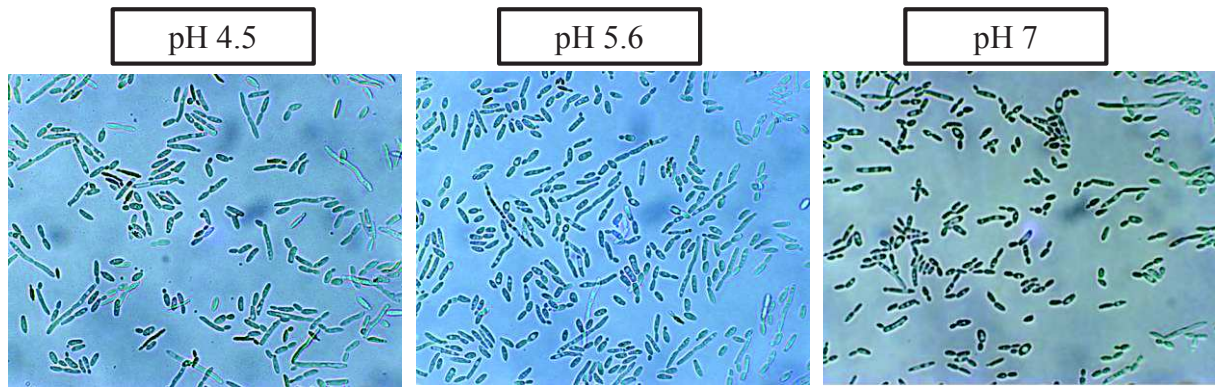


Figure III-10: Microscopic observations of the initial cell populations at pH 4.5; 5.6 and 7. Images were taken under a light microscope, without oil fixation and at magnifications of 40 \times . The image size (width x height) is 54 μm x 44 μm

Table III-8: Morphological characteristics of the initial populations: Mean values of the equivalent circle diameter (d_{CE}), aspect ratio (AR), fiber length (L_f) and fiber width (W_f) are expressed with their associated standard deviations

Parameter	pH 4.5	pH 5.6	pH 7
Diameter (d_{CE}) (μm)	8.08 \pm 2.12	7.94 \pm 2.13	7.34 \pm 1.86
Aspect ratio (/)	0.45 \pm 0.20	0.54 \pm 0.18	0.41 \pm 0.16
Fiber length (μm)	13.0 \pm 6.8	14.8 \pm 8.0	13.0 \pm 5.6
Fiber width (μm)	5.78 \pm 1.28	8.14 \pm 1.14	5.05 \pm 1.55

In addition, morphological similarities between the initial populations were statistically verified through parametric tests: Student's t-test and overlapping (OVL) coefficient determination. Assessing the normality of cell size distribution at the population level was required for executing these tests. Details on the statistical calculations used in the present study are presented in the “Materials and Methods” section of the thesis (*See § II.4.1.3.1.2*). As depicted in Figure III-11, number distribution of the equivalent circular diameter (d_{CE}) followed a normal law for the three independent initial cultures. Normality criteria C1 (mean/median) and C2 (MAD/STDV) were satisfied on both linear and logarithmic scales (Table III-9). Mean and standard deviation of each size distribution were approximately identical, notably with the logarithmic diameter. On another hand, morphological similarities between the three independent cultures were also validated with an overlapping coefficient of 0.8 emphasizing thus the standardization of inoculums morphology.

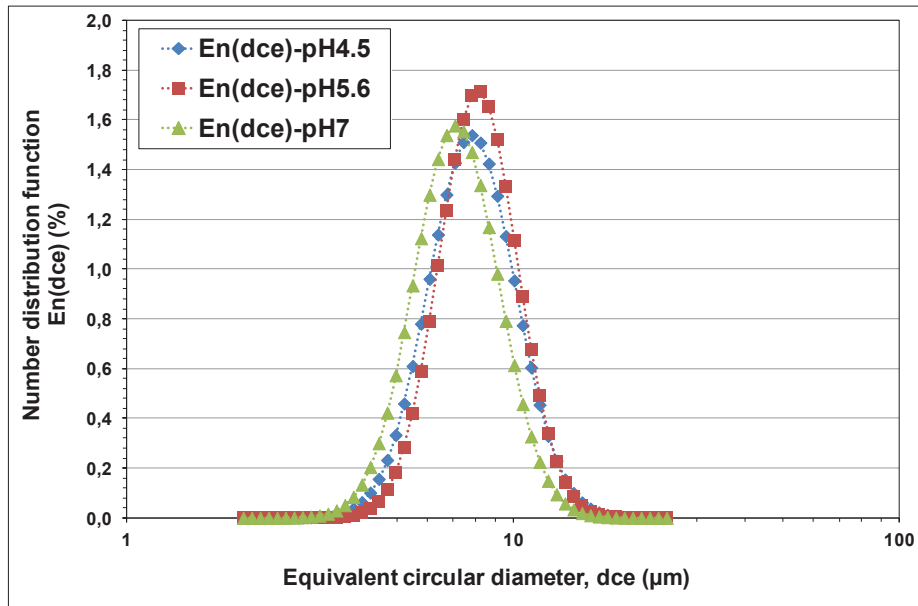


Figure III-11: Graphical illustration of the log-normality of the size distribution for the initial cell populations: comparing number distribution function of the equivalent circle diameter (d_{CE}) between the three pH conditions

Table III-9: Determination of mean, standard deviation and normality criteria for the initial cell populations

Normality criteria	pH 4.5		pH 5.6		pH 7	
	Linear	logarithmic	Linear	logarithmic	Linear	logarithmic
Mean d_{CE} (μm)	8.08	7.82	7.94	7.94	7.34	7.12
Standard deviation (μm)	2.12	1.30	2.13	1.26	1.86	1.29
C1=mean/median	1.02	0.99	1.05	1.01	1.02	0.99
C2=MAD/STDV	0.73	0.75	0.72	0.76	0.77	0.78

On the basis of the equivalent circle diameter, a threshold criterion of $15 \mu\text{m}$ representing the upper diameter of almost 99.7 % ($\bar{x} + 3\sigma$) of the initial cell cultures (in number) was therefore selected in order to distinguish between the ovoid-shaped and filamentous subpopulations. The mycelial behavior of *Y. lipolytica* was quantified by analyzing the evolutions in the filamentous fraction (cells with $d_{CE} > 15 \mu\text{m}$) during fermentation.

Similarly to the quantitative approach developed with the equivalent diameter (d_{CE}), a discriminatory threshold of $40 \mu\text{m}$ (slightly higher than the $\bar{x} + 3\sigma \approx 35 \mu\text{m}$, in number) on the fiber length was adopted to quantify the proportion of filamentous subpopulation.

III.2.3.2 Mycelial transition versus pH: quantification and magnitude

Considering the diameter (d_{CE}) and associated number and volume distributions, dynamic evolutions in the yeast morphology were assessed during growth at the different pH. Qualitative (mean diameters) and quantitative (filamentous fraction) analyses of the mycelial transition were performed based on number and volume distributions. Furthermore, deviations

between sphere and cylinder models were analyzed with respect to the mycelial trends. Additional morphological criteria (fiber length, width and aspect ratio) were examined in order to evaluate more precisely the propensity and the magnitude of the filamentous behavior. Microscopic images illustrating the morphological aspect of the cell population at the end of the fermentation at a given pH are depicted in Figure III-12. One can observe an induction of mycelial transition at pH 4.5 and 7.

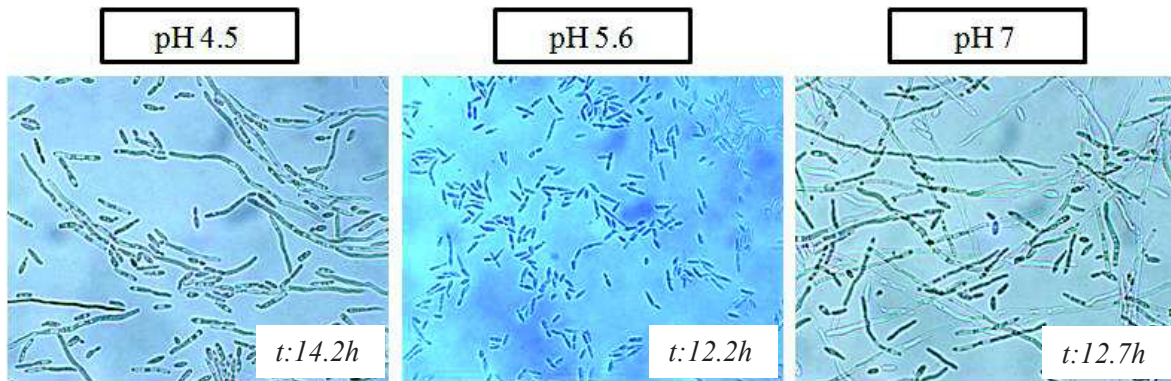


Figure III-12: Morphology of *Y. lipolytica* at the end of the culture under pH 4.5; 5.6 and 7. Observations were performed with a light microscope, without oil fixation and at magnifications of 40 \times . Image size (width x height): 54 μm x 44 μm

III.2.3.2.1 Equivalent circle diameter distribution

III.2.3.2.1.1 Number distribution of the equivalent circle diameter, $\text{En}(d_{\text{CE}})$

Changes in the cumulative d_{CE} distribution function in number, $\text{Fn}(d_{\text{CE}})$ as a function of the diameter (d_{CE}) were presented in Figure III-13 for the three pH tested. As growth progressed, transition towards higher diameter was observed for the cells cultivated under pH 4.5 and 7. On the contrary, the morphology has tendency to evolve into smaller sizes for the culture at pH 5.6. These results were confirmed with the quantification data on the filamentous subpopulation (cells with $d_{\text{CE}} > 15 \mu\text{m}$), as presented in Table III-10. The filamentous fraction evolved from 1.4, 2.0, and 0.4 up to 11.3, 0.5 and 7.7 % at pH 4.5, 5.6 and 7 respectively. Mycelial transition was demonstrated at pH 4.5 and 7 whereas ovoid-shaped cells predominated at pH 5.6. Considering number based calculations of the size distribution, mycelial trends were not significantly elucidated. Indeed when the data were number-weighted, each cell particle, regardless of its morphology, has equal statistical weight once the final distribution was calculated. However, when converting these results into volume distribution, the size distribution would shift into the elongated forms since the majority of total particle volume comes from the larger cell particles. Volume-based calculations are therefore potentially preferred to accurately elucidate the mycelial trends but the geometrical model should be accurately defined (*cf. Chapter III.1*).

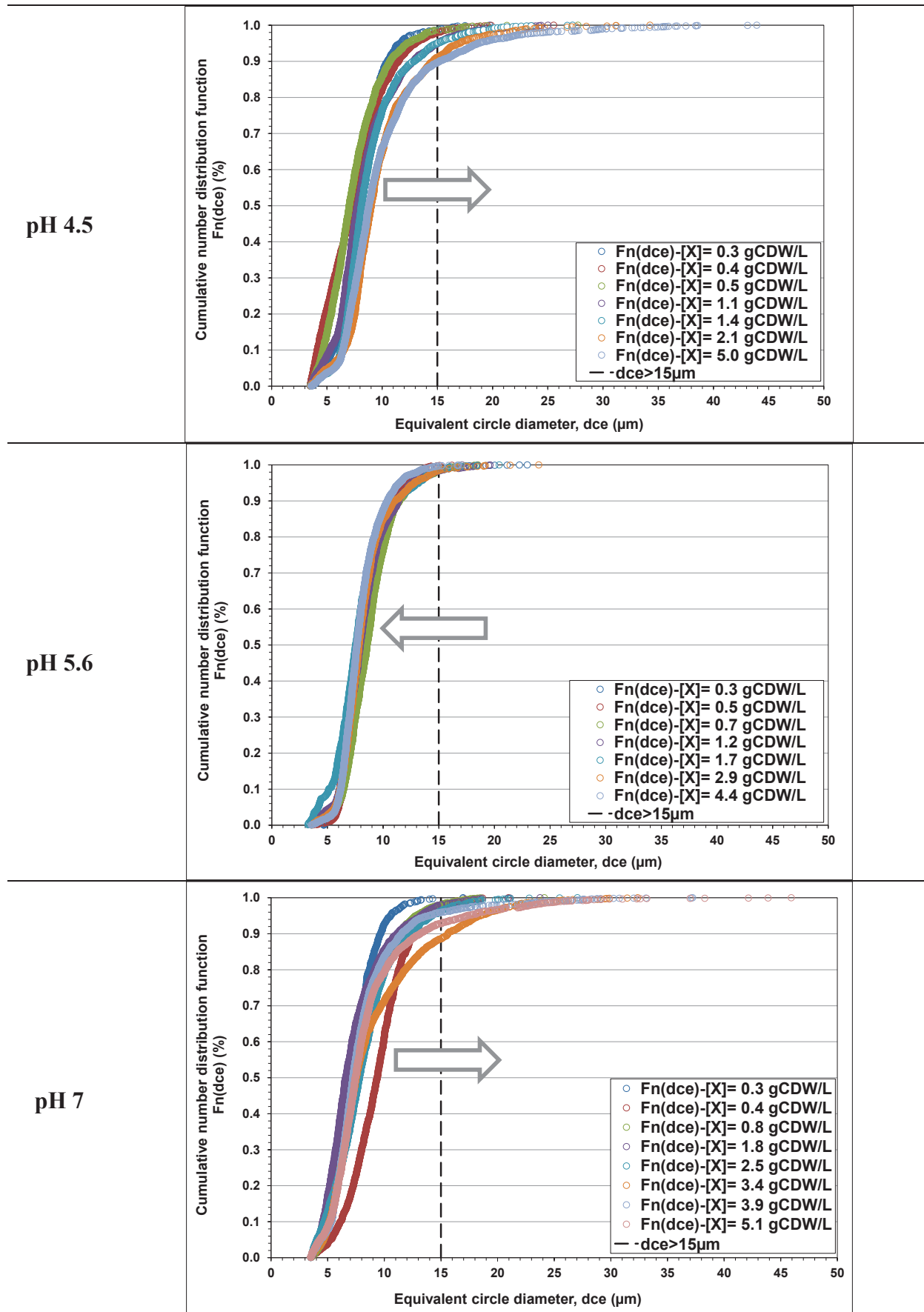


Figure III-13: Evolutions of the cumulative number distribution functions of the equivalent circle diameter, $F_n(d_{ce})$ during the cultures at pH 4.5, 5.6 and 7

Table III-10: Qualitative and quantitative investigation of the mycelial behavior of *Y. lipolytica* considering number-based distribution of the equivalent diameter (d_{CE})

	Qualitative analysis			Quantitative analysis		
	D[1,0] (μm)			Fn ($d_{CE} > 15 \mu\text{m}$) (%)		
	pH 4.5	pH 5.6	pH 7	pH 4.5	pH 5.6	pH 7
[X]=0.3 g CDW L ⁻¹	8.08±2.12	7.94±2.13	7.34±1.86	1.4	2.0	0.4
[X]=1 g CDW L ⁻¹	8.55±3.24	8.33±2.32	7.34±2.79	6.1	2.1	2.5
[X]=2 g CDW L ⁻¹	9.87±3.76	8.27±2.28	8.24±3.10	10.2	2.0	4.4
[X]=5 g CDW L ⁻¹	10.08±4.68	7.98±1.80	8.71±4.83	11.3	0.5	7.7

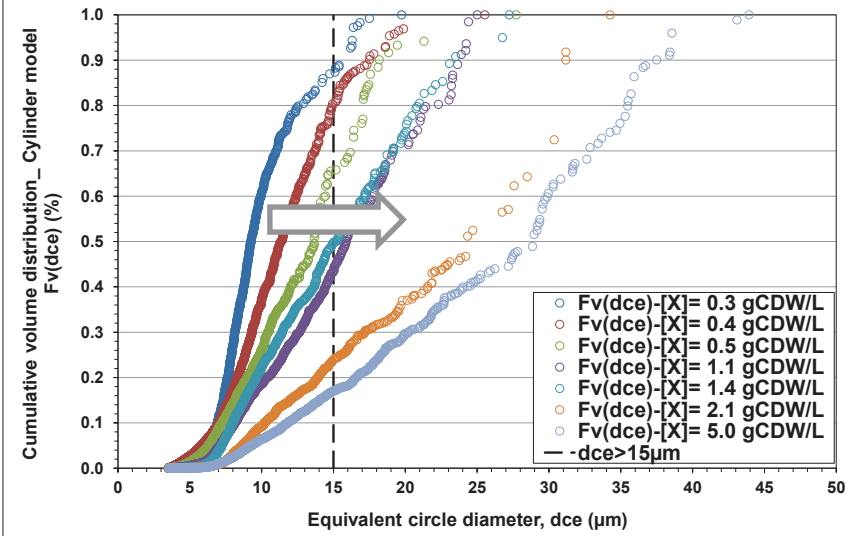
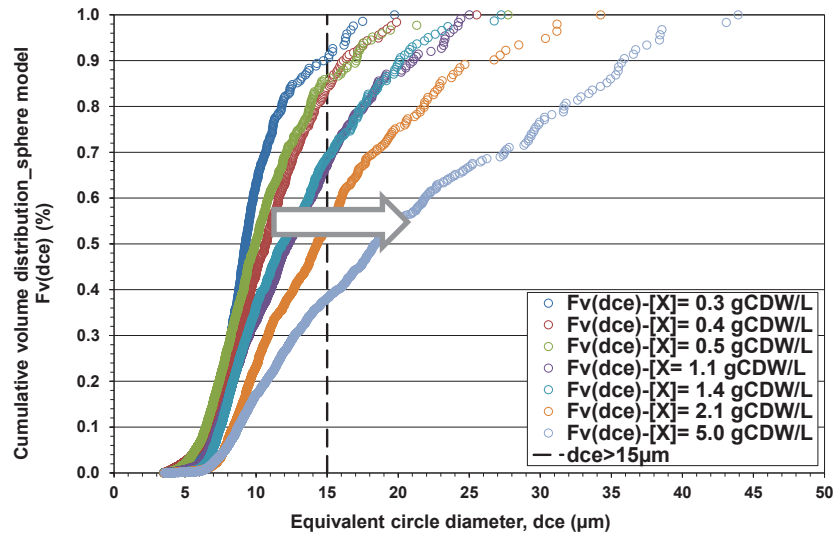
III.2.3.2.1.2 Volume distribution of the equivalent circle diameter, $Ev(d_{CE})$: comparison between sphere and cylinder models

Dynamics evolutions in the yeast morphology were characterized on the basis of volume-weighted distributions by the application of two different geometric models: sphere and cylinder. Details on the theoretical approach related to both models are presented in the chapter III.1 (§ III.1.3.4). Accurate measurements of the length and width of cells, as well as assumptions on a constant intrinsic cell density (so that the equivalence mass-volume could be considered) (Fillaudeau et al. 2009) were mandatory for the application of the cylinder model. Figure III-14 compares the cumulative distribution functions in volume of the d_{CE} for the different cultures with cylinder and sphere models. Average volume diameters $D[4,3]$, as well as fractions of the filamentous subpopulation at different biomass concentration (from 0.3 to 5 g CDW L⁻¹) were presented in Table III-11. Results showed that mycelial transition was demonstrated by the application of both models for the cultures at pH 4.5 and 7: cell diameters reached 20.9 (sphere model) and 26.3 μm (cylinder model) at pH 4.5. Under neutral conditions, cell diameters attained 20.2 and 31.2 μm with the sphere and cylinder model, respectively. A noticeable divergence between models was demonstrated as cell elongation increased. Filament formation was more properly described with the cylinder model. Based on the sphere model, the filamentous fraction increased from 10.0 and 3.5 up to 63.5 and 62.3 % for the cultures at pH 4.5 and pH 7, respectively. With the cylinder model approximation, the mycelial population evolved from 13.0 and 12.3 up to 84.1 and 92.7 % at pH 4.5 and 7, respectively. No mycelial transition was observed for the culture at pH 5.6: filamentous cells represented a small proportion of the population that did not exceed 3.5 % (in volume) at the end of fermentation. Difference between sphere and cylinder models was not detected with the ovoid-shaped cell populations (culture at pH 5.6). Applying geometric models for mycelial transition characterization, as provided by this study, has never been reported in the literature. Accordingly, confronting our results with existing research was not affordable.

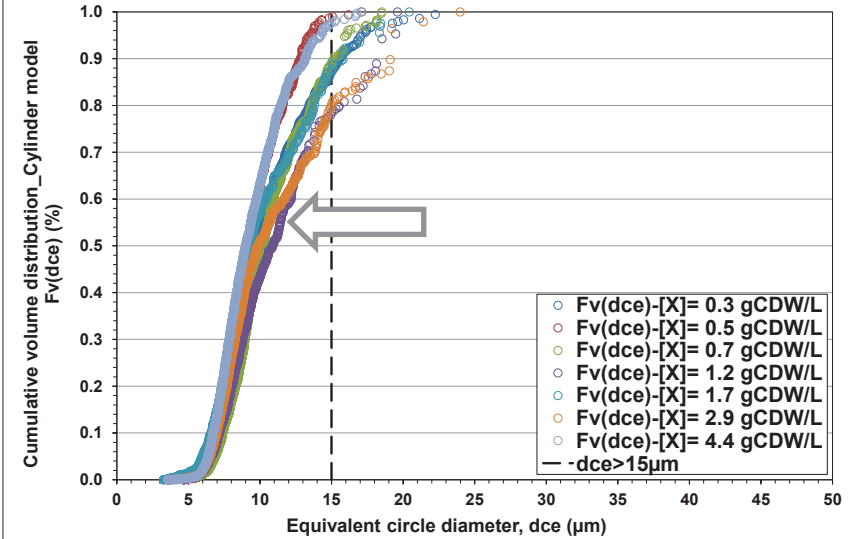
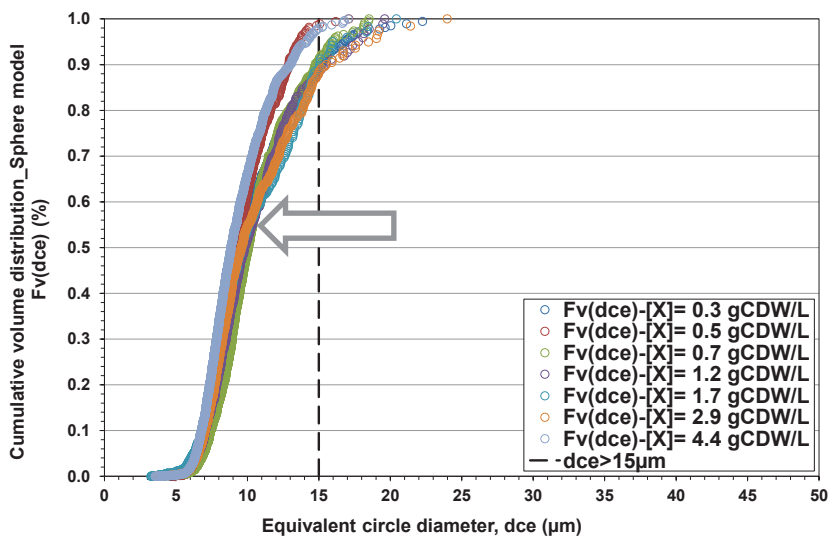
Sphere model

Cylinder model

pH 4.5



pH 5.6



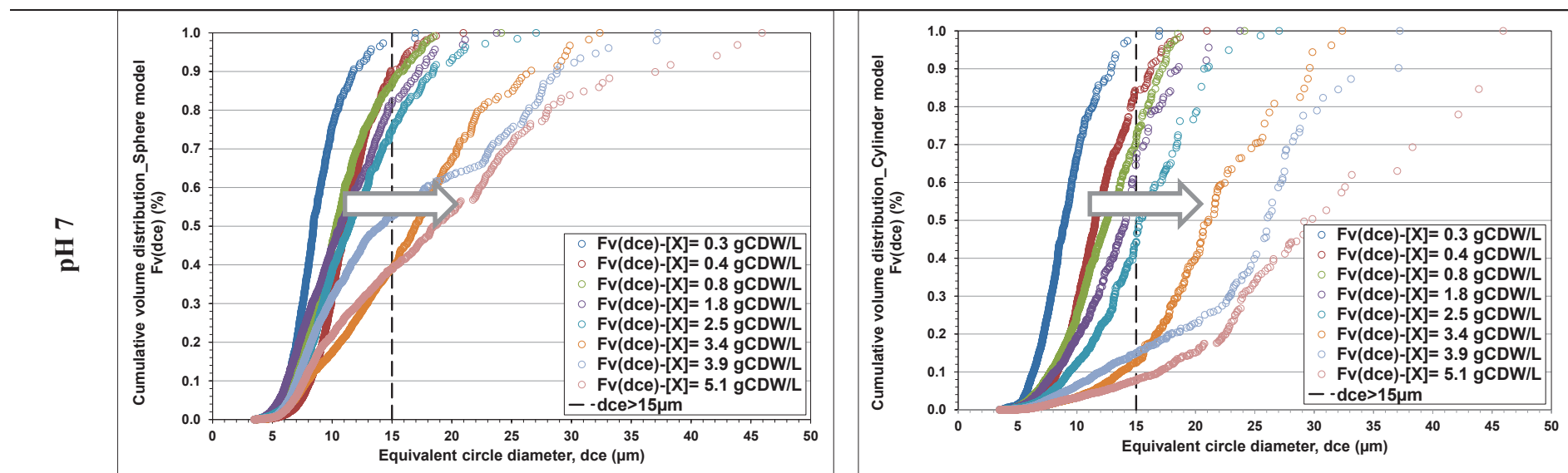


Figure III-14: Evolution of the cumulative distribution function in volume of the equivalent circle diameter, $Fv(d_{CE})$ during the time course of fermentation at the different pH considering the sphere and cylinder models

Table III-11: Qualitative and quantitative assessment of the filamentous behavior of *Y. lipolytica* based on the sphere and cylinder models: comparison between cultures at pH 4.5; 5.6 and 7

Biomass concentration (gCDW L ⁻¹)	Qualitative analysis D[4,3] (μm)						Quantitative analysis Fv (d _{CE} >15 μm) (%)					
	Sphere			Cylinder			Sphere			Cylinder		
	pH 4.5	pH 5.6	pH 7	pH 4.5	pH 5.6	pH 7	pH 4.5	pH 5.6	pH 7	pH 4.5	pH 5.6	pH 7
0.3	9.98±2.95	10.44±3.32	8.88±2.38	10.16±3.17	10.58±3.52	9.32±2.54	10.0	12.6	3.5	13.0	15.1	12.3
1	13.16±5.08	10.65±3.32	11.31±4.31	16.01±5.60	11.67±4.01	13.85±4.21	32.9	13.6	21.0	59.6	23.0	42.1
2	15.83±6.88	10.57±3.42	12.33±4.65	23.04±8.40	10.44±3.71	15.77±4.73	48.4	13.2	27.9	77.8	14.3	60.4
5	20.85±10.42	9.39±2.37	20.22±10.94	26.31±9.68	9.49±2.44	31.19±10.98	63.5	3.4	62.3	84.1	3.5	92.7

III.2.3.2.2 Fiber length distribution

The morphogranulometry instrument provides access to additional criteria, namely the fiber length, width, aspect ratio, circularity, etc. In our case, the fiber length may represent an appropriate parameter for describing the elongated patterns of cells. For this purpose, number and volume distributions based on fiber length were analyzed and dynamics evolutions were qualitatively and quantitatively compared between the pH conditions tested.

III.2.3.2.2.1 Number distribution of the fiber length, $En(l_f)$

The intensity of the filamentous behavior in response to pH stress was assessed through the comparison of the fiber length distribution profiles. Figure III-15 illustrates the cumulative number distribution of the fiber length, $En(l_f)$ for the cells grown at pH 4.5; 5.6 and 7. Results demonstrated that filament intensity was more noticeable at pH 4.5 and 7, compared to the culture at pH 5.6. Nevertheless, variabilities in cell elongation between pH conditions were not clearly elucidated on the basis of number-weighted distribution. Indeed, fiber elongation for 50 % of the population increased from 13.0 to 20.0 μm at pH 4.5, and from 13.0 to 19.2 μm at pH 7. This average value decreased from 14.8 up to 12.5 μm during the culture under pH 5.6. As depicted in Table III-12, quantitative data on the filamentous subpopulation (cells with $l_f > 40 \mu\text{m}$) revealed approximately similar proportions of elongated cells ($\approx 8\%$) at the end of fermentation at pH 4.5 and 7. Yeast subpopulations with fiber length higher than 100 μm did not exceed 1.3 % for both stressful pH.

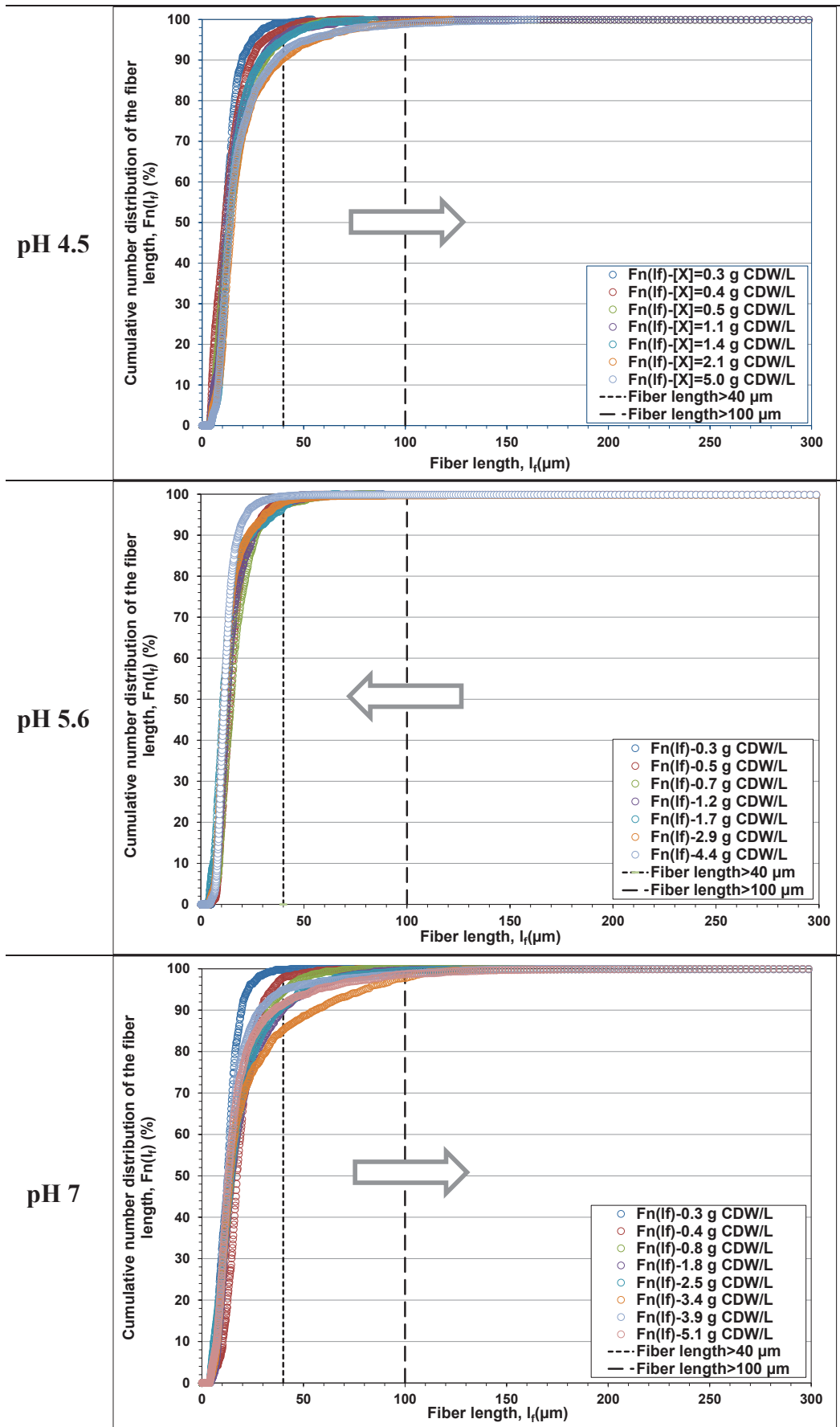


Figure III-15: Cumulative number distribution of the fiber length, $F_n(l_f)$ during the cultures at different pH.

Table III-12: Qualitative and quantitative characterization of the mycelial growth in *Y. lipolytica* based on number distribution of the cell length

Biomass concentration (g CDW L ⁻¹)	Qualitative analysis			Quantitative analysis					
	Fiber length: mean±SD (μm)			Fn (l _f >40 μm) (%)			Fn (l _f >100 μm) (%)		
	pH4.5	pH5.6	pH7	pH4.5	pH5.6	pH7	pH4.5	pH5.6	pH7
0.3	13.0±6.8	14.8±8.0	13.0±5.6	0.9	1.6	0.3	0.0	0.0	0.0
1	15.8±11.1	15.4±9.4	20.0±15.3	4.2	2.5	9.8	0.1	0.0	0.3
2	20.9±20.2	13.8±10.1	19.0±16.2	9.6	3.1	9.0	0.8	0.0	0.5
5	20.0±20.5	12.5±5.2	19.2±20.3	8.1	0.6	8.7	1.1	0.0	1.3

III.2.3.2.2.2 Volume distribution of the fiber length, Ev (l_f)

Based on a volume-weighted distribution, evolutions in fiber length measurements were monitored for biomass concentration in the range of 0.3–5 gCDW L⁻¹. As shown in (Figure III-16, Table III-13), mycelial trends were markedly demonstrated under neutral and acidic (pH 4.5) conditions. The yeast-to-mycelium transition was significantly more intensified at pH 7. Comparing evolutions in the mean length parameter for the three pH conditions (Figure III-17, Table III-13) highlighted a significant increase in the cell elongation that reached 69.0 and 74.9 μm at pH 4.5 and pH 7, respectively. However, the width of the cells remained relatively constant (≈ 6 μm) across the various conditions. Quantitative characterization of the mycelial trends (Table III-13) demonstrated greater effect of the neutral pH on the yeast morphology: filamentous cells represented more than 62.7 % of the entire population at pH 7, compared to 55.4 % at pH 4.5. More than 25.6 % (in volume) of the cells exhibited a length higher than 100 μm. In addition, it is important to highlight that standard deviations on the fiber length are significantly important, especially for the highly elongated samples. This pointed out a noticeable dispersion of the fiber length measures within the population, as was clearly shown with the data on the fiber length distributions (Figure III-16).

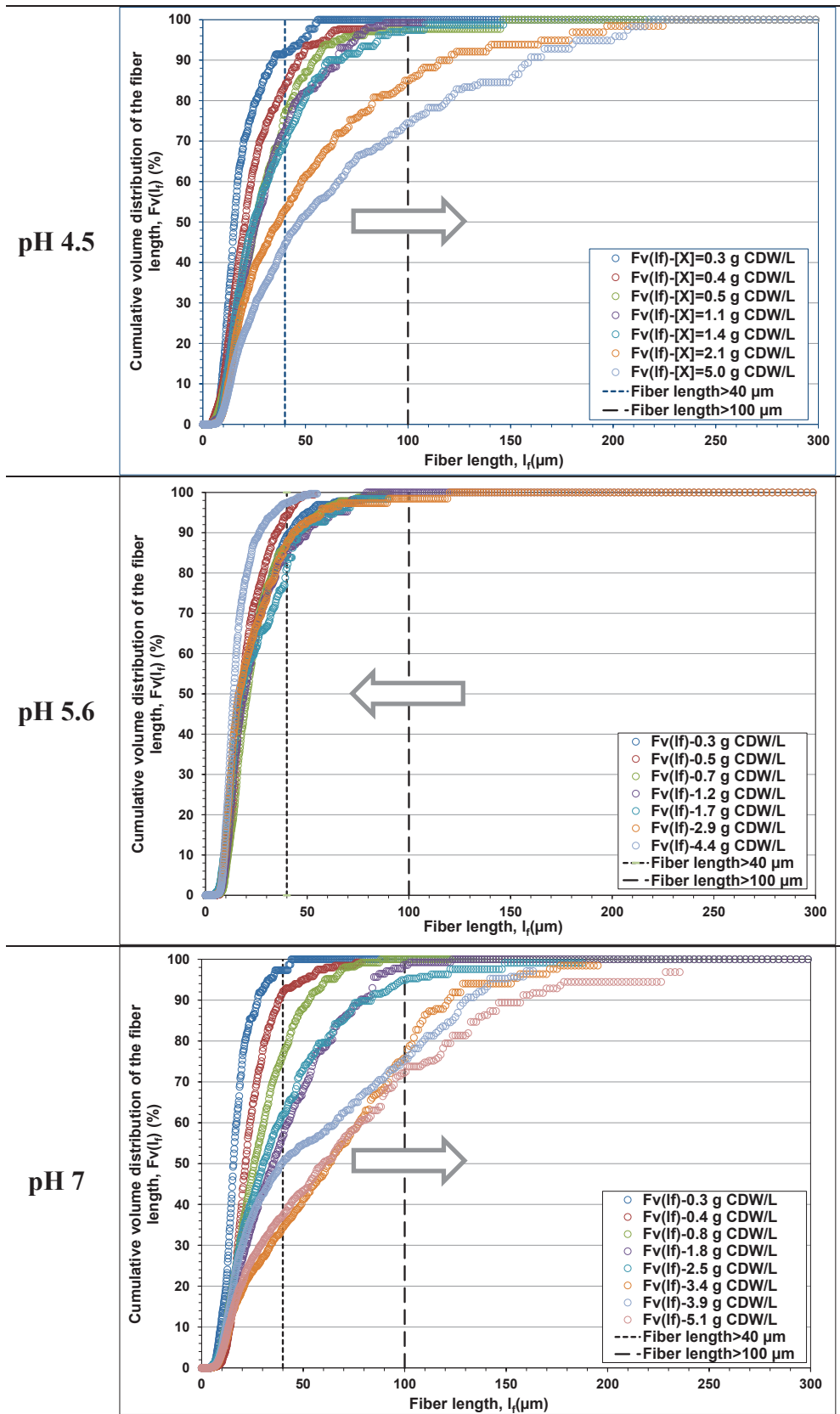
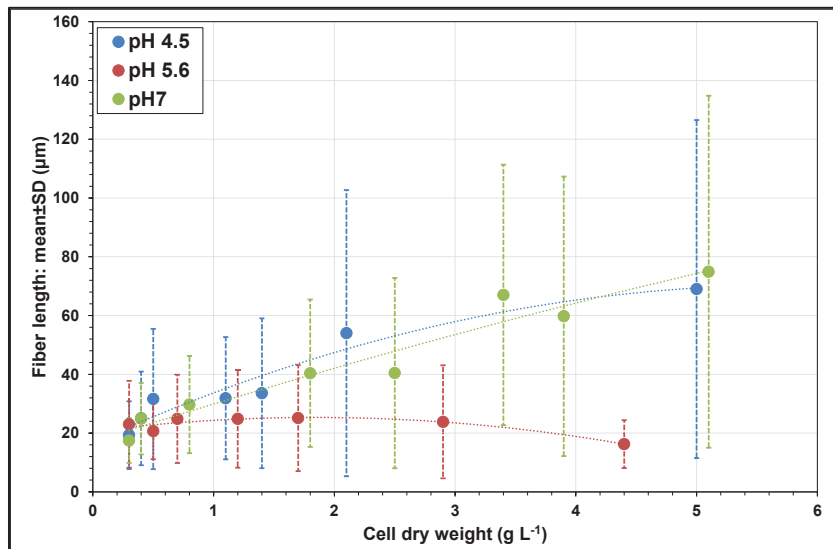


Figure III-16: Cumulative volume distribution of the fiber length, $Ev(l_f)$ during the cultures at different pH

Table III-13: Qualitative and quantitative analysis of mycelial growth intensity based on volume distribution of the cell length

Biomass concentration (g CDW L ⁻¹)	Qualitative analysis					
	Fiber length: mean \pm SD(μ m)			Fiber width: mean \pm SD(μ m)		
	pH4.5	pH5.6	pH7	pH4.5	pH5.6	pH7
0.3	19.3 \pm 11.5	23.0 \pm 14.8	17.5 \pm 7.6	5.78 \pm 1.3	8.14 \pm 1.1	5.05 \pm 1.5
1	31.9 \pm 20.8	24.9 \pm 16.6	40.4 \pm 25.1	6.08 \pm 3.2	5.63 \pm 1.6	5.40 \pm 2.9
2	54.0 \pm 48.7	25.1 \pm 18.0	40.4 \pm 32.4	6.76 \pm 3.6	5.41 \pm 1.1	5.28 \pm 4.2
5	69.0 \pm 57.5	16.2 \pm 8.1	74.9 \pm 59.9	7.49 \pm 4.7	5.85 \pm 1.5	6.54 \pm 6.8

Biomass concentration (g CDW L ⁻¹)	Quantitative analysis					
	Fv (l _f > 40 μ m) (%)			Fv (l _f > 100 μ m) (%)		
	pH4.5	pH5.6	pH7	pH4.5	pH5.6	pH7
0.3	8.0	10.7	2.7	0.0	0.0	0.0
1	27.4	15.4	43.2	2.3	0.0	1.4
2	47.0	18.7	38.0	15.1	0.0	5.1
5	55.4	2.7	62.7	25.6	0.0	27.5

**Figure III-17:** Evolution of the mean values for the fiber length, in volume, for the three pH conditions. Average values are expressed with their associated standard deviation

III.2.4 Conclusions

The use of morphogranulometry technique to quantify the mycelial transition of *Y. lipolytica* resulted in consistent and statistically representative morphological data. Considering diameters and associated number and volume distributions, dimorphism was observed and characterized by an increase in the proportion of the filamentous subpopulation (cells with d_{CE} greater than 15 μ m) until 84.1 and 92.7 % (v/v) at pH 4.5 and pH 7, respectively. In addition, the cylinder model that confined-well with the elongated patterns of the cells appeared to be more appropriate for describing the dimorphism phenomena in *Y. lipolytica*. The findings highlighted the relevance of the chosen model in our case of study. To describe adequately the

magnitude of the filamentous growth, quantitative measurements of the frequency volume distribution of the fiber length parameter should be considered: on the basis of the length criteria, mycelial population in volume reached 55.4 and 62.7 %, while it did not exceed 8.1 and 8.7 % in number under acidic (pH 4.5) and neutral pH respectively.

Qualitative and quantitative assessment of *Y. lipolytica* dimorphism, as provided by the current research is quite missing in the literature. Previous studies employed non-statistically representative methods (mainly the optical microscopy) without giving any information about the population distribution according to the size. The methodology presented in this chapter is of particular relevance since it allows a better monitoring of the impact of morphological changes (presence of filamentous cells) on the bioprocess productivity.

II.2.5 Results synthesis

The morphogranulometric characterization of the dimorphic behavior in *Y. lipolytica* resulted in the following conclusions:

- ⇒ Validation of the normality and morphological homogeneity of the independent initial cultures ($d_{CE} \approx 7.79 \pm 2.04 \mu\text{m}$; $AR \approx 0.47 \pm 0.18$). These results reflect an efficient control and standardization of the inoculum preparation steps.
- ⇒ Volume-based distributions are potentially preferred for the quantification of the elongation phenomena. The average d_{CE} attained 10.1 and 8.71 μm (in number) at the end of the culture at pH 4.5 and 7, respectively. The same populations presented mean diameters of 20.8 and 20.2 μm , respectively on the basis of a volume distribution. Similarly, the quantification data of the filamentous fraction are more significant with the volume-based calculations: more than 62.3 % of filaments (in volume) compared to 11.3 % (in number).
- ⇒ Differences between sphere and cylinder models are negligible with the ovoid-shaped populations (culture at pH 5.6). Indeed, the qualitative and quantitative measurements provided approximately similar results: mean- d_{CE} of 9.4 μm ; and filamentous subpopulation not exceeding 3.5 %.
- ⇒ Deviations between both models are considerable with the elongated samples (cultures at pH 4.5 and 5.6). With the cylinder approximation, the mycelial population reached more

than 84.1 % in volume. This fraction did not exceed 62.3 % using the sphere model. These findings highlighted the accuracy of the cylinder model for the description of the mycelial transition.

⇒ Fiber length and aspect ratio appeared as an appropriate parameter for describing the intensity of filament formation. Under acidic and neutral pH conditions, *Y. lipolytica* exhibited a heterogeneous morphology composed predominately of highly elongated cells: more than 25.6 % (v/v) of the cells showed a fiber length greater than 100 μm .

PART III: RESULTS AND DISCUSSION

Chapter III-3: Dynamic behavior of *Yarrowia lipolytica* in response to pH perturbations: dependence of the stress response on the culture mode

Chapter III-3: Dynamic behavior of *Yarrowia lipolytica* in response to pH perturbations: dependence of the stress response on the culture mode

III.3.1 Introduction

This chapter is presented in the form of a research article currently published in “Applied Microbiology and Biotechnology” (Timoumi et al. 2017).

In this work, the phenotypic plasticity (responses) of *Y. lipolytica* W29 strain to the exposure to different types of pH perturbation (pulse, Heaviside) was analyzed under two modes of culture: batch and continuous. The findings presented in this chapter are of particular relevance for industrial applications. It may provide deeper insights on the physiology of *Y. lipolytica* and can potentially contribute to more efficient control and monitoring of fermentation processes at the industrial scale where pH fluctuations are likely to occur.

pH is a critical parameter inducing the transition of *Y. lipolytica* from single-cells to mycelia (Gonzalez-Lopez et al. 2006; Ruiz-Herrera and Sentandreu 2002). Bibliographic analysis revealed the lack of research on the direct impact of pH stress (mono-factorial) on the yeast behavior. Up to now, studies were performed under partially culture conditions (shaken flask) which resulted in multi-factorial stress responses. Furthermore, it is still difficult to quantify at the population level the dimorphic response due to the multiplicity of methods, the disparity of morphological criteria and the poor statistical representativity of analyzed cells.

The first part of the work focused on the identification of the pH condition inducing a stress response (metabolic and/or morphological) in *Y. lipolytica*. To this end, batch cultures at different pH (4.5; 5.6 and 7) were carried out under well-controlled conditions in bioreactors. Second part was devoted to quantify the transient responses of cells subjected to pH perturbations at the most stressful pH condition, previously defined. Two modes of cultures (batch and continuous) were adopted in order to study the response of cells at different physiological states. In the third part, dynamics of morphological changes were compared, between both modes of culture, through analysis of cell size distribution at the population level. Finally, the last part presents a discussion of the results in the light of the existing research on the subject.

III.3.2 Publication: Dynamic behavior of *Yarrowia lipolytica* in response to pH perturbations: dependence of the stress response on the culture mode

Asma Timoumi¹, Mégane Cléret¹, Carine Bideaux¹, Stéphane E. Guillouet¹, Yohan Allouche², Carole Molina-Jouve¹, Luc Fillaudeau^{1§} and Nathalie Gorret^{1§*}

¹LISBP, Université de Toulouse, CNRS, INRA, INSA, Toulouse, France.

²Airbus Operations S.A.S, 316 Route de Bayonne, 31060 Toulouse, France.

§These authors contributed equally to the supervision of this work

*Corresponding author.

Tel.: +33 05 61 55 94 44; fax: +33 05 61 55 94 00.

E-mail address: nathalie.gorret@insa-toulouse.fr

Abstract

Yarrowia lipolytica, a non-conventional yeast with a promising biotechnological potential, is able to undergo metabolic and morphological changes in response to environmental conditions. The effect of pH perturbations of different types (pulses, Heaviside) on the dynamic behavior of *Y. lipolytica* W29 strain was characterized under two modes of culture: batch and continuous. In batch cultures, different pH (4.5, 5.6 (optimal condition) and 7) were investigated in order to identify the pH inducing a stress response (metabolic and/or morphologic) in *Y. lipolytica*. Macroscopic behavior (kinetic parameters, yields, viability) of the yeast was slightly affected by pH. However, contrary to the culture at pH 5.6, a filamentous growth was induced in batch experiments at pH 4.5 and 7. Proportions of the filamentous subpopulation reached 84 % and 93 % (v/v) under acidic and neutral conditions, respectively. Given the significant impact of neutral pH on morphology, pH perturbations from 5.6 to 7 were subsequently assayed in batch and continuous bioreactors. For both process modes, the growth dynamics remained fundamentally unaltered during exposure to stress. Nevertheless, morphological behavior of the yeast was dependent on the culture mode. Specifically, in batch bioreactors where cells proliferated at their maximum growth rate, mycelia were mainly formed. Whereas, in continuous cultures at controlled growth rates (from 0.03 to 0.20 h⁻¹) even closed to the maximum growth rate of the strain (0.24 h⁻¹), yeast-like forms predominated. This pointed out differences in the kinetic behavior of filamentous and yeast subpopulations, cell age distribution and pH adaptive mechanisms between both modes of culture.

Keywords: Batch; Chemostat; Dynamic response; Morphology; pH stress; *Yarrowia lipolytica*

III.3.2.1 Introduction

Yarrowia lipolytica (formerly known as *Candida*, *Endomycopsis* or *Saccharomycopsis lipolytica*) is a strictly aerobic non-conventional yeast (Barth and Gaillardin 1996; Barth and Gaillardin 1997), usually isolated from oily environments such as contaminated soils (Robak et al. 2011), raw poultry (Deak 2001) and dairy products (Yalcin and Ucar 2009). This yeast appears as a promising and potential microorganism with multiple biotechnological applications (Goncalves et al. 2014). It has the ability to metabolize a wide variety of carbon sources (e.g. glucose, alcohols, acetate and hydrophobic substrates) (Fickers et al. 2005; Finogenova et al. 2002; Papanikolaou et al. 2006), to degrade efficiently several low-value or toxic compounds (e.g. raw glycerol and olive mill wastewater) (Levinson et al. 2007; Makri et al. 2010; Rymowicz et al. 2006; Sarris et al. 2011) and to produce different valuable metabolites (e.g. organic acids, single cell oil, single cell protein, biosurfactants, heterologous proteins and enzymes) (Bellou et al. 2016; Bussamara et al. 2010; Lopes et al. 2009a; Madzak et al. 2004; Papanikolaou and Aggelis 2009; Papanikolaou et al. 2007; Parfene et al. 2013; Ron and Rosenberg 2002; Sauer et al. 2008). These potentialities, along with the versatility of metabolites produced, have increased interest in the exploitation of *Y. lipolytica* in numerous industrial sectors, notably in the areas of chemistry, food and energy.

Within the different phases of a new bioprocess development, the scale-up from laboratory to larger scale is still a critical issue, especially with the occurrence of unavoidable gradients (temperature, pH, dissolved oxygen, substrates and metabolites) in industrial bioreactors. These micro-environmental fluctuations may represent various stress conditions affecting microbial metabolism and physiology (Amanullah et al. 2001; Bylund et al. 1998; Delvigne et al. 2009; Enfors et al. 2001; Lara et al. 2006). Nature, intensity, duration and/or frequency of the stress encountered would be responsible for different cell behaviors, leading thereby to the generation of distinct subpopulations within the culture broth (Han et al. 2013; Jazini et al. 2014; Sunya et al. 2012). This is expected to cause performance variabilities in terms of yield, titer and/or productivity in industrial bioreactors comparing to small-scale bioreactors (Delvigne and Goffin 2014; Enfors et al. 2001; Lara et al. 2006).

Several metabolic activities displayed by *Y. lipolytica*, especially the synthesis of valuable metabolites, such as citric acid (Yalcin and Ucar 2009), lipids (Enshaeieh et al. 2013) and lipase (Kar et al. 2008) were influenced by changes in pH of the medium. Environmental pH

was also found to affect the morphology of *Y. lipolytica*. This yeast possesses the ability to undergo a dimorphic transition from yeast to filamentous forms in response to changes in pH conditions. Indeed, a maximum mycelial growth was detected at pH near neutrality and decreased as pH lowers to become almost null at pH 3 (Gonzalez-Lopez et al. 2006; Ruiz-Herrera and Sentandreu 2002). In the majority of previous studies, the effect of pH on *Y. lipolytica* morphology was coupled to other stimuli of dimorphism, mainly the carbon source (e.g. N-acetylglucosamine, serum), and often dependent on the chemical composition of the buffer used (citrate or phosphate buffer) (Gonzalez-Lopez et al. 2006; Ruiz-Herrera and Sentandreu 2002; Zinjarde et al. 1998). Studies correlating pH to yeast morphology are quite lacking. Indeed, all experiments were performed in partially controlled conditions under batch mode (shaken flasks), thus giving rise to multi-factorial stress responses.

The presence of different intermediate morphotypes (polymorphism), displaying a broad distribution of cell size and shape, greatly impacts the rheological behavior of the fermentation broth (Lim et al. 2002; Wucherpfennig et al. 2010), transfer phenomena inside bioreactors (Coelho et al. 2010; Kar et al. 2011; O'Shea and Walsh 2000), and consequently cell productivity (Fickers et al. 2009; Galvagno et al. 2011). In the case of *Y. lipolytica*, it was shown that the presence of 12 % of filamentous cells within the culture impacted the physico-chemical properties of the fermentation broth (rheometry, densimetry, conductimetry), and consequently the bioprocess performances (Kraiem et al. 2013). Moreover, several metabolic activities of industrial interest, displayed by *Y. lipolytica*, were related to the different cell forms. Higher efficiency of citric acid biosynthesis was found to be associated with an increase in the proportion of the smallest yeast cells (Rywinska et al. 2011). Furthermore, a predominant yeast form was shown to be required for an efficient secretion of various heterologous proteins in *Y. lipolytica*, such as the case of fungal *laccases* and human interferons (Gasmi et al. 2011; Madzak et al. 2005). In addition, according to the cell morphotype, a different hydrocarbon degradation potential was observed in two *Y. lipolytica* strains: yeast cells of a marine isolate (NCIM 3589) metabolized hexadecane with higher efficiency than the mycelial form, whereas the mycelial form of a terrestrial strain (W29) metabolized the hydrocarbon more efficiently (Palande et al. 2014; Zinjarde et al. 1998). Moreover, regarding aroma production, cells in the yeast form exhibited higher γ -decalactone production than the hyphal morphotype (*ca. 1.5-fold*) (Braga et al. 2016).

Optical microscopy was the most commonly used tool to describe morphological changes in *Y. lipolytica*. In previous reports, observations were often associated with direct counting measurements (Guevaraolvera et al. 1993; Ota et al. 1984; Zinjarde et al. 2008; Zinjarde et al. 1998) and automatic image processing methods (Botelho Nunes et al. 2013; Braga et al. 2016; Kawasse et al. 2003; Lopes et al. 2008). A few morphological criteria allowing the discrimination between filamentous and ovoid cells were employed (e.g. elongation factor (Botelho Nunes et al. 2013; Ota et al. 1984), cell length (Guevaraolvera et al. 1993), cell gravity (Novotny et al. 1994; Ota et al. 1984)). Regarding dimorphism quantification, in none of the studies, analysis of cell size distribution was presented. Quantification data were generally displayed as the proportion of the filamentous subpopulation within the culture.

Although it is commonly assumed that pH represents one of the major parameters affecting *Y. lipolytica* morphology and metabolism, assessing its direct impact (as only effector) on the yeast behavior, is still a complex issue: culture conditions were always partially controlled and morphological changes were rarely quantified on the basis of size distribution at the population level. Hence, in the current research, we aimed to characterize the influence of pH perturbations of different types (pulses and Heaviside) on the morphology and metabolism of *Y. lipolytica* cultivated in batch and continuous bioreactors. The objectives of this study were: i) to define, firstly the pH inducing a stress response (metabolic and/or morphologic) in *Y. lipolytica*, and ii) to subsequently quantify the transient responses of cells subjected to pH perturbations at the stressful pH condition, previously determined. Batch and continuous operating modes were preferentially employed, as it enabled respectively, the study of the stress response of cells growing at their maximum specific rate, and at various controlled specific growth rates in physiological steady-states. Furthermore, this work will give access to the specific kinetic parameters and yields determined under well-controlled growth conditions, which are still quite rare in literature for *Y. lipolytica*.

III.3.2.2 Materials and methods

III.3.2.2.1 Microbial strain

Wild-type *Y. lipolytica* strain W29 (ATCC® 20460™) was used in the present work and was maintained at -80 °C in Yeast extract Peptone Dextrose (YPD) medium (10 g L⁻¹ yeast extract, 10 g L⁻¹ peptone and 10 g L⁻¹ glucose), supplemented with 30 % (v/v) glycerol.

III.3.2.2.2 Minimum media composition

The defined minimum medium (MM) used for all batch and continuous experiments was the following (all compounds are expressed in g L⁻¹): (NH₄)₂SO₄ 3.0, KH₂PO₄ 6.0, MgSO₄ 2.0, EDTA-Na₂·2H₂O 0.0375, ZnSO₄·7H₂O 0.0281, MnCl₂·4H₂O 0.0025, CoCl₂·6H₂O 0.00075, CuSO₄·5H₂O 0.00075, Na₂MoO₄·2H₂O 0.00005, CaCl₂·2H₂O 0.0125, FeSO₄·7H₂O 0.00875, H₃BO₃ 0.0025, D-Biotin 0.00025, D-L Pantothenic acid 0.001, Nicotinic acid 0.001, Myo-inositol 0.00625, Thiamine. HCl 0.001, Pyridoxine 0.001 and Para-aminobenzoic acid 0.0002, prepared with deionized water. All chemicals used were of the highest grade commercially available. The pH was adjusted to 5.6 by addition of 2M potassium hydroxide solution.

After sterilization, 10 g L⁻¹ glucose and 1 mL L⁻¹ polypropylene glycol (antifoam PPG) were added in the medium.

III.3.2.2.3 Bioreactor cultures

Batch and continuous cultures were performed in a 1.6 L stainless-steel stirred tank bioreactor (11 cm diameter x 20 cm total height) with a working volume of 1 L (BIOSTAT® Bplus, Sartorius, Germany). The vessel was equipped with 2 six-bladed Rushton impellers, fitted with four equally spaced baffles (1 cm width), with dissolved oxygen, pH and temperature probes; stirred speed and airflow controls. Regulation and monitoring were done using MFCS/win 2.1 software package.

For each culture, one glycerol stock was streaked on a Petri dish and incubated at 30 °C for 48 h. Only one colony was used for the pre-culture. Three successive steps of pre-cultures were then carried out in baffled-shake flasks at 10 % (v/v) ratio with increasing culture volumes (5 mL YPD, 10 mL MM and 100 mL MM). One drop of polypropylene glycol (antifoam PPG) was added to the 100 mL pre-culture. The flasks were incubated at 28 °C for 12 h exactly at 130 rpm to have a well-standardized inoculum. The 100 mL inoculum was then used for inoculating the bioreactor at an initial biomass concentration of 0.3 gCDW L⁻¹.

Batch experiments were carried out at different pH conditions (4.5, 5.6 and 7). In order to ensure fully-aerobic conditions all along the cultures, a partial oxygen pressure (pO₂) higher than 40 % of saturation was maintained by manually increasing the agitation and aeration (from 100 to 800 rpm and 0.1 to 0.35 vvm, respectively). Temperature was regulated at 28 °C.

pH was maintained at the set-point and regulated by addition of 2M potassium hydroxide solution.

Glucose-limited chemostat cultures were performed at different dilution rates (0.03, 0.07, 0.10 and 0.20 h⁻¹). The continuous mode of operation was initiated, subsequently to the batch phase, by feeding fresh medium (MM supplemented with 10 g L⁻¹ glucose) and removing broth from the bioreactor by means of a stainless steel cannula placed at the upper level of the 1-L culture broth. To ensure highly-aerobic conditions, the reactor was stirred at 800 rpm and aerated at 0.5 vvm (pO₂ value almost stable at 65 % of saturation). Temperature was regulated at 28 °C and pH was maintained at 5.6 and regulated by addition of 2M potassium hydroxide solution. The Antifoam (polypropylene glycol) was periodically added by means of a peristaltic pump (controlled pulse-based addition) to maintain a nearly constant concentration (1 mL L⁻¹) within the bioreactor. The system was considered to be in a steady state after at least five residence times.

III.3.2.2.4 pH perturbation experiments

Under batch mode, a pulse perturbation from pH 5.6 to 7 was applied at the beginning of the exponential growth at a biomass concentration of almost 1 gCDW L⁻¹. The pulse was performed by a rapid injection of a potassium hydroxide solution (2M) using a sterile syringe through a septum placed on the top of the reactor. After the pulse induction, pH regulation stopped and the decrease in pH was only due to the acidifying activity of the microorganism. Samples were taken before and after the pulse for further ex-situ characterization.

During the chemostat runs, steady-state cultures were exposed to pulse and Heaviside pH perturbations from 5.6 to 7. Successive pulses (from 3 to 7 pulses) were carried out using the same protocol as described for the batch fermentation. Duration of each pulse was dependent on the activity of the microorganism which was in turn controlled by the imposed dilution rate. Heaviside changes were carried out by adding potassium hydroxide solution (2M) through a peristaltic pump after modification of the pH set point. Samples were characterized during the steady state, pulses and Heaviside stress phases.

III.3.2.2.5 Biomass characterization

III.3.2.2.5.1 Biomass concentration

Biomass concentration was determined by optical density and dry weight measurements. Spectrophotometric measurements were performed at 620 nm (OD_{620nm}) using a visible spectrophotometer (Biochrom Libra S4, UK) with a 2 mm absorption cell (Hellma). Cell dry weight was determined by filtration through 0.45 μ m pore-size polyamide membranes (Sartorius Biolab Product) and dried to a constant weight at 60°C (with the presence of gel silica) under a partial vacuum of 200 mmHg for at least 48 h (HERAEUS, France). The biomass formula used to convert cell dry weight into molar carbon concentration was $CH_{1.675}O_{0.523}N_{0.153}$ for a molecular weight of 25.59 g $Cmol^{-1}$ considering 5.7 % of ashes.

III.3.2.2.5.2 Cell cultivability

Enumeration of cultivable cells was determined using a simple plate count technique on Plate Count Agar (PCA) medium. 1 mL of culture broth was serially diluted with 9 mL sterile NaCl 0.85 % (*w/v*) physiological solution (BioMerieux®, France) and 50 μ L of the resulting cell suspension were plated out, in triplicate, onto PCA medium by means of a Whitley Automatic Spiral Plater-WASP (Don Whitley Scientific Limited, UK). The plates were incubated at 28 °C for 48 h and the colonies were manually counted.

III.3.2.2.5.3 Cell viability

Viability of cells was monitored with a BD Accuri C6® flow cytometer (BD Biosciences). The instrument is equipped with blue (488 nm) and red (640 nm) excitation lasers. Light scatter was collected at two angles: forward (FSC, 0 degrees, ± 13) and side (SSC, 90 degrees, ± 13) scatter. Fluorescence intensity was collected at FL1 (533/30nm), FL2 (585/40), FL3 (>670 nm) and FL4 (675/25) detectors. Carboxyfluorescein diacetate (cFDA), propidium iodide (PI) and Sytox® red stains (Molecular probes, Invitrogen, USA) were used to monitor esterase activity (cFDA) and membrane integrity (PI and Sytox), as indicators of yeast viability. Single and double staining (cFDA/PI and cFDA/Sytox) with these probes were performed during the time course of fermentations. A working solution (3 g L^{-1}) of cFDA was prepared by dissolving 5 mg of cFDA in 500 μ L of anhydrous DMSO and 1 mL of pluronic (F-127, Molecular probes, Invitrogen, USA). cFDA solution was then stored at room

temperature in the dark and was used at a concentration of 3 mg L^{-1} of cells. PI and Sytox® red were supplied by the manufacturer as 20 mM and 5 μM solutions in dimethyl sulfoxide solvent (DMSO) respectively, and were used as the working solutions at a concentration of 1 $\mu\text{L mL}^{-1}$ of cell suspension. Before staining, culture samples were washed twice in the McIlvaine buffer (pH 4.5) (McIlvaine 1921), diluted to reach approximately $10^6 \text{ cells mL}^{-1}$ and were then incubated in the dark for 20 min at 37 °C. Heat-treated cells (70 °C for 20 min) were used as the 100 % dead-cell control. A sample volume of 20 μL was analyzed at the slow flow rate setting ($14 \mu\text{L min}^{-1}$) using MilliQ water as sheath fluid. The FSC signal was used as a trigger channel (default value of 30000). The green fluorescence from the cFDA-stained cells was detected through the FL1 channel, and the red fluorescence of the PI and Sytox signal was collected in the FL3 and FL4 channels respectively. Data acquisition was processed using BD Accuri CFlow® software. Sample data were further analyzed with FlowJo software (Tree Star).

III.3.2.2.5.4 Cell morphology

Different methods were used to assess changes in cell morphology upon exposure to various pH conditions and perturbations under batch and continuous modes of culture:

Flow cytometry: the BD Accuri C6® flow cytometer (BD Biosciences) was used for single-cell light scattering measurements. FSC and SSC signals give information on cell size and internal complexity (granularity) respectively. A calibration curve established by polystyrene microspheres with diameters ranging from 1 to 15 μm (Flow Cytometry Size Calibration Kit (F-13838), Molecular probes, Invitrogen, USA) was used to relate FSC signals to cell size. The width (duration or time of flight) of the pulse from the forward scatter light was analyzed in order to estimate the length of cells. Measurements were performed at a pre-set flow rate of $14 \mu\text{L min}^{-1}$ using MilliQ grade water as sheath fluid and with a defined sample volume of 20 μL . Typically data were collected for $10^6 \text{ cells mL}^{-1}$; dilution (from 1:10 to 1:500) of culture sample was usually required. A threshold value of 30000 was applied on the forward scatter channel (FSCH) in order to subtract background noise events (salt particles and cell debris from the culture broth). The data collected were processed with BD Accuri CFlow® software and subsequently analyzed using FlowJo software (Tree Star).

Morphogranulometry: cell morphology was characterized using a morpho-granulometer (Mastersizer G3S, Malvern Instruments Ltd. SN: MAL1033756, software Morphologi v7.21).

The apparatus is composed of a system of lens (magnification: from x1 to x50, particle dimension: from 0.5 to 3000 μm), an optical device (Nikon CFI60 Bright/ Dark field) and a camera (IEEE1394a, Fire WireTM, 2592x1544 pixels). This optical apparatus allows the capture of composite images, on-line image processing and analysis of culture samples under dry or wet modes. After image acquisition on a defined area, individual cells were identified and analyzed. Different dimensional and morphometric parameters were calculated for each cell and associated distributions were generated for each parameter. In this paper, the equivalent circular diameter (d_{CE} , diameter of the sphere with the same projected area as the cell particle) was preferentially employed to track changes in biomass morphology. Before measurements, broth samples were diluted (from 1:1 to 1:10) up to concentrations ranging between 0.3 and 0.5 gCDW L^{-1} , and homogenized using a vortex. A Droplet of about 5 μL of the cell suspension was deposited between cover glasses and slides. A $2 \times 2 \text{ mm}^2$ surface was analyzed under standardized conditions (magnification x20, dark field, light intensity 100 %, exposure time 300 ms). After analysis, recorded images were filtered and analyzed in order to define the morphological properties of cells (diameter, aspect ratio, circularity, etc.) and their size distribution within the culture.

Diffraction light scattering: a diffraction light scattering device (Mastersizer 2000 Hydro, Malvern Instruments Ltd. SN: 34205-69, range from 0.02 to 2000 μm) was used for granulometric analysis of fermentation broth samples. This particle sizer converts the detected scattered light into a volume size distribution of the equivalent spherical diameter d_{SE} (diameter of the sphere that has the same volume as the particle). A defined volume (1 mL) of broth samples taken from bioreactor was added into a water circulation loop (refractive index of the dispersant agent: 1.33). Measurements were conducted at room temperature (20 °C) with obscuration rates (red $\lambda=632.8 \text{ nm}$ and blue $\lambda=470.0 \text{ nm}$ lights) ranging between 10 and 40 %. This analysis is based on the sphere-shaped model and employs by default the refractive index of organic compounds (1.569 at 20 °C).

Light microscopy: microscopic observations were performed using an Olympus BH-2 microscope (Olympus optical Co., Ltd, Tokyo, Japan), equipped with a colour digital camera (Nikon's Digital System DS-Ri1, Surrey, UK).

III.3.2.2.6 Sugar and organic acid analysis by high-performance liquid chromatography (HPLC) and ionic chromatography (HPIC) techniques

Broth culture supernatant was obtained by centrifuging (MiniSpin, Eppendorf, USA) fermentation samples in Eppendorf tubes at 13400 rpm for 3 min and stored at -20 °C. Before chromatographic analysis, supernatant was filtered on Minisart filters 0.45 µm pore diameter polyamide membranes (SARTORIUS, Germany) and diluted (when required) with Milli-Q grade water (18.2 mΩ-cm resistance).

During batch cultures, glucose and organic acids concentrations were determined by high performance liquid chromatography (Ultimate 3000, Dionex, USA) using an Aminex HPX-87H⁺ column (Bio-RAD, US) under the following conditions: a temperature of 50 °C with 5 mM H₂SO₄ as eluent (flow rate of 0.5 mL min⁻¹) and a dual detection (IR and UV at 210 nm). The metabolites searched for detection and quantification were glucose, acetate, pyruvate, succinate and citrate.

Quantification of glucose and organic acids, presents at low concentrations in the cultures under continuous mode, was carried out by high performance ionic chromatography using an ICS-3000 system (Dionex, USA) equipped with an ED 40 electrochemical detector (amperometry and conductivity detections). Glucose was separated on a CarboPacTM PA1 analytical and guard columns at an isocratic concentration of 25 % deionized water (eluent 1) and 75 % 200 mM NaOH (eluent 2), at a flow rate of 1.0 mL min⁻¹ at 30 °C for 15 min, followed by a pulsed amperometric detection (a working gold electrode and a reference electrode pH-Ag/AgCl combination). Organic acids (acetate, pyruvate, succinate, malate, fumarate and citrate) were separated on an IonPac AS11-HC analytical and AG11 guard columns equipped with a carbonate removal device (CRD 200, 4mm), a continuously regenerated anion trap column (CR-ATC) and an anion self-generating suppressor (ASRS[®] 300, 4mm) followed by a conductivity detection. The mobile phase was KOH solution (EGC II KOH cartridge) at a flow rate of 1.5 mL min⁻¹.

Chromatographic data were collected, analyzed and quantified using Chromeleon (version 6.80 SP4 Build 2361) software and autocalibration chromatograms. External standards (glucose and organic acids) were used at the beginning, the middle and the end of the sequence to ensure the stability along the sequence analysis.

III.3.2.2.7 Chemical products

The purchased chemicals were of the highest grade commercially available. Macroelements, oligo-elements except zinc sulfate (Sigma, USA), glucose, orthophosphoric acid and potassium hydroxide solutions were provided by Rectapur/Normapur/Prolabo. Vitamins and organic acids were purchased from Sigma (USA).

III.3.2.2.8 Gas analysis and monitoring

Inlet and outlet gas composition were analyzed using a fermentation gas monitor system (LumaSense Technologies Europe). The instrument combines a multipoint sampler 1309 (INNOVA 1309) with a gas analyzer (INNOVA 1313). Concentrations of oxygen (O_2) and carbon dioxide (CO_2) were determined using magneto and photo-acoustic spectroscopic measurements respectively.

III.3.2.2.9 Calculation methods

Off-gas rates: oxygen consumption (r_{O_2}) and carbon dioxide production (r_{CO_2}) rates were calculated from the mass balances in the gas and liquid phases taking into account the inlet and outlet gas compositions, and the evolutions of temperature, pH, salinity, and liquid volume in the bioreactor.

Glucose uptake and organic production rates: glucose consumption (r_g) and biomass production (r_x) rates were determined based on their experimental measurements and their respective mass balance equations. The inlet and outlet volumetric flow rates were considered in calculating these rates during the continuous cultures.

Statistical analysis: details on the statistical tests used in the current study are available in the Electronic supplementary material.

Analysis of cell size distribution of morphologically distinct subpopulations: basic principles of particle size analysis, size distribution calculations as well as the methodology adopted for the quantification of cell subpopulations with different morphology are explained in the Electronic supplementary material.

III.3.2.3 Results

III.3.2.3.1 Batch cultures

Oxidative batch fermentations were carried out at different pH 4.5, 5.6 and 7 in order to characterize and quantify the pH stress responses (metabolic and morphologic) of *Y. lipolytica* under well-controlled conditions in bioreactor. The pH choice made was based on literature and aimed to test acidic and alkaline conditions regarding the classical pH used for *Y. lipolytica* cultures. Macroscopic behavior of *Y. lipolytica* was characterized by quantifying the dynamics of growth, viability, cultivability, glucose uptake, oxygen consumption, organic acid and carbon dioxide production. Changes in cell morphology were monitored using different physical methods (microscopy, flow cytometry, morphogranulometry and diffraction light scattering).

III.3.2.3.1.1 Macroscopic behavior characterization

In order to monitor changes in the kinetic behavior of cells cultivated at different pH conditions, evolutions of biomass, substrates (glucose, oxygen) and carbon dioxide concentrations, as well as their associated specific rates were analyzed and compared (Figure III-18).

Analysis of culture supernatants revealed the absence of organic acids under all tested pH. Glucose was only converted to biomass and carbon dioxide. For all experiments, carbon and redox balances were recovered with a deficit of less than 5 %. The mean biomass yield on glucose ($Y_{X/S}$) was $0.67 \pm 0.02 \text{ CmolX CmolS}^{-1}$ and the mean carbon dioxide yield on glucose ($Y_{\text{CO}_2/S}$) was $0.30 \pm 0.03 \text{ CmolCO}_2 \text{ CmolS}^{-1}$. As shown in Figure III-18 (A-B), similar kinetic patterns of biomass growth and glucose uptake were observed for the three batch runs. A slight impact of pH changes on the maximum specific growth (Figure III-18C) and glucose consumption (Figure III-18D) rates was demonstrated: their mean values were $0.24 \pm 0.01 \text{ h}^{-1}$ and $0.38 \pm 0.02 \text{ Cmol CmolX}^{-1} \text{ h}^{-1}$ respectively. Particularly, the specific glucose uptake rate (q_S) increased rapidly at pH 5.6 compared to the other pH tested, but reached almost similar maximum values for all pH conditions.

However, respiration capabilities of the yeast seemed to be affected by varying pH levels (Figure III-18 E-F). Cells cultivated at pH 5.6 exhibited higher respiration activity (q_{O_2} , q_{CO_2}

and RQ patterns) compared to those grown at pH 4.5 and 7. Fluctuations in the specific respiration rates (qO_2 and qCO_2), and hence in the respiratory quotients profiles were observed during the first hours of fermentations carried out at pH 4.5 and 7. These variations were less pronounced under pH 5.6 and can therefore be attributed to the adaptation of cells to pH changes when transferred from the inoculum culture (pH 5.6) to the bioreactor (pH 4.5 or pH 7). Inaccurate measurements of the exhaust gas composition could also be expected at the beginning of the culture; due to the low biomass concentration and the inadequate air flow-rate (100 mL min^{-1}) for a reliable gas analysis (minimum required flow rate for the gas analyzer is 130 mL min^{-1}).

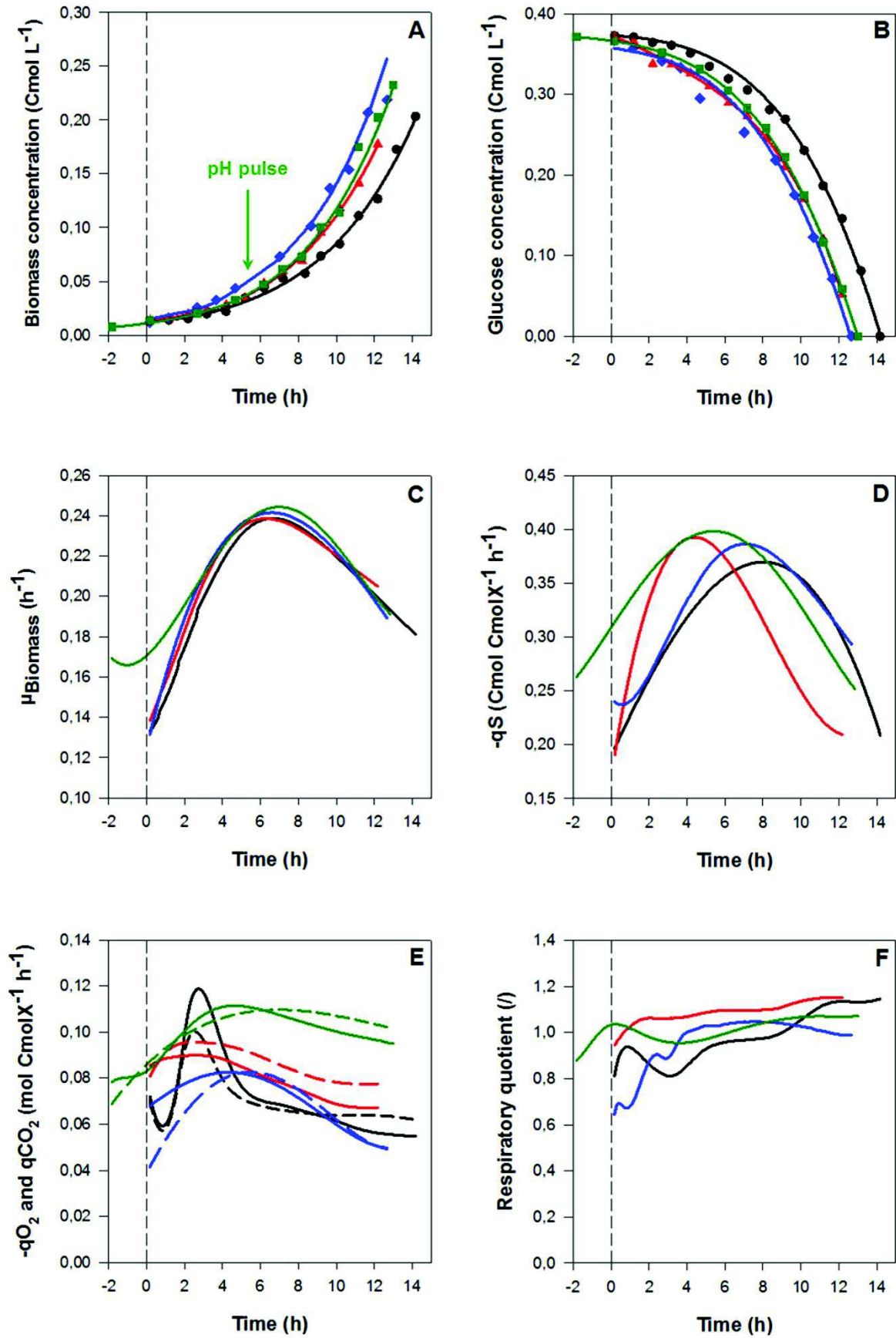


Figure III-18: Dynamic evolutions of biomass (A) and glucose (B) concentrations, biomass production (C), glucose uptake (D), oxygen consumption and carbon dioxide production (E) specific rates, and respiratory quotient (F) during batch cultures at different pH values: Black, red, blue and green lines correspond respectively to the cultures at pH 4.5; 5.6; 7 and with a pulse perturbation at pH 7. In Figures (A-B), the symbols indicate measured values; the lines correspond to smoothed data. Dash lines in Figure (E) represent the specific oxygen uptake rates. The arrow in Figure (A) indicates the moment of pH pulse application

III.3.2.3.1.2 Morphological changes monitoring

Changes in cell morphology were investigated during discontinuous cultures by means of granulometric measurements. Figure III-19A represents some microscopic observations of broth samples at different biomass concentrations for each pH condition. A homogeneous morphological behavior at the beginning of the culture in all tested pH was observed, emphasizing the use of well-standardized seed cultures. Distribution functions in number of the equivalent circle diameter (d_{CE}) were described by a normal law for the three independent inoculum cultures (normality criteria were satisfied on linear and logarithmic scales). Average diameters of each cell population were approximately identical: values ranged between 7.8 ± 1.3 ; 7.9 ± 1.3 and 7.1 ± 1.3 μm at pH 4.5, 5.6 and 7, respectively. Morphological similarities between the three independent cultures were also validated with an overlapping coefficient of 0.8, emphasizing therefore the standardization of inoculum morphology.

Contrary to the batch cultivation at pH 5.6, *Y. lipolytica* exhibited a mycelial transition when grown at pH 4.5 and pH 7. As shown in Figure III-19A, the microorganism displayed a heterogeneous morphology comprised of elongated cells and pseudomycelia. Elongated cells are unicellular with an elongation of the cell's major axis, whereas pseudomycelia represent elongated cells where each generation of buds remains attached to the parent cells (Walker and Oneill 1990). In the present study, changes in yeast morphology were quantified using the diameter corresponding to a circular area equivalent to the total cell projected area (d_{CE}). This one-dimensional measure provided a direct indication of the cell size and allowed subcategorization of yeast populations into the yeast-like (ovoid or spherical single cells) and filamentous (elongated cells and pseudomycelia) forms. To describe adequately the heterogeneity of the culture, quantitative measurement of the frequency distribution in number and in volume based on the equivalent diameter was required. Furthermore, to provide a better fit with the elongated shape of cells, a cylinder model was preferentially employed.

Figure III-19B represents the evolution of the filamentous fraction (percentage of cells with a mean d_{CE} higher than 15 μm), in number and in volume during the batch cultures at different pH. Results confirmed the morphological homogeneity of the initial populations for the three pH conditions: proportion of filamentous cells ranged between 1.4/ 13.0 %; 2.0/ 15.1 % and 1.2/ 12.3 % (in number/ in volume) for the batch runs at pH 4.5, 5.6 and 7 respectively. Furthermore, filamentous cells predominated during the cultures at pH 4.5 and 7. Their proportion increased from 1.4/ 13.0 % and 1.2/ 12.3 % (in number/ in volume) to reach almost 11.3/ 84.1 % and 7.7/ 92.7 % (in number/ in volume) at the end of the fermentation at pH 4.5 and 7, respectively. However, growth in the yeast-like form noticeably predominated during the culture at pH 5.6. Filamentous cells represented a small proportion of the population that did not exceed 3.5 % (in volume) at the end of the culture.

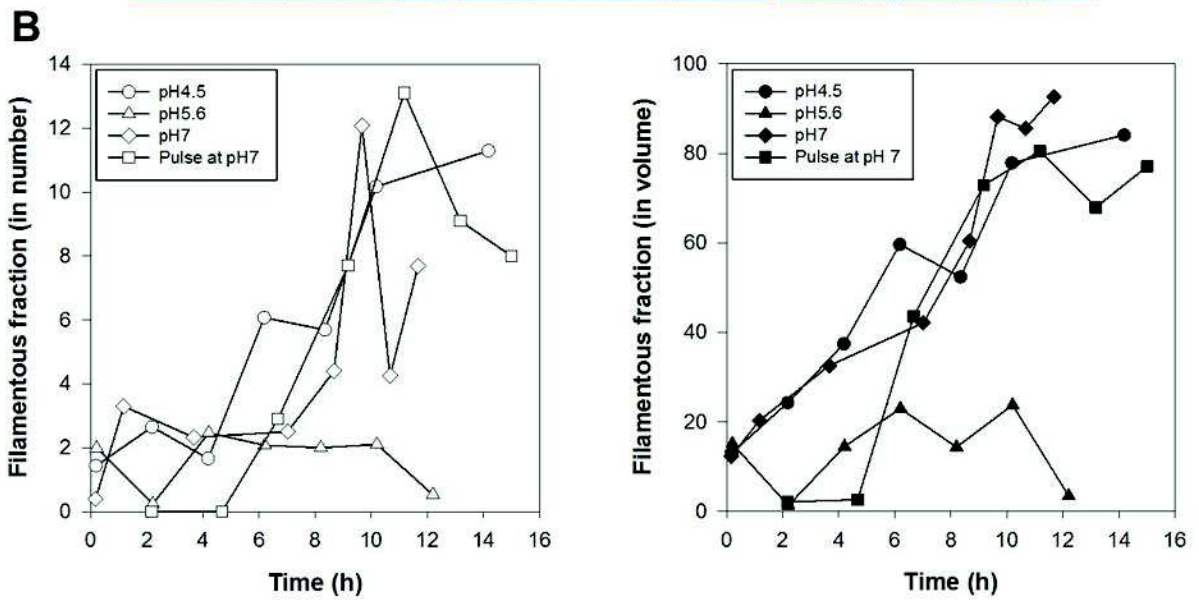
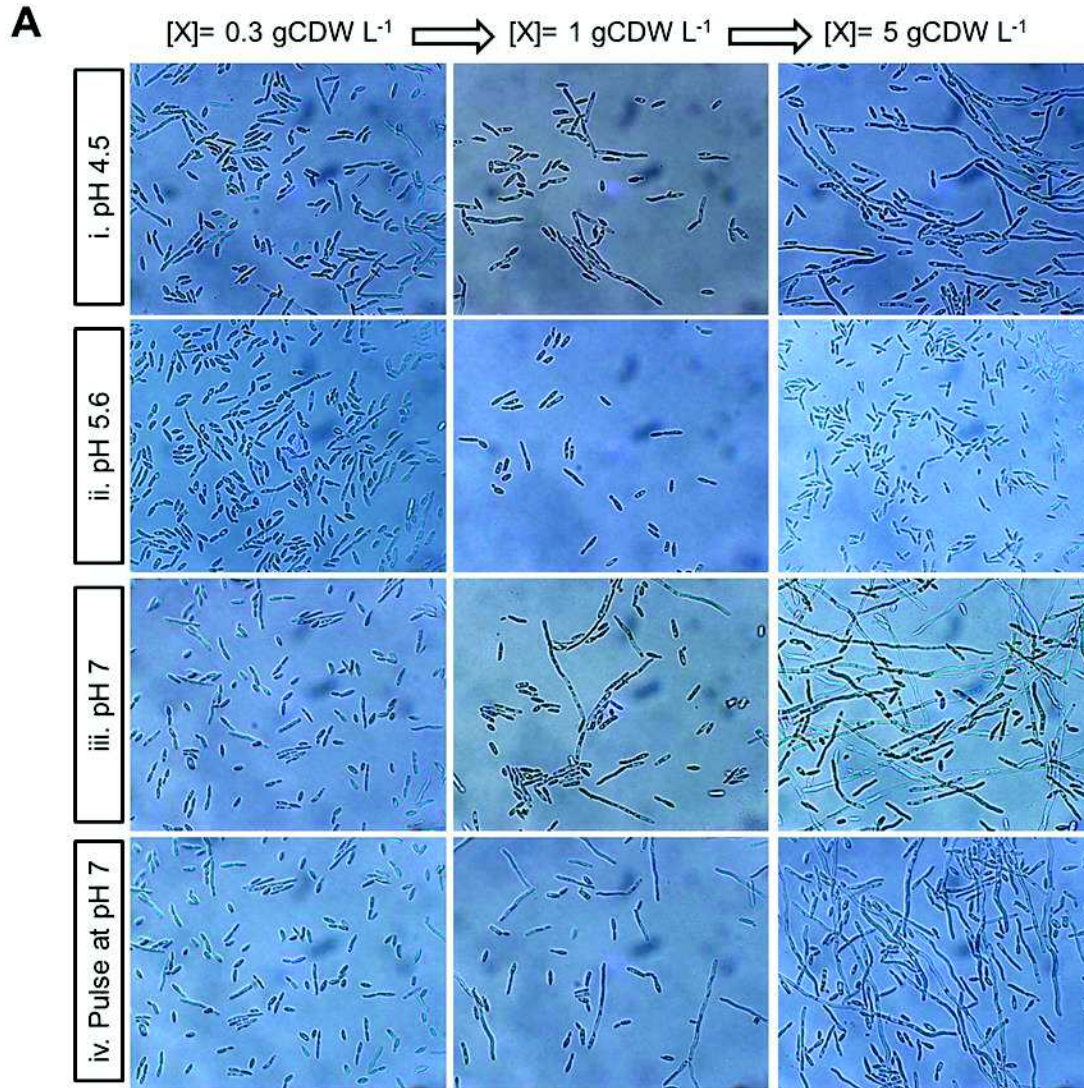


Figure III-19: A. Images taken during growth of *Yarrowia lipolytica* W29 under batch culture mode at various pH conditions (i, pH 4.5; ii, pH 5.6; iii, pH 7 and iv, pH pulse from 5.6 to 7) for biomass concentration of 0.3; 1 and 5 gCDW L⁻¹. The morphology was observed under a light microscope, without oil fixation and at magnifications of 40 x. Image size is 54 µm in width and 44 µm in height. B. Quantification of the mycelial transition of *Yarrowia lipolytica* W29 by morphogranulometric measurements. Evolutions of the filamentous subpopulation, in number and in volume, were followed during the time course of fermentation

III.3.2.3.1.3 Cell viability assessment

The fluorescent probes PI, cFDA and Sytox® red were used in a single and multiparameter flow cytometry analysis to assess the viability of *Y. lipolytica*. The dot plots presented in Figure III-20 indicated a dead population (Q3 quadrant) that did not exceed 3.4 % at the end of the culture under all pH conditions. Similar proportions were obtained during the time course of cultivations for all tested conditions.

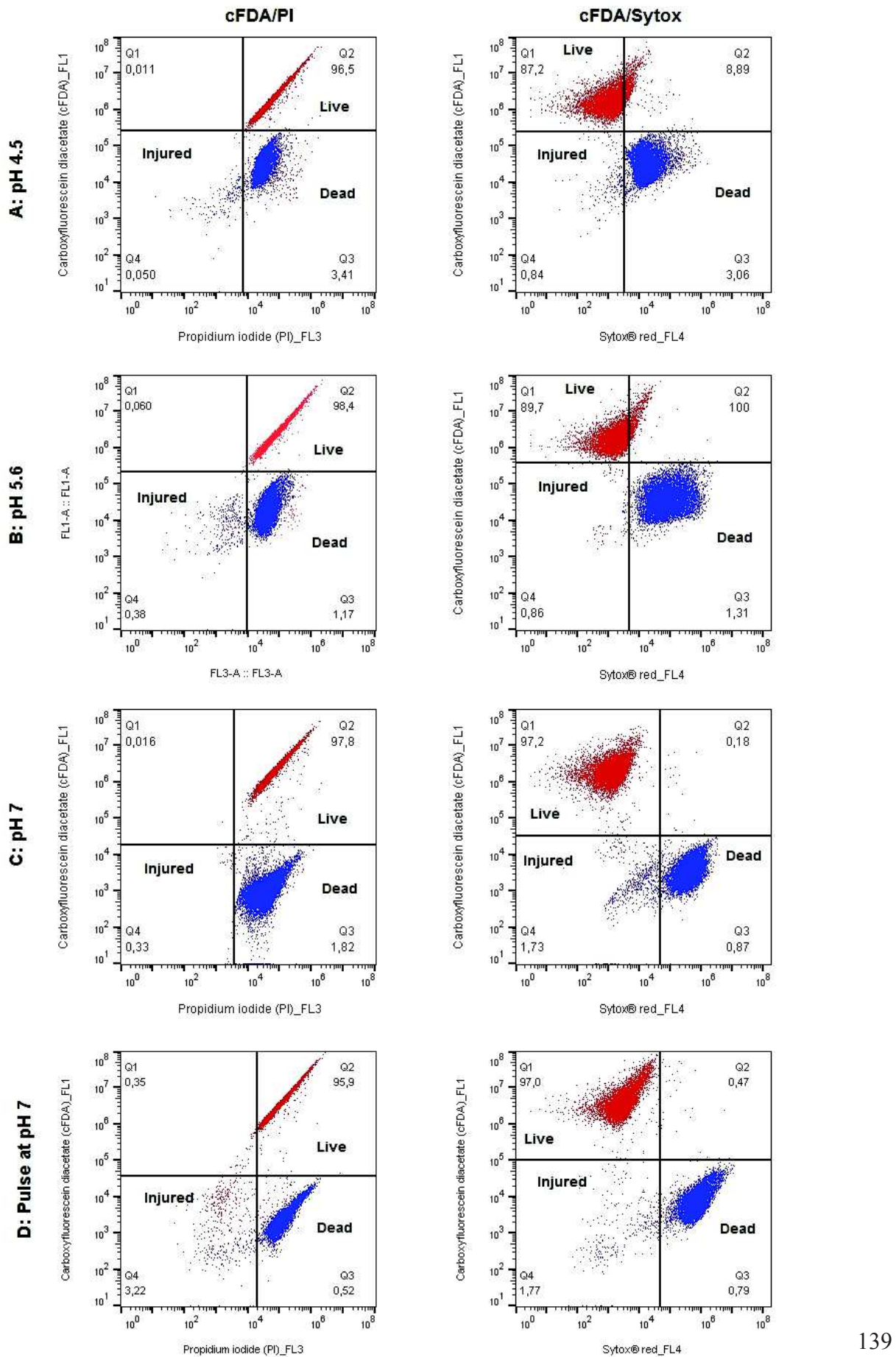


Figure III-20: Multiparameter dot plots of *Y. lipolytica* W29 representing cFDA (FL1) versus PI fluorescence (FL3) and cFDA (FL1) versus Sytox (FL4) fluorescence for the cFDA/PI and cFDA/Sytox double-stained cells respectively. Samples were taken at the end of each batch culture (A, pH 4.5; B, pH 5.6; C, pH 7 and D, pH pulse from 5.6 to 7). Two main subpopulations of untreated (culture sample/ red color) and dead (control sample/ blue color) cells can be readily differentiated through overlapping their respective plots. The quadrants of the dot plots were set on the double-stained dead cells that appeared in the lower left quadrant. Q1 and Q2 quadrants represent viable subpopulation in the cFDA/Sytox and cFDA/PI double-stained culture samples respectively. Q3 quadrant represents dead subpopulation. Q4 quadrant (represents injured damaged) cells. The indicated percentages in the four quadrants correspond to the untreated sample (culture sample / red color)

III.3.2.3.2 Batch culture with pH pulse perturbation

Taking into account the impact previously demonstrated of neutral pH on *Y. lipolytica* morphology, a batch experiment with pH pulse perturbation from 5.6 to 7 was carried out at pH 5.6. pH was greater than 6.5 during nearly the whole exponential growth phase. Results (Figure III-18) showed a non-significant effect of the stress applied on the macroscopic behavior of the yeast. Dynamics of growth, glucose uptake, oxygen consumption and carbon dioxide production were quite similar to the batch culture at pH 7. Furthermore, cell dimorphism was induced following exposure to the pH pulse (Figure III-19). Fraction of the filamentous population reached almost 8.0/ 77.1 % (in number/ in volume) at the end of the culture. These findings were expected since a pH close to neutrality was maintained throughout the entire duration of fermentation. In addition, as shown in Figure III-19, more than 99.2 % of cells remained viable after the pH shift.

III.3.2.3.3 Continuous cultures

Four independent chemostat cultures were carried out at different dilution rates (0.03, 0.07, 0.10 and 0.20 h⁻¹) in order to investigate the impact of the growth rates and the residence time of cells inside the bioreactor (via the dilution rates) on the pH stress responses. The steady state (SS: phase I) was considered to be achieved after a period of at least five residence times, and was assessed by a constant production of biomass and a stable composition of the exhaust gases. Characterization of each steady state was carried out by taking-up at least 5 samples within a period of 1 to 2 residence times. After characterization of each steady state, successive pH pulses from 5.6 to 7 (P: phase II) were carried out directly in the bioreactor. Following this phase, Heaviside changes at pH 7 (HS: phase III) were applied and the stress

response was characterized when a new steady state regime was established after pH disturbances.

III.3.2.3.3.1 Macroscopic behavior characterization

Specific consumption and production rates, biomass yields as well as carbon and redox recoveries were calculated from raw data and reported in Table III-14. Kinetic parameters were analyzed and compared between stressed and unstressed physiological states in order to assess the impact of pH perturbations on the macroscopic behavior of the yeast. Similarly to batch cultivations, no production of organic acids was observed under the various growth rates and pH stress conditions. The mean residual glucose concentration was lower than 10 mg L⁻¹ during the various phases. For all tested dilution rates, the calculated specific rates of glucose consumption under steady state, pH pulses and Heaviside stress phases were not significantly different (for example 0.15, 0.16 and 0.16 Cmol_{glucose} CmolX⁻¹ h⁻¹ respectively, for cells grown at 0.10 h⁻¹). Similarly, measured specific oxygen uptake and carbon dioxide rates were not affected by pH perturbations during these experiments. Respiratory quotients were always around 1.1 reflecting thus the conservation of an oxidative metabolism regardless of the type (pulses / Heaviside), frequency (pulses) and duration of the imposed stresses.

Table III-14: Comparison of kinetic parameters of the continuous cultures: Average values of specific rates, yields, respiratory quotients, carbon and redox recoveries were expressed with their associated standard deviations

Dilution rate	Phases	-qS	qCO ₂	-qO ₂	Y _{X/S}	RQ _{mean}	Carbon recovery	Redox recovery
(h ⁻¹)		(Cmol CmolX ⁻¹ h ⁻¹)			(Cmol Cmol ⁻¹)	(/)	(%)	
0.03	I ^{a)}	0.050±0.004	0.031±0.004	0.020±0.002	0.61±0.02	1.11±0.06	99.4±1.1	100.7±0.1
	II ^{b)}	0.043±0.001	0.024±0.003	0.021±0.004	0.60±0.03	1.03±0.03	100.3±0.2	100.5±0.4
	III ^{c)}	0.040±0.005	0.023±0.004	0.024±0.003	0.64±0.01	1.06±0.05	99.3±1.4	99.7±0.9
0.07	I ^{a)}	0.110±0.002	0.041±0.004	0.034±0.005	0.64±0.02	1.10±0.03	100.7±0.9	107.6±1.0
	II ^{b)}	0.094±0.009	0.034±0.005	0.040±0.004	0.65±0.01	1.08±0.04	102.6±1.6	108.5±0.5
	III ^{c)}	0.103±0.006	0.043±0.003	0.033±0.002	0.63±0.02	1.06±0.03	100.6±0.4	109.5±0.2
0.10	I ^{a)}	0.150±0.005	0.061±0.004	0.051±0.004	0.64±0.01	1.17±0.08	104.2±1.1	108.5±0.2
	II ^{b)}	0.163±0.003	0.060±0.007	0.050±0.002	0.62±0.02	1.17±0.07	100.4±2.3	102.1±1.1
	III ^{c)}	0.160±0.001	0.053±0.010	0.044±0.003	0.65±0.01	1.10±0.05	97.4±1.3	100.6±0.8
0.20	I ^{a)}	0.321±0.009	0.133±0.003	0.110±0.007	0.63±0.03	1.18±0.03	105.8±1.1	108.7±0.7
	II ^{b)}	0.303±0.013	0.121±0.011	0.103±0.010	0.64±0.02	1.18±0.05	107.6±0.5	112.5±0.1
	III ^{c)}	0.344±0.004	0.130±0.005	0.124±0.003	0.61±0.02	1.14±0.07	98.4±1.4	98.9±2.1

^{a)} Steady state^{b)} Pulses at pH 7^{c)} Heaviside at pH 7

III.3.2.3.3.2 Morphological changes monitoring

Yeast morphology was examined along continuous cultures through microscopic observations, flow cytometric, diffraction laser scattering and morphogranulometric measurements. In Figure III-21, representative microscopic images of cells were depicted for each experimental condition (steady state, pulses and Heaviside phases). For all tested dilution rates and stress perturbations, the culture consisted mainly of perfectly ovoid-shaped cells with a unimodal size distribution. From steady-state to stress phases, diameter of cells (determined by the different methods) did not exceed 6.2 μm . Coefficient of variation on the cell diameter varied between 8, 3, 4 and 2 % for the cultures at dilution rates of 0.03, 0.07, 0.10 and 0.20 h^{-1} respectively (data quantified by flow cytometry). Hence, irrespective of the stress conditions applied, morphological differences between the various cellular states were non-statistically significant.

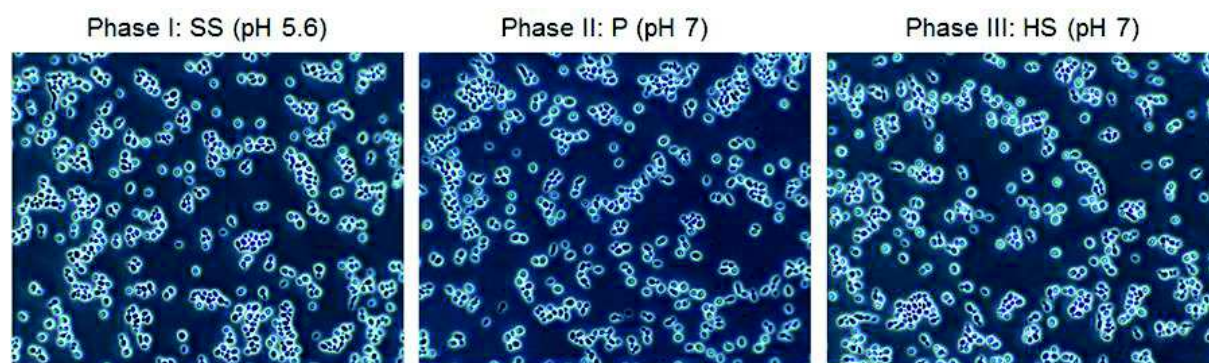


Figure III-21: Morphology of *Y. lipolytica* W29 during the steady state (SS, pH 5.6), pulses (P, pH 7) and Heaviside (HS, pH 7) stress phases of the continuous culture at a dilution rate of 0.10 h^{-1} . Images were taken through a light microscope, with oil fixation, under phase contrast mode, and at magnifications of 40 x. Image size is 54 μm in width and 44 μm in height

III.3.2.3.3.3 Cell viability assessment

Percentage of viable cells did not vary significantly between the different conditions at all dilution rates tested. Their proportions assessed either by cFDA/PI or cFDA/Sytox double staining methods were greater than 97, 95 and 94 % at steady state, pulses and Heaviside phases respectively.

III.3.2.3.4 Comparison between batch and continuous cultures: analysis of cell size distribution

In order to understand the dynamics of morphological evolutions of *Y. lipolytica* in response to pH stress, profiles of cell size distribution were preferentially analyzed and compared between the batch and continuous modes. The width (duration) of the forward scatter light (FSC), measured by flow cytometry was used to discriminate subpopulations of different sizes within the culture broth. Indeed, it represents the time of flight of a cell by passage through the laser beam, reflecting hence its length. Distributions in number based on cell length measurements were determined during the time course of fermentation, and data were displayed as box plots (Figure III-22).

Under batch operating mode, dispersion of cell length was reduced as growth proceeded at pH 5.6 (Figure III-22A) whereas it increased at neutral pH (Figure III-22B). The time of flight of 95 % of cells across the laser beam decreased from 130 to 119 during the culture at pH 5.6, while it increased from 121 to 140 at pH 7.

In continuous cultivation, cells exhibited a smaller size and much narrower size distribution at steady states (phase I, pH 5.6) for all dilution rates, compared the batch culture at pH 5.6, as shown in Figure III-22A. Stress applied in the form of successive pulses (phase II, at least 3 pulses at pH 7) did not induce noticeable variations on the size distribution, comparing to the distribution of unstressed cells at steady state phases (phase I, for each dilution rate) (Figure III-22A). Furthermore, despite exposure to a continuous stress (phase III, pH 7) during 25 to 200 h (depending on the dilution rate), no dimorphic transition was induced by pH perturbations in the form of Heaviside (Figure III-22B). Minor morphological changes were observed over the broad range of dilution rates tested; from 0.03 until 0.20 h⁻¹ which was closed to the maximum growth rate of the strain (0.24 h⁻¹). This showed that the cell growth rate did not impact the sensibility of *Y. lipolytica* to pH stress, neither in the form of pulses nor Heaviside.

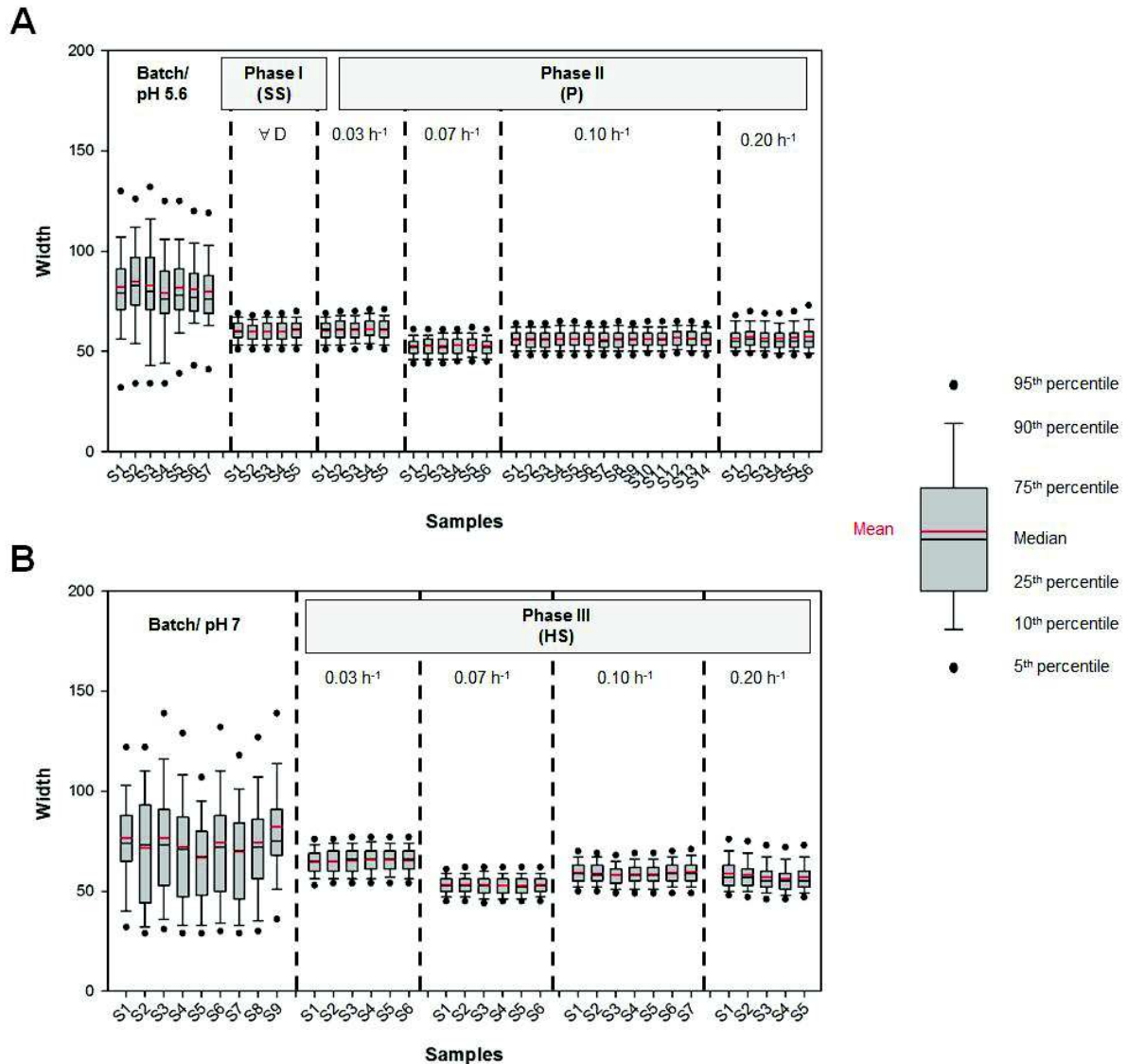


Figure III-22: A. Box plots comparing the evolution of cell length distribution during the batch culture at pH 5.6, the phase I (steady state at pH 5.6) and the phase II (pluses at pH 7) of the continuous experiments performed at dilution rates of 0.03, 0.07, 0.10 and 0.20 h⁻¹. B. Box plots comparing the dynamics of cell length distribution between the batch culture at pH 7 and the phase III (Heaviside at pH 7) of the chemostat experiments carried out at dilution rates from 0.03 to 0.20 h⁻¹. The boundary of the box closest to zero indicates the 25th percentile, a black line within the box marks the median, a red line within the box marks the mean and the boundary of the box farthest from zero indicates the 75th percentile. Whiskers above and below the box indicate the 90th and 10th percentiles. The black dot indicates the 95th and 5th percentiles

III.3.2.4 Discussion

Due to insufficient mixing, heterogeneities regularly occur in industrial fermentation processes. Dynamic behavior of microbial populations faced to such fluctuations should be taken into account in order to optimize bioprocess performances. Focusing on the effect of pH

gradients within bioreactor, we investigated how *Y. lipolytica*, a microorganism with multiple industrial applications, adjusted its metabolic behavior, morphology and/or physiology in response to pH perturbations under well-controlled culture conditions.

During bioreactor batch cultures, the macroscopic behavior of the yeast was slightly affected by the pH of culture. Compared to acidic and neutral conditions, cells cultivated at pH 5.6 reached more rapidly their maximum glucose consumption rate, exhibited less fluctuating respiration rates and showed stable respiratory quotients. This is probably related to the adaptation of the microorganism to pH changes when transferred from inoculum into bioreactor. Indeed, in order to establish a standardized non-filamentous seed cultures, all inoculums were produced at the same pH (5.6). For the culture at pH 4.5, absence of excreted metabolites as well as values of maximum growth rate (μ_{\max}), specific oxygen uptake rate ($-qO_2$), and yields of biomass ($Y_{x/s}$) and carbon dioxide ($Y_{CO_2/s}$) from glucose were in concordance with previous results from *Y. lipolytica* CECT 1240 discontinuous cultures on minimal medium with glucose as carbon source (Workman et al. 2013). Detailed quantitative data on the kinetic parameters during growth of *Y. lipolytica* are quite rare in the literature. Furthermore, accurate analysis and interpretation of the results are complicated as partially controlled conditions (shaken flasks cultures) have been often employed and complex medium components have been usually added to the growth medium.

Regarding morphology of the yeast, a dimorphic growth was induced during the batch cultivations under pH 4.5, pH 7 and after the pH pulse from 5.6 to 7 (fraction of filamentous population higher than 77 % in volume for all conditions), whereas ovoid-shaped cells predominated during the culture under pH 5.6 (proportion of filamentous cells not exceeding 3.5% in volume). Filament formation can only be attributed to pH changes in the growth medium since morphological homogeneities were demonstrated between the independent inoculum cultures and experimental conditions were efficiently controlled along fermentations. Several studies (Gonzalez-Lopez et al. 2006; Ruiz-Herrera and Sentandreu 2002; Zinjarde et al. 2008) reported the role of neutral pH on the induction of dimorphism in *Y. lipolytica*, which is in agreement with the experimental results presented in the current paper. Nevertheless, in none of these studies the effect of pH on yeast morphology was only considered. Indeed, experiments were performed under uncontrolled culture conditions (Erlenmeyers, tubes) leading thereby to multifactorial stress responses (Gonzalez-Lopez et al.

2006; Ruiz-Herrera and Sentandreu 2002; Zinjarde et al. 1998). Moreover, the effect of pH was usually studied simultaneously with other dimorphism inducers, notably the carbon source such as N-acetylglucosamine or serum. Previous results (Ruiz-Herrera and Sentandreu 2002) showed that mycelial growth decreased as pH lowers from pH 7 to pH 3 (with only 34 % of short mycelial cells at pH 4.0). In the current study, pH 4.5 was found to affect yeast morphology, as noticeable filamentous growth predominated during the culture. These results are controversial and may probably be explained by a strain-dependent effect of pH on the dimorphic capacity in *Y. lipolytica* species. The strain dependent dimorphic capacity was previously demonstrated in the work of Rodriguez and Dominguez (1984) and Perez-Campo and Dominguez (2001) as different *Y. lipolytica* species exhibited different morphological behaviors when exposed to dimorphism inducers.

Subsequently, a continuous operating mode was preferentially employed as it enabled the study of the stress response of cells stabilized in the same metabolic and morphological state. The above results concerning the effect of pH on morphological transition during batch fermentations directed the choice of pH perturbation on the alkaline stress. Controlled perturbations in the form of consecutive pulses and Heaviside at pH 7 were then assayed at various cell growth rates during these cultures.

Characterization and comparison of the growth kinetic parameters during continuous cultivations of *Y. lipolytica* showed no significant variations between the steady state and pH stressed conditions for each dilution rate. Studies presenting a quantitative assessment of the growth dynamics of *Y. lipolytica* under continuous culture conditions, as provided by this study are lacking. Indeed, most of the papers looked at the synthesis of various valuable by-products (lipids, organic acids, enzymes...) under specific cultures conditions (nitrogen, phosphorus deficiencies...) using different substrates (glucose, glycerol, olive oil...) (Deive et al. 2010; Ochoa-Estopier and Guillouet 2014; Rakicka et al. 2015; Rywinska et al. 2011). pH fluctuations appear to have no detectable effect on the macroscopic behavior of cells grown at different rates. This response is thought to be attributed to the high adaptive potential of *Y. lipolytica* to survive under alkaline conditions (Barth and Gaillardin 1996). Previous reports showed an increased production of mitochondrial reactive oxygen species and increased activity of superoxide dismutase enzymes in conjunction with the exposure to alkaline stress (Sekova et al. 2015).

Under batch and continuous modes of cultures, *Y. lipolytica* cells exhibited no loss of viability (esterase activity, membrane integrity) with pH perturbation indicating thereby their robustness against pH stress. This evidenced that filamentation, induced during batch fermentation was not a prerequisite for cell death. These findings were expected since a set of genes involved in maintenance of cell wall integrity were identified as up-regulated during dimorphic transition of *Y. lipolytica* (Topiltin Morales-Vargas et al. 2012).

Regarding the morphological evolutions in continuous fermentations, no dimorphic transition was induced by the alkaline stress, in contrast to batch cultivations. The culture consisted mainly of single cells showing a perfectly ovoid /spherical shape with a unimodal size distribution. Bellou et al. (2014) conducted the only study to date examining morphological changes in *Y. lipolytica* under continuous mode. Even though culture conditions (restricted oxygen supply, lipid accumulation conditions, glycerol substrate) were different than the present study, their results indicated the ability of *Y. lipolytica* to grow in the mycelial form in a chemostat operating mode at a low dilution rate of 0.032 h^{-1} . In the present study, the cell morphology displayed by the microorganism was similar over the broad range of dilution rates tested (from 0.03 to 0.20 h^{-1}). This suggests that the growth rate have no impact on the stress response, which is in accordance with Shepherd and Sullivan (1976) who observed a non-significant effect of varying the dilution rate on the morphology of *Candida albicans* grown on different carbon sources in continuous cultures. In contrast, several researchers emphasized the relationship between the dilution rate and growth morphology. Wiebe and Trinci (1991) observed a decreased fragment concentration and increased hyphal diameter of *Fusarium graminearum* cells when the dilution rate was increased from 0.07 to 0.19 h^{-1} in glucose-limited continuous cultures. At specific growth rates lower than 0.12 h^{-1} , changes in mycelial morphology were observed during chemostat cultivation of *Aspergillus niger*: hypha were branched and conidiation occurred. Whereas, hyphal branching was less pronounced at dilution rates higher than 0.12 h^{-1} (Schrickx et al. 1993).

It is apparent from this study that the effect of pH perturbation on *Y. lipolytica* morphology is predominately determined by the culture mode. In batch cultivations, where cells proliferated at their maximum growth rates, mycelia were mainly formed. Whereas in chemostat cultivations at controlled growth rates even closed to the maximum growth rate of the strain (0.24 h^{-1}), yeast-like cells predominated. No such data were previously described for *Y. lipolytica*. Nevertheless, similar observations were made by O'Shea and Walsh (2000) who

attributed morphological alterations in *Kluyveromyces marxianus*, induced by restricted aeration, to differences in the culture mode (batch and chemostat) imposed on the microorganism.

This dependence of the stress response on the culture mode may be either attributed to differences in the kinetic behavior between yeast-like and filamentous populations, to differences in cell age distribution (history dependence) in batch and chemostat bioreactors, or related to variabilities in the pH adaptive mechanisms dependent on the culture mode. In continuous bioreactors, all the cells are in the same physiological state and grow at the same specific rate, while in batch cultures cell subpopulations with different physiological states growing at various specific rates may cohabit at the same time. Despite advances in the knowledge of the molecular mechanisms regulating dimorphism in *Y. lipolytica* (signaling pathways (Cervantes-Chavez et al. 2009; Cervantes-Chavez and Ruiz-Herrera 2006; Cervantes-Chavez and Ruiz-Herrera 2007), genomic (Hurtado et al. 2000; Martinez-Vazquez et al. 2013; Topiltin Morales-Vargas et al. 2012) and proteomic approaches (Morin et al. 2007)), understanding the effect of the culture mode on the dimorphic transition of *Y. lipolytica* in response to pH stress requires further research and investigation.

This work reports for the first time the impact of the culture mode on the pH stress responses in *Y. lipolytica*, and provides a detailed quantitative data on the growth kinetic parameters (specific rates, yields, RQ) of this yeast. Such data are still quite rare, although the increasing interest in the application of *Y. lipolytica* for biotechnological advances.

Acknowledgements

Financial support for this study was provided by Airbus, Agence Nationale de la Recherche (ANR) and Commissariat aux Investissements d'Avenir via the project ProBio3 “Biocatalytic production of lipidic bioproducts from renewable resources and industrial by-products : BioJet Fuel Application” (ref. ANR-11-BTBT-0003).

Compliance with ethical standards

Conflict of interest: The authors declare that they have no conflict of interest.

Ethical approval: This article does not contain any studies with human participants or animals performed by any of the authors.

III.3.3 Results synthesis

- ⇒ Dynamics of growth, metabolism and morphology of *Y. lipolytica* W29 strain in response to different types of pH perturbation (pulses, Heaviside) were assessed under well-controlled conditions (mono-factorial investigation approach) in batch and continuous bioreactors (cells in distinct physiological states).
- ⇒ Changes in biomass morphology were qualitatively and quantitatively characterized at the population scale. Quantitative measurements of the frequency distribution (in number and in volume) of the equivalent cell diameter enabled the classification of cells into the yeast-like and filamentous subpopulations, providing therefore a realistic description of the heterogeneity of the culture.
- ⇒ Detailed quantitative data on the growth kinetic parameters (specific rates, yields, rates) of *Y. lipolytica* at different pH was provided in well-controlled culture conditions: these data are not yet described in literature.
- ⇒ For both process modes, the macroscopic behavior (growth dynamics, viability) of *Y. lipolytica* was not markedly affected by the pH of the culture:
- Batch mode:
 - No production of organic was observed for all tested pH (4.5; 5.6; 7 and pulse from pH 5.6 to 7): glucose was completely converted to biomass and carbon dioxide.
 - Kinetics of biomass growth and glucose uptake followed broadly similar trends during the different batch runs.
 - Respiratory activity of the yeast (qO_2 , qCO_2 and RQ) was slightly affected at acidic (pH 4.5) and neutral pH compared to cells cultivated at pH 5.6.
 - No loss in cell viability (dead population not exceeding 3.4 %) was caused by changes in pH conditions.
 - Continuous mode:
 - Under the various growth rates (dilution rates) and pH perturbation applied, no organic acid secretion was detected.
 - No significant differences in the growth kinetic parameters between steady state

and pH stress phases for each of the dilution rate (0.03; 0.07; 0.10 and 0.2 h⁻¹).

- The low percentage of cell death along fermentation revealed the high adaptive potential of *Y. lipolytica* to withstand pH stress.

⇒ The morphological behavior of the yeast appeared to be dependent on the culture mode:

- Batch mode:

- A yeast-to-mycelium transition was induced at pH 4.5, pH 7 and after the pH pulse from 5.6 to 7: proportion of filamentous cells was higher than 77 % (v/v).

- Cells cultivated at pH 5.6 exhibited, predominantly, a yeast-like morphology: no more than 3.5 % (v/v) of elongated cells.

- Continuous mode:

- No morphological changes were observed in continuous experiments although exposure to stress during at least five residence times. The culture consisted mainly of ovoid-shaped cells with normal size distribution (average diameter below 6.2 μm).

- The growth rate of the yeast had no impact on the stress response: the morphology of the yeast remained unaltered by varying the dilution rate from 0.03 until 0.20 h⁻¹, which was closed to the maximum growth rate of the strain (0.24 h⁻¹).

PART III: RESULTS AND DISCUSSION

Chapter III-4: Investigation of the effect of oxygen availability on the metabolism and morphology of *Yarrowia lipolytica*: more insights into the impact of glucose levels on dimorphism

Chapter III-4: Investigation of the effect of oxygen availability on the metabolism and morphology of *Yarrowia lipolytica*: more insights into the impact of glucose levels on dimorphism

III.4.1 Introduction

This chapter is presented in the form of a scientific article currently submitted to “Applied Microbiology and Biotechnology”.

It presents a study on the impacts of fluctuating, low and limited dissolved oxygen (DO) conditions on the dynamic behavior of *Y. lipolytica* W29 strain in batch and glucose-limited chemostat cultures. The choice of evaluating the oxygen availability on the stress response was based on the operational feedback provided by the industrial partner of the ProBio3 project (Tereos), and was also justified by literature data. Indeed, DO gradients were frequently encountered at the industrial production scale (Oosterhuis and Kossen 1984; Reuss et al. 1994; Zahradnik et al. 2001). Additionally, *Y. lipolytica*, the microorganism of interest in this study, was characterized by its ability to undergo metabolic and morphological shifts in response to fluctuations in DO levels (Bellou et al. 2014).

Although the impact of oxygen deficiency on *Y. lipolytica* physiology was widely recognized, studies under controlled culture conditions (in bioreactor) during biomass propagation phase are missing. As well, the yeast behavior in response to DO perturbations representatives of the heterogeneous conditions experienced in large scale bioreactors has never been reported in previous research. In addition, characterization of the dimorphic transition of *Y. lipolytica* at the population level through analysis of cell size distribution within the culture represented an original method to monitor changes in morphology during fermentation.

First part of this study was devoted to characterize and quantify the dynamic responses of *Y. lipolytica* to controlled perturbations in DO concentrations under batch mode of culture. Continuous operation mode was subsequently employed to examine the yeast behavior during exposure to fluctuated, low and limited oxygen supply. The resulting microbial responses were then characterized at the metabolic and morphological levels, and compared between both modes of cultures. At the end of this chapter, results were discussed and compared with bibliographic data. This study opens up new avenues in the investigation of the mechanisms underlying differences in stress responses of *Y. lipolytica* between batch and continuous modes of cultures.

III.4.2 Publication: Investigation of the effect of oxygen availability on the metabolism and morphology of *Yarrowia lipolytica*: more insights into the impact of glucose levels on dimorphism

Asma Timoumi¹, Carine Bideaux¹, Stéphane E. Guillouet¹, Yohan Allouche², Carole Molina-Jouve¹, Luc Fillaudeau^{1§} and Nathalie Gorret^{1§*}

¹LISBP, Université de Toulouse, CNRS, INRA, INSA, Toulouse, France.

²Airbus Operations S.A.S, 316 Route de Bayonne, 31060 Toulouse, France.

§These authors contributed equally to the supervision of this work

*Corresponding author.

Tel.: +33 05 61 55 94 44; fax: +33 05 61 55 94 00.

E-mail address: nathalie.gorret@insa-toulouse.fr

Abstract

Dynamic behavior of *Yarrowia lipolytica* W29 under conditions of fluctuating, low and limited oxygen supply were characterized in batch and glucose-limited chemostat cultures. In batch cultures, transient oscillations between oxygen-rich and -deprived environments induced the production of citric acid by the yeast. By contrast, no citric acid was detected in continuous fermentations for all stress conditions: full anoxia (zero pO₂ value, 100 % N₂), low (pO₂ close to 2 %) and limited (zero pO₂ value, 75 % of cell needs) dissolved oxygen (DO) levels. The macroscopic behavior (kinetic parameters, yields, viability) of *Y. lipolytica* was not significantly affected by the exposure to DO fluctuations under both modes of cultures. Nevertheless, conditions of oxygen limitation have led to the destabilization of the glucose-limited growth during the continuous cultivations. Morphological responses of *Y. lipolytica* to DO oscillations were different between batch and chemostat runs. Indeed, a yeast-to-mycelium transition was induced and progressively intensified during the batch fermentations (filamentous subpopulation reaching 74 % in volume). While, in chemostat bioreactors, the culture consisted mainly of yeast-like cells (mean diameter not exceeding 5.7 μm) with a normal size distribution. In continuous cultures, growth at low DO concentration did not inflict any changes in *Y. lipolytica* morphology. Dimorphism (up to 80.5 % (v/v) of filamentous cells) was only detected in conditions of oxygen limitation with the presence of excess glucose (more than 0.75 g L⁻¹). These data suggest an impact of glucose levels on the signaling pathways regulating dimorphic response in *Y. lipolytica*.

Keywords: Batch; Chemostat; Dissolved oxygen concentration; Dynamic response; Morphology; *Yarrowia lipolytica*

III.4.2.1 Introduction

Yarrowia lipolytica is an obligate aerobic non-conventional yeast that has attracted great attention due to its particular physiological and biochemical characteristics (Coelho et al. 2010). It represents an industrially important microorganism capable of producing a broad spectrum of valuable metabolites (e.g. organic acids, lipids, enzymes, and proteins) (Bussamara et al. 2010; Madzak et al. 2004; Papanikolaou and Aggelis 2009; Parfene et al. 2013), and having potentialities to degrade a wide variety of carbon sources (e.g. glucose, alcohols, acetate and hydrophobic substrates) (Fickers et al. 2005; Finogenova et al. 2002; Papanikolaou et al. 2006) as well as several types of low-value or harmful by-products (e.g. raw glycerol and olive mill wastewater) (Makri et al. 2010; Sarris et al. 2011).

Bioreactors are designed to provide a controlled environment for optimal cell growth and/or product synthesis. However, the scale up of a bioprocess is limited by practical constraints that entail frequently transfer and mixing problems, and the concomitant occurrence of local gradients in process parameters (e.g. temperature, pH, dissolved oxygen (DO), substrate and metabolite concentration) (Enfors et al. 2001; Hewitt and Nienow 2007; Lara et al. 2006). Microorganisms are highly sensitive to these heterogeneities and may exhibit different metabolic and physiological behaviors, potentially leading to the generation of phenotypic variabilities at the population level (Amanullah et al. 2001; Bylund et al. 1998; Delvigne et al. 2009; Han et al. 2013).

At the large scale, DO gradients are part of the fluctuations that are likely to occur as a result of the interaction between oxygen transfer, circulation time and microbial kinetics (Amanullah et al. 2004; Oosterhuis 1984; Palomares and Ramírez 2003). Several experimental and computational approaches were employed to predict oxygen gradients in large scale bioreactors (Oosterhuis and Kossen 1984; Reuss et al. 1994; Sweere et al. 1987; Vlaev et al. 2000; Zahradnik et al. 2001; Zhang et al. 2009). Spatial fluctuations in oxygen concentrations ranging from 22 to 0 % (with respect to air saturation) were identified respectively in ideal mixed and stagnant zones of 19 m³ bioreactor, equipped with six-bladed Rushton turbine impellers (Oosterhuis and Kossen 1984). Furthermore, a 64-fold difference between maximum and minimum oxygen concentrations were predicted inside a 100 L bioreactor (Reuss et al. 1994). Spatial non-uniformities in DO concentrations varying between 3 and 49 % (with a mean value of 35 ± 0.24 %) were also identified in different zones of a 3 m³ triple-impeller stirred reactor (Zahradnik et al. 2001).

Being a strictly aerobic microorganism, oxygen is a key substrate in *Y. lipolytica* cultivation. The amount of oxygen available to yeast cells may directly influence their growth, metabolism and morphology. An increase in the oxygen availability, imposed either by pressure rise or oxygen transfer enhancement (through agitation and aeration rates modulation), had been shown to enhance cellular growth (Finogenova et al. 1991; Lopes et al. 2009a), lipase synthesis (Kar et al. 2008; Lopes et al. 2008), γ -decalactone secretion (Braga and Belo 2015) and organic acid production (Ferreira et al. 2016a; Rane and Sims 1994; Rywińska et al. 2012) in *Y. lipolytica*. Nonetheless, low ($\leq 5\%$ of saturation) and/or limited (0 % of saturation) DO levels were often required for more efficient production of some extracellular metabolites (such as mannitol, arabitol, citric acid and succinic acid) by this yeast (Jost et al. 2015; Kamzolova et al. 2003; Workman et al. 2013). Furthermore, DO concentrations have been considered as one of the major factor affecting *Y. lipolytica* morphology. Indeed, mycelia were mainly formed under low aerated conditions, whereas high aeration induced the growth in the yeast-like form (Bellou et al. 2014). In most of the previous studies, the effect of oxygen availability on the morphology of *Y. lipolytica* has been investigated under uncontrolled culture conditions, either in sealed bottles (with gradually decreasing DO levels by varying the headspace volume) (Zinjarde et al. 1998), tubes (under layer of mineral oil) (Ruiz-Herrera and Sentandreu 2002) or flasks (by addition of an oxidizing agent) (Kawasse et al. 2003; Kim et al. 2000). A recent study (Bellou et al. 2014) analyzed the influence of DO concentrations on the dimorphism of *Y. lipolytica* under controlled conditions in bioreactor, but in lipid-producing conditions (nitrogen limitation) and not during biomass propagation phase.

Regulation of the dimorphic transition in *Y. lipolytica* is based on the operation of the mitogen-activated protein kinase (MAPK) and the cyclic-AMP (cAMP) dependent protein kinase A (PKA) signaling pathways. These pathways operate in opposition during the yeast-to-mycelium transition: MAPK pathway is necessary for mycelial growth whereas PKA pathway is required for growth in the yeast-like form (Cervantes-Chavez et al. 2009; Cervantes-Chavez and Ruiz-Herrera 2006; Cervantes-Chavez and Ruiz-Herrera 2007). Specifically, increasing cAMP levels in cells inhibited mycelial growth in *Y. lipolytica* (Cervantes-Chavez and Ruiz-Herrera 2007; Ruiz-Herrera and Sentandreu 2002). cAMP concentration can be increased either by adenylate cyclase activation or by entry of exogenous nucleotides into the cell (Cervantes-Chavez and Ruiz-Herrera 2007)

The impacts of the filamentous morphology on broth rheology, transfer phenomena inside bioreactor, and related productivity have been extensively studied in the literature (Coelho et al. 2010; Fickers et al. 2009; Galvagno et al. 2011; Kar et al. 2011; Lim et al. 2002; O'Shea and Walsh 2000; Wucherpfennig et al. 2010). In the case of *Y. lipolytica*, a filamentous subpopulation representing 12 % (in volume) of the culture has been shown to affect physico-chemical properties of the fermentation broth, which consequently resulted in deterioration of bioprocess performances (Kraiem et al. 2013). Furthermore, some metabolic activities of industrial interest in *Y. lipolytica*, such as aroma production, organic acid biosynthesis, hydrocarbon degradation and heterologous protein secretion, were dependent on the cell morphology (Braga et al. 2016; Gasmi et al. 2011; Madzak et al. 2005; Palande et al. 2014; Rywinska et al. 2011; Zinjarde et al. 1998). Understanding and control of *Y. lipolytica* dimorphic behavior is thus of major importance for improving bioprocesses based on this microorganism.

Light microscopy, sometimes combined with image analysis and processing was the most commonly used method for describing morphological changes in *Y. lipolytica* (Botelho Nunes et al. 2013; Braga et al. 2016; Guevaraolvera et al. 1993; Kawasse et al. 2003; Ota et al. 1984; Zinjarde et al. 2008). Analysis of size distribution profiles of *Y. lipolytica* cells within the culture broth was recently employed to characterize the dynamics of filamentous growth at the population level (Timoumi et al. 2017). Such methodology may provide a realistic description of the morphological heterogeneity of the culture, and allows subcategorization of yeast subpopulations into the yeast-like (ovoid or spherical single cells) and filamentous (elongated cells and pseudomycelia) forms. On another hand, studies on the morphological behavior of *Y. lipolytica* in response to DO fluctuations under controlled culture conditions are quite lacking. These approaches/ data allow to approximate DO gradients occurring in large-scale equipments, which would help to improve the scale up process.

In the current research, the impact of DO fluctuations of different frequencies and durations on the metabolic and morphological characteristics of *Y. lipolytica* were studied in controlled batch and glucose-limited continuous bioreactors. Dynamics of stress responses were characterized on yeast populations with different physiological states: (i) in continuous cultivations, where the environment is constant, the entire cell population grows at a constant growth rate, and exhibits the same physiological state, and (ii) on the opposite, yeast subpopulations with different physiological states, and growing at various specific rates may coexist within the culture under batch mode. In addition, the influence of low ($pO_2 \approx 2\%$) and

limited ($pO_2 = 0\%$) DO levels on the dimorphism and physiology of *Y. lipolytica* was analyzed in glucose-limited steady state cultures using a similar investigative approach.

III.4.2.2 Materials and methods

III.4.2.2.1 Microorganism, media and growth conditions

The strain used in this study was the wild-type *Y. lipolytica* W29 (ATCC® 20460™). Culture conditions and medium composition were performed as previously reported (Timoumi et al. 2017). All chemicals used (glucose, salts, oligo-elements, vitamins, orthophosphoric acid, potassium hydroxide and polypropylene glycol) were of the highest grade commercially available.

III.4.2.2.2 Bioreactor cultures

Batch and glucose-limited continuous cultures were performed in a 1.6 L stainless-steel stirred tank bioreactor with a working volume of 1 L (BIOSTAT® Bplus, Sartorius, Germany). Reactor equipment and configuration, as well as inoculum preparation steps were as previously described (Timoumi et al. 2017). Special attention was paid to the standardization of pre-growth conditions (pH 5.6, temperature 28 °C, agitation speed 130 rpm, incubation time 12 h exactly) in order to avoid filament formation prior to inoculation into the bioreactor for cellular stress responses studies. The temperature was regulated at 28 °C and the pH at 5.6 by addition of 2 M potassium hydroxide solution. During the batch runs, 1 mL L⁻¹ of polypropylene glycol (antifoam PPG) was added in the medium after sterilization. For chemostat experiments, the antifoam was periodically added by means of a peristaltic pump (pulse-based addition) to maintain a nearly constant concentration (1 mL L⁻¹) in the bioreactor. All continuous cultures were carried out at dilution rates close to 0.10 h⁻¹. Steady-state phases were achieved after at least five residence times.

III.4.2.2.3 Oxygen perturbation experiments

Under batch cultivation mode, perturbations in DO concentrations from highly aerobic (pO_2 value above 40 % of saturation) to anoxic (pO_2 value of 0 %) conditions were achieved by sterilely injecting nitrogen gas inside the bioreactor. In order to create oscillatory environments between stressed (100 % N₂; $pO_2 = 0\%$) and unstressed (100 % air; $pO_2 \geq 40\%$) states, two intermitted aeration strategies were applied, by means of an external gas valve, during two independent batch experiments: i) 1-h period of continuous anoxia intermittent

with 1-h period under air supply; ii) 1-h period of discontinuous anoxia (switch between air and nitrogen gas every 20 min) alternating with 1-h of air feed. Cells were exposed to DO fluctuations from the beginning of the exponential growth phase (at a biomass concentration of almost 1 gCDW L⁻¹). For each batch run, three sets of anoxic perturbations were applied until glucose depletion in the medium. Samples were taken before, during and after stress application, for further ex-situ characterization.

During continuous experiments, steady-state cultures were exposed to transient perturbations in DO concentrations. Oxygen fluctuations were carried out using the same strategy as described for the batch cultivations. Additional perturbations with higher frequency (oscillations between air and nitrogen gas every 5 min) and same duration (1 h) were also applied during these cultures. Samples were collected during the steady state phase and upon stress exposure at time intervals of 2 h for analysis.

In addition, glucose-limited chemostat cultures at low (pO₂ value around 1.9 ± 0.3 % of saturation) and limited (zero pO₂ value) amounts of DO were carried out by modulating agitation speed and/or aeration rate. For the low DO concentration studies (pO₂ close to 2 %), pO₂ levels were regulated through a cascade controller varying the impeller speed (from 420 to 430 rpm) and keeping constant the aeration rate at 0.35 L min⁻¹. Subsequently, oxygen-limited conditions (pO₂ = 0 %) were obtained by manually reducing the air flow rate by almost 25 % of the initially set flow rate (0.35 L min⁻¹), and adjusting agitation at 430 rpm (the cascade controller was shuttled down during this phase). Samples were characterized along the steady state and stress phases.

III.4.2.2.4 Biomass characterization

III.4.2.2.4.1 Biomass concentration

Biomass concentration was quantified by spectrophotometric (OD_{620nm}) and dry weight measurements following the protocol described by Timoumi et al. (2017). The biomass formula CH_{1.675}O_{0.523}N_{0.153} with molecular weight of 25.59 g Cmol⁻¹ considering 5.7 % of ashes was used to convert cell dry weight measurements into molar carbon concentration.

III.4.2.2.4.2 Cell viability

During batch and chemostat runs, cell viability was assessed by flow cytometry using a BD Accuri C6[®] flow cytometer (BD Biosciences) equipped with blue (488 nm) and red (640 nm) excitation lasers. Different fluorescent probes: carboxyfluorescein diacetate (cFDA),

propidium iodide (PI) and Sytox® red were used to monitor esterase activity and membrane integrity, as indicators of yeast viability. Two staining combinations (cFDA/PI and cFDA/Sytox) were optimized to identify and quantify live and dead subpopulations within the culture. Previously published procedure (Timoumi et al. 2017) was rigorously followed for preparing dye solutions, staining cells and analyzing samples. Fluorescence emitted by cFDA, PI and Sytox® red stained cells were collected at FL1 (533/30nm), FL3 (>670 nm) and FL4 (675/25) detectors respectively.

III.4.2.2.4.3 Cell morphology

In this study, different methods were used to assess changes in yeast morphology upon exposure to stress conditions:

Flow cytometry: single cell behavior within the microbial population was analyzed by the BD Accuri C6® flow cytometer (BD Biosciences). Cell size and internal granularity were correlated with forward scattered (FSC, 0 degrees, ± 13) and side scattered (SSC, 90 degrees, ± 13) light respectively. Cell size was determined from the FSC signal using a calibration curve established by a set of polystyrene microspheres of diameters ranging between 1 and 15 μm (Flow Cytometry Size Calibration Kit (F-13838), Molecular probes, Invitrogen, USA). The width of the FSC signal representing the time of flight of the cell through the laser beam was examined in order to determine the length distribution of cells within the population. Measurements were performed according to a previously published protocol (Timoumi et al. 2017). The acquired data were analyzed using FlowJo software (Tree Star).

Morphogranulometry: morphological characterization of cell subpopulations were performed using a morpho-granulometer (Mastersizer G3S, Malvern Instruments Ltd. SN: MAL1033756, software Morphologi v7.21). This optical device includes a system of lens (magnification: from x1 to x50, dimension min/ max: 0.5/ 3000 μm) and a camera (Nikon CFI60) with a resolution close to 0.06 μm / pixel. Samples were diluted, homogenized and observed between cover glass and slide. A surface of 2 x 2 mm² was examined under standardized conditions (magnification x20, dark field mode, light intensity 100 %, exposure time 300 ms). Recorded images were filtered and analyzed to identify individual cells and their geometrical properties (diameter, aspect ratio, circularity, etc.). Number and volume distribution associated to each parameter were automatically generated.

Diffraction light scattering: size distribution of cells within the culture was characterized by means of a diffraction light scattering device (Mastersizer 2000 Hydro, Malvern Instruments Ltd. SN: 34205-69, range from 0.02 to 2000 μm). A defined volume (1 mL) of culture samples was added to a circulation loop (dispersant agent: water; refractive index: 1.33). Measurements were performed at room temperature (20 °C) with obscuration rates (red $\lambda=632.8$ nm and blue $\lambda=470.0$ nm lights) varying between 10 and 40 %. Detected scattered lights were converted into a volume size distribution of the equivalent spherical diameter d_{SE} (diameter of the sphere of the same volume as the particle).

Light microscopy: cell photographs were taken using an Olympus BH-2 microscope (Olympus optical Co., Ltd, Tokyo, Japan) equipped with a color digital camera (Nikon's Digital System DS-Ri1, Surrey, UK).

III.4.2.2.5 Sugar and organic acid analysis by high-performance liquid chromatography (HPLC) and ionic chromatography (HPIC) techniques

During batch experiments, glucose and organic acid (acetate, pyruvate, succinate and citrate) concentrations were determined by high performance liquid chromatography (Ultimate 3000, Dionex, USA) using an Aminex HPX-87H⁺ column (Bio-RAD, US). Quantification of glucose and organic acids (acetate, pyruvate, succinate, malate, fumarate and citrate) present at low concentrations in the culture under continuous mode was carried out by high performance ionic chromatography (ICS-3000, Dionex, USA) using the CarboPacTM PA1 and IonPac AS11-HC columns respectively. All procedures and precisions of these apparatus were followed according to previously described methods (Timoumi et al. 2017).

III.4.2.2.6 Gas analysis and monitoring

The online analysis of the composition of inlet and outlet gas streams during bioreactor cultivations was performed using a fermentation gas monitor system (LumaSense Technologies Europe) composed of a multipoint sampler 1309 (INNOVA 1309) and a gas analyzer (INNOVA 1313). Measurements of oxygen (O₂) and carbon dioxide (CO₂) concentrations were carried out by means of two acoustic-based methods: magneto-acoustic spectroscopy for O₂ measurements and photo-acoustic spectroscopy for CO₂ measurements.

III.4.2.2.7 Calculation methods

Off-gas rates: oxygen consumption (r_{O_2}) and carbon dioxide production (r_{CO_2}) rates were determined from mass balances in gas and liquid phases as previously reported (Timoumi et al. 2017), with considering the inlet and outlet gas compositions, as well as the evolutions of temperature, pH, salinity, and liquid volume in the bioreactor.

Glucose consumption and biomass production rates: glucose uptake (r_S) and biomass production (r_X) rates were calculated using their measured data and as their respective mass balance equations. For the chemostat experiments, the inlet and outlet volumetric flow rates were included in calculating these rates.

Statistical analysis: principles of statistical tests used in this study are presented in the Electronic supplementary material (Timoumi et al. 2017).

Analysis of cell size distribution at the population level: basic principles of particle size analysis, size distribution calculations, as well as the methodology applied for the quantification of cell subpopulations of different morphology are presented in the Electronic supplementary material (Timoumi et al. 2017).

III.4.2.3 Results

III.4.2.3.1 Batch cultures

Batch cultures of *Y. lipolytica* were performed in bioreactor under fluctuating DO levels. Transient oscillations of cells between well-aerated and anoxic environments were carried out using two distinct stress implementation strategies. During their exponential growth phase, cells were submitted to three- and nine-successive anoxic perturbations intermittent with a 1-hour exposure to high concentrations of DO. The resulting microbial response was then characterized at the metabolic and morphological levels. The macroscopic behavior of the yeast was assessed through comparing the patterns of growth, viability, glucose uptake, oxygen consumption, organic acid and carbon dioxide production rates, before and upon stress exposure. Changes in yeast morphology were characterized at the cell population level by means of flow cytometry, morphogranulometry and diffraction light scattering techniques.

III.4.2.3.1.1 Macroscopic behavior characterization

Kinetics of growth of *Y. lipolytica* were analyzed and compared between stressed and unstressed physiological states. Evolutions of biomass concentrations, changes in respiration rates, as well as fluctuations in DO levels were illustrated in Figure III-23. Small amounts of citric acid were detected in culture supernatants upon stress application. Maximum concentrations of 23 and 29 mg L⁻¹ were reached during the stress phase of the batch cultivation with three- and nine-successive perturbations respectively. Citric acid produced was consumed by the microorganism when adequate oxygen supply was restored. As shown in Figure III-23, cells stopped growing during the periods of stress. An exponential growth was immediately resumed under favorable aeration conditions. Indeed, the growth rate reached a maximum value (0.24 h⁻¹) similar to that previously determined during oxidative cultivations of *Y. lipolytica* W29 on the same culture medium (Timoumi et al. 2017). Average growth rates during the perturbation phase attained 0.12 and 0.15 h⁻¹ when cells were exposed, respectively to three- and nine-consecutive fluctuations in DO concentrations. Furthermore, respiration rates (r_{O_2} and r_{CO_2}) as well as respiratory quotients (RQ) were synchronously affected by oxygen perturbations. An oxidative metabolism (RQ value around 1.1) was rapidly restored after repeated exposure to stressful conditions.

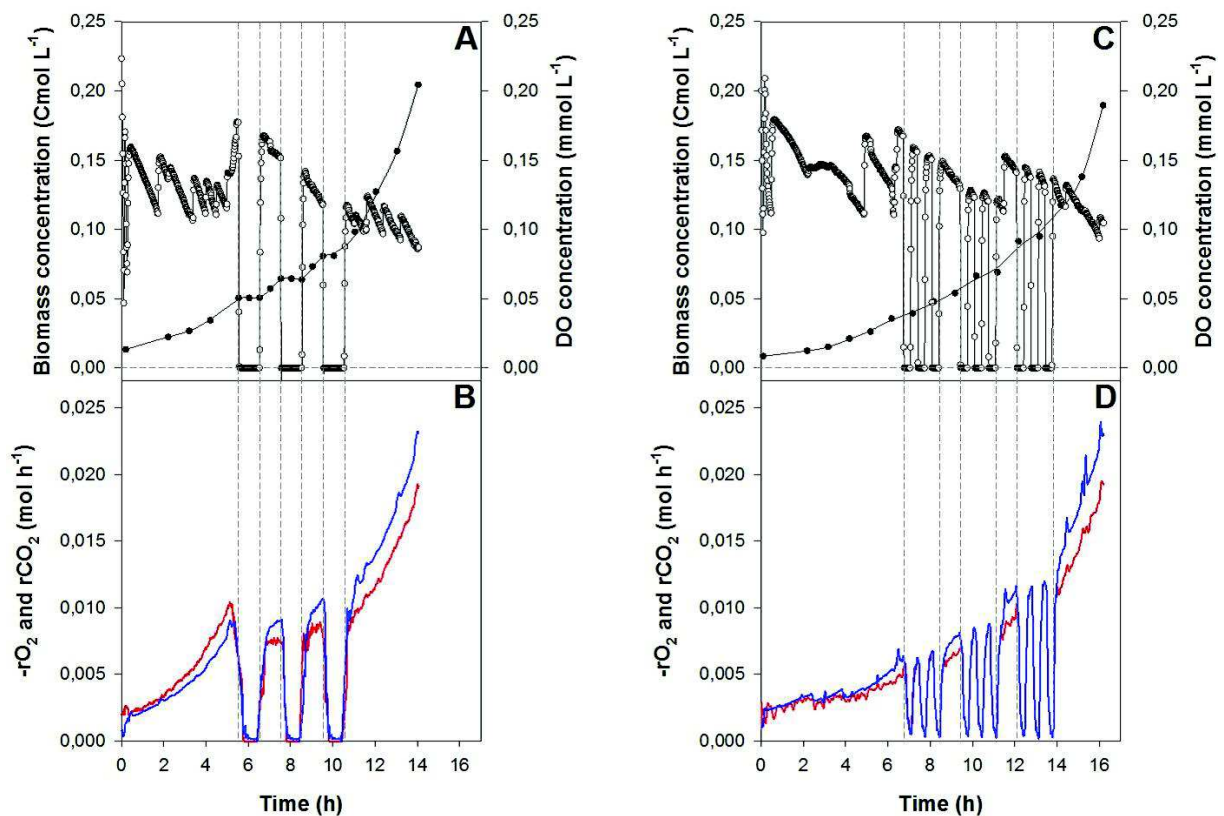


Figure III-23: Dynamic evolutions of biomass concentration, oxygen uptake and carbon dioxide production rates of *Y. lipolytica* W29 in response to controlled fluctuations in dissolved oxygen (DO) levels under batch cultivation mode. (A, B) Measured values from the continuous anoxic perturbations of 1 h. (C, D) Measured values from the discontinuous (switch between air and nitrogen gas every 20 min) anoxic perturbations of 1 h. In Figures (A, C), open symbols represent changes in DO levels, and filled symbols correspond to biomass concentrations. In Figures (B, D), red and blue lines correspond to oxygen consumption and carbon dioxide production rates, respectively. The vertical dashed lines (grey) delimit the stress phases

III.4.2.3.1.2 Morphological changes monitoring

Yeast morphology was examined by microscopy and characterized by size distribution analysis during fermentation. Figure III-24A compares the morphology of *Y. lipolytica* cells before and following exposure to DO fluctuations of different frequencies. Cells oscillating between oxygen-rich and -deprived environments developed a heterogeneous morphology composed predominantly of filamentous forms.

The equivalent circular diameter (d_{CE} , diameter of the circle with the same projected area as the cell particle) was employed to quantify changes in biomass morphology. This parameter provides a direct indication of the cell size and allows subcategorization of yeast populations into the yeast-like (ovoid or spherical single cells) and filamentous (elongated cells and pseudomycelia) forms. To describe adequately the heterogeneity of the culture, quantitative measurements of the frequency distribution in number and in volume based on the equivalent diameter was performed. A cylinder model based on accurate measurements of the length and width of cells was also applied in order to better approximate the elongated shape of cells. Granulometric methods measure different geometric properties of individual cells and generate number and volume distribution of each parameter at the population level. A mean equivalent diameter of 15 μm (calculated on the basis of the cylinder model), was employed as a threshold criterion to classify cells into the yeast-like and filamentous subpopulations (more details of these calculations are provided in the Electronic supplementary material (Timoumi et al. 2017)). Quantification data describing the dynamic evolution of the filamentous subpopulation during the course of the batch culture are presented in Figure III-24B: proportions of elongated cells reached 6.6/42.7 and 7.3/73.5 % (in number/ in volume) at the end of the batch fermentation submitted to three- and nine-consecutive perturbations, respectively.

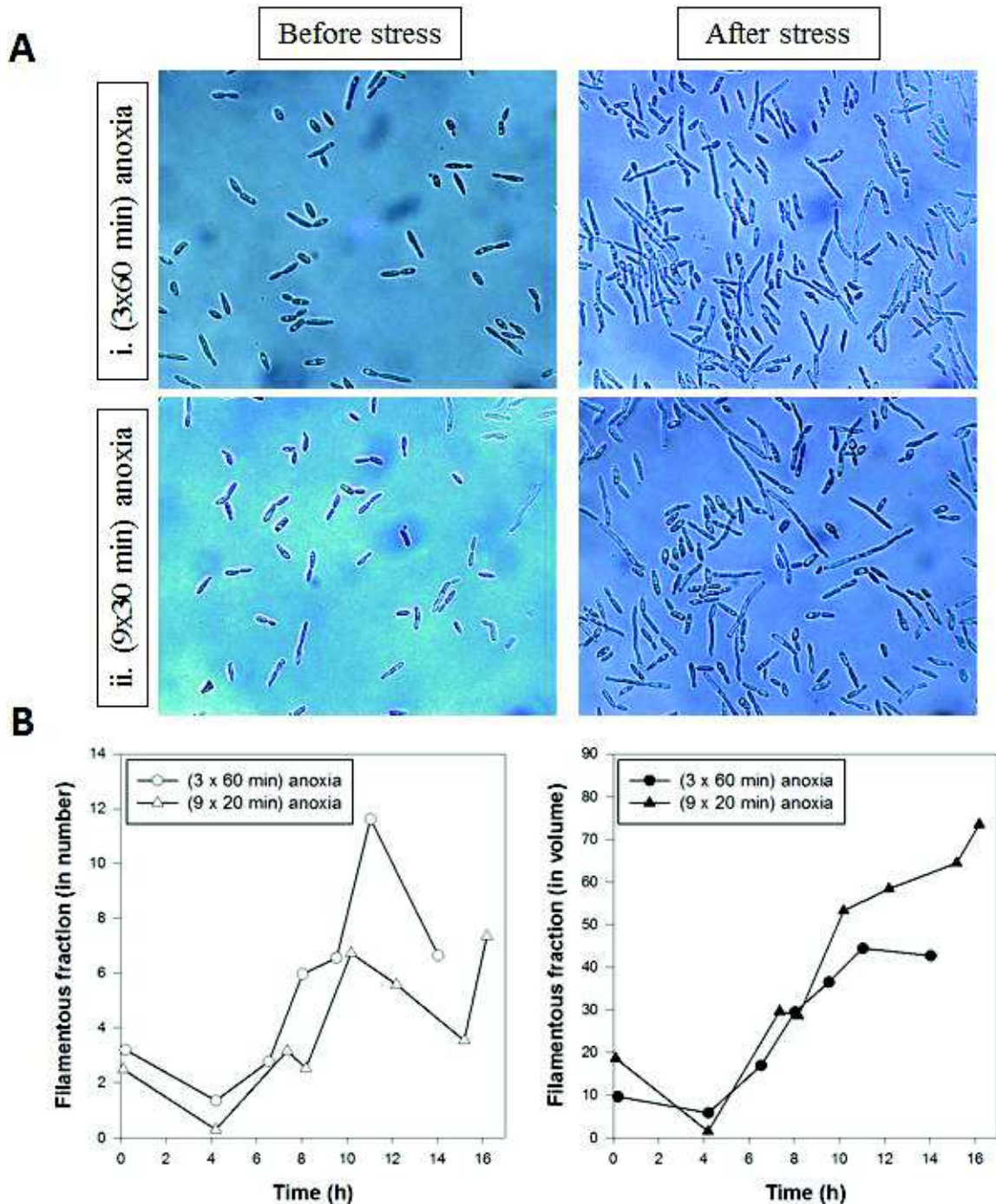


Figure III-24: A. Light micrographs showing morphological changes of *Yarrowia lipolytica* W29 in response to fluctuations in dissolved oxygen (DO) concentration during the batch cultures. The morphology was compared before and after exposure to (i) three and (ii) nine successive anoxic perturbations of 60 and 20 min, respectively. As growth progressed, observations were performed using a light microscope, without oil fixation, and at magnifications of 40 x. Image size is 54 μm in width and 44 μm in height. B. Dynamic evolution of the filamentous subpopulation, in number and in volume, during the DO oscillating batch cultures of *Y. lipolytica*. Data were quantified by morphogranulometric measurements based on the cylinder model (for calculation details, see the Electronic supplementary material (Timoumi et al. 2017))

III.4.2.3.1.3 Cell viability assessment

Flow cytometry in combination with the fluorescent probes (PI, cFDA and Sytox® red) was applied to rapidly assess the impact of DO fluctuations on the viability status of *Y. lipolytica*. The dual-parameter dot plots in Figure III-25 indicate a dead subpopulation that did not exceed 3 % at the end of the culture regardless of the perturbation's frequency imposed. Nonetheless, proportion of injured (damaged) cells seemed to be more important (almost 4-fold higher) when oscillating more frequently between oxygen-rich and -deprived environments.

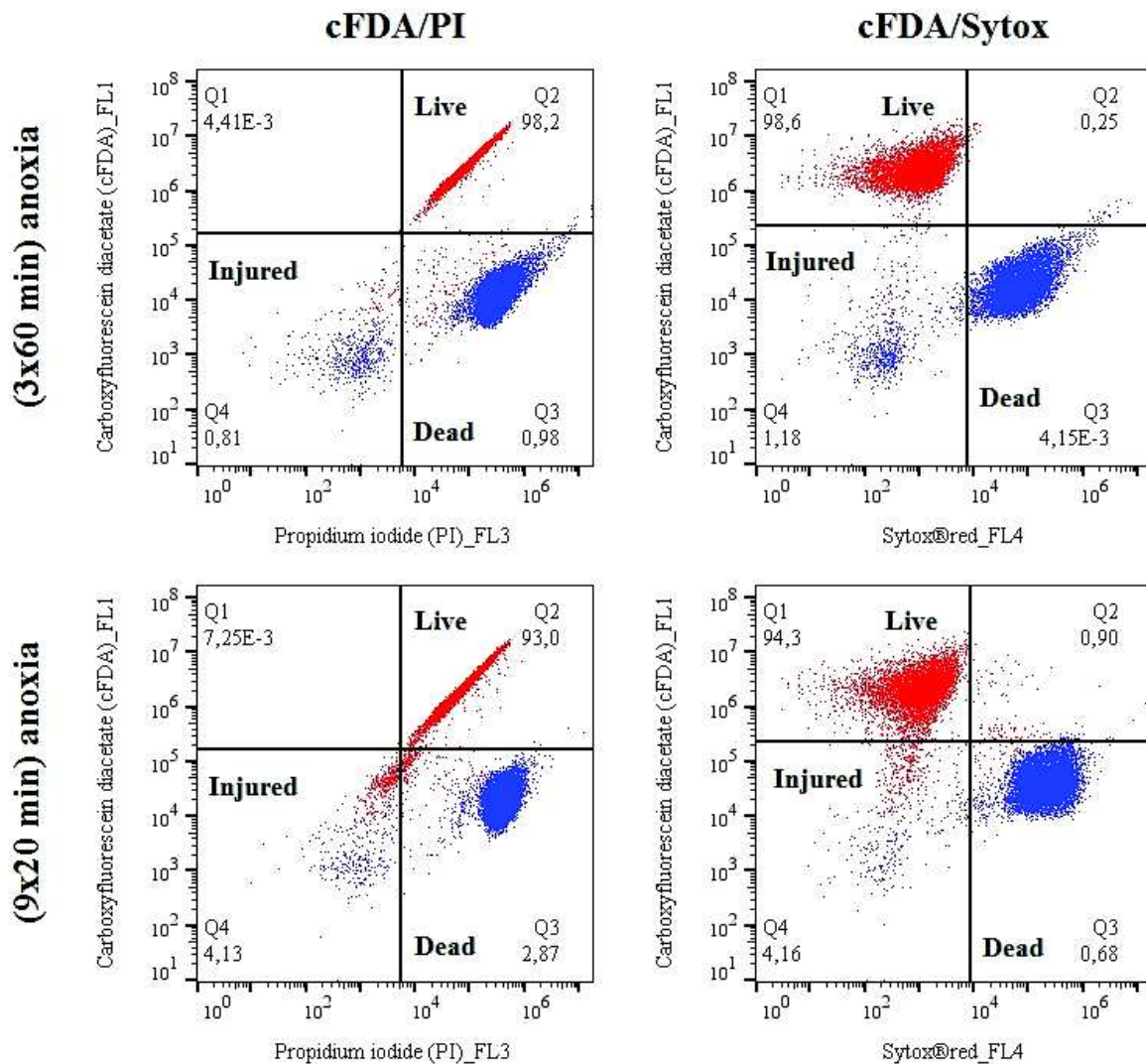


Figure III-25: Flow cytometry multiparameter dot plots representing cFDA (FL1) versus PI fluorescence (FL3) and cFDA (FL1) versus Sytox (FL4) fluorescence of the cFDA/PI and cFDA/Sytox double-stained *Y. lipolytica* cells, respectively. Data is presented for biomass samples taken at the end of each batch run (A, three DO perturbations of 60 min; B, nine DO perturbations of 20 min). Untreated (culture sample/ red color) and dead (control sample/ blue color) cells can be clearly discriminated by overlapping their respective plots. The quadrants

were set so that the double-stained dead cells appeared in the lower left quadrant. Percentages of cells indicated in each quadrant correspond to the culture sample (red color). Q1 and Q2 quadrants represent viable subpopulations in the cFDA/Sytox and cFDA/PI double-stained cells, respectively. Q3 quadrant represents the dead subpopulation. Q4 quadrant represents injured (damaged) cells

III.4.2.3.2 Continuous cultures

The effect of oscillating DO concentration on the metabolism and morphology of *Y. lipolytica* was investigated in glucose limited chemostat cultures at a dilution rate of 0.10 h^{-1} . Controlled oscillations from highly aerobic (unstressed) to anoxic (stressed) conditions were attained by manipulating the oxygen and nitrogen gas supply into the bioreactor. Periods of 60, 20 and 5 min of anoxia were tested on steady states cultures. In addition, continuous cultivations under low ($p\text{O}_2 \approx 2 \%$) and limited oxygen conditions ($p\text{O}_2 = 0 \%$ corresponding to 75 % of microorganism needs) were carried out in order to assess the impact of oxygen availability on the microbial response.

III.4.2.3.2.1 Macroscopic behavior characterization

Growth kinetic parameters of *Y. lipolytica* were calculated and compared between stressed and unstressed physiological states, as reported in Table III-15. At steady states, negligible amounts of residual glucose (lower than 8 mg L^{-1}) were quantified in the medium confirming thus the carbon-limited growth, and no organic acids were detected in the culture broth.

For the experiments with DO fluctuations, the specific uptake and production rates were quite similar to those quantified under steady state conditions, and this is irrespective of the duration and frequency of the stress applied. The average specific rates of glucose consumption ($-q_S$), oxygen uptake ($-q_{\text{O}_2}$) and carbon dioxide production (q_{CO_2}) were 0.148 ; 0.049 ; $0.057 \text{ Cmol CmolX}^{-1} \text{ h}^{-1}$ respectively under steady state, and 0.147 ; 0.048 ; $0.057 \text{ Cmol CmolX}^{-1} \text{ h}^{-1}$ respectively at the higher frequency of oxygen oscillations (perturbations every 5 min). Similarly to batch cultivations, *Y. lipolytica* cells resumed normal respiratory activity (RQ always higher than 1.1) after exposure to the various stress conditions. Despite the application of DO perturbations, even more frequent than those applied during the batch cultures, no production of organic acids was quantified during the chemostat runs.

Under conditions of low DO concentration ($p\text{O}_2 \approx 2 \%$), *Y. lipolytica* exhibits similar kinetic behavior compared to cells grown at high oxygen levels in the culture medium (steady-state phase) (Table III-15). These findings were expected since the oxygen supply to the broth, primarily through the inlet air path and in a much lesser extent via the medium feeding,

largely covers the oxygen requirements for *Y. lipolytica* growth at dilution rate of 0.10 h^{-1} . In the oxygen limitation studies ($p\text{O}_2 = 0 \%$), reduced aeration resulted in a 0.1-fold lower biomass production (as compared to fully-aerated media), and in an increased residual glucose concentration (up to 0.98 g L^{-1}) within nearly one residence time (8 h) after the $p\text{O}_2$ shift from 2 to 0 % (Figure III-27C). Cell growth became oxygen-limited and no longer limited by the carbon source. Furthermore, exposure to low and limited DO levels did not trigger any production of organic acids by the yeast.

Table III-15: Effect of different conditions of oxygen availability on the kinetic growth parameters of *Y. lipolytica* in glucose-limited chemostat cultures: values of specific rates, yields, respiratory quotients, carbon and redox recoveries were expressed as mean±standard deviation

Perturbation duration (min)	Number of perturbations (/)	-qS (Cmol CmolX ⁻¹ h ⁻¹)	qCO ₂ (Cmol CmolX ⁻¹ h ⁻¹)	-qO ₂ (Cmol CmolX ⁻¹ h ⁻¹)	Y _{X/S} (Cmol Cmol ⁻¹)	Y _{CO₂/S} (Cmol Cmol ⁻¹)	Y _{O₂/S} (Cmol Cmol ⁻¹)	RQ _{mean} (/)	Carbon recovery (%)	Redox recovery (%)
Steady state (fully oxidative condition)		0.148±0.002	0.057±0.002	0.049±0.001	0.62±0.01	0.38±0.01	0.33±0.01	1.17±0.02	100.1±1.1	102.2±1.8
60	2 ^{a)}	0.153±0.001	0.058±0.004	0.050±0.005	0.60±0.00	0.38±0.03	0.33±0.03	1.17±0.06	97.9±2.4	99.3±2.4
		0.151±0.001	0.057±0.004	0.050±0.004	0.61±0.00	0.38±0.03	0.33±0.03	1.16±0.06	98.4±4.3	100.1±4.1
20	6 ^{b)}	0.149±0.002	0.058±0.003	0.051±0.002	0.61±0.01	0.39±0.01	0.34±0.01	1.13±0.03	99.7±0.7	102.9±1.0
		0.148±0.002	0.058±0.002	0.050±0.002	0.61±0.01	0.39±0.01	0.34±0.01	1.17±0.02	100.1±1.4	102.1±1.7
5	24 ^{c)}	0.147±0.002	0.057±0.001	0.048±0.001	0.61±0.01	0.39±0.00	0.33±0.01	1.18±0.01	99.9±0.7	99.7±1.3
		0.147±0.003	0.056±0.001	0.047±0.001	0.62±0.01	0.38±0.01	0.32±0.01	1.18±0.01	101.4±1.9	101.3±2.9
Low DO concentration (pO ₂ ≈ 2 %)		0.152±0.003	0.050±0.001	0.043±0.002	0.64±0.01	0.33±0.01	0.28±0.01	1.17±0.02	96.7±1.2	98.6±2.5

^{a)} Average value after each perturbation

^{b)} Average value after each set of 3 perturbations

^{c)} Average value after each set of 12 perturbations

The total duration of anoxia (120 min) was strictly identical between the different DO fluctuation profiles
DO: Dissolved oxygen

III.4.2.3.2.2 Morphological changes monitoring

Optical microscopy, light scattering by flow cytometry, and size distributions measurements by diffraction laser scattering and morphogranulometry methods were compared to evaluate the morphological changes in cells upon exposure to the various forms of oxidative stress.

In Figure III-26A, microscopic observations of broth samples were illustrated for each experimental condition (steady state and DO perturbation phases). Regardless of the oscillations' frequency and duration, *Y. lipolytica* cells kept an ovoid/spherical form with average diameter not exceeding 5.7 μm . Distributions of cell length within the culture (Figure III-26B) follow a normal law for the different conditions tested. Similar observations were also found for the cells cultivated under low DO concentrations (Figure III-27B). On the contrary, a mycelial growth was clearly induced when cultures were grown under oxygen limitation (Figure III-27, A-B). These morphological changes were accompanied with an increase in the residual glucose concentration in the chemostat culture (Figure III-27C). Dimorphism was detected at a residual glucose concentration of 0.75 g L^{-1} (around 17.2 % (v/v) of filamentous cells) and progressively intensified until a concentration of 0.98 g L^{-1} (filamentous subpopulation of 80.5 %).

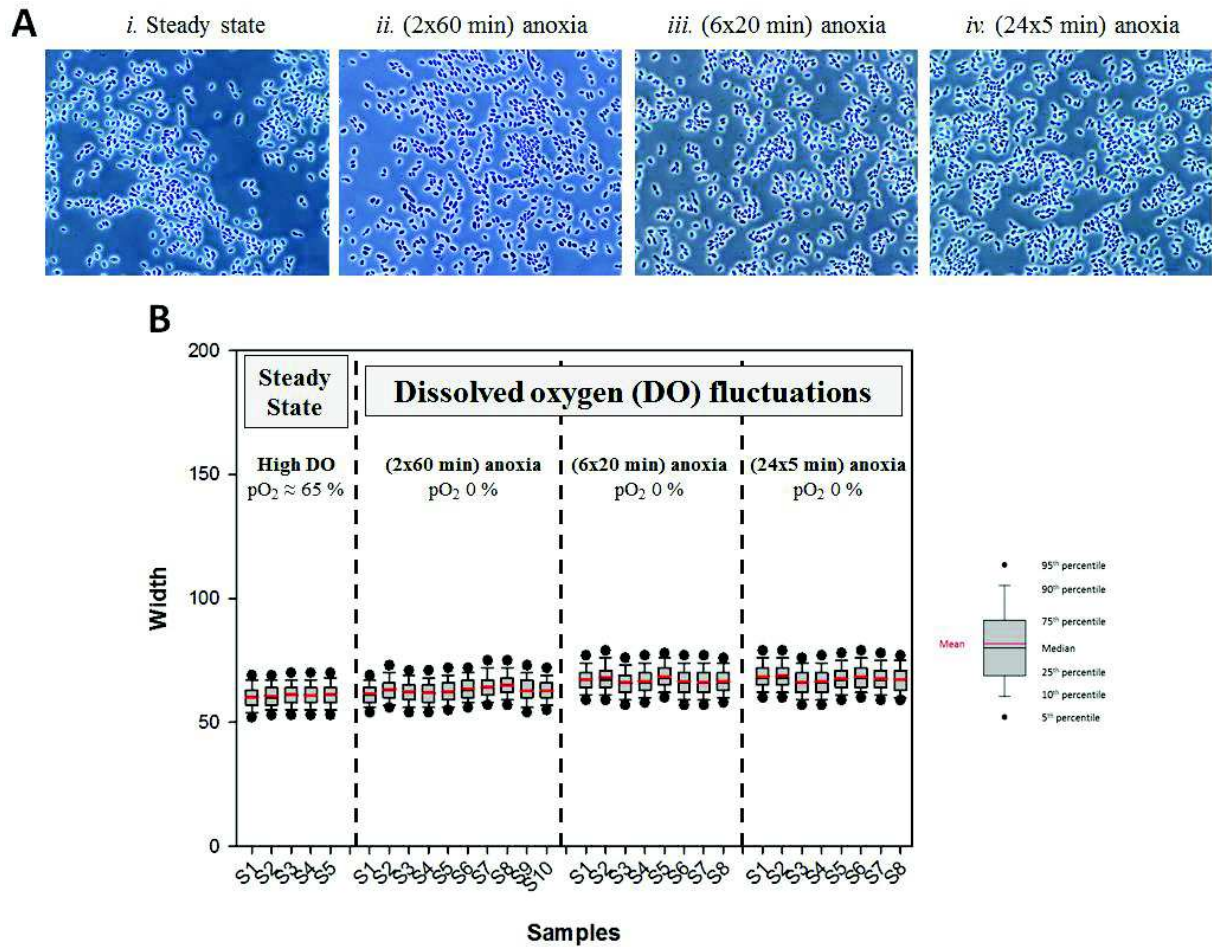


Figure III-26: A. Effect of dissolved oxygen (DO) fluctuations on *Y. lipolytica* morphology in glucose-limited chemostat cultures at a dilution rate of 0.10 h^{-1} . Microscopic observations comparing (i) unstressed (steady state phase), and stressed cells exposed to consecutive DO fluctuations of (ii) 60, (iii) 20 and (iv) 5 min. Images were taken at magnifications of 40 x under oil immersion using phase contrast mode. The image size (width x height) is $54 \mu\text{m} \times 44 \mu\text{m}$. B. Box plots comparing the time-evolution of length distribution measurements for cells under steady state and oxygen perturbed environments (data quantified by flow cytometry). The boundary of the box closest to zero indicates the 25th percentile, a black line within the box marks the median, a red line within the box marks the mean and the boundary of the box farthest from zero indicates the 75th percentile. Whiskers above and below the box indicate the 90th and 10th percentiles. The black dot indicates the 95th and 5th percentiles

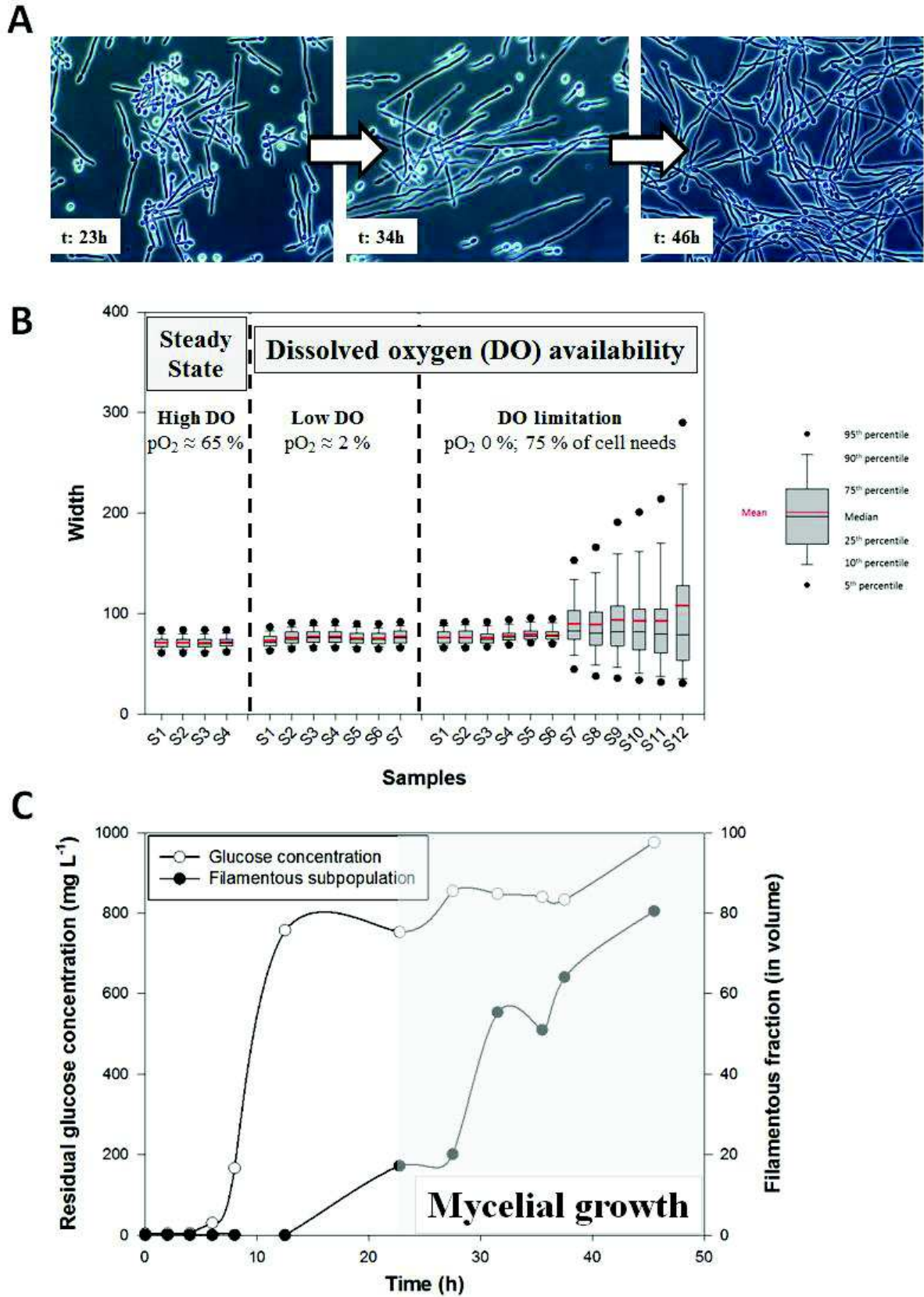


Figure III-27: A. Light micrographs illustrating the morphological changes of *Y. lipolytica* following the transition from low ($pO_2 \approx 2\%$) to limited DO conditions ($pO_2 = 0\%$, 75% of cell needs). The morphology was examined under phase contrast mode using an oil

immersion objective at a magnification of 40 x. Image dimension (width x height): 54 μm x 44 μm . B. Dynamics of cell length distribution of *Y. lipolytica* subpopulations in the continuous cultures at high (steady state phase), low (pO_2 2 %) and limited (pO_2 0 %) oxygen supply. Cell length measurements were performed by flow cytometry C. Evolution of the filamentous subpopulation (in volume) and the residual glucose concentration during the oxygen-limited phase of the chemostat culture.

III.4.2.3.2.3 Cell viability assessment

The impact of oxygen availability on the viability of *Y. lipolytica* was characterized by the data in Table III-16. Proportions of viable subpopulations did not vary significantly across the three conditions: DO fluctuations, low DO (pO_2 2 %) and oxygen limitation (pO_2 0 %). Cell viability was maintained at levels greater than 93.3 % throughout fermentation.

Table III-16: Average percentage of viable cells during the chemostat experiments

Perturbation duration (min)	Number of perturbations (/)	Percentage of viable cells (%)	
		Type of staining	
		cFDA/PI	cFDA/Sytox
60	2 ^{a)}	99.6 \pm 0.1	93.3 \pm 7.5
		99.3 \pm 0.5	93.4 \pm 6.4
20	6 ^{b)}	99.6 \pm 0.3	99.8 \pm 0.1
		99.6 \pm 0.2	98.2 \pm 1.3
5	24 ^{c)}	99.7 \pm 0.2	99.8 \pm 0.1
		99.5 \pm 0.2	99.6 \pm 0.3
Low DO concentration ($\text{pO}_2 \approx 2$ %)		99.9 \pm 0.1	100 \pm 0.2
Oxygen limitation ($\text{pO}_2 = 0$ %)		99.6 \pm 0.1	99.5 \pm 0.6

^{a)} Average value after each perturbation

^{b)} Average value after each set of 3 perturbations

^{c)} Average value after each set of 12 perturbations

The total duration of anoxia (120 min) was strictly identical between the different DO fluctuation profiles

DO: Dissolved oxygen

III.4.2.4 Discussion

In industrial bioreactors, microbial cultures are continuously exposed to local gradients in fundamental process parameters such as substrate, DO, pH and temperature. These heterogeneities may have detrimental effects on cellular growth, metabolism and morphology, depending on the nature, intensity, duration and/or frequency of the fluctuations encountered. The aim of this study was to investigate the impact of oxygen availability on the dynamic behavior of *Y. lipolytica*, at both physiological and metabolic levels, in a 1-L scale-down bioreactor under batch and continuous modes of culture. To this end, different DO fluctuation

profiles were adopted in order to highlight the effect of the duration and frequency of cell exposure to anoxic conditions on the microbial response. In addition, the impact of low and limited DO concentration on *Y. lipolytica* dynamic behavior was also considered in the current research.

In batch cultivations, subjecting cells to drastic fluctuations in oxygen levels (pO₂ values from more than 40 % up to 0 %) caused repetitive interruptions of the yeast growth. During the periods of oxygen deprivation, the specific growth rate declined steeply from its maximum level (0.24 h⁻¹) to zero. The growth arrest in the absence of oxygen was expected since the microorganism is strictly aerobic. The inability of *Y. lipolytica* to grow under hypoxic conditions (anaerobiosis) was thought to be related, in part, to the repression of the mitochondrial ADP/ATP carrier encoding gene (*YLAAC1*) expression (Mentel et al. 2005). The absence of a functional ADP/ATP carrier, due to repression of the corresponding gene, was also involved in growth arrest under anaerobic conditions of other obligate aerobic yeasts, such as *Kluyveromyces lactis*, *Schizosaccharomyces pombe* and *Candida parapsilosis* (Nebohacova et al. 1999; Trezeguet et al. 1999). Interestingly, upon restoration of the air supply, the growth rate of *Y. lipolytica* cells recovered to a level similar to that observed prior the interruption. This behavior pointed out an astonishing degree of robustness against DO fluctuations in *Y. lipolytica* W29 strain.

In addition, transient oscillations of cells between aerated and non-aerated environments resulted in sudden changes on the metabolic activity of yeast that are revealed by an accumulation of citric acid during the cultures under batch mode. Small amounts of citric acid not exceeding 29 mg L⁻¹ were produced during the temporary anoxic periods, and rapidly re-assimilated by the yeast when favorable aeration was restored. Similar observations were made by Rakicka et al. (2015) who attributed citric acid secretion to oxygen limitation in a nitrogen-limited chemostat culture of *Y. lipolytica* JMY4086 grown on glycerol. The re-consumption of citric acid produced was in agreement with Papanikolaou et al. (2002) who observed some consumption of accumulated citrate by a *Y. lipolytica* LGAM strain, upon exhaustion of the carbon source in the culture medium. The production of citric acid by *Y. lipolytica* mainly occurs under nitrogen limitation and excess of carbon source (Papanikolaou et al. 2002), which were not the conditions of the present study. Indeed, exhaustion of the nitrogen source in the medium provokes a rapid drop in the intracellular AMP (adenosine monophosphate) concentration, causing inactivation of the isocitrate dehydrogenase (enzyme responsible for the transformation of iso-citric to α -ketoglutaric acid, allosterically activated

by AMP) and therefore accumulation of citric acid inside the mitochondrion. Upon reaching a critical level, citric acid is secreted into the cytosol (Papanikolaou and Aggelis 2009; Ratledge and Wynn 2002). Generally, citric acid biosynthesis by *Y. lipolytica* was favored under efficient aeration conditions (Ferreira et al. 2016b; Rywińska et al. 2012). However, our results pointed-out the production of citric acid upon oxygen starvation. Repeated transitions from exponential phase ($\mu_{\max} = 0.24 \text{ h}^{-1}$) to growth arrest ($\mu = 0 \text{ h}^{-1}$) could lead to perturbations in the energy balance at the cellular level. A redirection of excess carbon flux towards the accumulation of an intermediate metabolite might therefore be expected in the absence of oxygen, as the tricarboxylic acid (TCA) cycle was blocked under these conditions.

Regarding the yeast morphology, filamentous cells became progressively predominant upon transient exposures to anoxia during the batch runs. The intensity of filament formation was more pronounced in the batch culture with the higher frequency of DO fluctuation, even though the total duration of the stress period was strictly identical (180 min) for both DO oscillating profiles. Indeed, proportions of the filamentous subpopulation attained 73.5 % (v/v) when cells were exposed to nine-consecutive fluctuations of 20 min, compared to 42.7 % (v/v) with three-successive perturbations of 60 min. Previous reports have correlated oxygen availability with dimorphism in *Y. lipolytica* strains: cells exhibited mycelial growth in poorly aerated environments, while the yeast-like form was favored under high aerated conditions (Bellou et al. 2014; Ruiz-Herrera and Sentandreu 2002; Zinjarde et al. 1998). Nonetheless, in none of the studies, the effect of transient fluctuations in DO levels on the morphological behavior of this fungus has been investigated. On another hand, citrate has been considered as a positive effector of mycelium formation in *Y. lipolytica*, being effective at even small concentrations (5 mM) (Ruiz-Herrera and Sentandreu 2002). Its accumulation (up to 29 mg L⁻¹; approx. 0.15 mM) during the DO oscillating batch cultures would probably induce filamentous growth in this strain. Accordingly, it remained unclear whether the absence of oxygen or the presence of citrate was primarily responsible for triggering the yeast-to-mycelium transition in *Y. lipolytica* under the conditions of the present study.

Similarly to the batch runs, different DO oscillating aerobic/anoxic profiles were assayed in glucose-limited chemostat cultures. The continuous cultivation mode is particularly adapted as it enables the analysis of stress responses of cell populations in a defined physiological state and growing at the same specific rate. Our results showed that, unlike batch experiments, DO fluctuations did not induce any production of citric acid, even at transient exposure to anoxic condition as short as 5 min. This can be attributed to the carbon-limited growth

imposed during the chemostat experiments. The concentration of the carbon source is important for an efficient production of citric acid (Anastassiadis et al. 2002; Antonucci et al. 2001). According to Sarris et al. (2011), low citric acid yields were quantified as a result of the insufficient amount of carbon present in the growth medium, for different strains of *Y. lipolytica* cultivated in carbon-limited shake-flasks cultures. Alternatively, it might be possible that the transition from maximum (0.24 h^{-1}) to zero growth rates in the batch cultivations impacted more considerably the energy status of the cells, compared to the shift from a growth rate of 0.10 h^{-1} to zero (two-fold lower) during the continuous cultivations. As a result, the reorientation of the carbon flux into the accumulation of citric acid was probably less pronounced in the case of continuous growth. At the macroscopic level, differences in the growth kinetic parameters (specific rates, yields, RQ) between the steady state phase and following the aerobic/anoxic transition period were quite negligible, irrespective of the duration and frequency of the fluctuation. To our knowledge, this is the first report examining the growth dynamics of *Y. lipolytica* in response to fluctuations in DO levels. In the literature, a special emphasis was given to elucidate the impact of DO gradients on lipase synthesis by *Y. lipolytica*, without providing any quantitative assessment of the kinetic parameters during the growth phase of the yeast (Kar et al. 2008; Kar et al. 2010). Besides, their culture conditions (complex medium convenient for lipase production), perturbation approaches (scale-down reactor systems), as well as yeast strain (*Y. lipolytica* JMY775) were different from those employed in the current study.

In continuous cultivations of *Y. lipolytica* under relatively low $p\text{O}_2$ levels (around 2 % of saturation), the macroscopic behavior of the yeast remained fundamentally unaltered, since its oxygen needs at a growth rate of 0.10 h^{-1} were satisfied. Particularly, a slight decrease in specific respiration rates was observed during this phase. This is probably due to the increased energy requirements for cell maintenance under low oxygen tensions (Gustafsson et al. 1993). The effect of low DO concentration (around $0.003 \text{ mmolO}_2 \text{ L}^{-1}$) on the physiology of *Y. lipolytica* in continuous cultivation was previously reported by Bellou et al. (2014). Nevertheless, the study was conducted under lipid producing conditions (nitrogen limitation, low dilution rate (0.032 h^{-1}), and not during biomass production phase as was the case for the present research.

A decrease of the partial oxygen pressure from 2 to 0 % was thereafter tested in a chemostat culture with glucose limitation. Providing cells with about 75 % of their oxygen needs caused a decrease in biomass production with a concomitant increase in residual glucose

concentration within almost one residence time upon the pO₂ shift: only cells being sufficiently supplied with oxygen were able to undergo fully oxidative growth. Due to oxygen limitation, no other medium compound was totally consumed, and thus a switch from glucose to oxygen limitation took place. Similar observations were made by Jost et al. (2015) who observed 3.5 times lower biomass generation under oxygen limitation (agitation 500 rpm; airflow 0.4 l min⁻¹; pO₂ 0%) than when the oxygen was unlimited (agitation 500 rpm; airflow regulation from 0.2 to 1 l min⁻¹; pO₂ 50%) during bioreactor cultivations of different *Y. lipolytica* strains. Their findings also showed that no citrate was detected when oxygen limitation occurred.

For both process modes, cell viability was maintained at high levels (≥ 93.3 %) under the different conditions of oxygen availability: fluctuating, low (pO₂ 2 %) and limited (pO₂ 0 %) DO tensions. Cells exhibited esterase activity and no alteration of membrane integrity, even when their morphology evolved towards mycelial forms (a physiological adaptive response to stressful environments). These findings were consistent with our previous observation that filamentation, induced by pH stress, was not a prerequisite for cell death in *Y. lipolytica* (Timoumi et al. 2017). Indeed, a multitude of genes involved in vital cellular functions, such as remodeling and biogenesis of the cell wall, membrane trafficking and N- or O-glycosylation, were identified as up-regulated during mycelial transition of *Y. lipolytica* (Morales-Vargas et al. 2012).

With regard to the morphological response to oxygen availability under continuous culture mode, *Y. lipolytica* cells grew constitutively in the yeast-like form at both fluctuating and low DO levels (pO₂ \approx 2 %). A normal distribution of cell size within the population was maintained over the whole period of fermentation for all tested conditions. To date, there are no published data on the influence of DO fluctuation on *Y. lipolytica* morphology. Nevertheless, *Y. lipolytica* behavior at low DO tension (\approx 0.003 mmolO₂ L⁻¹) was previously examined in a nitrogen-limited chemostat operating in synthetic medium at low dilution rate (0.032 h⁻¹) (Bellou et al. 2014). In contrast to our data, their results showed the induction of a mycelial growth at low DO concentration. Our results demonstrate that dimorphism of *Y. lipolytica* (up to 80.5 % (v/v) of filamentous cells) was only observed in conditions of oxygen limitation (pO₂ = 0 %) with the presence of excess glucose (more than 0.75 g L⁻¹) during continuous cultivation. No such data was previously reported for *Y. lipolytica* species.

The morphological behavior of the yeast face to variations in oxygen availability was different between both modes of culture. When the yeast was cultured in batch with excess glucose, the morphology evolved into a mycelial form following the exposure to DO perturbation. However, if the yeast was cultured in a glucose-limited chemostat under DO fluctuation, at even higher frequencies (every 5 min), the primary morphology of the culture was yeast-like. These results were in concordance with our previous findings on effects of pH stress on *Y. lipolytica* dimorphism (Timoumi et al. 2017), where we have shown that neutral pH induced mycelial growth during batch cultivations of the yeast in the presence of excess sugar. On the opposite, no mycelial transition was triggered in glucose-limited chemostat runs at different dilution rates although prolonged exposure to pH stress. Indeed, in our previous work, residual glucose concentrations lower than 10 mg L⁻¹ was maintained in all conditions of pH perturbation (different dilution rates / stress modulation strategies). The ability of *Y. lipolytica* to grow in the filamentous form was only demonstrated in glucose-excess environments in combination with an oxygen limitation. Taken together, these results suggest an impact of glucose availability and/or glucose signal transduction mechanism on the regulation of dimorphic transition in *Y. lipolytica*. Evidence exists that exogenous addition of cAMP, an important mediator of environmental stimuli, inhibited filamentous growth in *Y. lipolytica* through the activation of the cAMP-PKA regulating pathway (Cervantes-Chavez and Ruiz-Herrera 2007; Ruiz-Herrera and Sentandreu 2002). However, the mechanisms by which glucose levels modulate filament formation and how glucose-induced signals are transmitted to *Y. lipolytica* cells remain unknown. Basically, yeast cells were shown to develop an interlocking network of signaling pathways that receive glucose-dependent signals and affect various cellular responses (Broach 2012; Gancedo 2008; Kim et al. 2013; Rolland et al. 2002). This signaling network employs three major glucose signaling pathways: (i) the Rgt2/Snf3 glucose induction pathway required for glucose uptake (Ozcan and Johnston 1999); (ii) the Snf1/Mig1 glucose repression pathway responsible for the repression of genes involved in the utilization of alternative carbon sources as well as in gluconeogenesis and respiration (Carlson 1999; Gancedo 1998); and (iii) the cAMP-PKA pathway that mediates glucose effects on biosynthetic capacity and stress responses (Broach 2012). Glucose signaling systems were extensively studied in various yeast species, most notably in the model fungus *Saccharomyces cerevisiae* (for review, see references (Conrad et al. 2014; Santangelo 2006)). However, in the yeast *Y. lipolytica* glucose signaling is poorly understood, even though glucose transport system in this fungus is starting to be elucidated (Lazar et al. 2017; Ryu et al. 2016). Understanding the underlying molecular mechanisms responsible for

the adaptation process to changes in glucose availability would certainly help to monitor the morphological behavior of *Y. lipolytica*.

In conclusion, the present results enhance the understanding of the effect of fluctuating, low and limited DO levels on the dynamic behavior of *Y. lipolytica*, cultivated under batch and continuous modes. Oxygen availability was shown to have an impact on the yeast morphology, only in glucose excess environments. Controlling residual glucose concentrations in *Y. lipolytica* fermentation may contribute to a better monitoring of its morphological changes in response to environmental stimuli. Such data would help to optimize bioprocess performances at the industrial scale since it alleviates physico-chemical impacts due to filamentous cells.

Acknowledgements

Financial support for this study was provided by Airbus, Agence Nationale de la Recherche (ANR) and Commissariat aux Investissements d'Avenir via the project ProBio3 “Biocatalytic production of lipidic bioproducts from renewable resources and industrial by-products : BioJet Fuel Application” (ref. ANR-11-BTBT-0003).

Compliance with ethical standards

Conflict of interest: The authors declare that they have no conflict of interest.

Ethical approval: This article does not contain any studies with human participants or animals performed by any of the authors.

III.4.3 Results synthesis

- ⇒ The effect of controlled fluctuations in dissolved oxygen (DO) levels, of different frequencies and durations, on the dynamic behavior of *Y. lipolytica* was studied and characterized at the metabolic and morphological levels in batch and glucose-limited chemostat cultures.
- ⇒ Dynamics of growth, metabolism and morphology of *Y. lipolytica* were examined in low (pO_2 close to 2 %) and limited (zero pO_2 value, 75 % of cell needs) oxygen environments under continuous mode of culture.
- ⇒ Mycelial transition of *Y. lipolytica* was characterized at the population level through analysis of cell size distribution patterns within the culture broth. Evolutions of the proportion of yeast-like and filamentous subpopulations were followed during the time course of fermentation by means of different granulometric methods.
- ⇒ Consecutive oscillations between oxygen-rich and -deprived environments induced the production of citric acid by *Y. lipolytica*. By contrast, no citric acid was detected in glucose-limited continuous cultures for the different types of stress conditions applied: controlled perturbations (anoxic periods of 60, 20 and 5 min), low ($pO_2 \approx 2$ %) and limited ($pO_2 = 0$ %) oxygen supply.
- ⇒ Macroscopic behavior (kinetic parameters, yields, viability) of the yeast was fundamentally unaltered upon exposure to oxygen perturbations (in the range of tested conditions) for both modes of cultures. However, conditions of oxygen limitation resulted in the destabilization of the glucose-limited growth in the continuous cultivations.
- ⇒ Morphological responses of *Y. lipolytica* to repeated cycles of anoxia were different between batch and continuous modes of cultures: a dimorphic transition was induced and progressively intensified during batch fermentations (proportion of filamentous cells reaching 74 % in volume). While, in chemostat bioreactors, the culture consisted mainly of yeast-like cells with a normal size distribution.

⇒ Growth at low DO levels did not inflict any changes in *Y. lipolytica* morphology. Nevertheless, dimorphism was detected in conditions of oxygen limitation at a residual glucose concentration of 0.75 g L⁻¹ (around 17.2 % (v/v) of filamentous cells) and progressively intensified until a concentration of 0.98 g L⁻¹ (filamentous subpopulation representing 80.5 % in volume).

General discussion, conclusions and perspectives

GENERAL DISCUSSION, CONCLUSIONS AND PERSPECTIVES

The ultimate goal of developing a biotechnological process is the successful commercialization of added value products. However, the scale-up of a bioprocess from laboratory to pilot and production scale represents a limiting step in the success of industrial fermentation. This step is typically accompanied by unavoidable changes in the micro-environmental conditions that may impact the behavior of the microorganism, and thereby the industrial viability of the process. To increase product yields and to ensure consistent product quality, it is of utmost importance to gain insight into the dynamic interactions between the biological and physiological systems within complex and evolutive environments.

This research study focuses on the influence of physico-chemical environmental perturbations on the dynamic behavior of microbial populations. Differences in the cellular responses might be induced according to the nature, magnitude, and frequency of the perturbation considered. The aim of the thesis was to characterize metabolic responses and morphological states distribution within a microbial population, using the dimorphic yeast *Yarrowia lipolytica* as a model system. Increasing interest in *Y. lipolytica* was observed over the recent years due to its particular biochemical features and relevant industrial applications (Bankar et al. 2009; Goncalves et al. 2014). Bibliographic analysis revealed an impact of pH and dissolved oxygen concentration on the morphology of *Y. lipolytica* (Bellou et al. 2014; Gonzalez-Lopez et al. 2006; Ruiz-Herrera and Sentandreu 2002). Nevertheless, the yeast behavior were most commonly examined under uncontrolled culture conditions (shaken flasks cultures) leading to multifactorial stress stimuli. Well-controlled fermentations (in bioreactors) and modulated perturbations may be proposed in order to establish a direct causal relationship between the stress and the cell response.

The research approach adopted, the analytical methods developed, and the experimental results obtained within this study enable to draw answers to the following scientific questions:

- ⇒ What are the methods to be developed for the characterization of the morphological response at the cell population level? What is the methodology implemented to quantify subpopulations with distinct morphotypes within the culture?
- ⇒ What are the dynamics of metabolic and morphological behavior of *Y. lipolytica* in response to pH stress? What are the effects of the cell growth rate and culture mode on the microbial response?

⇒ What are the impacts of fluctuations in dissolved oxygen (DO) levels on the metabolism and morphology of *Y. lipolytica*? How this yeast behaves in perturbed, low ($pO_2 \approx 2\%$) and limited DO ($pO_2 \approx 0\%$) environments?

Methods of characterization of the morphological changes in Y. lipolytica: development and validation

The first step of our scientific investigation was to develop appropriate methodologies for a rigorous characterization of the morphological evolutions in *Y. lipolytica*. Owing to their ability to provide statistically representative results of the target population, three complementary methods were implemented; flow cytometry (CYT), morphogranulometry (MG) and dynamic light scattering (DLS). Model matrices of well-defined geometry (spherical particles with diameter ranging from 1 to 80 μm) were used as a reference to assess accuracy, precision and reliability of the techniques.

The CYT technique provide an estimation of the diameter and length of particles based on a power-law calibration of the FSC and width signals according to an equivalent sphere model (by means spherical calibration beads of diameter in the range of 1 to 15 μm). Whereas, MG measurements, which are based on microscopic observations and image analysis, provided a direct measurement of the particle dimensions (without an approximation model). For the DLS instrument, equivalent diameters of the particles were calculated according to a sphere model. In terms of mean values, both CYT and MG generate comparable measures of the particle diameter, which were in agreement with the provider specifications. The largest difference between the estimated diameter and the provider information was observed with the DLS method (mean size underestimation of 14 %). Data derived from DLS measurements should therefore be carefully considered. With regards to the standard deviation, the use of the calibration curve in CYT to convert FSC and width signals into a particle dimension has been shown to induce errors of about 10 and 32 % on the estimated diameter and length, respectively. Considering these observations, only the raw data (width parameter) were examined for CYT results, and no correlation with the diameter or length of the equivalent sphere was used in the following part of the thesis (stress responses studies: Chapter III-3 and III-4). With the morphogranulometer, the error on the particle diameter did not exceed 5 %. This relatively low error committed with MG was expected since the determination of the

diameter is directly measured on the 2D composite image, unlike CYT where the diameter is estimated through a power-law correlation of the corresponding signal.

Furthermore, a comparative study between the three methods was conducted at the size distribution level for individual and mixed particulate samples. Results illustrated the ability of CYT and MG to accurately identify centered narrow peak of the population. However, the derived distribution was much more boarder with the DLS device. In addition, the techniques allowed to differentiate and to quantify individual populations of similar sized particles in mixed suspensions.

A particular attention should be addressed to some specific points regarding the implementation of CYT and MG methods for cell morphology characterization:

- ✓ The statistical representativity of the analyzed samples at the population level was different between both techniques: the number of particles analyzed by MG was approximately 20-fold (≈ 1000 particles) lower than that examined by CYT (≈ 20000 events).
- ✓ The analyzed zone examined with the morphogranulometer was selected by the operator. Accordingly, the subjectivity of the results has to be kept in mind. Randomly selected microscopic fields would remove the bias.
- ✓ Due to the technical difficulty to carry out the MG analyses during the course of the fermentation, cell samples have to be kept at 4 °C between sealed slide and cover slip for at least 24 h before analysis. During this storage period, cells are kept within different environments depending on the time point of fermentation and the culture mode. In particular, they might be prone to oxygen and substrate limitation which may induce an evolution in the morphology in the sample.
- ✓ With flow cytometry, the size calibration was established over a diameter range from 1 to 15 μm . This calibration cannot be employed for samples with higher diameter, which is the case for *Y. lipolytica* cells when their morphology evolved toward more elongated forms.

Considering the dimorphic behavior of *Y. lipolytica* under stress conditions, developing an appropriate methodology for quantifying this behavior appeared therefore necessary. To this end, a theoretical comparative approach was carried out on different geometric models (ellipse, cylinder) that would better approximate the elongated shape of the cells compared to the usual sphere model (for CYT and DLS). Our analysis revealed the adequacy of elliptic

and cylinder models for the description of the elongation phenomena. However, the sphere model was completely inadequate as it induces errors on particle volume higher than 35 % for cells with aspect ratio (AR) greater than 0.5. In the thesis, the cylinder model was preferentially used for the characterization of morphological responses of *Y. lipolytica*.

Application of the cylinder model required access to morphometric parameters for each cell in the population being analyzed. Among the three methods reviewed (Chapter III-1), MG is the only technique presenting this feature. The aptitude of this technique to characterize and quantify the mycelial transition was accordingly evaluated with biological samples (yeast cells with different morphological states). Our findings confirmed the accuracy of the cylinder approximation for elongated-shaped materials, and emphasized the importance of examining length, width and AR parameters to assess the dimorphism magnitude. Besides, a threshold criteria was statistically defined to differentiate between ovoid and filamentous subpopulations. This is the first time that a strategy quantifying the morphological changes in *Y. lipolytica* at the population level is proposed and implemented. Such data are quite lacking in previous research.

The morphological methods developed were subsequently used to characterize the morphological changes of *Y. lipolytica* in response to pH and DO perturbations. Additionally, the dynamics of yeast growth, viability, glucose uptake, oxygen consumption, organic acid and carbon dioxide production rates were scrutinized in detail in Chapters III-3 and III-4.

Effect of pH stress on Y. lipolytica metabolism and morphology

The first part of this study aimed to determine the pH level inducing a stress response on the yeast either on the metabolic and/or morphological level. The neutral pH was known by its positive impact on *Y. lipolytica* dimorphism (Gonzalez-Lopez et al. 2006; Ruiz-Herrera and Sentandreu 2002; Zinjarde et al. 2008). The literature review (Chapter I) highlighted the lack of research on the direct impact of pH (mono-factorial) on the yeast morphology. Most of the studies carried out under partially controlled conditions resulting thereby on multi-factorial stress responses. Besides, the multiplicity of the analytical methods, the disparity of the morphological criteria, as well as the poor statistical representativity of the analyzed samples makes the findings difficult to interpret. For this purpose, bioreactor cultures (batch mode) where the environment was perfectly controlled were proposed. Under these conditions, process parameters such as pH, dissolved oxygen concentration, temperature, agitation and

aeration were always controlled, and the physiological changes, whenever occurring, were only due to changes in pH conditions imposed on the microorganism (mono-factorial stress response). The analysis of the microbial dynamics of *Y. lipolytica* under distinct pH conditions (4.5, 5.6 and 7) in batch bioreactors revealed that:

- ✓ The culture pH did not have a significant effect on the macroscopic behavior (kinetic parameters, yields, viability) of the yeast.
- ✓ The yeast-to-mycelium transition was triggered at both acidic (pH 4.5) and neutral conditions. The pH 5.6 promotes growth in the yeast-like forms.
- ✓ The magnitude of mycelial transition was more pronounced at pH 7 than pH 4.5: filamentous cells represented 93 % (v/v) under neutral pH, compared to 84 % (v/v) during the culture at pH 4.5.

In view of these results, controlled perturbations at the most stressful pH condition (pH 7) were carried out in batch and glucose-limited chemostat cultivations. Metabolic and morphological behaviors of *Y. lipolytica* were examined with regards to the type of the perturbation applied (pulse or Heaviside), the nature of the culture mode (batch or continuous), and the microorganism growth rate (from 0.03 to 0.24 h⁻¹). On the morphological level, our findings demonstrated that:

- ✓ The influence of the perturbation type was different between both modes of culture. In batch cultivations, successive pulses or Heaviside fluctuations induced noticeable transition from yeast to elongated morphotypes. For the chemostat runs, the yeast morphology remained unaffected whatever the type of perturbation: cells maintained a perfectly ovoid shape across the various conditions.
- ✓ The morphological response was dependent on the culture mode: no dimorphism was detected in the continuous cultures, by contrast to the batch experiments. Different hypothesis have been stated: the difference in the morphological behavior may be attributed to variabilities in the cell history and/or to differences in the kinetic behavior of ovoid and filamentous subpopulations between batch and continuous modes. In fact, the difference between both cultivation modes rely on the cell history. In the continuous bioreactor, the environment is constant (residual glucose concentration is null) and the entire population grows at a constant growth rate with the same physiological state after 5 to 6 residence times. While during the batch cultures, the environment is constantly changing (residual glucose concentration in

excess) and cell subpopulations at various physiological states may cohabit within the fermentation broth. On another hand, macroscopically (kinetically) ovoid and filamentous cells may behave differently, which would probably lead to the separation of yeast subpopulations, with respect to their morphology, by the hydraulic outlet flow in the case of the chemostat cultures.

- ✓ No effect of the cell growth rate on the stress response was detected. Cells maintained a yeast-like morphology across the board range of growth rates (0.03; 0.07; 0.10 and 0.20 h⁻¹) examined.

On the metabolic level, the pH stress did not inflict significant changes on the macroscopic behavior of *Y. lipolytica*, irrespective of the type of perturbation, the mode of culture and the yeast growth rate. A high robustness of the strain against pH perturbation was also demonstrated by the maintenance of cell viability: dead subpopulation did not exceed 3.4 % under the different conditions.

Impact of dissolved oxygen availability on Y. lipolytica metabolism and morphology

In order to investigate the influence of dissolved oxygen (DO) levels on the cellular response of *Y. lipolytica*, assays were conducted in batch and glucose-limited chemostat bioreactors under fluctuating, low and limited oxygen supply. In this study, the effect of frequency and duration of the DO fluctuation were examined. In addition, as the results obtained in Chapter III-3 (pH stress studies) proved that the growth rate had no impact on *Y. lipolytica* behavior regarding the response of the stress, continuous experiments were performed at the same growth rate (0.10 h⁻¹).

Regarding the yeast physiology, our results showed that:

- ✓ Subjecting cells to repeated oscillations between oxygen-rich (pO₂ ≥ 40%) and deprived (full anoxia, pO₂ 0%) environments caused an arrest of the microbial growth in batch and continuous bioreactor, as well. This was not surprising as *Y. lipolytica* is strictly aerobic.
- ✓ An accumulation of citric acid was detected under fluctuating DO conditions, only under batch culture mode. No citrate production was revealed in continuous fermentation although exposure to DO fluctuation with higher frequency (every 5 min). Likewise, low and limited DO did not induce any production of organic acid. It should be stressed that high sensitive analytical methods allowing the quantification of

organic acid at very low concentrations (from 0 to 10 mg L⁻¹) were implemented. The redirection of the carbon flux towards an accumulation of an intermediate metabolite of the TCA cycle was expected to be related to the abrupt shift of the growth rate from its maximum level (0.24 h⁻¹) to zero in the batch cultures, compared to the transition from 0.10 h⁻¹ to growth arrest in the chemostat runs.

- ✓ The kinetic parameters, yields and viability of the yeast were fundamentally unaltered across the various conditions of oxygen availability. Under batch mode, *Y. lipolytica* exhibited an astonishing ability to withstand anoxic perturbations: an instantaneous recovery of growth and respiratory activities upon stress exposure was observed. For the continuous cultivations, the transition from low (pO₂ 2 %) to limited (pO₂ 0 %) DO tensions resulted in a slight decline in biomass production, and an increase in the residual glucose concentration within approximately one residence time after the pO₂ shift. The growth of *Y. lipolytica* was no longer limited by the carbon source, but obviously by the oxygen supply.

On the morphological level, dimorphism (up to 73.5 % (v/v) of filaments) was detected in the batch cultures with excess glucose as a response to the exposure to DO fluctuation. Similarly to what was observed with the pH stress (Chapter III-3), the primary morphology of the cells was yeast-like during the glucose-limited chemostat cultures under both perturbed and low pO₂ levels. These findings were not in agreement with a previous study (Bellou et al. 2014) showing the ability of *Y. lipolytica* to grow in the mycelial form in a chemostat operating at low DO concentration. Mycelial transition was only demonstrated under oxygen limitation in glucose-excess environments. Overall, all the data obtained on the impact of pH and DO perturbation (Chapter III-3 and III-4) suggests a possible impact of glucose availability on the regulation of dimorphism in *Y. lipolytica*. In fact, the regulation of the dimorphic transition in this yeast is based on the operation of two opposite signaling pathways: the mitogen-activated protein kinase (MAPK) and the cyclic-AMP (c-AMP) dependent protein kinase A (PKA) pathways (Cervantes-Chavez et al. 2009; Cervantes-Chavez and Ruiz-Herrera 2006; Cervantes-Chavez and Ruiz-Herrera 2007). The exogenous addition of cAMP, which represents an important mediator of environmental stimuli has been shown to inhibit filament formation through activating the cAMP-PKA regulating pathway (Cervantes-Chavez and Ruiz-Herrera 2007; Ruiz-Herrera and Sentandreu 2002). Glucose levels on the medium may probably influence the operation of the filament formation pathway. However, the mechanisms by which glucose-induced signals are transmitted to cells, and how glucose

concentration modulate the filamentous behavior remain still unknown for *Y. lipolytica* species. Glucose signaling pathways in *Y. lipolytica* and their implications on the regulation of the yeast morphology is a topic of interest that requires in-depth research and investigation.

In conclusion, the results presented in the manuscript might be of particular relevance for industrial applications. It provides deeper insights on the physiology of *Y. lipolytica* and can potentially contribute to more efficient control and monitoring of fermentation processes at the industrial scale where pH and pO₂ fluctuation are likely to occur. In fact, data on specific kinetic parameters under optimal growth conditions, pH and DO perturbed environments are quite missing in literature. Besides, analysis of the size distribution patterns at the population level represented an original method to quantify mycelial transition in *Y. lipolytica*. This allowed a better monitoring and control of the impact of morphology (presence of filamentous cells) on bioprocess productivity. The results achieved in the thesis were promoted through publications and talks at national and international conferences.

Perspectives

Regarding the results obtained in the thesis, some suggestions for future work are presented:

- ✓ Development of a dynamic model to describe the kinetic behavior of filamentous subpopulations using the data acquired in dimorphism quantification by morphogranulometry analyses (Chapter III-2). Different scenarios on whether a filamentous cell may divide into an ovoid or filamentous form are conceivable. Cell sorting assays according to the size are therefore proposed to separate ovoid and filamentous populations, and to follow subsequently their morphological evolutions under controlled conditions.
- ✓ Understanding the molecular mechanisms regulating the morphological responses of *Y. lipolytica* to pH and DO perturbations. Comparative analyses of the transcriptome of yeast and mycelial forms of *Y. lipolytica* were conducted on broth samples taken during the pH and DO experiments. Our purpose was to characterize the major molecular changes that are associated with the morphological switch in *Y. lipolytica*. Transcriptome analysis were performed using the RNA-seq methodology. Three replicates for each sample were examined, and different comparative combinations were suggested in order to examine the effect of the perturbation nature (pH and pO₂) the culture mode (batch, chemostat), and the perturbation type (pulse, Heaviside). This

study could also provide answers/interpretation to the influence of glucose concentration on dimorphism regulation. Currently, transcriptomic results were collected, but result interpretation is still ongoing. Such data has never been reported in previous research: no such studies are nowadays available on the regulatory mechanisms underlying stress responses in *Y. lipolytica*.

- ✓ As residual glucose concentration may have an effect on the regulation of the dimorphic behavior of *Y. lipolytica* through the MAPK and cAMP-PKA signaling pathways, it would be interesting to examine the morphology of the yeast in well-controlled glucose-limited cultures with pulse additions of cAMP. Such approach would allow to confirm or reject the hypothesis on the cross effect between glucose level and dimorphism (Chapter III-4).
- ✓ Some metabolic activities of industrial relevance have been found to be dependent on the various cell forms of *Y. lipolytica*. However, studies looking at the influence of the yeast form on lipid synthesis and accumulation are still lacking. Investigation of the impact of the morphology on lipid production (specific yields, lipid profiles) could be examined for further optimization of *Y. lipolytica*-based processes at the industrial scale.

References

REFERENCES

Website references related to the introduction of the aviation sector:

1. Aviation civile magazine, n° 355, décembre 2010, p10-15, Carburants alternatifs, les efforts s'intensifient.
2. SWAFEA (Sustainable Way for Alternative Fuels and Energy in Aviation), State of the art on alternative fuels in aviation – executive summary, April 2010, www.swafea.eu.
3. IATA Economics, 2009.
4. Rapport annuel IATA 2013 alternative fuel report, <http://www.iata.org/publications/documents/2013-reportalternative-fuels.pdf>.
5. Parorama 2015, présentation d'Olivier Appert, <http://www.ifpenergiesnouvelles.fr/Actualites/Evenements/Nous-organisons/Panorama-2015>.

-
- Allen T (1968) Particle size measurement. Fourth edition, Powder technology Series, Chapman et hall, The Netherlands
- Amanullah A, Buckland BC, Nienow AW (2004) Mixing in the Fermentation and Cell Culture Industries. In: Handbook of Industrial Mixing. John Wiley & Sons, Inc., pp 1071-1170. doi:10.1002/0471451452.ch18
- Amanullah A, McFarlane CM, Emery AN, Nienow AW (2001) Scale-down model to simulate spatial pH variations in large-scale bioreactors Biotechnology and Bioengineering 73:390-399 doi:10.1002/bit.1072
- Anastassiadis S, Aivassidis A, Wandrey C (2002) Citric acid production by *Candida* strains under intracellular nitrogen limitation. Applied Microbiology and Biotechnology 60:81-87. doi:10.1007/s00253-002-1098-1
- Andreishcheva EN et al. (1999) Adaptation to salt stress in a salt-tolerant strain of the yeast *Yarrowia lipolytica* Biochemistry-Moscow 64:1061-1067
- Antonucci S, Bravi M, Bubbico R, Di Michele A, Verdone N (2001) Selectivity in citric acid production by *Yarrowia lipolytica*. Enzyme and Microb Technology 28:189-195. doi:10.1016/s0141-0229(00)00288-x
- Asenjo JA, Merchuk JC (1994) Bioreactor system design:648
- Babau M, Cescut J, Allouche Y, Lombaert-Valot I, Fillaudeau L, Uribelarrea JL, Molina-Jouve C (2013) Towards a Microbial Production of Fatty Acids as Precursors of Biokerosene from Glucose and Xylose Oil & Gas Science and Technology-Revue D Ifp Energies Nouvelles 68:899-911 doi:10.2516/ogst/2013148
- Baert J et al. (2016) Microbial population heterogeneity versus bioreactor heterogeneity: Evaluation of Redox Sensor Green as an exogenous metabolic biosensor Engineering in Life Sciences 16:643-651 doi:10.1002/elsc.201500149
- Bankar AV, Kumar AR, Zinjarde SS (2009) Environmental and industrial applications of *Yarrowia lipolytica* Applied Microbiology and Biotechnology 84:847-865 doi:10.1007/s00253-009-2156-8
- Barth G, Gaillardin C (1996) Nonconventional yeasts in Biotechnology:313-388
- Barth G, Gaillardin C (1997) Physiology and genetics of the dimorphic fungus *Yarrowia lipolytica* Fems Microbiology Reviews 19:219-237
- Bellou S, Makri A, Triantaphyllidou I-E, Papanikolaou S, Aggelis G (2014) Morphological and metabolic shifts of *Yarrowia lipolytica* induced by alteration of the dissolved oxygen concentration in the growth environment Microbiology-Sgm 160:807-817 doi:10.1099/mic.0.074302-0

- Bellou S, Triantaphyllidou IE, Aggeli D, Elazzazy AM, Baeshen MN, Aggelis G (2016) Microbial oils as food additives: recent approaches for improving microbial oil production and its polyunsaturated fatty acid content *Current Opinion in Biotechnology* 37:24-35 doi:10.1016/j.copbio.2015.09.005
- Benson BB, Krause D (1984) The concentration and isotopic fractionation of oxygen dissolved in freshwater and seawater in equilibrium with the atmosphere *Limnology and Oceanography* 29:620-632
- Beopoulos A, Cescut J, Haddouche R, Uribe-larrea J-L, Molina-Jouve C, Nicaud J-M (2009) *Yarrowia lipolytica* as a model for bio-oil production *Progress in Lipid Research* 48:375-387 doi:10.1016/j.plipres.2009.08.005
- Berne BJ, Pecora R (2000) *Dynamic light scattering: with applications to chemistry, biology, and physics*. Courier Corporation,
- Biryukova EN, Medentsev AG, Arinbasarova AY, Akimenko VK (2006) Tolerance of the yeast *Yarrowia lipolytica* to oxidative stress *Microbiology* 75:243-247
- Botelho Nunes PM, da Rocha SM, Fonseca Amaral PF, Miguez da Rocha-Leao MH (2013) Study of trans-trans farnesol effect on hyphae formation by *Yarrowia lipolytica* *Bioprocess and Biosystems Engineering* 36:1967-1975 doi:10.1007/s00449-013-0973-8
- Boyer F, Pouliquen O, Guazzelli E (2011) Dense suspensions in rotating-rod flows: normal stresses and particle migration *Journal of Fluid Mechanics* 686:5-25 doi:10.1017/jfm.2011.272
- Braga A, Belo I (2015) Production of gamma-decalactone by *Yarrowia lipolytica*: insights into experimental conditions and operating mode optimization *Journal of Chemical Technology and Biotechnology* 90:559-565 doi:10.1002/jctb.4349
- Braga A, Mesquita DP, Amaral AL, Ferreira EC, Belo I (2016) Quantitative image analysis as a tool for *Yarrowia lipolytica* dimorphic growth evaluation in different culture media *Journal of Biotechnology* 217:22-30 doi:10.1016/j.jbiotec.2015.10.023
- Brígida AIS, Amaral PF, Gonçalves LR, Coelho MAZ (2007) Characterization of an extracellular lipase from *Yarrowia lipolytica* *Proceedings of European Congress of Chemical Engineering (ECCE-6) Copenhagen, 16-20 September 2007*
- Brittain HG (2001) Particle-size distribution. Part I. Representations of particle representations of particle shape, size, and distribution *Pharmaceutical technology* 25:38-45
- Broach JR (2012) Nutritional Control of Growth and Development in Yeast. *Genetics* 192:73-105. doi:10.1534/genetics.111.135731
- Bussamara R et al. (2010) Isolation of a lipase-secreting yeast for enzyme production in a pilot-plant scale batch fermentation *Bioresource Technology* 101:268-275 doi:10.1016/j.biortech.2008.10.063
- Bylund F, Collet E, Enfors SO, Larsson G (1998) Substrate gradient formation in the large-scale bioreactor lowers cell yield and increases by-product formation *Bioprocess Engineering* 18:171-180 doi:10.1007/s004490050427
- Carlquist M et al. (2012) Physiological heterogeneities in microbial populations and implications for physical stress tolerance *Microbial Cell Factories* 11 doi:10.1186/1475-2859-11-94
- Carlson M (1999) Glucose repression in yeast. *Curr Opin in Microbiology* 2:202-207. doi:[http://dx.doi.org/10.1016/S1369-5274\(99\)80035-6](http://dx.doi.org/10.1016/S1369-5274(99)80035-6)
- Cervantes-Chavez JA, Kronberg F, Passeron S, Ruiz-Herrera J (2009) Regulatory role of the PKA pathway in dimorphism and mating in *Yarrowia lipolytica* *Fungal Genetics and Biology* 46:390-399 doi:10.1016/j.fgb.2009.02.005

- Cervantes-Chavez JA, Ruiz-Herrera J (2006) STE11 disruption reveals the central role of a MAPK pathway in dimorphism and mating in *Yarrowia lipolytica* Fems Yeast Research 6:801-815 doi:10.1111/j.1567-1364.2006.00084.x
- Cervantes-Chavez JA, Ruiz-Herrera J (2007) The regulatory subunit of protein kinase A promotes hyphal growth and plays an essential role in *Yarrowia lipolytica* Fems Yeast Research 7:929-940 doi:10.1111/j.1567-1364.2007.00265.x
- Cescut J (2009) Accumulation d'acylglycérols par des espèces levuriennes à usage carburant aéronautique: physiologie et performances de procédés. PhD Thesis, Institut National des Sciences Appliquées de Toulouse (INSAT)-France
- Chapman GV (2000) Instrumentation for flow cytometry Journal of Immunological Methods 243:3-12 doi:10.1016/s0022-1759(00)00224-6
- Chisti Y (2001) Hydrodynamic damage to animal cells Critical Reviews In Biotechnology 21:67-110
- Coelho MAZ, Amaral PFF, Belo I (2010) *Yarrowia lipolytica*: an industrial workhorse Current Research, Technology and Education Topics in Applied Microbiology and Microbial Biotechnology Advances:930-940
- Collignon ML, Dossin D, Delafosse A, Crine M, Toye D (2010) Quality of mixing in a stirred bioreactor used for animal cells culture: heterogeneities in a lab scale bioreactor and evolution of mixing time with scale up Biotechnologie Agronomie Societe Et Environnement 14:585-591
- Conrad M, Schothorst J, Kankipati HN, Van Zeebroeck G, Rubio-Teixeira M, Thevelein JM (2014) Nutrient sensing and signaling in the yeast *Saccharomyces cerevisiae*. FEMS Microbiology Reviews 38:254-299. doi:10.1111/1574-6976.12065
- Cortes JT, Flores N, Bolivar F, Lara AR, Ramirez OT (2016) Physiological effects of pH gradients on *Escherichia coli* during plasmid DNA production Biotechnology and Bioengineering 113:598-611 doi:10.1002/bit.25817
- Corzo G, Revah S (1999) Production and characteristics of the lipase from *Yarrowia lipolytica* 681 Bioresource Technology 70:173-180
- Cruz PE, Cunha A, Peixoto CC, Clemente J, Moreira JL, Carrondo MJT (1998) Optimization of the production of virus-like particles in insect cells Biotechnology And Bioengineering 60:408-418
- Danckwerts PV (1953) Continuous flow systems Chemical Engineering Science 2:1-13 doi:[http://dx.doi.org/10.1016/0009-2509\(53\)80001-1](http://dx.doi.org/10.1016/0009-2509(53)80001-1)
- Dart T, Chatellier G (2002) Comment décrire la distribution d'une variable ? Test de normalité et traitement des valeurs extrêmes. Rev. Mal. Respir., 20, 946-951
- Deak T (2001) Identification of yeasts isolated from poultry meat Acta Biologica Hungarica 52:195-200 doi:10.1556/ABiol.52.2001.2-3.3
- Deive FJ, Angeles Sanroman M, Longo MA (2010) A comprehensive study of lipase production by *Yarrowia lipolytica* CECT 1240 (ATCC 18942): from shake flask to continuous bioreactor Journal of Chemical Technology and Biotechnology 85:258-266 doi:10.1002/jctb.2301
- Delvigne F, Boxus M, Ingels S, Thonart P (2009) Bioreactor mixing efficiency modulates the activity of a prpoS::GFP reporter gene in *E. coli* Microbial Cell Factories 8
- Delvigne F, Goffin P (2014) Microbial heterogeneity affects bioprocess robustness: Dynamic single-cell analysis contributes to understanding of microbial populations Biotechnology Journal 9:61-72 doi:10.1002/biot.201300119
- Diaz M, Herrero M, Garcia LA, Quiros C (2010) Application of flow cytometry to industrial microbial bioprocesses Biochemical Engineering Journal 48:385-407 doi:10.1016/j.bej.2009.07.013

- Dominguez A, Ferminan E, Gaillardin C (2000) *Yarrowia lipolytica*: an organism amenable to genetic manipulation as a model for analyzing dimorphism in fungi Contributions to microbiology 5:151-172
- Elliott AC, Woodward WA (2006) Statistical Analysis Quick Reference Guidebook: With SPSS Examples. Sage Publications Pvt. Ltd.,
- Enfors SO et al. (2001) Physiological responses to mixing in large scale bioreactors Journal of Biotechnology 85:175-185 doi:10.1016/s0168-1656(00)00365-5
- Enshaeieh M, Abdoli A, Nahvi I (2013) Medium optimization for biotechnological production of single cell oil using *Candida gali* and *Yarrowia lipolytica* M7 Journal of Cell and Molecular Research 5:17-23
- Epova E et al. (2012) Identification of Proteins Involved in pH Adaptation in Extremophile Yeast *Yarrowia lipolytica* Proteomic Applications in Biology 209-224
- Faure L (2002) Optimisation de la production de lipases recombinantes chez *Yarrowia lipolytica* DEA Biologie-Santé-Biotechnologie, Laboratoire Biotechnologie-Bioprocédés
- Fernandes RL et al. (2012) Experimental methods and modeling techniques for description of cell population heterogeneity Biotechnology Advances 29:575-599
- Ferreira P, Lopes M, Mota M, Belo I (2016a) Oxygen mass transfer impact on citric acid production by *Yarrowia lipolytica* from crude glycerol Biochemical Engineering Journal 110:35-42 doi:10.1016/j.bej.2016.02.001
- Ferreira P, Lopes M, Mota M, Belo I (2016b) Oxygen transfer rate and pH as major operating parameters of citric acid production from glycerol by *Yarrowia lipolytica* W29 and CBS 2073. Chemical Papers 70:869-876. doi:10.1515/chempap-2016-0024
- Fickers P, Benetti PH, Wache Y, Marty A, Mauersberger S, Smit MS, Nicaud JM (2005) Hydrophobic substrate utilisation by the yeast *Yarrowia lipolytica*, and its potential applications Fems Yeast Research 5:527-543 doi:10.1016/j.femsyr.2004.09.004
- Fickers P, Destain J, Thonart P (2009) Improvement of *Yarrowia lipolytica* lipase production by fed-batch fermentation Journal of Basic Microbiology 49:212-215 doi:10.1002/jobm.200800186
- Fickers P, Marty A, Nicaud JM (2011) The lipases from *Yarrowia lipolytica*: Genetics, production, regulation, biochemical characterization and biotechnological applications Biotechnology Advances 29:632-644 doi:10.1016/j.biotechadv.2011.04.005
- Fillaudeau L, Cescut J, Anne-Archard D, Nicaud JM, Uribelarrea JL, Molina-Jouve C (2009) Morphology and rheological behaviour of *Yarrowia lipolytica* during production of intra-cellular energetic molecules. Impact of lipid accumulation and genetic modifications Conference Paper 8th World Congress of Chemical Engineering, At Montréal, Quebec, Canada, Volume: In: Proceeding of 8th World Congress of Chemical Engineering Eds Canadian Society for Chemical Engineering (Ontario, Canada)
- Finogenova TV et al. (2002) Biosynthesis of citric and isocitric acids from ethanol by mutant *Yarrowia lipolytica* N 1 under continuous cultivation Applied Microbiology and Biotechnology 59:493-500 doi:10.1007/s00253-002-1022-8
- Finogenova TV, Shishkanova NV, Fausek EA, Eremina SS (1991) Biosynthesis of isocitric acid from ethanol by yeasts Applied Microbiology and Biotechnology 36:231-235
- Fissan H, Ristig S, Kaminski H, Asbach C, Epple M (2014) Comparison of different characterization methods for nanoparticle dispersions before and after aerosolization Analytical Methods 6:7324-7334 doi:10.1039/c4ay01203h
- Fontanille P, Kumar V, Christophe G, Nouaille R, Larroche C (2012) Bioconversion of volatile fatty acids into lipids by the oleaginous yeast *Yarrowia lipolytica* Bioresource Technology 114:443-449 doi:10.1016/j.biortech.2012.02.091

- Fu ZB, Verderame TD, Leighton JM, Sampey BP, Appelbaum ER, Patel PS, Aon JC (2014) Exometabolome analysis reveals hypoxia at the up-scaling of a *Saccharomyces cerevisiae* high-cell density fed-batch biopharmaceutical process *Microbial Cell Factories* 13 doi:10.1186/1475-2859-13-32
- Galvagno MA, Iannone LJ, Bianchi J, Kronberg F, Rost E, Carstens MR, Cerrutti P (2011) Optimization of biomass production of a mutant of *Yarrowia lipolytica* with an increased lipase activity using raw glycerol *Revista Argentina De Microbiologia* 43:218-225
- Gancedo JM (1998) Yeast carbon catabolite repression. *Microbiology and molecular biology reviews* : MMBR 62:334-+
- Gancedo JM (2008) The early steps of glucose signalling in yeast. *FEMS Microbiology Reviews* 32:673-704. doi:10.1111/j.1574-6976.2008.00117.x
- Gao Q, Fang A, Pierson DL, Mishra SK, Demain AL (2001) Shear stress enhances microcin B17 production in a rotating wall bioreactor, but ethanol stress does not *Applied Microbiology And Biotechnology* 56:384-387
- Garland S, Gauthier G, Martin J, Morris JF (2013) Normal stress measurements in sheared non-Brownian suspensions *Journal of Rheology* 57:71-88 doi:10.1122/1.4758001
- Gasmi N, Ayed A, Nicaud J-M, Kallel H (2011) Design of an efficient medium for heterologous protein production in *Yarrowia lipolytica*: case of human interferon alpha 2b *Microbial Cell Factories* 10 doi:10.1186/1475-2859-10-38
- Ghasemi A, Zahediasl S (2012) Normality tests for statistical analysis: a guide for non-statisticians *International journal of endocrinology and metabolism* 10:486-489 doi:10.5812/ijem.3505
- Givan AL (2001) *Flow Cytometry: First Principles, Second Edition* 2nd Edition, John Wiley & Sons, Inc, New York
- Goncalves FAG, Colen G, Takahashi JA (2014) *Yarrowia lipolytica* and Its Multiple Applications in the Biotechnological Industry *Scientific World Journal* doi:10.1155/2014/476207
- Gonzalez-Lopez CI, Ortiz-Castellanos L, Ruiz-Herrera J (2006) The ambient pH response Rim pathway in *Yarrowia lipolytica*: Identification of YIRIM9 and characterization of its role in dimorphism *Current Microbiology* 53:8-12
- Gonzalez-Lopez CI, Szabo R, Blanchin-Roland S, Gaillardin C (2002) Genetic control of extracellular protease synthesis in the yeast *Yarrowia lipolytica* *Genetics* 160:417-427
- Gorenflo VM et al. (2007) Acoustic cell processing for viral transduction or bioreactor cell retention. In: *Cell Technology for Cell Products*. pp 273-278
- Guevaraolvera L, Calvomendez C, Ruizherrera J (1993) The role of polyamine metabolism in dimorphism of *Yarrowia lipolytica* *Journal of General Microbiology* 139:485-493
- Guseva MA, Epova EY, Kovalev LI, Shevelev AB (2010) The study of adaptation mechanisms of *Yarrowia lipolytica* yeast to alkaline conditions by means of proteomics *Applied Biochemistry and Microbiology* 46:307-312 doi:10.1134/s0003683810030105
- Gustafsson L, Olz R, Larsson K, Larsson C, Adler L (1993) Energy balance calculations as a tool to determine maintenance energy requirements under stress conditions. *Pure Applied Chemistry* 65:1893-1898. doi:10.1351/pac199365091893
- Ham JH, Platzer B (2004) Semi-empirical equations for residence time distributions in disperse systems - Part 1: Continuous phase *Chemical Engineering & Technology* 27:1172-1178 doi:10.1002/ceat.200407038
- Han S, Delvigne F, Brognaux A, Charbon GE, Sorensen SJ (2013) Design of growth-dependent biosensors based on destabilized GFP for the detection of physiological

- behavior of *Escherichia coli* in heterogeneous bioreactors *Biotechnology Progress* 29:553-563 doi:10.1002/btpr.1694
- Herrero AB, Lopez MC, Fernandez-Lago L, Dominguez A (1999) *Candida albicans* and *Yarrowia lipolytica* as alternative models for analysing budding patterns and germ tube formation in dimorphic fungi *Microbiology-Sgm* 145:2727-2737
- Hewitt CJ, Nienow AW (2007) The scale-up of microbial batch and fed-batch fermentation processes. In: Laskin AI, Sariaslani S, Gadd GM (eds) *Advances in Applied Microbiology*, Vol 62, vol 62. *Advances in Applied Microbiology*. pp 105-135. doi:10.1016/s0065-2164(07)62005-x
- Hewitt CJ, Onyeaka H, Lewis G, Taylor IW, Nienow AW (2007) A comparison of high cell density fed-batch fermentations involving both induced and non-induced recombinant *Escherichia coli* under well-mixed small-scale and simulated poorly mixed large-scale conditions *Biotechnology And Bioengineering* 96:495-505
- Hurtado CAR, Beckerich JM, Gaillardin C, Rachubinski RA (2000) A Rac homolog is required for induction of hyphal growth in the dimorphic yeast *Yarrowia lipolytica* *Journal of Bacteriology* 182:2376-2386
- Jazini M, Cekici G, Herwig C (2014) Quantifying the Effects of Frequency and Amplitude of Periodic Oxygen-Related Stress on Recombinant Protein Production in *Pichia pastoris* *Bioengineering*:47-61
- Jost B, Holz M, Aurich A, Barth G, Bley T, Muller RA (2015) The influence of oxygen limitation for the production of succinic acid with recombinant strains of *Yarrowia lipolytica* *Applied Microbiology and Biotechnology* 99:1675-1686 doi:10.1007/s00253-014-6252-z
- Kamzolova SV, Shishkanova NV, Morgunov IG, Finogenova TV (2003) Oxygen requirements for growth and citric acid production of *Yarrowia lipolytica* *Fems Yeast Research* 3:217-222 doi:10.1016/s1567-1356(02)00188-5
- Kar T, Delvigne F, Destain J, Thonart P (2011) Bioreactor scale-up and design on the basis of physiologically relevant parameters: application to the production of lipase by *Yarrowia lipolytica* *Biotechnologie Agronomie Societe Et Environnement* 15:585-595
- Kar T, Delvigne F, Masson M, Destain J, Thonart P (2008) Investigation of the effect of different extracellular factors on the lipase production by *Yarrowia lipolytica* on the basis of a scale-down approach *Journal of Industrial Microbiology & Biotechnology* 35:1053-1059
- Kar T, Destain J, Thonart P, Delvigne F (2010) Impact of scaled-down on dissolved oxygen fluctuations at different levels of the lipase synthesis pathway of *Yarrowia lipolytica*. *Biotechnologie Agronomie Societe Et Environnement* 14:523-529
- Kawasse FM, Amaral PF, Rocha-Leao MHM, Amaral AL, Ferreira EC, Coelho MAZ (2003) Morphological analysis of *Yarrowia lipolytica* under stress conditions through image processing *Bioprocess And Biosystems Engineering* 25:371-375
- Kaye BH, Alliet D, Switzer L, TurbittDaoust C (1997) The effect of shape on intermethod correlation of techniques for characterizing the size distribution of powder .1. Correlating the size distribution measured by sieving, image analysis, and diffractometer methods *Particle & Particle Systems Characterization* 14:219-224
- Kebabci O, Cihangir N (2012) Comparison of three *Yarrowia lipolytica* strains for lipase production: NBRC 1658, IFO 1195, and a local strain *Turkish Journal of Biology* 36:15-24 doi:10.3906/biy-1102-10
- Kent JA (2012) *Handbook of Industrial Chemistry and Biotechnology*, Ch-30: Industrial Biotechnology: Discovery to Delivery 2:1131-1227

- Khidas Y, Haffner B, Pitois O (2015) Critical size effect of particles reinforcing foamed composite materials *Composites Science and Technology* 119:62-67 doi:10.1016/j.compscitech.2015.09.024
- Kim J, Cheon SA, Park S, Song Y, Kim JY (2000) Serum-induced hypha formation in the dimorphic yeast *Yarrowia lipolytica* *Fems Microbiology Letters* 190:9-12
- Kim JH, Roy A, Jouandot D, Cho KH (2013) The glucose signaling network in yeast. *Biochim Biophys Acta-Gen Subj* 1830:5204-5210. doi:10.1016/j.bbagen.2013.07.025
- Kraiem H, Ben Gaïda L, Manon Y, Anne-Archard D, Fillaudeau L (2013) Impact of cell physiology and densities during oxidative axenic cultures of *Yarrowia lipolytica* on physico-chemical properties of broth Conference Paper 9th World Congress of Chemical Engineering, 18 August 2013 - 23 August 2013 (Seoul, Korea, Republic Of)
- Krull R, Cordes C, Horn H, Kampen I, Kwade A, Neu TR, Nortemann B (2010) Morphology of filamentous fungi: linking cellular biology to process engineering using *Aspergillus niger* *Advances in biochemical engineering/biotechnology* 121:1-21 doi:10.1007/10_2009_60
- Kuschel M, Siebler F, Takors R (2017) Lagrangian Trajectories to Predict the Formation of Population Heterogeneity in Large-Scale Bioreactors *Bioengineering* 4:27
- Lakhotia S, Bauer KD, Papoutsakis ET (1992) Damaging Agitation Intensities Increase Dna-Synthesis Rate And Alter Cell-Cycle Phase Distributions Of Cho Cells *Biotechnology And Bioengineering* 40:978-990
- Lambert M, Blanchin Roland S, LeLouedec F, Lepingle A, Gaillardin C (1997) Genetic analysis of regulatory mutants affecting synthesis of extracellular proteinases in the yeast *Yarrowia lipolytica*: Identification of a RIM101/pacC homolog *Molecular and Cellular Biology* 17:3966-3976
- Lanciotti R, Gianotti A, Baldi D, Angrisani R, Suzzi G, Mastrocola D, Guerzoni ME (2005) Use of *Yarrowia lipolytica* strains for the treatment of olive mill wastewater *Bioresource Technology* 96:317-322 doi:10.1016/j.biortech.2004.04.009
- Langheinrich C, Nienow AW (1999) Control of pH in large-scale, free suspension animal cell bioreactors: Alkali addition and pH excursions *Biotechnology and Bioengineering* 66:171-179 doi:10.1002/(sici)1097-0290(1999)66:3<171::aid-bit5>3.0.co;2-t
- Lara AR, Galindo E, Ramirez OT, Palomares LA (2006) Living with heterogeneities in bioreactors *Molecular Biotechnology* 34:355-381 doi:10.1385/mb:34:3:355
- Larsson G, Tornkvist M, Wernersson ES, Tragardh C, Noorman H, Enfors SO (1996) Substrate gradients in bioreactors: Origin and consequences *Bioprocess Engineering* 14:281-289
- Lazar Z et al. (2017) Characterization of hexose transporters in *Yarrowia lipolytica* reveals new groups of Sugar Porters involved in yeast growth. *Fungal Genetics Biology* 100:1-12. doi:<http://dx.doi.org/10.1016/j.fgb.2017.01.001>
- Ledesma-Amaro R, Nicaud JM (2016) Metabolic Engineering for Expanding the Substrate Range of *Yarrowia lipolytica* *Trends in Biotechnology* 34:798-809 doi:10.1016/j.tibtech.2016.04.010
- Lejeune A, Frank D, Thonart P (2013) Physiological response of yeast to process perturbations: A mini-bioreactor approach *Cerevisia* 38:15-19 doi:<http://dx.doi.org/10.1016/j.cervis.2013.04.004>
- Levinson WE, Kurtzman CP, Kuo TM (2007) Characterization of *Yarrowia lipolytica* and related species for citric acid production from glycerol *Enzyme and Microbial Technology* 41:292-295 doi:10.1016/j.enzmictec.2007.02.005

- Lim JS, Kim JH, Kim C, Kim SW (2002) Morphological and rheological properties of culture broth of *Cephalosporium acremonium* M25 Korea-Australia Rheology Journal 14:11-16
- Liu HH, Ji XJ, Huang H (2015) Biotechnological applications of *Yarrowia lipolytica*: Past, present and future Biotechnology Advances 33:1522-1546 doi:10.1016/j.biotechadv.2015.07.010
- Lopes M (2013) Characterization of non-conventional yeasts under hyperbaric conditions: cellular responses to oxidative stress. PhD Thesis. University of Minho-Portugal
- Lopes M, Gomes N, Goncalves C, Coelho MAZ, Mota M, Belo I (2008) *Yarrowia lipolytica* lipase production enhanced by increased air pressure Letters In Applied Microbiology 46:255-260
- Lopes M, Gomes N, Mota M, Belo I (2009a) *Yarrowia lipolytica* Growth Under Increased Air Pressure: Influence on Enzyme Production Applied Biochemistry And Biotechnology 159:46-53
- Lopes M, Mota M, Belo I (2009b) *Yarrowia lipolytica* adaptation to oxidative stress induced by increased air pressure New Biotechnology 25:S77-S78
- Lopes M, Mota M, Belo I (2013) Comparison of *Yarrowia lipolytica* and *Pichia pastoris* Cellular Response to Different Agents of Oxidative Stress Applied Biochemistry And Biotechnology 170:448-458
- Lu GZ, Thompson BG, Suresh MR, Gray MR (1995) Cultivation Of Hybridoma Cells In An Inclined Bioreactor Biotechnology And Bioengineering 45:176-186
- Lueker TJ, Dickson AG, Keeling CD (2000) Ocean pCO₂ calculated from dissolved inorganic carbon, alkalinity, and equations for K₁ and K₂: validation based on laboratory measurements of CO₂ in gas and seawater at equilibrium Marine Chemistry 70:105-119 doi:[http://dx.doi.org/10.1016/S0304-4203\(00\)00022-0](http://dx.doi.org/10.1016/S0304-4203(00)00022-0)
- Madzak C, Gaillardin C, Beckerich JM (2004) Heterologous protein expression and secretion in the non-conventional yeast *Yarrowia lipolytica*: a review Journal of Biotechnology 109:63-81 doi:10.1016/j.jbiotec.2003.10.027
- Madzak C, Otterbein L, Chamkha M, Moukha S, Asther M, Gaillardin C, Beckerich JM (2005) Heterologous production of a laccase from the basidiomycete *Pycnoporus cinnabarinus* in the dimorphic yeast *Yarrowia lipolytica* Fems Yeast Research 5:635-646 doi:10.1016/j.femsyr.2004.10.009
- Makri A, Fakas S, Aggelis G (2010) Metabolic activities of biotechnological interest in *Yarrowia lipolytica* grown on glycerol in repeated batch cultures Bioresource Technology 101:2351-2358 doi:10.1016/j.biortech.2009.11.024
- Manfredini R, Cavallera V, Marini L, Donati G (1983) Mixing and oxygen-transfer in conventional stirred fermenters Biotechnology and Bioengineering 25:3115-3131 doi:10.1002/bit.260251224
- Martinez-Vazquez A, Gonzalez-Hernandez A, Dominguez A, Rachubinski R, Riquelme M, Cuellar-Mata P, Torres Guzman JC (2013) Identification of the Transcription Factor Znc1p, which Regulates the Yeast-to-Hypha Transition in the Dimorphic Yeast *Yarrowia lipolytica* Plos One 8 doi:10.1371/journal.pone.0066790
- McDowell CL, Papoutsakis ET (1998) Increased agitation intensity increases CD13 receptor surface content and mRNA levels, and alters the metabolism of HL60 cells cultured in stirred tank bioreactors Biotechnology And Bioengineering 60:239-250
- McIlvaine TC (1921) A buffer solution for colorimetric comparison Journal of Biological Chemistry 49:183-186
- Meng X, Yang JM, Xu X, Zhang L, Nie QJ, Xian M (2009) Biodiesel production from oleaginous microorganisms Renewable Energy 34:1-5 doi:10.1016/j.renene.2008.04.014

- Mentel M, Piskur J, Neugeglise C, Rycovska A, Cellengova G, Kolarov J (2005) Triplicate genes for mitochondrial ADP/ATP carriers in the aerobic yeast *Yarrowia lipolytica* are regulated differentially in the absence of oxygen. *Mol Genet Genomics* 273:84-91. doi:10.1007/s00438-005-1107-z
- Metting FB (1996) Biodiversity and application of microalgae *Journal of Industrial Microbiology & Biotechnology* 17:477-489 doi:10.1007/bf01574779
- Morales-Vargas AT, Dominguez A, Ruiz-Herrera J (2012) Identification of dimorphism-involved genes of *Yarrowia lipolytica* by means of microarray analysis. *Research in Microbiology* 163:378-387. doi:10.1016/j.resmic.2012.03.002
- Morin M, Monteoliva L, Insenser M, Gil C, Dominguez A (2007) Proteomic analysis reveals metabolic changes during yeast to hypha transition in *Yarrowia lipolytica* *Journal of Mass Spectrometry* 42:1453-1462 doi:10.1002/jms.1284
- Muller S, Harms H, Bley T (2010) Origin and analysis of microbial population heterogeneity in bioprocesses *Current Opinion in Biotechnology* 21:100-113 doi:10.1016/j.copbio.2010.01.002
- Nagy E, Neubeck M, Mayr B, Moser A (1995) Simulation Of The Effect Of Mixing, Scale-Up And Ph-Value Regulation During Glutamic-Acid Fermentation *Bioprocess Engineering* 12:231-238
- Najjar A, Robert S, Guerin C, Violet-Asther M, Carriere F (2011) Quantitative study of lipase secretion, extracellular lipolysis, and lipid storage in the yeast *Yarrowia lipolytica* grown in the presence of olive oil: analogies with lipolysis in humans *Applied Microbiology and Biotechnology* 89:1947-1962 doi:10.1007/s00253-010-2993-5
- Nakamura M, Ishimura K (2010) Rapid Size Evaluation of Nanoparticles Using Flow Cytometry *Advanced Science Letters* 3:130-137 doi:10.1166/asl.2010.1096
- Nebohacova M, Mentel M, Nosek J, Kolarov J (1999) Isolation and expression of the gene encoding mitochondrial ADP/ATP carrier (AAC) from the pathogenic yeast *Candida parapsilosis*. *Yeast* 15:1237-1242. doi:10.1002/(sici)1097-0061(19990915)15:12<1237::aid-yea446>3.0.co;2-3
- Nguyen TC (2014) In-situ and ex-situ multi-scale physical metrologies to investigate the destructuration mechanisms of lignocellulosic matrices and release kinetics of fermentescible cellulosic carbon Thèse de doctorat- INSA de Toulouse (France) doi:<http://www.theses.fr/2014ISAT0036>
- Novotny C, Dolezalova L, Lieblova J (1994) Dimorphic Growth And Lipase Production In Lipolytic Yeasts *Folia Microbiologica* 39:71-73
- Nunes PMB, da Rocha SM, Amaral PFF, da Rocha-Leao MHM (2013) Study of trans-trans farnesol effect on hyphae formation by *Yarrowia lipolytica* *Bioprocess And Biosystems Engineering* 36:1967-1975
- O'Beirne D, Hamer G (2000) Oxygen availability and the growth of *Escherichia coli* W3110: A problem exacerbated by scale-up *Bioprocess Engineering* 23:487-494 doi:10.1007/s004499900185
- O'Shea DG, Walsh PK (2000) The effect of culture conditions on the morphology of the dimorphic yeast *Kluyveromyces marxianus* var. *marxianus* NRRLy2415: a study incorporating image analysis *Applied Microbiology and Biotechnology* 53:316-322
- Ochoa-Estopier A (2012) Analyse systématique des bascules métaboliques chez les levures d'intérêt industriel : application aux bascules du métabolisme lipidique chez *Yarrowia lipolytica* PhD Thesis, Institut National des Sciences Appliquées de Toulouse (INSAT)-France
- Ochoa-Estopier A, Guillouet SE (2014) D-stat culture for studying the metabolic shifts from oxidative metabolism to lipid accumulation and citric acid production in *Yarrowia lipolytica* *Journal of Biotechnology* 170:35-41 doi:10.1016/j.jbiotec.2013.11.008

- Ochoa Estopier A (2012) Analyse systématique des bascules métaboliques chez les levures d'intérêt industriel : application aux bascules du métabolisme lipidique chez *Yarrowia lipolytica* PhD thesis, INSA Toulouse, France
- Olmos E, Mehmood N, Husein LH, Goergen JL, Fick M, Delaunay S (2013) Effects of bioreactor hydrodynamics on the physiology of *Streptomyces* Bioprocess and Biosystems Engineering 36:259-272 doi:10.1007/s00449-012-0794-1
- Onyeaka H, Nienow AW, Hewitt CJ (2003) Further studies related to the scale-up of high cell density *Escherichia coli* fed-batch fermentations: The additional effect of a changing microenvironment when using aqueous ammonia to control pH Biotechnology and Bioengineering 84:474-484 doi:10.1002/bit.10805
- Oosterhuis NMG (1984) Scale-up of bioreactors, a scale-down approach PhD thesis, Delft University of Technology Delft, The Netherlands
- Oosterhuis NMG, Kossen NWF (1984) Dissolved oxygen concentration profiles in a production-scale bioreactor Biotechnology and Bioengineering 26:546-550 doi:10.1002/bit.260260522
- Oshea DG, Walsh PK (1996) Morphological characterization of the dimorphic yeast *Kluyveromyces marxianus* var *marxianus* NRRLy2415 by semi-automated image analysis Biotechnology and Bioengineering 51:679-690 doi:10.1002/(sici)1097-0290(19960920)51:6<679::aid-bit6>3.0.co;2-e
- Ota Y, Oikawa S, Morimoto Y, Minoda Y (1984) Nutritional Factors Causing Mycelial Development of *Saccharomycopsis lipolytica* Agricultural and Biological Chemistry 48:1933-1939
- Ozcan S, Johnston M (1999) Function and regulation of yeast hexose transporters. Microbiology and Molecular Biology Reviews 63:554-+
- Pakpour M (2013) Rheology of dry, partially saturated and wet granular materials PhD thesis, Faculty of Science (FNWI)- Van der Waals-Zeeman Institute (WZI)
- Palande AS, Kulkarni SV, Leon-Ramirez C, Campos-Gongora E, Ruiz-Herrera J, Deshpande MV (2014) Dimorphism and hydrocarbon metabolism in *Yarrowia lipolytica* var. *indica* Archives of Microbiology 196:545-556 doi:10.1007/s00203-014-0990-2
- Palomares LA, Estrada-Mondaca S, Ramirez OT (2006) Principles and Applications of the Insect Cell-Baculovirus Expression Vector System Cell culture technology for pharmaceutical and cellular applications (Ozturk, S and Hu, W S, eds):627-692
- Palomares LA, Ramirez OT (2000) Bioreactor Scale-Up, in *The Encyclopedia of Cell Technology* 1:183-201
- Palomares LA, Ramirez OT (2003) Bioreactor Scale-Down. In: *Encyclopedia of Cell Technology*. John Wiley & Sons, Inc. doi:10.1002/0471250570.spi022
- Papagianni M (2004) Fungal morphology and metabolite production in submerged mycelial processes Biotechnology Advances 22:189-259 doi:10.1016/j.biotechadv.2003.09.005
- Papanikolaou S, Aggelis G (2009) Biotechnological valorization of biodiesel derived glycerol waste through production of single cell oil and citric acid by *Yarrowia lipolytica* Lipid Technology 21:83-87
- Papanikolaou S, Chevalot I, Galiotou-Panayotou M, Komaitis M, Marc I, Aggelis G (2007) Industrial derivative of tallow: a promising renewable substrate for microbial lipid, single-cell protein and lipase production by *Yarrowia lipolytica* Electronic Journal of Biotechnology 10:425-435 doi:10.2225/vol10-issue3-fulltext-8
- Papanikolaou S, Chevalot I, Komaitis M, Aggelis G, Marc I (2001) Kinetic profile of the cellular lipid composition in an oleaginous *Yarrowia lipolytica* capable of producing a cocoa-butter substitute from industrial fats Antonie Van Leeuwenhoek International Journal of General and Molecular Microbiology 80:215-224 doi:10.1023/a:1013083211405

- Papanikolaou S, Galiotou-Panayotou M, Chevalot I, Komaitis M, Marc I, Aggelis G (2006) Influence of glucose and saturated free-fatty acid mixtures on citric acid and lipid production by *Yarrowia lipolytica* Current Microbiology 52:134-142 doi:10.1007/s00284-005-0223-7
- Papanikolaou S, Muniglia L, Chevalot I, Aggelis G, Marc I (2002) *Yarrowia lipolytica* as a potential producer of citric acid from raw glycerol Journal of Applied Microbiology 92:737-744 doi:10.1046/j.1365-2672.2002.01577.x
- Papanikolaou S, Muniglia L, Chevalot I, Aggelis G, Marc I (2003) Accumulation of a cocoa-butter-like lipid by *Yarrowia lipolytica* cultivated on agro-industrial residues Current Microbiology 46:124-130 doi:10.1007/s00284-002-3833-3
- Parfene G, Horincar V, Tyagi AK, Malik A, Bahrim G (2013) Production of medium chain saturated fatty acids with enhanced antimicrobial activity from crude coconut fat by solid state cultivation of *Yarrowia lipolytica* Food Chemistry 136:1345-1349 doi:10.1016/j.foodchem.2012.09.057
- Perez-Campo FM, Dominguez A (2001) Factors affecting the morphogenetic switch in *Yarrowia lipolytica* Current Microbiology 43:429-433
- Phue JN, Shiloach J (2005) Impact of dissolved oxygen concentration on acetate accumulation and physiology of *E coli* BL21, evaluating transcription levels of key genes at different dissolved oxygen conditions Metabolic Engineering 7:353-363 doi:10.1016/j.ymben.2005.06.003
- Portelli B (2011) Biologie systématique et intégrative pour l'amélioration de l'accumulation et de la sélectivité des acides gras accumulés dans les espèces levuriennes. PhD Thesis, Institut National des Sciences Appliquées de Toulouse (INSAT)-France
- Rakicka M, Lazar Z, Dulermo T, Fickers P, Nicaud JM (2015) Lipid production by the oleaginous yeast *Yarrowia lipolytica* using industrial by-products under different culture conditions Biotechnology for Biofuels 8 doi:10.1186/s13068-015-0286-z
- Rakotomalala R (2011) Tests de normalité - Techniques empiriques et tests statistiques, Université Lumière Lyon 2
- Rane KD, Sims KA (1994) Oxygen uptake and citric acid production by *Candida lipolytica* Y 1095 Biotechnology and Bioengineering 43:131-137 doi:10.1002/bit.260430205
- Ranjan V, Waterbury R, Xiao ZH, Diamond SL (1996) Fluid shear stress induction of the transcriptional activator c-fos in human and bovine endothelial cells, HeLa, and Chinese hamster ovary cells Biotechnology And Bioengineering 49:383-390
- Ratledge C (1982) Single cell oil Enzyme and Microbial Technology 4:58-60 doi:10.1016/0141-0229(82)90014-x
- Ratledge C, Wynn JP (2002) The biochemistry and molecular biology of lipid accumulation in oleaginous microorganisms. In: Laskin AI, Bennett JW, Gadd GM (eds) Advances in Applied Microbiology, Vol 51, vol 51. Advances in Applied Microbiology. pp 1-51. doi:10.1016/s0065-2164(02)51000-5
- Reuss M, Schmalzriedt S, Jenne M (1994) Structured Modelling of Bioreactors. In: Galindo E, Ramirez OT (eds) Advances in Bioprocess Engineering. Springer Netherlands, Dordrecht, pp 207-215. doi:10.1007/978-94-017-0641-4_29
- Robak M, Boruckowski T, Drozd W, Lazar Z, Baranowska M, Przado D, Steininger M (2011) Application of the Yeasts *Yarrowia lipolytica* for in-situ Bioremediation of Soil Contaminated with Creosote Oil A Case Study Ochrona Srodowiska 33:27-33
- Roberts RL, Fink GR (1994) Elements Of A Single Map Kinase Cascade In Saccharomyces-Cerevisiae Mediate 2 Developmental Programs In The Same Cell-Type - Mating And Invasive Growth Genes & Development 8:2974-2985
- Robinson JP (2004) Flow cytometry, in: G.L. Bowlin, G. Wnek (Eds.), Encyclopaedia of Biomaterials and Biomedical Engineering, Marcel Dekker, Inc., New York, :630-640

- Rodriguez C, Dominguez A (1984) The growth characteristics of *Saccharomycopsis lipolytica*: morphology and induction of mycelium formation Canadian Journal of Microbiology 30:605-612
- Rolland F, Winderickx J, Thevelein JM (2002) Glucose-sensing and -signalling mechanisms in yeast. FEMS Yeast Res 2:183-201. doi:10.1111/j.1567-1364.2002.tb00084.x
- Ron EZ, Rosenberg E (2002) Biosurfactants and oil bioremediation Current Opinion in Biotechnology 13:249-252 doi:10.1016/s0958-1669(02)00316-6
- Ruiz-Herrera J, Sentandreu R (2002) Different effectors of dimorphism in *Yarrowia lipolytica* Archives Of Microbiology 178:477-483
- Rymowicz W, Rywinska A, Zarowska B, Juszczak P (2006) Citric acid production from raw glycerol by acetate mutants of *Yarrowia lipolytica* Chemical Papers-Chemicke Zvesti 60:391-394 doi:10.2478/s11696-006-0071-3
- Ryu S, Hipp J, Trinh CT (2016) Activating and Elucidating Metabolism of Complex Sugars in *Yarrowia lipolytica*. Appl Environ Microbiol 82:1334-1345. doi:10.1128/aem.03582-15
- Rywinska A, Juszczak P, Wojtatowicz M, Rymowicz W (2011) Chemostat study of citric acid production from glycerol by *Yarrowia lipolytica* Journal of Biotechnology 152:54-57 doi:10.1016/j.jbiotec.2011.01.007
- Rywińska A, Musiał I, Rymowicz W, Żarowska B, Boruckowski T (2012) Effect of agitation and aeration on the citric acid production by *Yarrowia lipolytica* grown on glycerol Preparative Biochemistry and Biotechnology 42:279-291 doi:10.1080/10826068.2012.656868
- Sahoo S, Rao KK, Suraishkumar GK (2006) Reactive oxygen species induced by shear stress mediate cell death in *Bacillus subtilis* Biotechnology and Bioengineering 94:118-127 doi:10.1002/bit.20835
- Santangelo GM (2006) Glucose signaling in *Saccharomyces cerevisiae*. Microbiol Mol Biol Rev 70:253-282. doi:10.1128/mmbr.70.1.253-282.2006
- Sarris D, Galiotou-Panayotou M, Koutinas AA, Komaitis M, Papanikolaou S (2011) Citric acid, biomass and cellular lipid production by *Yarrowia lipolytica* strains cultivated on olive mill wastewater-based media Journal of Chemical Technology and Biotechnology 86:1439-1448 doi:10.1002/jctb.2658
- Sauer M, Porro D, Mattanovich D, Branduardi P (2008) Microbial production of organic acids: expanding the markets Trends in Biotechnology 26:100-108 doi:10.1016/j.tibtech.2007.11.006
- Schricks JM, Krave AS, Verdoes JC, Vandenhondel C, Stouthamer AH, Vanverseveld HW (1993) Growth and product formation in chemostat and recycling cultures by *Aspergillus niger* N402 and a glucoamylase overproducing transformant, provided with multiple copies of the *glaA* gene Journal of General Microbiology 139:2801-2810
- Schweder T, Kruger E, Xu B, Jurgen B, Blomsten G, Enfors SO, Hecker M (1999) Monitoring of genes that respond to process-related stress in large-scale bioprocesses Biotechnology and Bioengineering 65:151-159
- Sekova VY, Gessler NN, Isakova EP, Antipov AN, Dergacheva DI, Deryabina YI, Trubnikova EV (2015) Redox status of extremophilic yeast *Yarrowia lipolytica* during adaptation to pH-stress Applied Biochemistry and Microbiology 51:649-654 doi:10.1134/s0003683815060137
- Senger RS, Karim MN (2003) Effect of shear stress on intrinsic CHO culture state and glycosylation of recombinant tissue-type plasminogen activator protein Biotechnology Progress 19:1199-1209
- Shapiro HM (2003) Practical Flow Cytometry 4th Edition, Wiley-Liss, New York

- Shepherd MG, Sullivan PA (1976) The production and growth characteristics of yeast and mycelial forms of *Candida albicans* in continuous culture *Journal of General Microbiology* 93:361-370
- Sinigaglia M, Lanciotti R, Guerzoni ME (1994) Biochemical And Physiological-Characteristics Of *Yarrowia-Lipolytica* Strains In Relation To Isolation Source *Canadian Journal Of Microbiology* 40:54-59
- Soetaert W, Vandamme EJ (2010) *Industrial Biotechnology: Sustainable Growth and Economic Success*:476
- Staniforth JN, Hart JP (1987) Particle size characterization for pharmaceuticals: Use of image processing and bulk powder measurements for shape analysis of microcrystalline cellulose particles *Anal Proc* 24:78-80
- Sunya S (2012) Dynamique de la réponse physiologique d'*Escherichia coli* à des perturbations maîtrisées de son environnement : vers le développement de nouveaux outils de changement d'échelle PhD thesis, INSA Toulouse, France
- Sunya S, Delvigne F, Uribelarrea JL, Molina-Jouve C, Gorret N (2012) Comparison of the transient responses of *Escherichia coli* to a glucose pulse of various intensities *Applied Microbiology and Biotechnology* 95:1021-1034 doi:10.1007/s00253-012-3938-y
- Sweere APJ, Luyben K, Kossen NWF (1987) Regime analysis and scale-down: Tools to investigate the performance of bioreactors *Enzyme and Microbial Technology* 9:386-398 doi:10.1016/0141-0229(87)90133-5
- Szabo R, Stofanikova V (2002) Presence of organic sources of nitrogen is critical for filament formation and pH-dependent morphogenesis in *Yarrowia lipolytica* *Fems Microbiology Letters* 206:45-50
- Takors R (2012) Scale-up of microbial processes: Impacts, tools and open questions *Journal of Biotechnology* 160:3-9 doi:10.1016/j.jbiotec.2011.12.010
- Taticek RA, Mooyoung M, Legge RL (1991) The Scale-Up Of Plant-Cell Culture - Engineering Considerations *Plant Cell Tissue And Organ Culture* 24:139-158
- Timoumi A et al. (2017) Dynamic behavior of *Yarrowia lipolytica* in response to pH perturbations: dependence of the stress response on the culture mode *Applied Microbiology and Biotechnology* 101:351-366 doi:10.1007/s00253-016-7856-2
- Toma MK et al. (1991) Inhibition Of Microbial-Growth And Metabolism By Excess Turbulence *Biotechnology And Bioengineering* 38:552-556
- Topiltin Morales-Vargas A, Dominguez A, Ruiz-Herrera J (2012) Identification of dimorphism-involved genes of *Yarrowia lipolytica* by means of microarray analysis *Research in Microbiology* 163:378-387 doi:10.1016/j.resmic.2012.03.002
- Tourbin M (2006) Caractérisation et comportement de suspension concentrées de nanoparticules sous écoulement : application aux processus d'agrégation et de rupture. PhD thesis, INP Toulouse. 294 pages
- Trezeguet V, Zeman I, David C, Lauquin GJM, Kolarov J (1999) Expression of the ADP/ATP carrier encoding genes in aerobic yeasts; phenotype of an ADP/ATP carrier deletion mutant of *Schizosaccharomyces pombe*. *Biochim Biophys Acta-Bioenerg* 1410:229-236 doi:10.1016/s0005-2728(98)00180-7
- Troussellier M, Courties C, Lebaron P, Servais P (1999) Flow cytometric discrimination of bacterial populations in seawater based on SYTO 13 staining of nucleic acids *Fems Microbiology Ecology* 29:319-330 doi:10.1111/j.1574-6941.1999.tb00623.x
- Tsao EI, Bohn MA, Numsuwan V, Omstead DR, Munster MJ (1992) Effects Of Heat-Shock On The Production Of Human Erythropoietin From Recombinant Cho Cells *Biotechnology And Bioengineering* 40:1190-1196

- Vanderheijden R, Romein B, Heijnen JJ, Hellinga C, Luyben K (1994) Linear constrain relations in biochemical reaction systems III. Sequential application of data reconciliation for sensitive detection of systematic errors *Biotechnology and Bioengineering* 44:781-791 doi:10.1002/bit.260440703
- Varma A, Palsson BO (1994) Stoichiometric Flux Balance Models Quantitatively Predict Growth And Metabolic By-Product Secretion In Wild-Type *Escherichia-Coli* W3110 *Applied And Environmental Microbiology* 60:3724-3731
- Villiermaux J (1993) Génie de la réaction chimique : conception et fonctionnement des réacteurs:Ed. Tech & Doc Lavoisier
- Vlaev D, Mann R, Lossev V, Vlaev SD, Zahradnik J, Seichter P (2000) Macro-mixing and *Streptomyces fradiae* - Modelling oxygen and nutrient segregation in an industrial bioreactor *Chemical Engineering Research & Design* 78:354-362 doi:10.1205/026387600527473
- Walker GM, Oneill JD (1990) Morphological and metabolic changes in the yeast *Kluyveromyces marxianus* var. *marxianus* NRRLy2415 during fermentation of lactose *Journal of Chemical Technology and Biotechnology* 49:75-89
- Webb PA (2000) A Primer on Particle Sizing by Static Laser Light Scattering. Micromeritics Instrument Corp. Technical Workshop Series: Introduction to the Latest ANSI/ISO Standard for Laser Particle Size Analysis. http://w.w.w.particletesting.com/docs/primer:particle_sizing_laser.pdf. (December 11, 2007) Norcross, Ga.: Micromeritics Instruments Corp.
- Weiss RF (1974) Carbon dioxide in water and seawater: the solubility of a non-ideal gas *Marine Chemistry* 2:203-215 doi:[http://dx.doi.org/10.1016/0304-4203\(74\)90015-2](http://dx.doi.org/10.1016/0304-4203(74)90015-2)
- Wick LM, Quadroni M, Egli T (2001) Short- and long-term changes in proteome composition and kinetic properties in a culture of *Escherichia coli* during transition from glucose-excess to glucose-limited growth conditions in continuous culture and vice versa *Environmental Microbiology* 3:588-599 doi:10.1046/j.1462-2920.2001.00231.x
- Wiebe MG, Trinci APJ (1991) Dilution rate as a determinant of mycelial morphology in continuous culture *Biotechnology and Bioengineering* 38:75-81 doi:10.1002/bit.260380110
- Workman M, Holt P, Thykaer J (2013) Comparing cellular performance of *Yarrowia lipolytica* during growth on glucose and glycerol in submerged cultivations *Amb Express* 3 doi:10.1186/2191-0855-3-58
- Wucherpennig T, Kiep KA, Driouch H, Wittmann C, Krull R (2010) Morphology and Rheology in Filamentous Cultivations. In: Laskin AI, Sariaslani S, Gadd GM (eds) *Advances in Applied Microbiology*, Vol 72, vol 72. *Advances in Applied Microbiology*. pp 89-136. doi:10.1016/s0065-2164(10)72004-9
- Xing ZZ, Kenty BN, Li ZJ, Lee SS (2009) Scale-Up Analysis for a CHO Cell Culture Process in Large-Scale Bioreactors *Biotechnology and Bioengineering* 103:733-746 doi:10.1002/bit.22287
- Xiong Z, Oriss TB, Cavaretta JP, Rosengart MR, Lee JS (2012) Red cell microparticle enumeration: validation of a flow cytometric approach *Vox Sanguinis* 103:42-48 doi:10.1111/j.1423-0410.2011.01577.x
- Xu B, Jahic M, Blomsten G, Enfors SO (1999) Glucose overflow metabolism and mixed-acid fermentation in aerobic large-scale fed-batch processes with *Escherichia coli* *Applied Microbiology and Biotechnology* 51:564-571
- Xu H, Miao XL, Wu QY (2006) High quality biodiesel production from a microalga *Chlorella protothecoides* by heterotrophic growth in fermenters *Journal of Biotechnology* 126:499-507 doi:10.1016/j.jbiotec.2006.05.002

- Yalcin HT, Ucar FB (2009) Isolation and characterization of cheese spoiler yeast isolated from Turkish white cheeses *Annals of Microbiology* 59:477-483
- Yalcin SK, Tijen Bozdemir M, Yesim Ozbas Z (2010) Citric acid production by yeasts: Fermentation conditions, process optimization and strain improvement *Current Research, Technology and Education Topics in Applied Microbiology and Microbial Biotechnology* A Méndez-Vilas (Ed) ©FORMATEX 2010
- Yu W, Erickson K (2008) Chord length characterization using focused beam reflectance measurement probe - methodologies and pitfalls *Powder Technology* 185:24-30 doi:10.1016/j.powtec.2007.09.011
- Zahradnik J, Mann R, Fialova M, Vlaev D, Vlaev SD, Lossev V, Seichter P (2001) A networks-of-zones analysis of mixing and mass transfer in three industrial bioreactors *Chemical Engineering Science* 56:485-492 doi:10.1016/s0009-2509(00)00252-9
- Zhang H, Zhang K, Fan S (2009) CFD simulation coupled with population balance equations for aerated stirred bioreactors *Engineering in Life Sciences* 9:421-430 doi:10.1002/elsc.200800074
- Zinjarde SS (2014) Food-related applications of *Yarrowia lipolytica* *Food Chemistry* 152:1-10 doi:10.1016/j.foodchem.2013.11.117
- Zinjarde SS, Kale BV, Vishwasrao PV, Kumar AR (2008) Morphogenetic behavior of tropical marine yeast *Yarrowia lipolytica* in response to hydrophobic substrates *Journal of Microbiology and Biotechnology* 18:1522-1528
- Zinjarde SS, Pant A, Deshpande MV (1998) Dimorphic transition in *Yarrowia lipolytica* isolated from oil-polluted sea water *Mycological Research* 102:553-558

Titre : Étude des dynamiques de réponses physiologiques et métaboliques de *Yarrowia lipolytica* à des perturbations environnementales physico-chimiques

Auteur : Asma TIMOUMI

Directeurs de thèse: Luc FILLAUDEAU (DR INRA, LISBP, Toulouse), Carole MOLINA-Jouve (PR INSA, LISBP, Toulouse), Nathalie GORRET (CR INRA, LISBP, Toulouse)

Ecole doctorale : ED SEVAB : Ingénieries microbienne et enzymatique

Laboratoire de recherche : Laboratoire d'Ingénierie des Systèmes Biologiques et des Procédés (LISBP, CNRS UMR5504, INRA UMR792, INSA)

Résumé :

En raison d'un mélange non-idéal, des hétérogénéités au sein des bioréacteurs se produisent régulièrement soit à l'échelle pilote, soit lors de l'extrapolation à l'échelle industrielle. En conséquence, les microorganismes circulant au sein de ces bioréacteurs sont continuellement exposés à des gradients locaux de paramètres tels que le pH, la température, la concentration en substrat et/ou en oxygène dissous. Ces fluctuations spatiales et temporelles peuvent affecter la physiologie des cellules (croissance, métabolisme, morphologie) en fonction de leur nature, intensité, durée et/ou fréquence. L'objectif de ce travail est l'étude qualitative et quantitative de l'impact des fluctuations de pH et d'oxygène dissous sur le comportement dynamique (morphologique et métabolique) de *Yarrowia lipolytica*, une levure avec un potentiel biotechnologique prometteur. Pour répondre à cet objectif, des cultures en bioréacteur en conditions d'environnement contrôlé ont été mises en œuvre afin d'établir un lien de causalité entre la perturbation et la réponse observée. L'implémentation de deux modes de cultures différents (discontinu et continu) a permis de caractériser le comportement dynamique des populations cellulaires dans des états physiologiques différents. En mode continu (régime permanent), l'état physiologie pseudo-stationnaire est déterminé sur la base de la stabilité des paramètres macroscopiques mesurés (vitesses spécifiques de production, de consommation, de croissance et de respiration, rendement et viabilité des cellules). Par opposition, en mode discontinu, la distribution d'âge interne évolue avec l'accroissement de la biomasse et le temps de culture. L'hétérogénéité de la population peut alors impliquer une dispersion importante des états physiologiques. Un effort important a été consacré au développement et validation des méthodes (à partir de particules modèles et de cellules) pour une quantification rigoureuse des évolutions morphologiques de *Y. lipolytica*. Le comportement macroscopique de la levure a été caractérisé par l'évaluation des dynamiques de croissance, la viabilité, les vitesses de consommation du glucose et d'oxygène, ainsi que les vitesses de production d'acide organique et de dioxyde de carbone. Trois techniques, à savoir la cytométrie en flux (CYT), la morphogranulométrie (MG) et la diffraction dynamique de la lumière laser (DLS) ont été employé pour la quantification et la caractérisation de la transition mycélienne. Les résultats ont démontré l'adéquation du modèle cylindre pour quantifier la population filamentée, ainsi que l'importance de la longueur (complémentaire du diamètre équivalent) pour qualifier l'intensité du dimorphisme. Aucun effet significatif des fluctuations de pH et d'oxygène dissous sur le comportement macroscopique (vitesses spécifiques, rendements, viabilité) de la levure n'a été observé et ce quelque soit la perturbation (pulse, Heaviside ou créneau) et le mode de culture (discontinu ou continu). En revanche, une transition mycélienne a été induite en réponse aux deux facteurs de stress (pH and pO₂) seulement en conditions d'excès de glucose durant les cultures en mode discontinu (perturbations sous forme de pulse, Heaviside ou créneau) et continu (induite uniquement par une limitation d'oxygène en régime transitoire), suggérant ainsi un rôle de la concentration résiduelle de glucose sur la régulation de dimorphisme chez *Y. lipolytica*. Le contrôle et la régulation de la concentration en glucose dans le milieu pourrait ainsi contribuer à une meilleure maîtrise des changements morphologiques de *Y. lipolytica* en réponse à des stimuli de l'environnement.

Mots clés : *Yarrowia lipolytica*, Mode discontinu, Mode continu, Réponse dynamique, Métabolisme, Morphologie, Sous-populations, Cytométrie, Perturbation, Stress pH, Disponibilité d'oxygène

RESUME ETENDU

Actuellement, un des enjeux mondiaux majeurs est la réduction de l'impact de l'Homme sur son environnement. Dans ce contexte, l'industrie aéronautique, en croissance perpétuelle, investit dans le développement de biocarburants afin de réduire les impacts environnementaux de son activité, mais surtout d'assurer son indépendance énergétique et de sécuriser ses approvisionnements [1, 2]. Parmi les sources d'énergie alternatives aux carburants fossiles se trouvent les lipides. Les lipides peuvent être extraits à partir des plantes oléagineuses, préférentiellement à partir de cultures non-alimentaires comme la cameline ou la jatropha. Les microorganismes oléagineux tels que les bactéries, champignons, levures et microalgues peuvent également accumuler des réserves lipidiques jusqu'à 86% de leur masse sèche sous des conditions spécifiques de culture [3, 4, 5, 6, 7]. Parmi les microorganismes capables d'accumuler d'importantes quantités de lipides, *Yarrowia lipolytica* se distingue par un profil lipidique intéressant pour les applications aéronautiques [8, 9].

Au cours du développement d'un nouveau procédé, le passage du laboratoire à l'échelle industrielle représente souvent une étape critique du fait de l'existence d'hétérogénéités (gradients locaux de température, pH, concentration en oxygène dissous, substrat et métabolite) au sein des réacteurs de grandes dimensions. Ces effecteurs et leurs fluctuations, assimilées à des stress, peuvent impacter la physiologie des microorganismes et de ce fait affecter les performances du bioprocédé en fonction de leur nature, intensité, durée et/ou fréquence. Les hétérogénéités peuvent impacter de manière conséquente les performances des bioréacteurs industriels (rendement, productivité et qualité des produits d'intérêt) en comparaison avec les résultats obtenus à l'échelle laboratoire. L'identification et la quantification de l'impact de ces fluctuations sur la réactivité des cellules doivent donc être maîtrisées afin d'optimiser les bioperformances.

Les travaux de recherche présentés dans ce manuscrit se focalisent sur la caractérisation et la quantification des dynamiques de la réponse microbienne à des perturbations maîtrisées de l'environnement (en bioréacteur). *Y. lipolytica*, une levure avec un potentiel biotechnologique prometteur est utilisée comme modèle d'étude. La démarche expérimentale adoptée (Figure 1) consiste tout d'abord à établir une revue bibliographique des travaux antérieurs concernant les hétérogénéités au sein des bioréacteurs industriels et leur impact sur le métabolisme et la morphologie de *Y. lipolytica*. L'objectif est d'identifier la

Étude des dynamiques de réponses physiologiques et métaboliques de *Yarrowia lipolytica* à des perturbations environnementales physico-chimiques

nature, l'origine et l'amplitude de ces fluctuations, les inducteurs potentiels de stress chez cette levure, ainsi que les méthodologies et les outils expérimentaux utilisés pour l'analyse des réponses résultantes. Des fluctuations de pH et d'oxygène dissous ont été ensuite examinées en bioréacteur sous conditions d'environnement contrôlé afin d'établir un lien de causalité directe entre la perturbation et la réponse observée. Deux modes de culture (continu et discontinu) ont été mises en œuvre afin de caractériser le comportement dynamique des populations cellulaires dans des états physiologiques différents. Par ailleurs, un effort important a été consacré au développement des méthodes appropriées pour une caractérisation rigoureuse des évolutions morphologiques chez *Y. lipolytica* (transition de la forme ovoïde à la forme mycéliale/filamenteuse en réponse à un stress).

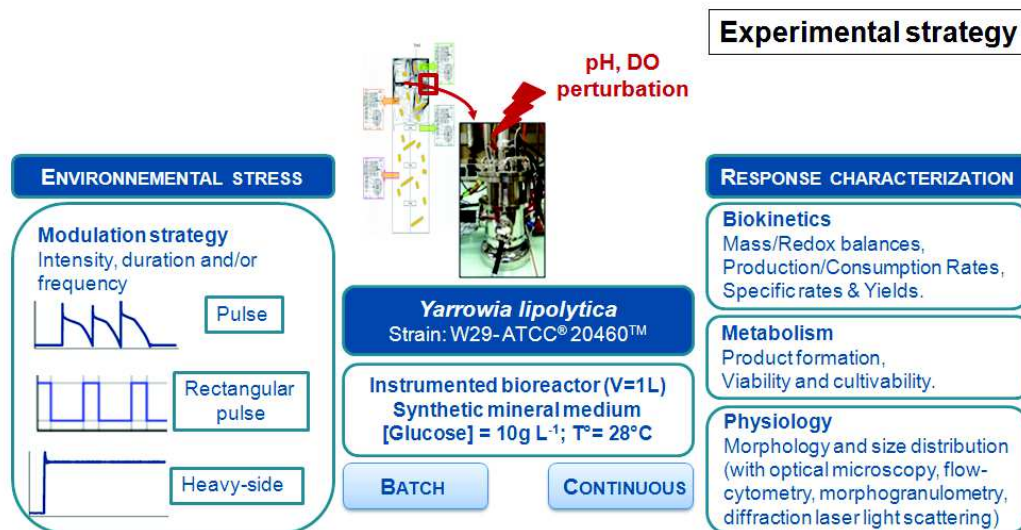
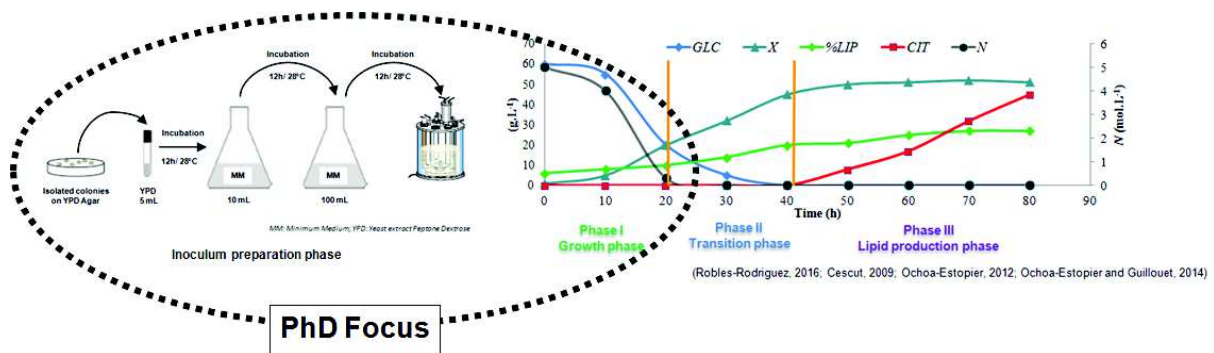


Figure 1: Centre d'intérêt de la thèse et la démarche expérimentale

Le manuscrit de thèse est structuré en quatre parties :

I. Synthèse bibliographique

La première partie de ces travaux de recherche est une **Synthèse Bibliographique** relative aux hétérogénéités rencontrées au sein des bioréacteurs industriels. La physiologie du microorganisme modèle choisi "*Y. lipolytica*", et l'état des connaissances relatives à l'analyse de son comportement vis-à-vis des fluctuations de l'environnement sont également décrites. Cette analyse bibliographique a permis de conclure sur la limite des connaissances présentes dans la littérature concernant l'étude de la transition mycélienne de *Y. lipolytica* en réponse à un stress. En effet, la plupart des études ($\approx 82\%$ des travaux) ont été effectuées dans des conditions partiellement maîtrisées (Erlenmeyer, tubes) conduisant ainsi à des réponses multifactorielles. A ce jour, une seule étude a été effectuée en bioréacteur sous un environnement contrôlé mais dans des conditions de limitation en azote et non pas en condition de croissance [10]. Par ailleurs, la comparaison des évolutions morphologiques entre les différents travaux semble être assez complexe, compte tenu de la multiplicité des méthodes, la disparité des critères morphologiques et la faible représentativité statistique des cellules analysées. En effet, La microscopie optique a été la méthode la plus largement utilisée pour la caractérisation des changements morphologiques de *Y. lipolytica*. De plus, des critères discriminatoires subjectifs ont été souvent employés pour discriminer des populations cellulaires de différentes formes. Néanmoins, aucune analyse de la distribution de la taille de cellules au niveau de la population n'a été rapportée dans les travaux antérieurs.

De cet état de l'art, il ressort **les questions scientifiques** auxquels ces travaux ont l'ambition d'apporter des éléments de réponse:

- ⇒ **Quel est l'impact des fluctuations de pH et d'oxygène dissous sur métabolisme et la morphologie de *Y. lipolytica* ?**
- ⇒ **Quels sont les effets de la nature, intensité, durée et/ou fréquence de la perturbation sur le comportement dynamique de *Y. lipolytica* ?**
- ⇒ **Comment caractériser et quantifier les changements morphologiques de *Y. lipolytica* à l'échelle de la population ?**

II. Matériels et Méthodes

Dans la deuxième partie, une description détaillée des **Matériels et Méthodes** utilisés est présentée. Cette partie comprend une présentation de la souche et des milieux de cultures utilisés, les conditions de culture employées, ainsi que les caractéristiques des particules

modèles utilisées pour la validation des techniques morphologiques. Les méthodes analytiques utilisées pour caractériser les dynamiques de croissance, le métabolisme et la morphologie de *Y. lipolytica* sont également décrites. Le Tableau 1 présente l'ensemble des méthodes morphologiques utilisées dans le cadre de ses travaux. Enfin, la méthodologie employée pour le traitement des données cinétiques (vitesses, rendements, bilans carbone et redox ...), ainsi que le lissage et la réconciliation des données expérimentales sont dûment présentés. Le schéma récapitulatif du dispositif expérimental et de l'ensemble des analyses effectuées est présenté dans la Figure 2.

Tableau 1: Les méthodes de caractérisation morphologique des cellules de *Y. lipolytica*

Méthode	Dimension	Paramètre mesuré	Représentativité statistique
Microscopie optique	2D	d_{CE} , L, W, AR	∅
Morphogranulométrie (MG)	3D	d_{CE} , L, W, AR, perimeter, area, circularity	⊕
Diffraction dynamique de la lumière (DLS)	3D	d_{SE}	⊕
cytométrie en flux (CYT)	3D	d_{SE} , L	⊕

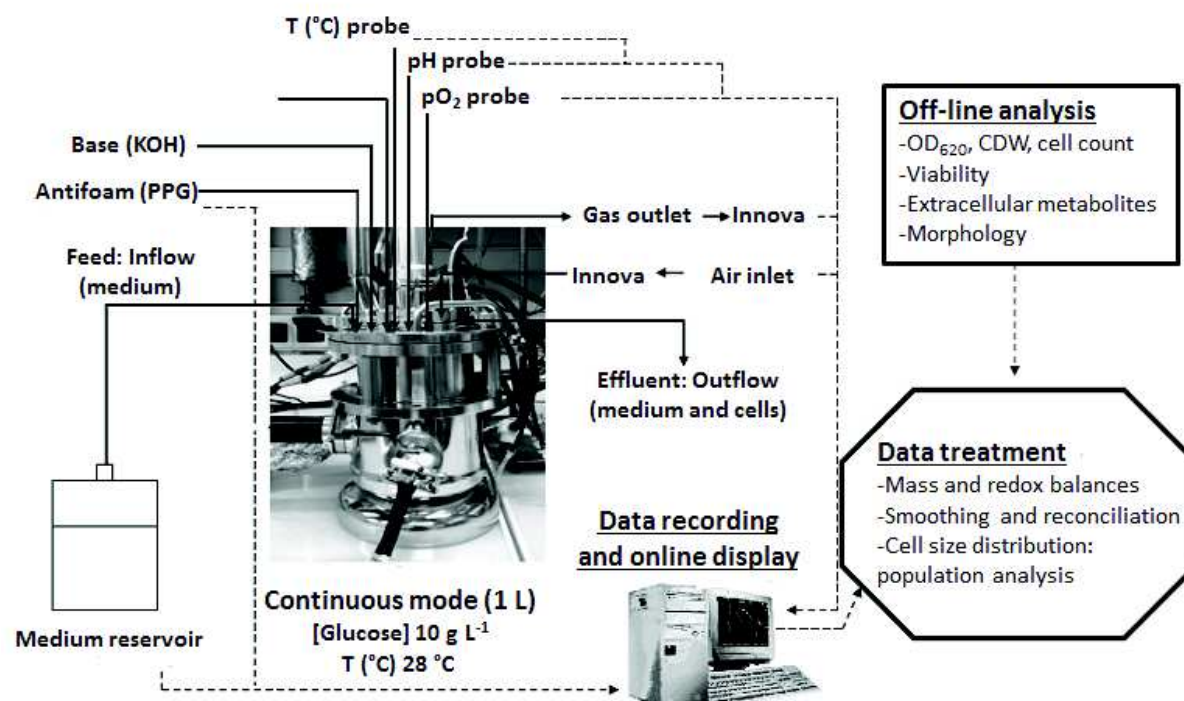


Figure 2: Description du dispositif expérimental, son instrumentation, les analyses et le traitement des données effectués.

III. Résultats et Discussion

La troisième partie “**Résultats et Discussion**” présente les résultats obtenus ainsi que la discussion organisée en quatre chapitres :

1. Développement et validation des méthodes pour la quantification et la caractérisation des changements morphologiques de *Y. lipolytica*.
2. Caractérisation qualitative et quantitative de la transition mycélienne de *Y. lipolytica* par morphogranulométrie.
3. Etude de l'impact des perturbations du pH sur la physiologie (métabolisme, morphologie) de *Y. lipolytica* cultivée en modes continu et discontinu.
4. Influence des fluctuations en oxygène dissous sur le comportement dynamique de *Y. lipolytica* lors des cultures continues et discontinues.

Dans le **Chapitre III-1**, l'aptitude de trois techniques optiques (cytométrie en flux, morphogranulométrie et diffraction dynamique de la lumière laser) à quantifier les changements morphologiques de *Y. lipolytica* est évaluée en utilisant des particules sphériques de diamètres variant de 1 à 80 μm (Figure 3).

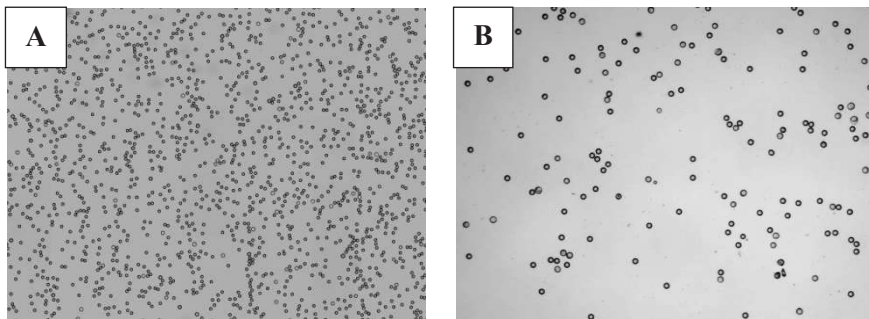


Figure 3: Images microscopiques pour les billes de diamètre de 15 μm (A ; grossissement x20; taille de l'image 362 x 272 μm^2) et 40 μm (B ; grossissement: x2,5; taille de l'image 2903 x 2177 μm^2)

Les données brutes générées par chacune des méthodes sont différents. En effet, la cytométrie en flux fournit une estimation du diamètre et de la longueur des particules en se basant sur une courbe de calibration des signaux FSC (Forward Scatter) et width-FSC en fonction du diamètre de billes selon un modèle sphère (en utilisant des billes standardisées sphériques de diamètre compris entre 1 et 15 μm). La morphogranulométrie, qui est une technique basée sur des observations microscopiques couplées à une analyse automatique d'images, fournit une mesure directe de la taille et des paramètres morphologiques des particules (sans avoir recours

à aucun modèle géométrique). Alors que, la technique de DLS mesure un diamètre équivalent de la particule selon un modèle sphère. Les résultats obtenus ont montré que la cytométrie en flux et la morphogranulométrie permettent une mesure correcte du diamètre moyen des particules, tandis que la méthode de la diffraction dynamique de la lumière a abouti une sous-estimation du diamètre d'environ 14%. En terme de précision de mesure, l'utilisation de la courbe de calibration pour convertir les signaux obtenues par cytométrie en flux (FSC et width) en une dimension de particule, a induit des imprécisions de l'ordre de 10 et 32% au niveau du diamètre et de la longueur, respectivement. Ainsi, seulement les signaux bruts de cytométrie ont été examinés et aucune corrélation avec le diamètre ou la longueur de la sphère n'a été appliquée dans la suite des travaux. Avec le morphogranulomètre, l'erreur induite sur la mesure du diamètre ne dépassait pas 5%. Cet écart-type relativement faible est attendu puisque le diamètre est directement mesuré sur l'image composite (2D), à la différence de la cytométrie en flux, où le diamètre est estimé à travers une corrélation selon une loi en puissance du signal correspondant. Figure 4 compare les profils de distribution du taille obtenus par les différents techniques pour les particules de 15 μm de diamètre. Par ailleurs, **les résultats ont démontré la capacité des trois techniques à différencier et à quantifier des sous-populations de billes de taille proches (4 et 6 μm) et/ou différentes (1 et 15 μm).**

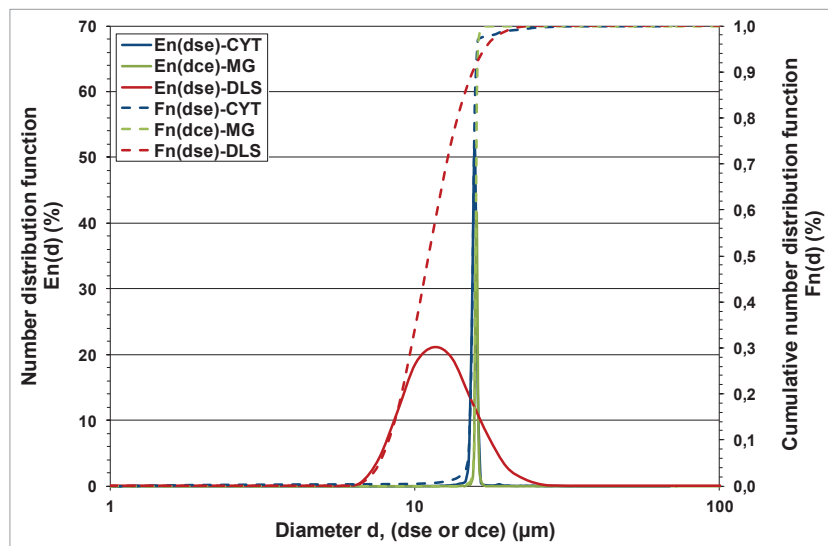


Figure 4 : Comparaison des fonctions de distribution, En et de distribution cumulée, Fn du diamètre, en nombre, issues de trois méthodes (MG, CYT, DLS) pour des particules sphériques (diamètre : 15 μm)

Le **Chapitre III-2** est consacré à la caractérisation de la morphologie et la distribution de la taille des cellules durant la transition mycéliale de *Y. lipolytica* par morphogranulométrie.

Parmi les trois techniques précédemment évaluées, la morphogranulométrie a été préférentiellement sélectionnée car elle fournit différents critères morphologiques pour chacune des particules (diamètre, longueur, largeur...), et permet ainsi l'application du modèle cylindre pour la quantification des sous-populations filamentées. Dans ce chapitre, le pH a été choisi comme inducteur de dimorphisme chez la levure. Trois conditions de pH (4,5 ; 5,6 et 7) ont été testées. Dans cette étude, un effort important a été dédié à la standardisation de la morphologie des populations initiales (pré-cultures) avant l'inoculation en bioréacteur, afin de fournir des interprétations précises des évolutions morphologiques induites par les changements du pH. Dans les pré-cultures à différent pH, *Y. lipolytica* présente une morphologie homogène composée principalement de cellules ovoïdes. Les caractéristiques morphologiques des populations initiales à pH 4,5 ; 5.6 et 7 sont présentées dans le tableau 2.

Tableau 2 : Caractéristiques morphologiques des populations initiales de *Y. lipolytica*

Paramètres	pH 4.5	pH 5.6	pH 7
Diamètre (d_{CE}) (μm)	8.08±2.12	7.94±2.13	7.34±1.86
Aspect ratio (/)	0.45±0.20	0.54±0.18	0.41±0.16
Longueur (μm)	13.0±6.8	14.8± 8.0	13.0±5.6
Largeur (μm)	5.78±1.28	8.14±1.14	5.05±1.55

Les profils de distribution de la taille des cellules, en nombre et en volume, ont été évalués durant les fermentations à différents pH. Deux modèles géométriques (sphère et cylindre) ont été également comparés afin d'évaluer leur aptitude à quantifier le phénomène d'élongation chez la levure étudiée. Par ailleurs, d'autres paramètres morphologiques, à savoir la longueur et l'aspect ratio (AR : rapport largeur/longueur) ont été analysés afin d'étudier l'intensité de la filamentation. Les résultats obtenues ont démontré que les modèles de calcul tenant en compte de la distribution en fonction de volume sont plus adéquats, comparés au modèle de la distribution en fonction du nombre pour la quantification du dimorphisme (plus de 62,3% de cellules filamentées en volume, comparé à 11,3% en nombre). L'utilisation du modèle cylindre a permis également une meilleure description du phénomène d'élongation chez cette levure, comparé au modèle de la sphère (Figure 5). Avec l'approximation cylindre, la population mycéliale représente plus de 84,1% (v/v) pour les cellules cultivées à pH 7. Cette fraction ne dépasse pas 62,3 % avec le modèle de la sphère.

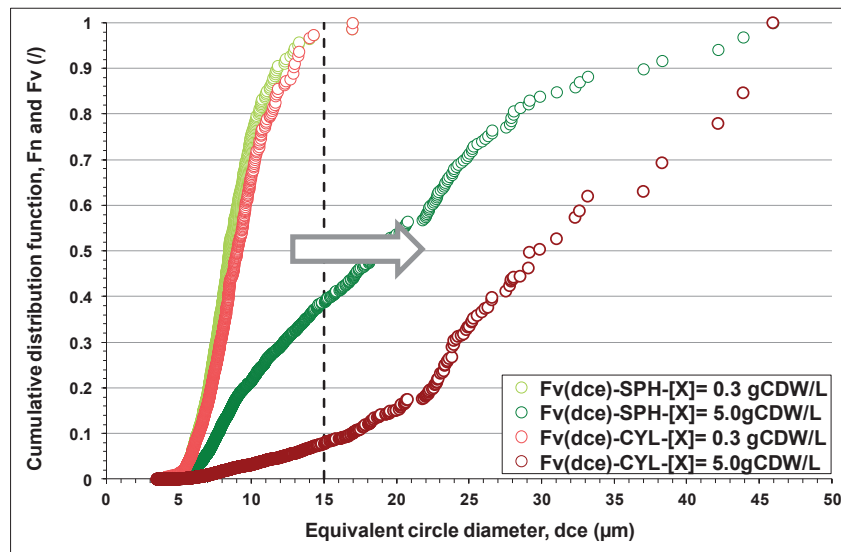


Figure 5 : Comparaison et évolution des fonctions de distribution cumulatives en volume du diamètre de cercle équivalent, d_{CE} en fonction de la concentration en biomasse cellulaire (0.3 et 5.0gcdw/L) selon les modèles sphérique et cylindrique (*Yarrowia lipolytica*, culture discontinue, pH=7).

Par ailleurs, les résultats présentés dans ce chapitre soulignent l'importance d'examiner d'autres paramètres morphologiques, tel que la longueur des cellules et l'aspect ratio pour quantifier la magnitude du dimorphisme

Le **Chapitre III-3**, analyse le comportement dynamique de *Y. lipolytica* en réponse à des perturbations de pH dans des conditions maîtrisées de culture (Timoumi et al. 2017a [11]-DOI: [10.1007/s00253-016-7856-2](https://doi.org/10.1007/s00253-016-7856-2)). Dans la première partie de cette étude, des cultures en mode batch ont été réalisées à différents pH (4,5 ; 5,6 et 7). La transition mycéliale a été induite au cours des cultures batch à pH 4,5 et 7, alors qu'à pH 5,6, la forme ovoïde (levure) a été largement prédominante. De plus, l'intensité de la filamentation a été plus prononcée à pH 7 qu'à pH 4,5: les cellules filamenteuses représentaient 93% (v/v) à pH neutre, comparé à 84% (v/v) durant la culture à pH 4,5 (Figure 6). Néanmoins, le comportement macroscopique (paramètres cinétiques, rendements, viabilité) de la levure n'a pas été significativement affectée par le pH de culture.

Dans une seconde partie, des perturbations contrôlées de pH 5.6 à pH 7 ont été appliquées durant des cultures en modes batch et continu (limité en glucose). Les réponses métaboliques et morphologiques de *Y. lipolytica* ont été examinées en fonction du type de perturbation imposé (pulses successives, paliers), de la nature du mode de culture (batch ou chemostat), et du taux de croissance du microorganisme (de 0.03 à 0.20 h⁻¹). Au niveau morphologique, aucune transition dimorphique de la forme levure au mycélium n'a été observée en mode

continu, contrairement aux cultures batch. En mode continu, quel que soit le type de perturbations, la morphologie de la levure n'a pas été affecté : les cellules ont conservé une forme parfaitement ovoïde (diamètre moyen $\approx 6,2 \mu\text{m}$) dans les différentes conditions étudiées (type de perturbation, taux de dilution). Sur le plan métabolique, le stress pH n'a pas induit des variations significatives sur les dynamiques de croissance, de consommation de substrat et d'oxygène, et de production de dioxyde de carbone. Une forte robustesse de la souche aux changements de pH a été également démontrée par le maintien d'une viabilité cellulaire élevée ($\geq 97\%$).

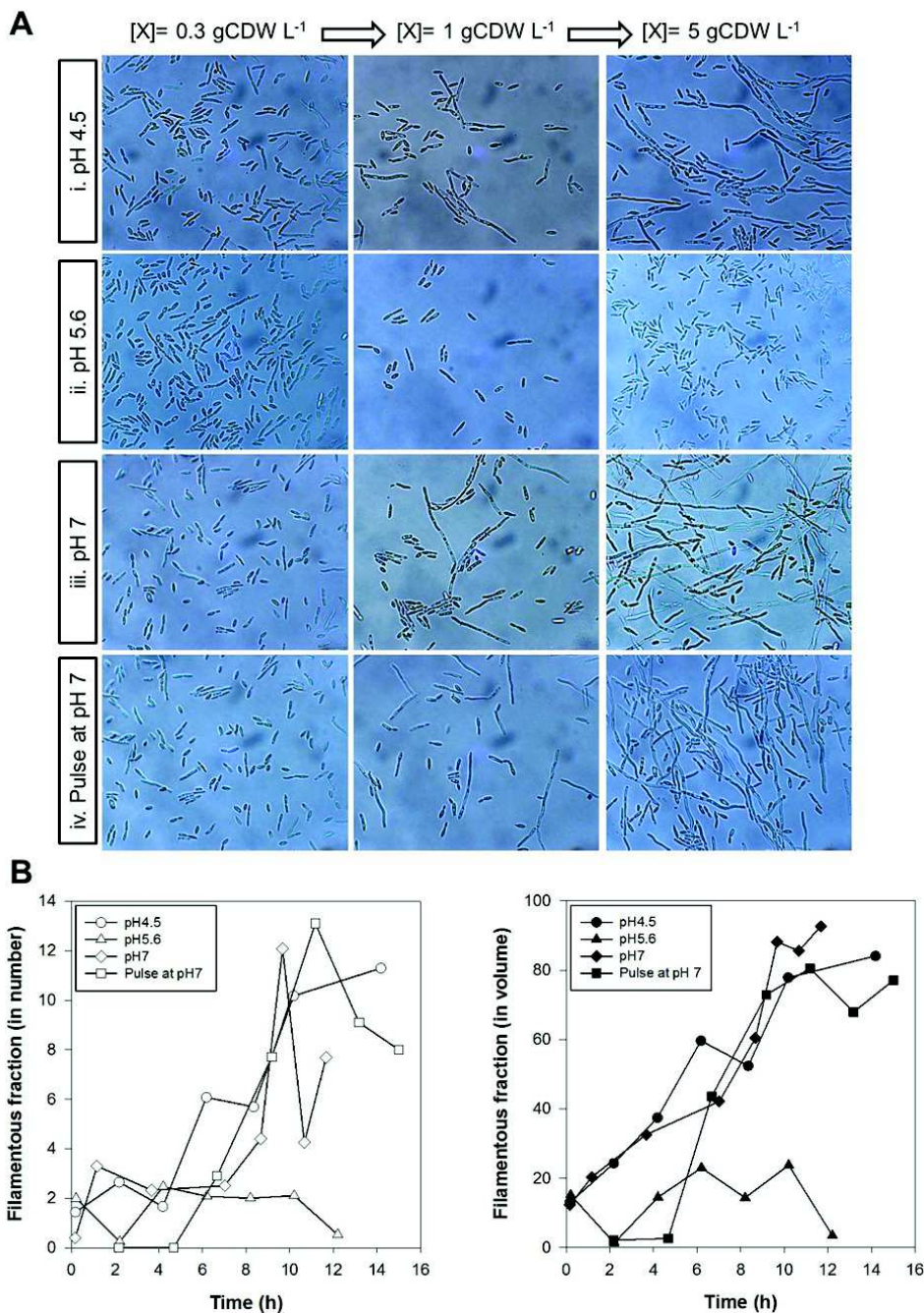


Figure 6 : A. Images microscopiques de cellules de *Y. lipolytica* cultivées dans des conditions de pH différentes (i, pH 4,5, ii, pH 5,6, iii, pH 7 et iv, pH de 5,6 à 7). B. Pourcentage de la population filamentée ($d_{CE} > 15 \mu\text{m}$) de *Yarrowia lipolytica* par des mesures morpho-granulométriques.

Les résultats issus de cette étude ont permis d'apporter une analyse quantitative des paramètres cinétiques de croissance chez *Y. lipolytica* dans des conditions maîtrisées de culture (approche mono-factorielle). Par ailleurs, une méthode de quantification du phénomène du dimorphisme à l'échelle de la population cellulaire (représentativité statistique) a été également mise au point dans le cadre de ces travaux.

Dans le **Chapitre III-4**, l'influence des variations au niveau de la concentration en oxygène dissous sur les réponses cellulaires de *Y. lipolytica* est présentée (Timoumi et al. 2017b [12]-DOI: [10.1007/s00253-017-8446-7](https://doi.org/10.1007/s00253-017-8446-7)). La levure a été cultivée en mode discontinu et continu dans différentes conditions d'oxygénation: Fluctuations en oxygène dissous (Figure 7), anoxie totale (pO_2 0% ; 100% N_2), et sous un apport faible (pO_2 2%) ou limité (pO_2 0% ; 75% des besoins) en oxygène. Les comportements dynamiques de la levure aux niveaux métabolique et morphologique ont été par la suite caractérisés et discutés.

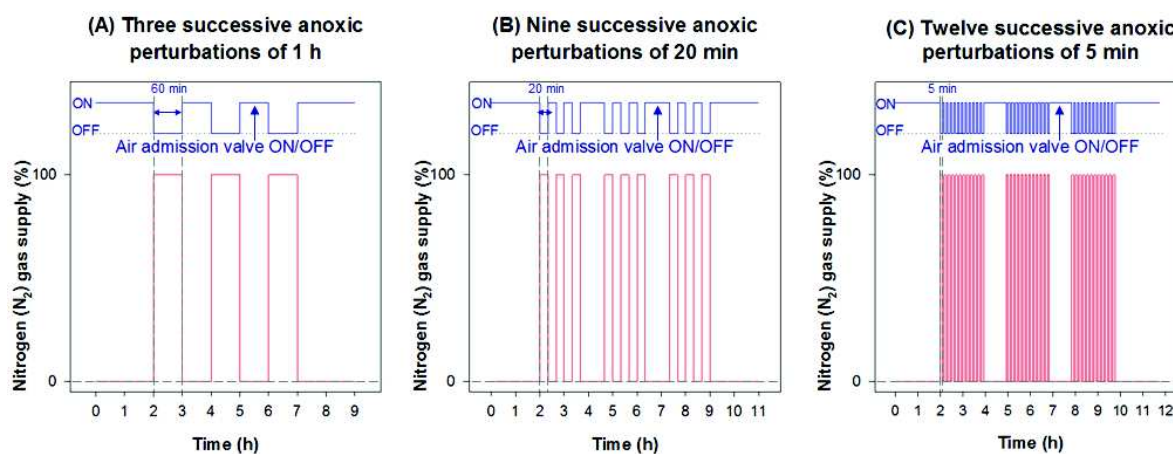
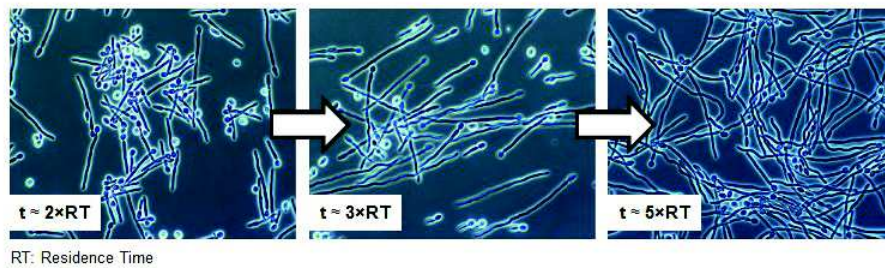


Figure 7: Profils des fluctuations en oxygène dissous appliqués durant les cultures continues et discontinues de *Y. lipolytica* (A : 3x60min, B : 9x20min et C : 36x5min)

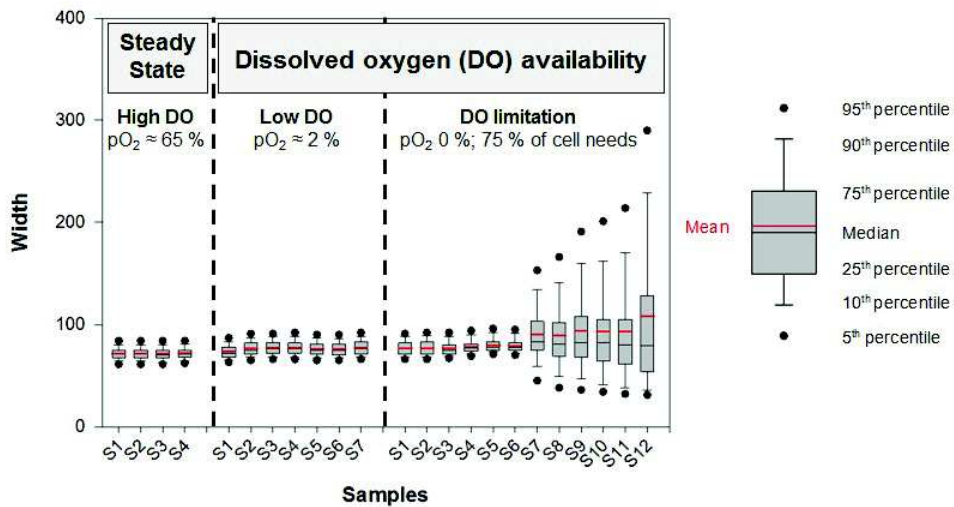
Les résultats de cette étude ont montré qu'en mode discontinu, les transitions entre des environnements riches et dépourvus en oxygène ont induit une légère accumulation d'acide citrique par les cellules de *Y. lipolytica* ($\leq 29 \text{ mg L}^{-1}$). Cependant, aucune production d'acide citrique n'a été détectée en culture continues malgré l'exposition à des perturbations plus fréquentes en oxygène dissous. Les paramètres cinétiques, rendements et viabilité de la levure n'ont pas été significativement affectés sous les deux modes de culture. En revanche, une accumulation du glucose résiduel (jusqu'à $0,98 \text{ g L}^{-1}$) dans le milieu a été observée dans les

conditions de limitation en oxygène (pO_2 0%) durant les cultures en chemostat. Sur le plan morphologique, une transition micellaire (jusqu'à 74% de cellules filamenteuses) a été induite en réponse aux fluctuations d'oxygène durant les cultures discontinues (condition d'excès de glucose). Néanmoins, en mode continu (limité en glucose), la forme ovoïde a été majoritaire. Le dimorphisme a été observé uniquement dans les conditions où l'oxygène dissous était limitant, et est corrélé avec une accumulation de glucose dans le milieu de culture (à partir d'une concentration de $0,75 \text{ g L}^{-1}$) (Figure 8).

A



B



C

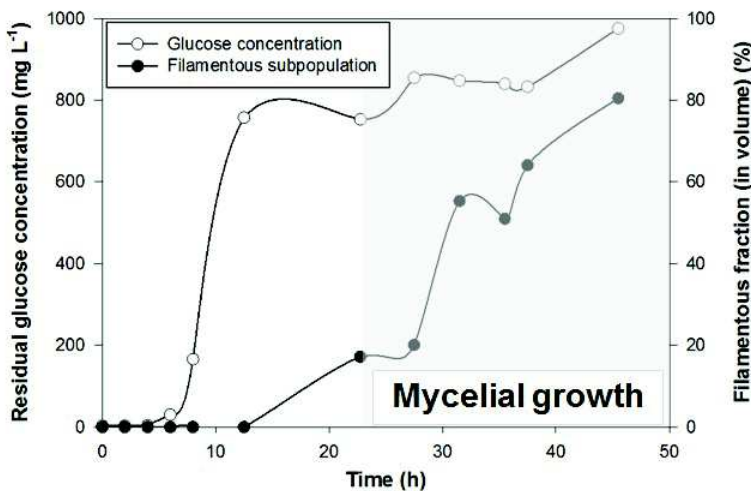


Figure 8 : A. Images microscopiques illustrant les changements morphologiques de *Y. lipolytica* induis par un passage des conditions sous un apport faible (pO_2 2%) à limité en oxygène. B. Evolution de la distribution en nombre de la longueur des cellules cultivées en mode continu sous les différentes conditions d'oxygénation. C. Evolution de la sous-population mycéliale (en volume) et de la concentration de glucose résiduelle pendant la phase limitée en oxygène de la culture continue

L'ensemble de ces résultats suggèrent un rôle possible du niveau du glucose dans le milieu sur la régulation du dimorphisme chez *Y. lipolytica*. **La régulation de la transition morphologique chez cette levure repose sur le fonctionnement de deux voies de signalisation opposées: MAPK (Mitogen-Activated Protein Kinase), et cAMP-PKA (cyclic-AMP dependent Protein Kinase A). La voie de la MAPK est impliquée dans la croissance sous forme filamenteuse, tandis que la voie PKA est nécessaire pour le développement sous la forme ovoïde. Le niveau de glucose pourrait probablement influencer la régulation de la voie impliquée dans la filamentation.**

IV. Conclusions et perspectives

En conclusion, ces travaux de recherche identifient et quantifient les interactions dynamiques entre la physiologie microbienne de *Y. lipolytica* et le stress environnemental, aux échelles métabolique et morphologique. **Ces travaux ont permis d'une part d'obtenir, en mettant en œuvre des outils d'investigation originaux, des données sur les cinétiques de croissance de la levure en conditions d'environnement contrôlé, et d'autre part de quantifier et qualifier le phénomène du dimorphisme de la population microbienne.** L'analyse des travaux menés dans ce projet permet de proposer **plusieurs perspectives**:

- ⇒ Le développement d'un modèle dynamique décrivant le comportement cinétique des sous-populations filamenteuses en se basant sur les données de quantification du dimorphisme obtenues par morphogranulométrie.
- ⇒ Compréhension des mécanismes moléculaires régulant les changements morphologiques de *Y. lipolytica* en réponse à des fluctuations de pH et d'oxygène dissous. A cet égard, une analyse comparative du transcriptome de la levure sous la forme ovoïde et filamentée a été effectuée en utilisant la méthodologie du RNA-seq. Trois répliquas par échantillon ont été analysés et différents scénarii de comparaison ont été examinés afin d'évaluer l'effet de la nature de stress (pH et pO_2), le mode de

culture (discontinu, continu) et le type de perturbation (pulse, créneau et palier) sur la réponse cellulaire.

- ⇒ Etude de l'influence de la concentration résiduelle en glucose sur la transition mycélienne (voie de la cAMP-PKA) de *Y. lipolytica*. L'analyse des évolutions morphologiques de la levure durant des cultures en bioréacteur sous limitation glucose en présence d'un ajout pulsé de l'AMPc et/ou une quantification de l'AMPc intracellulaire pourraient être envisageables.
- ⇒ Investigation de l'impact de la morphologie cellulaire sur la production et l'accumulation de lipides (rendements, profils lipidiques) par *Y. lipolytica*.

Publications et Communications

Revue internationale

Timoumi A, Cléret M, Bideaux C, E. Guillouet S, Allouche Y, Molina-Jouve C, Fillaudeau L, Gorret N (2017): Dynamic behavior of *Yarrowia lipolytica* in response to pH perturbations: dependence of the stress response on the culture mode. *Appl Microbiol Biotechnol* 101:351-366 doi:10.1007/s00253-016-7856-2

Timoumi A, Bideaux C, E. Guillouet S, Allouche Y, Molina-Jouve C, Fillaudeau L, Gorret N: Influence of oxygen availability on the metabolism and morphology of *Yarrowia lipolytica*: insights into the impact of glucose levels on dimorphism. *Appl Microbiol Biotechnol* 101:351-366 doi:10.1007/s00253-016-7856-2

Timoumi A, Nguyen T.C, Molina-Jouve C, Gorret N, Fillaudeau L: Comparison of optical methodologies for morphology and size distribution characterization of model particles and complex-shaped biological matrices (*under preparation*).

Conférences internationales

➤ Présentation orale

Timoumi A, Cléret M, Allouche Y, Molina-Jouve C, Fillaudeau L, Gorret N. (2015): Study of the dynamics of metabolic and physiological responses of *Yarrowia lipolytica* to pH perturbations under well-controlled conditions in batch and continuous modes of culture. *Microbial Stress Congress: From Molecules to Systems, Sitges, Spain*.

Timoumi A, Cléret M, Allouche Y, Molina-Jouve C, Fillaudeau L, Gorret N. (2016): Dynamic behavior of *Yarrowia lipolytica* to well-controlled pH and oxygen perturbations: dependence of the stress response on the culture mode. *17th European Congress on Biotechnology (ECB), Krakow, Poland*.

Timoumi A, Cléret M, Allouche Y, Molina-Jouve C, Fillaudeau L, Gorret N. (2016): Dynamics of metabolic and physiological responses of *Yarrowia lipolytica* to well-controlled pH and oxygen perturbations in batch and continuous operating modes. *6th Conference on Physiology of Yeasts and Filamentous Fungi (PYFF6), Lisbon, Portugal*.

Timoumi A, Nguyen T.C, Le T, Anne-archard D, Bideaux C, Cameleyre X, Lombard E, Molina-Jouve C, To K.A, Gorret N, Fillaudeau L. (2016): Optical methods and their limitation to characterize the morphology and granulometry of complex shape biological materials. *Journées Internationales de Biotechnologie, Sousse, Tunisie*.

➤ Présentation par affiche

Timoumi A, Allouche Y, Plateau J, Molina-Jouve C, Fillaudeau L, Gorret N. (2015): Comparison of optical methods to characterize morphology and size distribution of model particles and mycelial transition of *Yarrowia lipolytica*. *ECCE10-ECAB3-EPIC5 Congress, Nice, France*.

Timoumi A, Allouche Y, Plateau J, Molina-Jouve C, Fillaudeau L, Gorret N. (2015): Comparison of optical methods to characterize morphology and size distribution of model particles and mycelial transition of *Yarrowia lipolytica*. *Journées Internationales de Biotechnologie, Djerba, Tunisie*.

Références

1. Rapport annuel IATA 2013 alternative fuel report, <http://www.iata.org/publications/documents/2013-reportalternative-fuels.pdf>.
2. Parorama 2015, présentation d'Olivier Appert, <http://www.ifpenergiesnouvelles.fr/Actualites/Evenements/Nous-organisons/Panorama-2015>.
3. Babau M, Cescut J, Allouche Y, Lombaert-Valot I, Fillaudeau L, Uribelarrea JL, Molina-Jouve C (2013) Towards a Microbial Production of Fatty Acids as Precursors of Biokerosene from Glucose and Xylose Oil & Gas Science and Technology-Revue D Ifp Energies Nouvelles 68:899-911 doi:10.2516/ogst/2013148
4. Meng X, Yang JM, Xu X, Zhang L, Nie QJ, Xian M (2009) Biodiesel production from oleaginous microorganisms Renewable Energy 34:1-5 doi:10.1016/j.renene.2008.04.014
5. Metting FB (1996) Biodiversity and application of microalgae Journal of Industrial Microbiology & Biotechnology 17:477-489 doi:10.1007/bf01574779
6. Ratledge C (1982) Single cell oil Enzyme and Microbial Technology 4:58-60 doi:10.1016/0141-0229(82)90014-x
7. Xu H, Miao XL, Wu QY (2006) High quality biodiesel production from a microalga *Chlorella protothecoides* by heterotrophic growth in fermenters Journal of Biotechnology 126:499-507 doi:10.1016/j.jbiotec.2006.05.002
8. Papanikolaou S, Muniglia L, Chevalot I, Aggelis G, Marc I (2003) Accumulation of a cocoa-butter-like lipid by *Yarrowia lipolytica* cultivated on agro-industrial residues Current Microbiology 46:124-130 doi:10.1007/s00284-002-3833-3
9. Ratledge C, Wynn JP (2002) The biochemistry and molecular biology of lipid accumulation in oleaginous microorganisms. In: Laskin AI, Bennett JW, Gadd GM (eds) Advances in Applied Microbiology, Vol 51, vol 51. Advances in Applied Microbiology. pp 1-51. doi:10.1016/s0065-2164(02)51000-5
10. Bellou S, Makri A, Triantaphyllidou I-E, Papanikolaou S, Aggelis G (2014) Morphological and metabolic shifts of *Yarrowia lipolytica* induced by alteration of the dissolved oxygen concentration in the growth environment Microbiology-Sgm 160:807-817 doi:10.1099/mic.0.074302-0
11. Timoumi A, Cléret M, Bideaux C, Guillouet SE, Allouche Y, Molina-Jouve C, Fillaudeau L, Gorret N (2017a) Dynamic behavior of *Yarrowia lipolytica* in response to pH perturbations: dependence of the stress response on the culture mode Appl Microbiol Biotechnol 101:351-366 doi:10.1007/s00253-016-7856-2
12. Timoumi A, Bideaux C, Guillouet SE, Allouche Y, Molina-Jouve C, Fillaudeau L, Gorret N (2017b) Influence of oxygen availability on the metabolism and morphology of *Yarrowia lipolytica*: insights into the impact of glucose levels on dimorphism Appl Microbiol Biotechnol doi:10.1007/s00253-017-8446-7